

39 MAG
NN08201
40951 1999-05-12

CA
2618

SWIMMING AND MUSCLE STRUCTURE IN FISH

Igor L. Y. Spierts



Swimming and muscle structure in fish

Igor L.Y. Spierts

Proefschrift

ter verkrijging van de graad van doctor
op gezag van de rector magnificus
van de Landbouwniversiteit te Wageningen,
dr. C.M. Karssen,
in het openbaar te verdedigen
op vrijdag 28 mei 1999
des namiddags te half twee in de aula

Abstract

Spierts, I.L.Y. 1999. Swimming and muscle structure in fish. Doctoral thesis, Experimental Zoology Group, Wageningen Agricultural University, P.O. Box 338, 6700 AH Wageningen, The Netherlands

ISBN: 90-9012702-X

Subject headings: Carp axial muscle, fish swimming, myotendinous junctions, force transmission, titin isoforms, muscle activity, carp larvae, ontogeny, elastic energy, *Cyprinus carpio* L.

The scope of this series of studies was to determine (from micro- to macro-level) how the structure of axial muscles of fish is adapted to the functional, sometimes contrasting, demands of different modes of swimming (e.g. continuous swimming and fast-starts) in relation to fish size and age. Posterior fibres of adult carp have a longer phase of eccentric activity (active while being stretched) than anterior fibres and will therefore develop greater forces. Posterior and red fibres are subjected to larger sarcomere strains during continuous swimming and have special adaptations to these functional demands: (1) stronger MTJs, and (2) larger isoforms of the giant elastic muscle protein titin. A quantitative electron-microscopical study showed that a linear correlation exists between the surface area of MTJs (measure for strength) and the size and duration of the load on a junction. Fibres with larger surface areas consequently can bear larger loads during swimming. Gel-electrophoresis and micro-mechanical experiments revealed that fibres with larger titin isoforms require less passive tension for the same sarcomere strain. As larval muscle fibres possessed smaller titins than that of any adult muscle fibre the titin isoform changes during ontogeny. The shorter titin isoform is thought to help restricting form changes of fast swimming carp larvae and to increase the elastic contribution to the tail beat by elastic energy storage in this titin isoform during the initial bending that is subsequently released in the following bending. This study corroborates the idea that (small) differences in muscle function during swimming, turning and escaping can be used to predict and possibly explain structural differences between various types of muscles in fish of different age and size.

This research were supported by the Life Sciences Foundation (project 805-28.266, NWO-SLW), which is subsidised by the Netherlands Organisation for Scientific Research.

Cover design: Wim Valen.

STELLINGEN

- 1 Spieren die aan verschillende mechanische eisen moeten voldoen blijken bij die eisen passende (ultra) structuren te bezitten.
Dit proefschrift.
- 2 De elastische eigenschappen van een spier worden in belangrijke mate bepaald door het elastische spiereiwit titine. Aangezien zeer kort na de dood van een vis het titine door proteolytische enzymen afgebroken wordt zijn de resultaten van vele micro-mechanische experimenten, waarbij aan spiervezels getrokken werd, onbetrouwbaar. De belangrijke elastische bijdrage van titine aan dergelijke kracht-lengte metingen is dan namelijk niet met zekerheid bekend.
Dit proefschrift.
- 3 Het is tegenwoordig niet alleen mogelijk maar het wordt ook noodzakelijk om structuur-functie relaties in de morfologie tot op moleculair niveau te onderzoeken.
Dit proefschrift.
- 4 Tijdens snelle starten van karpers (C- en S- ontsnappingsreacties) zijn niet alleen witte maar ook rode spieren langs de lichaamsas van de vis actief. Ik neem daarom aan dat rode spieren tijdens deze krachtige en snelle bewegingen een (geringe) bijdrage leveren aan de productie van kracht.
Dit proefschrift (hoofdstuk 6, 7).
- 5 Het is als wetenschapper belangrijk om niet met alle winden mee te waaien, doch het luisteren naar de wind in de bomen van het eigen onderzoeksveld blijft essentieel.
- 6 Wetenschap bedrijven zonder regelmatig een second opinion te krijgen is als roeien zonder peddels.
- 7 'De onnodige oorlog'. Nooit is er een oorlog geweest, die gemakkelijker vermeden had kunnen worden dan die, welke zojuist heeft verwoest wat door de vorige worsteling nog van de wereld was overgelaten.
Sir Winston Leonard Spencer-Churchill. De Tweede Wereldoorlog. 1. Van oorlog tot oorlog, 1919-1938 (1989). Tirion-Baarn, 374 pp.

- 8 De uiteenlopende belangen van de huidige Europese partners én het ontbreken van een goede democratische structuur in Europa verhinderen een éénduidig Europees optreden dat noodzakelijk is om een crisis als in de Balkan snel aan te kunnen pakken, c.q. te kunnen vermijden.
- 9 Een omscholing naar de Informatiserings Technologie is tegenwoordig de meest succesvolle carrièrewijziging voor langdurig werkeloze academici.
- 10 De geschiedenis leert ons dat ervaringen slechts deels overdraagbaar zijn. Elke generatie zal zelf ervaringen moeten opdoen en een weg uit problemen moeten bepalen, want de tevoren door anderen aangedragen oplossingen worden nauwelijks opgevolgd. Dit kan ook niet want kennis en ervaring zijn twee verschillende vormen van weten.
G.H.M.A. Spierts.
- 11 De dikte van een proefschrift is positief gecorreleerd met de gehanteerde ondermarge van de pagina.

Stellingen bij het proefschrift:

'Swimming and muscle structure in fish' van Igor L.Y. Spierts, Wageningen, 28 mei 1999.

Pijn in mijn hart...

Mijn eerste leermeester in het spiergebeuren,
zal mijn verdere leven zeker inkleuren.
Al die discussies en hete vuren,
ik zou nú willen dat ze voor eeuwig konden duren.
Rie je hebt altijd veel voor mij betekend,
en wat er gebeurt, daar had ik nooit op gerekend.

Ik wou dat ik de klok terug kon draaien,
en nog eens ouderwets met jou kon kraaien,
om het hoogste woord in die ene ruimte,
en nú wou ik dat ik geen enkel gesprek verzuimde.
Wat er ook zal gebeuren,
ik hoop dat ik je af en toe nog op kan fleuren.

Met mijn eigenwijsheid die jij toch óók hebt,
hoop ik dat mijn band met jou nooit meer verlept.
Rie bedankt voor alles wat je me tot nog toe hebt gegeven,
kennis, aandacht, ruzies en de ervaringen uit jou leven.
Ik heb diep respect voor jouw enorme kracht,
en dat je ondanks 't gebeuren van het afgelopen jaar toch áltijd weer lacht.

Rie ik heb je erg leren waarderen,
en dit alles zal ik maar heel moeilijk kunnen verteren.
Maar één ding staat in elk geval voorop,
jouw aanwezigheid verlicht váák mijn (soms) duistere kop.
Voor de toekomst ben ik niet bang,
al is de weg vóór ons toch nog erg lang.

Igor

voor Rie

CONTENTS/INHOUD

Chapter 1	General introduction.....	7
Chapter 2	Swimming. To be published in a German textbook on fish for students (as one chapter): J.W.M. Osse and I.L.Y. Spierts (1999).....	25
Chapter 3	Muscle growth and swimming in larvae of <i>Clarias gariepinus</i> (Burchell). Published: H.A. Akster, J.A.J. Verreth, I.L.Y. Spierts, T. Berbner, M. Schmidbauer and J.W.M. Osse (1995) <i>ICES Marine Science Symposia</i> 201: 45-50.....	79
Chapter 4	Local differences in myotendinous junctions in axial muscle fibres of carp (<i>Cyprinus carpio</i> L.). Published: I.L.Y. Spierts, H.A. Akster, I.H.C. Vos and J.W.M. Osse (1996). <i>Journal of Experimental Biology</i> 199: 825-833.....	89
Chapter 5	Expression of titin isoforms in red and white muscle fibres of carp (<i>Cyprinus carpio</i> L.) exposed to different sarcomere strains during swimming. Published: I.L.Y. Spierts, H.A. Akster and H.L. Granzier (1997). <i>Journal of Comparative Physiology B</i> 167: 543-551.....	107
Chapter 6	Kinematics and muscle dynamics of C- and S-starts of carp (<i>Cyprinus carpio</i> L.). Published: I.L.Y. Spierts and J.L. van Leeuwen (1999). <i>Journal of Experimental Biology</i> 202 (4): 393-406.....	125
Chapter 7	How carp (<i>Cyprinus carpio</i> L.) activate the trunk muscles during C- and S-starts. In preparation: I.L.Y. Spierts, J.L. van Leeuwen, A. Terlouw and J.W.M. Osse.....	153
Chapter 8	Expression of titin isoforms during the ontogeny of carp (<i>Cyprinus carpio</i> L.) in relation to fast swimming. In preparation: I.L.Y. Spierts.....	175
Summary/ Samenvatting	Swimming and muscle structure in fish. Submitted: I.L.Y. Spierts (1999). <i>Netherlands Journal of Zoology</i>	193
References.....		203
Dankwoord.....		217
Curriculum vitae.....		219
List of publications.....		220

1

General introduction

Igor L.Y. Spierts

Experimental Zoology Group, Wageningen Institute of Animal Sciences (WIAS), Wageningen
Agricultural University, P.O. Box 338, 6700 AH Wageningen;
The Netherlands

CONTENTS

- 1.1. Outline of this thesis**
- 1.2. Chapter 2: Swimming**
- 1.3. Chapter 3: Muscle growth and swimming of larval *Clarias gariepinus* (Burchell)**
- 1.4. Chapter 4: Differences in force transmission and in myotendinous junctions in axial muscle of carp (*Cyprinus carpio* L.)**
- 1.5. Chapter 5: The relation between differences in sarcomere strain in swimming carp and the expression of titin isoforms**
- 1.6. Chapter 6: Kinematics and muscle dynamics of C- and S-starts of adult carp**
- 1.7. Chapter 7: Muscle performance during C- and S-starts of adult carp**
- 1.8. Chapter 8: Expression of titin isoforms during the ontogeny of carp in relation to fast swimming**
- 1.9. Scientific significance**
- 1.10. Relevance for society**

1.1. OUTLINE OF THIS THESIS

The scope of the present thesis is to determine how the structure of axial muscles of fish is adapted to the functional, sometimes contrasting, demands of different modes of swimming. Changes of the muscular system with fish size and age belong to this question. Studies of larval muscle development, of myotendinous junctions (MTJs, the connections between muscle fibres and tendons), of the giant elastic muscle protein titin and of strains in sarcomeres during continuous and fast swimming in larval and adult carp were performed. Only a few highlights of the obtained results can be mentioned.

During swimming posterior muscle fibres of adult carp have a longer phase of eccentric activity (active while being stretched) than anterior fibres and will therefore develop greater forces. Posterior and red fibres are subjected to larger sarcomere strains during continuous swimming and have special adaptations to these functional demands: (1) stronger MTJs, and (2) larger titin isoforms. A quantitative electron-microscopical study showed that a linear correlation exists between the surface area of the MTJ (measure for the strength of the joint) and the size and duration of the load on a junction. Fibres with larger surface areas consequently can bear larger loads during swimming. Gel-electrophoresis and micro-mechanical experiments showed that fibres with larger titin isoforms require less passive tension for the same sarcomere strain. As larval muscle fibres possessed smaller titins than that of any adult muscle fibre the titin isoform changes during ontogeny. The shorter titin isoform is thought to help restricting form changes of fast swimming carp larvae and to increase the elastic contribution to the tail beat.

The largest loads are imposed on the muscle system during very fast escape or attack movements. The ultrastructure and protein composition is very well fitted to perform such tasks. This study corroborates the idea that (small) differences in muscle function during swimming, turning and escaping can be used to predict and possibly explain structural differences between various types of muscles in fish of different age and size.

1.2. CHAPTER 2: SWIMMING

This chapter will present an overview of fish swimming in general. As the present thesis is about fish swimming this co-production seems to be a proper introduction. A similar approach was chosen in an earlier book about fish for biology students (in Dutch). The text is intended to be published as one chapter in a German monograph of fish, designed as a textbook for biology students. As the second author I importantly updated previous paragraphs and added new elements and considerations of fish muscle. Fish swimming is quite a large field of study and many aspects require attention. An overview is presented in which the fish body plan e.g. skeleton, skin and other supporting tissues are introduced together with the different types of muscle tissue and their specific features. Thereafter the paired and unpaired fins and their specific roles in diverse swimming modes (e.g. slow continuous swimming, intermediate swimming and fast-starts) will be explained, as well as buoyancy and swimbladders. Hydrodynamic interactions between fish and water, the influence of fish size and speed on these interactions and the energetic costs are dealt with. Some generally distinguished

swimming modes are explained with respect to the overcoming of drag and the thrust creation as well as in relation with ecological and feeding demands. The last five paragraphs of this chapter are devoted to the form of the tail fin, energetics, swimming adaptations in different fish species and larval swimming. This chapter is useful as a general reference about swimming required to understand subsequent more specific chapters.

1.3. CHAPTER 3: MUSCLE GROWTH AND SWIMMING OF LARVAL *CLARIAS GARIEPINUS* (BURCHELL)

This study was conducted to get more insight in the characteristics of the behaviour of the anguilliform swimming *Clarias gariepinus* larvae compared to the carangiform swimming carp (*Cyprinus carpio* L.). The ultimate aim was to determine the effects of these different swimming modes on the forces acting upon the larval body and hence on muscle development. The influence of different diets (fast-growing larvae fed with *Artemia* and slow-growing larvae fed with dry food and larvae that were starved for 5 days) on muscle growth and development of larvae was investigated because larval muscles are in many aspects (e.g. aerobic or anaerobic metabolism, type of myosin ATPase) very different from adult muscles. The relation between muscle development and swimming was investigated in *Artemia*-fed *Clarias* larvae.

In the early developmental stages (approximately 3.5-14 mm total length, *TL*) changes take place, both hydrodynamical and physiological. *Clarias* larvae hatch 24 hours after fertilisation with a total length of approximately 3.5-4 mm. At that time the larvae showed 'resistive swimming' to overcome the dominating viscous forces in that particular Reynolds-regime. The yolk-sac larvae had an inner 'larval white' muscle mass surrounded by a superficial red monolayer. Both white and red muscle had an aerobic metabolism at that time, although their myosin ATPase differed. The larvae aggregated in a corner of the tank, but showed almost continuously tail beat activity. At approximately 5 mm *TL* (1 day after hatching) the larvae showed almost continuously stationary activity, interrupted by slow swimming movements (2.4 ± 0.9 bodylength s^{-1} , $BL s^{-1}$). These activities are very likely powered by superficial red muscles. When stimulated by touching them with a probe these larvae reached very high velocities of up to approximately $17 BL s^{-1}$, most probably powered by the inner 'larval white' muscles. Three days after hatching the yolk-sac was absorbed and the *Clarias* larvae (8.5 mm *TL*) were much less active (the continuous activity was lacking). At 11 mm *TL* (larvae fed on *Artemia* for 3 days) the larvae developed the adult pattern of muscle fibre type distribution with different metabolic and functional properties between red (aerobic) fibres and white (anaerobic) fibres. The larvae now showed 'reactive' swimming in the inertial Reynolds-regime ($Re \geq 500$). The changes in muscle structure probably occurred in relation to size dependent differences in swimming and in relation to development of gills and the decrease in relative importance of the red fibre zone.

Larvae fed on *Artemia* for 3 days were similar in total length to larvae fed for 5 days with dry food. This similarity in total length was accompanied by a similarity in white fibre number and size. The development of the red muscle zone was also similar in both treatment groups and the monolayer of red fibres was acquiring additional fibres along the horizontal septum, resulting in a double layer of

red fibres at this location. In the inner white muscle zone of growing larvae, fibre number and diameter increased linearly with increasing total length of the larvae. This shows that muscles of free-swimming *Clarias* larvae grow by both the addition of fibres (hyperplasia) as well as by the growth of existing fibres (hypertrophy). The similarities in muscle development between the two treatment groups indicated that inadequate feeding of larvae with dry food (Verreth and den Bieman, 1987) does influence the growth rate and survival, but does not influence the development of muscle growth (fibre type distribution, fibre numbers and fibre size). The latter is related to larval length rather than to larval age, which is in contrast to data on gut development in *Clarias* larvae (Verreth *et al.*, 1992). The growth potential of muscles is not likely to be affected by inadequate feeding. This seems in itself an important adaptation as food distribution is quite unpredictable, especially in the marine environment. The relation between muscle growth and larval length is not unexpected, since the Reynolds number is length- and speed-dependent (Batty, 1984; Osse, 1990).

1.4. CHAPTER 4: DIFFERENCES IN FORCE TRANSMISSION AND IN MYOTENDINOUS JUNCTIONS IN AXIAL MUSCLE OF CARP (*CYPRINUS CARPIO* L.)

The results of the previous chapter showed that different size classes of fish had various swimming modes, due to different kinds of forces acting on the swimming fish body. Force differences, however, are not only related to different swimming modes, but also differ internally, locally along the body axis of a swimming fish. The myotendinous junction (MTJ), the connection between the actual muscle fibre and the tendon, represents the structure that actually transmits the forces necessary to swim. At electron-microscopical level the membrane at MTJs (called the interfacial membrane or junctional sarcolemma) shows extensive folding, resulting in a great increase of membrane area. Differences in the amount of force transmitted at the MTJ (local differences due to e.g. the type of swimming mode and the form of the fish's body), contraction velocity and frequency of use are expected to be expressed in the structural features of this joint.

Computer models (van Leeuwen *et al.*, 1990; van Leeuwen, 1995) based on electromyographic and motion analysis of carp (*Cyprinus carpio* L.) predicted that, during continuous and intermittent swimming, muscle fibres in the tail region (together with the connective tissue) would play an important role in the transmission of force produced by more anterior muscle fibres. The hypothesis is that, due to the shape of a fish's body, the forces produced at the biggest cross-sectional area of muscle tissue (typically found at the centre of the body cavity) must be transmitted to the tail fin by a decreasing cross-sectional area of muscle in posterior direction. Therefore posteriorly MTJs must be stronger. Furthermore, posterior axial muscle fibres of swimming carp experience a longer phase of eccentric activity (muscle activity during lengthening) than the more anterior fibres, resulting in a negative contraction velocity and work output (van Leeuwen *et al.*, 1990; van Leeuwen, 1995). As a result these posterior fibres will develop greater forces than the anterior fibres, an expectation that was confirmed by simulation experiments of Davies *et al.* (1995).

We therefore studied the membrane amplification at MTJs (due to characteristic foldings) of anterior and posterior red and white axial muscle fibres of adult carp, using electron-microscopy, morphometric sampling procedures, stereology and an appropriate correction required for the anisotropy of the tissue (degree of orientation). We compared the interfacial ratio, the ratio between the area of the junctional sarcolemma and the cross-sectional fibre area, of these muscle fibres. This ratio differed significantly between the investigated groups, with red fibres and posterior fibres having the larger ratios. The higher interfacial ratio of posterior fibres compared to anterior ones is in accordance with the hypothesis mentioned above.

Mechanical experiments on MTJs of single muscle fibres of frog semitendinosus (*Rana pipiens*) showed that failure of the MTJ was independent of strain and of strain rate over a biological relevant range (Tidball and Chan, 1989). Although red fibres are exposed to larger sarcomere strain fluctuations during continuous swimming than white fibres (due to their more lateral position) we therefore do not expect that the larger membrane amplification at the MTJs of red fibres found in this study is attributed to these differences in strain. It is however unknown in what way particular strains invariably mean a certain amount of stress on MTJs. Red fibres are active at lower tail beat frequencies (longer cycle times) than white fibres and for longer periods of time, resulting in a longer duration of the load on the junction of red fibres. Tidball and Daniel (1986) proposed that the degree of membrane amplification at MTJs not only depends on the magnitude but also on the duration of load on the junction. Curtis (1961) and Rand (1964) showed that the mechanical behaviour of cell membranes is dependent on loading time. Cells can survive a certain shear load (caused by applying either a large load for a short time or a small load for a longer time) by reducing the stress on the membrane through an amplification of the membrane area. It was therefore suggested that the larger membrane amplification at the MTJs of carp red muscle fibres may be related to the longer duration of the load on the junction in this fibre type.

It is more likely that the large strain fluctuations in the different muscle fibres during swimming (Rome and Sosnicki, 1991) will impose high demands on the series elastic elements within the sarcomere unit of these fibres, such as titin filaments (Wang *et al.*, 1991). This may be reflected in the type and structure of these elements as different isoforms of titin seem to exist (Wang *et al.*, 1991; Granzier and Wang, 1993a,b). An investigation of possible differences in the type and structure of this huge elastic muscle protein in different muscle fibre types and at different locations along the body axis is therefore the main goal of my next study.

1.5. CHAPTER 5: THE RELATION BETWEEN DIFFERENCES IN SARCOMERE STRAIN IN SWIMMING CARP AND THE EXPRESSION OF TITIN ISOFORMS

Although a relationship between the MTJ of a muscle fibre and the amount of strain this fibre is exposed to is not likely (Tidball and Chan, 1989), we do expect a relation between the sarcomere strain a fibre is exposed to during cyclic swimming and the size of the giant elastic muscle protein titin. Titin is also known as connectin and is a giant striated-muscle specific protein that spans the

distance between the Z- and M-lines of the sarcomere (Wang, 1985; Maruyama, 1986, 1994; Trinick, 1991). Our understanding of the molecular basis of muscle elasticity has made good progress as a result of the discovery of this muscle protein. The elastic segment of the titin molecule is situated in the I-band and consists of series-coupled immunoglobulin (Ig)-like domains, each containing approximately 100 residues, and an unique domain rich in proline (P), glutamate (E), lysine (K) and valine (V), referred to as the PEVK domain (Labeit and Kolmerer, 1995). This region is thought to function as a molecular spring that maintains the central position of the thick filaments in contracting sarcomeres. Titin is also held responsible for developing passive tension upon stretch of the sarcomere (Horowitz *et al.*, 1986; Fürst *et al.*, 1988; Wang *et al.*, 1991, 1993; Granzier *et al.*, 1996). As a result of differential splicing in the elastic region of titin, different muscle types express size variants of titin that differ in molecular mass (Labeit and Kolmerer, 1995).

During a tail beat of a swimming fish elastic energy is stored in the stretched muscle fibres at the convex side of the body, which is produced by the muscle fibres at the concave side. This investment might, depending on the stress-strain curve of the involved elastic material, serve two functions: 1) it prevents a disorganisation of sarcomere construction in a stretched condition, and 2) it enlarges the force at the moment the tail changes its direction of motion. In the latter case the restriction of sarcomere stretch beyond the thick-thin filament overlapping zone is of primary importance. Muscle fibres exposed to larger strains during cyclic swimming of adult carp (with relatively low total energetic costs) might be better off with a larger titin isoform, as the energy loss during cyclic loading of these muscle fibres is expected to be lower (less hysteresis) compared to a situation when a shorter isoform is concerned. It might however be clear that the exact shapes of the stress-strain curves of muscle fibres with different titin isoforms determine the best choice in situations where the biological strain ranges of various swimming modes are known. To investigate possible relations between differences in titin isoforms and the strains different muscle fibres are exposed to during cyclic swimming we conducted the research presented in this chapter.

We tried to elucidate the relation between the occurrence of titin isoforms and the functional properties of different fibre types by investigating the presence of different titin isoforms in red and white anterior and posterior fibres of the axial muscles of carp. Gel-electrophoresis of single fibres revealed that red fibres had larger titin isoforms (higher molecular mass) than white fibres. When comparing anterior and posterior fibres we also found that the molecular mass of titin was larger in posterior fibres than in anterior, for both red and white axial muscle fibres. So, within one fibre type different titin isoforms are expressed, depending on their location along the body axis. These different locations also are subjected to different functional demands. In earlier studies a positive correlation between the size of the expressed titin isoform and the passive tension-sarcomere length relationship of rabbit muscle fibres was found (Wang *et al.*, 1991; Horowitz, 1992). With similar hypotheses we determined the contribution of titin to passive tension and stiffness of red anterior and posterior carp muscle fibres. The relations between sarcomere length and passive tension and passive stiffness were determined using single skinned muscle fibres. In order to study the forces developed by the intermediate filament system we selectively removed the actin and myosin filaments (KCl/KI treatment). Measurements were made before and after extracting thin and thick filaments. The passive tension-sarcomere length curve of titin increased steeper in red anterior fibres than in red posterior

fibres and the curve reached a plateau at a shorter sarcomere length. Thus, the smaller titin isoform of anterior fibres results in more passive tension and stiffness for a given sarcomere strain.

The longitudinal oriented intermediate filaments in skeletal muscle are thought to function as a safety device, preventing damaged sarcomeres from being over-stretched and torn apart during activation by adjacent undamaged sarcomeres (Wang *et al.*, 1993). Torn sarcomeres would be disastrous as the severed myofibrils would highly shorten during contraction, ruling out any simple repair of the damaged areas. Are these mechanisms comparable in fish and in terrestrial vertebrates? Intermediate filaments of carp muscle developed high levels of tension and stiffness in both anterior and posterior fibres, compared to mammalian skeletal muscle (e.g. rabbit skeletal muscle). These findings imply that sarcomeres of carp fibres are even more vulnerable to such damage than those of rabbit skeletal muscle. This may very well be related to the phase of eccentric activation that occurs during the rhythmic strain cycles of the swimming movements. During this phase of eccentric activation, which is longer in posterior than in anterior carp fibres, high demands are imposed on the stress-bearing structures (van Leeuwen *et al.*, 1990; van Leeuwen, 1995; Wardle *et al.*, 1995; Spierts *et al.*, 1996).

The results of this study showed that in carp exactly those fibres that experienced the largest sarcomere strains during cyclic and intermittent swimming (red fibres and posterior fibres) possessed the largest titin isoforms, allowing these fibres to attain large strain amplitudes with relatively low tensions. We therefore suggest that sarcomere strain is one of the functional parameters that modulates the expression of different titin isoforms in axial muscle fibres of carp, although the causal pathways are still unknown. The results also showed that red posterior fibres are 'equipped' with an intermediate filament system that contributed more to passive tension at a certain sarcomere length compared to red anterior fibres. As in the previous study it was shown that posterior fibres transmit larger forces (and possess stronger MTJs), apparently even detailed aspects of functional demands seem to be reflected in structural features of muscle fibres. Although the above hypothesised relation between the molecular size of titin and sarcomere strain is indeed confirmed by this study when considering cyclic swimming of carp, it is still very unsure whether during really extreme swimming movements, such as C- and S-shaped escape responses, comparable sarcomere strain ranges occur in red and white anterior and posterior muscle fibres. Energetic considerations during such fast swimming modes probably are no longer of importance for the size of titin in muscle fibres at different positions along the body axis, in view of the extreme consequences of failure for survival. To investigate this aspect we performed our next study on the kinematics and muscle dynamics of C- and S-starts of adult carp.

1.6. CHAPTER 6: KINEMATICS AND MUSCLE DYNAMICS OF C- AND S-STARTS OF ADULT CARP

Many studies were devoted to the sarcomere strain in different muscle fibre types during cyclic swimming, but little is known about sarcomere strain during fast-starts. In an effort to understand the sarcomere structure in different strain situations we studied that problem. In the previous study we

hypothesised that a correlation exists between the strain a muscle fibre is subjected to during cyclic swimming and the size of the elastic muscle protein titin (larger strains \longleftrightarrow larger titin isoform). Energetic costs of swimming were hypothesised to be of importance for this possible structure-function relationship. During fast-starts of adult carp however, energetic costs are not expected to be a factor of importance in the process of natural selection of the molecular structure of titin. As no *in vivo* data were available on sarcomere strain of different carp muscle fibres at different locations along the body axis during fast-starts we decided to measure them.

Fast-starts of fish are characterised by unsteady manoeuvres and used to avoid predators and to capture prey. Two major types of fast-start swimming have been described for subcarangiform swimming (in teleosts) (Hertel, 1966; Weihs, 1973; Eaton *et al.*, 1977; Webb, 1975, 1976, 1978a,b; Webb and Blake, 1985). Either the body bends into a C-shape, usually occurring during an escape or startle response (Weihs, 1973; Webb, 1978a; Frith and Blake, 1991) or the body adapts an S-shape (Webb, 1976; Harper and Blake, 1990). During an S-shaped predatory attack the posterior part of the body curves much more than the anterior part (Hoogland *et al.*, 1956) and only a limited angle of turn is present. During an S-shaped escape response on the contrary considerable angles of turn are found, although smaller than in C-starts. C-starts are considered to be mediated by the Mauthner system (among others the giant cells in the hindbrain, Eaton *et al.*, 1977; Kimmel *et al.*, 1980), whereas little is known about the mechanisms controlling S-starts.

In the present study we analysed body curvature, acceleration and muscle strain during fast-starts of carp. The fast-starts investigated here were reactions of flight and escape to a certain stimulus. C- and S-starts were filmed at 200 frames s^{-1} at 23 °C. Curvatures and accelerations of mid-body axes were calculated from digitised outlines. Maximum accelerations at 0.3 *FL* (fork length, close to the centre of gravity) from the snout were 54 $m s^{-2}$ for C-starts and 40 $m s^{-2}$ for S-starts. For C-starts the total angle of turn was approximately 150°, whereas in escape S-starts this angle was 70°. This is significantly larger than for predatory S-starts in other species. Calculated sarcomere strains of axial muscle fibres at 0.4 and 0.8 *FL* revealed that during C-starts white muscle fibres were exposed to maximum sarcomere strains of up to approximately 16 %, and posterior fibres had similar strains as anterior fibres (red: 27 %; white: 16 %). During S-starts, however, maximum strain in anterior fibres (red: 39 %; white: 24 %) was more than twice that of posterior fibres (red: 17 %; white: 10 %). The question rises why a carp responds with a C-start in one situation and with an S-start in other situations.

In a C-start, the fish can make a large angle of turn directed away from the stimulus by bending its tail strongly and thereby producing a large thrust. The maximum curvature of the anterior trunk during escape S-starts of carp is strikingly large and is associated with fairly big turning angles. Based on these observations, it is expected that the final 'swim away' direction can be determined least accurately in C-starts and most accurately in predation S-starts (where precision of aiming is of vital importance). Escape S-starts seem to have an intermediate position in this respect. The largest loading of titin is likely to occur in red anterior fibres (at approximately 0.4 *FL*) during these S-starts. During cyclic and intermittent swimming, red posterior fibres experience the largest strains, fibres that also possessed the largest titin isoform and the lowest passive stiffness. This allows these fibres to attain large strain amplitudes with relatively low passive tensions. Further research is required to quantify

the energetic consequences as well as the mathematical relation between strain and tension in sarcomeres with different isoforms of titin.

As precise knowledge of the timing of muscle performance during fast-starts is of the utmost importance to understand how such movements are generated, the differences in electromyograms (EMG) between the various types of fast-starts were investigated in the next study.

1.7. CHAPTER 7: MUSCLE PERFORMANCE DURING C- AND S-STARTS OF ADULT CARP

In the previous study the kinematics and muscle dynamics of C- and S-starts were investigated to clarify the bending patterns during these escape responses. With these bending patterns (e.g. lateral curvature of the fish body) muscle strains were calculated and subsequently used to interpret structural differentiation of the system. In addition to this previous study on kinematics and muscle dynamics of fast-starts we needed important extra information concerning muscle activities during the fast-starts.

In this study we therefore examined simultaneously sampled movements, strain data and EMGs during fast-starts of adult carp. Fast-starts were filmed at 500 frames s^{-1} at 23 °C. We measured and from there calculated lateral body curvatures and calculate strain waves of anterior (0.4 *FL*) and posterior (0.8 *FL*) red and white axial muscle fibres during C- and S-starts. The recruitment patterns of these different muscle fibres were recorded continuously with a differentially electromyographic technique and synchronised with the strain variations during the starts. These combined data were used to analyse if and when red and white muscle fibres, at different positions along the trunk, were active during fast-starts and how these activities produced the actual kinematic profiles of C- and S-starts. We hypothesised that during C-starts both anterior and posterior fibres started their activity simultaneously as it is considered that C-starts are mediated by the (extremely fast) Mauthner system. In this way the fish accomplishes an initial C-shape as quickly as possible. S-starts are characterised by successive opposite S-shapes, making simultaneous activations of anterior and posterior fibres not necessary. These latter starts are controlled by a still unknown neuronal mechanism. The comparison of both strain- and EMG-data of C-starts with those of S-starts may therefore reveal some interesting differences.

A recurrent finding for vertebrate locomotion is that as power output and speed of movement increase, faster fibres are sequentially recruited in addition to (but not at the exclusion of) slower fibre types (Grillner, 1981; Armstrong, 1981). Jayne and Lauder (1993, 1994) found in bluegill sunfish (*Lepomis macrochirus*) that both red and white fibres were utilised at high speeds. They suggested that during rapid unsteady swimming the intensity of red muscle activity decreased (although present) while the intensity of white muscle activity increased. In this view slower fibres are mainly used to power slow- and medium-speed movements, whereas both slow and fast fibres are used during fast movements (Jayne and Lauder, 1994). This 'additive' model of muscle fibre function could also be applied to all fast-starts we investigated, as we found only red muscle activity during continuous swimming whereas red and white muscle activity occurred simultaneously during fast-starts. As red

muscle were active during all fast-starts investigated we believe that these muscle do contribute to force enhancement.

Our results also showed that red and white muscle activity periods at a given longitudinal location needed not to be necessarily synchronous and could be uncoupled (more or less), depending on the type of escape response. In our study this uncoupling took place during escape S-starts of carp and we suggest that in this way mechanically sub-optimal patterns of force generation can be avoided. During C-starts, on the contrary, the red and white muscle activity periods were coupled, possibly because it is incompatible with Mauthner-initiated starts. The antero-posterior delay in EMG onset was virtually absent during the first tail beat of C-starts (less than 1 ms), which must be due to very high conduction velocities of the Mauthner system, thus making a very fast escape possible. During S-starts this delay was clearly present which might be connected to the different neural patterns controlling these starts. In S-starts and in stage 1 of C-starts the EMGs generally showed posterior propagation, resulting in longer durations of posterior EMGs. Carp were at any time able to override continuous swimming motor patterns with escape S-starts or C-starts.

In the next study we concentrated on larval fast swimming and measured sarcomere strain ranges of different muscle fibres. The differences in swimming behaviour between carp larvae and adults led us to investigate whether these differences are accompanied by differences in titin isoforms. We therefore decided to determine the size of carp larval muscle titin using gel-electrophoresis and compared this with the strain data.

1.8. CHAPTER 8: EXPRESSION OF TITIN ISOFORMS DURING THE ONTOGENY OF CARP IN RELATION TO FAST SWIMMING

Larval swimming is very different from adult swimming due to a more viscous environment for fish larvae where friction can not be neglected. In addition to chapter 5, where we already related fish swimming to the expression of titin isoforms in adult carp muscle, in this study I tried to clarify the titin isoform of these small larvae and compared it with the sarcomere strain ranges of different muscle fibre types.

Teleost larvae often hatch at quite small lengths (Moser, 1996). As in most cases the larval body form differs substantially from their juvenile form, a metamorphosis must occur during larval development. Several functional systems are incomplete for adult functioning but adjusted for larval needs at hatching (Osse and van den Boogaart, 1997). The larvae start feeding on external energy sources soon after hatching because eggs mostly have little yolk, especially in pelagic fish. Rapid growth of organs and systems is observed during the early larval period.

In growing carp larvae the swimming behaviour changes remarkably from more anguilliform towards more carangiform swimming (Osse, 1990). Young carp larvae swam with a large amplitude over their entire body. Part of this swimming behaviour are attempts to hold station in flowing water by undulatory movements of the body and the finfolds. The burst-like mode of swimming found in older fish also occurs here. Fish larvae are subjected to low Reynolds-number regimes ($Re < 500$)

during fast swimming and therefore require special features to overcome effects of friction. Possibly, the viscous environment favours an anguilliform type of swimming of the larvae. Axial muscle of fish larvae differ from those of adult fish. Yolk-sac larvae have an inner 'larval white' muscle mass surrounded by a superficial red monolayer. During the free-swimming larval stage the adult patterns of muscle fibre type distribution and the differences in metabolism between the red aerobic fibres and the white anaerobic fibres develop (Hinterleitner *et al.*, 1987). It is suggested that red muscle fibres in larvae are mainly involved in the uptake and transfer of oxygen until the gills are fully developed (see chapter 3 of this thesis and El-Fiky *et al.*, 1987; Hinterleitner *et al.*, 1987). So regarding the early differentiation of muscle the question rises: how exactly are the inner 'larval white' muscles able to generate enough power to overcome the effects of friction and reach velocities over $20 BL s^{-1}$?

In chapter 5 we suggested a correlation between the function of different muscle fibres of carp and the size (and other properties) of the giant elastic muscle protein titin. My hypothesis is that in larvae shorter titin isoforms (requiring larger stress for the same strain) will be found to restrict the form changes of the swimming larvae and to increase the elastic contribution to the tail beat. Such molecules might also increase the resonant frequency of the beating tail and thereby facilitate the required high frequency for swimming in a low Reynolds-regime. In this study high-speed motion films ($500 \text{ frames s}^{-1}$) were made to determine sarcomere length changes (muscle strain) during fast swimming at two positions along the body, 0.4 and 0.8 *TL* (measured from the tip of the snout), in larval red and white axial muscle fibres of carp (6.5-8 mm *TL*). Gel-electrophoresis was used to investigate the presence of titin isoforms in carp larvae and a comparison with titin isoforms of adult carp was made. Gel-electrophoresis revealed that the titin isoform was larger in all adult muscle fibres than in larval muscle. Apparently the molecular structure of titin changed in the course of ontogeny.

The strains inner 'larval white' muscle fibres are exposed to during fast swimming are expected to be considerable, as initially the inner 'larval white' muscle fibres run almost parallel to the body axis without the complex three-dimensional folding pattern, as seen in adult white muscle. One limiting factor for very high strains is that these inner 'larval muscle' fibres are situated very close to the body axis, compared to the position of adult muscle fibres. This fact also accounts for the small differences in the mean maximum sarcomere strain that were found between red and white and between anterior and posterior fibres of carp larvae (all approximately 20 %), a difference that becomes however larger in older fish. Although the mean maximum sarcomere strains for fast swimming carp larvae were indeed considerable, they were not extremely high compared to mean maximum strains of adult muscle fibres during fast-starts. As superficial red fibres of Cyprinid larvae are mainly used as a respiratory organ (see above), larval swimming behaviour is mainly powered by the inner 'larval white' fibres (El-Fiky *et al.*, 1987). But how exactly are these inner 'larval white' fibres able to generate enough power to overcome the friction effects and reach maximum sarcomere strains of approximately 20 % during fast swimming and velocities of over $20 \text{ bodylength s}^{-1}$? The smaller a titin isoform, the more passive tension is required to stretch the muscle fibre to a certain extend. During fast swimming the power required for the considerable passive pre-stretching of fibres at the convex side (partly stored as elastic energy) of the body axis is generated by the activity of fibres at the concave side. Fish larvae may increase the elastic contribution to the tail beat during swimming by elastic energy storage in their titin isoform during the initial bending that is subsequently released in

the following bending.

1.9. SCIENTIFIC SIGNIFICANCE

This research provided new insights into the properties of fish axial muscle and their relations with the mechanical demands imposed on these structures during swimming. As we know much less of fish locomotion and the involved material properties than of locomotion of e.g. tetrapods and especially mammals and birds, this research was urgently needed. Fish are very different in their muscular mechanical systems than tetrapods because gravity is nearly absent in their natural habitat, the water. This also enables fish to easily use the third dimension. How such environmental features are reflected in micro- and macro-design of fish muscle-skeletal systems is urgently in need of more knowledge. The current knowledge of the system of segmental body muscles, the shape and size of myotomes and myosepts and their exact role in the generation of body curvature and power necessary for various swimming modes is still very incomplete. This thesis however revealed new aspects of fish muscle construction and functioning during swimming and increased the knowledge of the muscular system in general.

New views on molecular structure of muscle, e.g. the giant elastic muscle protein titin, and the influence of ontogeny on these structures are presented. Lots of work is done in the field of molecular biology. Direct links to organismic biology and functioning of animals and their systems however are still not made very often. In this thesis we tried to relate the molecular approach and the more organismic approach of biological research (including behavioural aspects like escape swimming etc.) by directly connecting structural features of organisms to functional properties of those materials and of the animals in general. Although the gap between the two fields of studies is sometimes big, we made some successful connections and discovered interesting, new, fields of muscle research.

1.10. RELEVANCE FOR SOCIETY

The relevance of this thesis for our society is threefold and at least important for two fields of practice.

In the first place there is the relevance of fundamental science in general for a western society like The Netherlands. It is quite essential for a university to maintain a certain quality standard concerning its research and its educational courses. In approximately the last 10 years the financial cuts on science in general, and fundamental science in particular, endangered the quality of science and education. For the Agricultural University of Wageningen for example a governmental cut of fl 24.403.000,- has to be realised from the year 2002 on. Also within the university itself financial problems, resulting from trying to maintain a well balanced budget, lead to extra structural cuts. To realise their studies appropriately researchers from the Agricultural University have to compensate for these financial cuts in their research by trying to acquire substantial financial support from research institutes and industry, mainly consisting of applied research. Partly, such a switch from fundamental to applied

research does not seem to be wrong. However, when simultaneously governmental cuts continue and actually even go on deeper than before, this development becomes harmful. Applied and fundamental research ought to be practised side by side, and the equilibrium between the two certainly should not be disturbed by governmental cuts. Applied research is still, and will always be, in need of a solid base from which it can operate, and this base, partly shaped by fundamental as well as strategic research, is being reduced slowly but steadily in the last decade. The Netherland government spends far less than other European nations to fundamental and strategic research. Dutch research is consequently quickly losing its lead to other countries and for employment and industry science is all important. When the Netherland government does not soon recognise the seriousness of the situation, negative effects of this ongoing process are unavoidable. Thus I am convinced that the fundamental and strategic research, as described in this particular thesis, is of major importance for society as a whole.

In the second place it is important to gain insight into changes that take place in muscle after an animal has been killed, muscle that is used for consumption. In industrial preparation of reared smoked salmon occasionally problems occur because of a process called 'gaping': the post-mortem deterioration of the connection between muscles and tendons (myotendinous junctions) throughout muscles. The phenomenon causes great loss of value of the particular product. This particular problem only occurs in reared fish and not in fish captured from their natural habitat. As reared fish probably swim much less than their wild colleagues it is thought that training of fish in reared conditions might improve the muscle quality. It is important to find possible solutions for such practical problems. Therefore a good start is to study to the myotendinous junctions itself (connections between muscle fibres and collagen fibres that transmit forces) and clarify the factors influencing these junctions. With such knowledge effects of different rearing conditions of fish, e.g. immobilised or trained fish, on their muscles can be investigated more fruitful. In this thesis the structure of myotendinous junctions in red and white muscle are investigated, including some factors that might be of influence on the strength of these junctions. With both scientific aims and the aim to provide useful information I call this research strategic.

Finally, knowledge of factors causing various kinds of muscle damage in general is still very poor. Myotendinous junctions appear to be the 'weak chain', both *in vivo* (e.g. during accidents) as well as *in vitro* (e.g. the above mentioned process of 'gaping') in transmission of forces. Next to the myotendinous junctions mentioned above elastic elements in muscle tissue are also important. Detailed knowledge of the effects of magnitude, duration and frequency of loads on various elements of the muscular system during different swimming modes of fish (e.g. continuous swimming, kick-and-glide swimming and escape fast-starts) is still very incomplete. One of the important structural elements in sarcomeres of striated muscle are the force-bearing structures, like e.g. myotendinous junctions and intermediate filaments (small cyto-skeletal bundles of short transverse filaments and continuous longitudinal filaments). Other important constituents of muscle are the series elastic elements within the sarcomere unit, such as titin filaments (giant elastic muscle proteins that act as dual springs and maintain the central position of thick filaments in contracting sarcomeres). At this moment important research efforts are made to clarify the structural and functional aspects of this molecule, especially in heart muscle. Here the principle of 'unity' in biology helps to show the

importance of animal research to serve as a source for data in treating diseases in human systems. Studying these titin isoforms in various muscles of swimming fish of different age and size as performed in this thesis, in relation to the functions of these muscles, contributes to this knowledge. Muscle damages that may happen require increased knowledge to treat them. Increased insight into the effects of different functional demands during swimming of fish is important. This thesis contributes to the above mentioned problems, elucidating structural features and their adaptations to specific functional demands in swimming fish.

REFERENCES

- ARMSTRONG, R.B. (1981). Recruitment of muscles and fibres within muscles in running animals. *Symp. Zool. Soc. Lond.* **48**, 289-304.
- BATTY, R.S. (1984). Development of swimming movements and musculature of larval herring (*Clupea harengus*). *J. Exp. Biol.* **110**, 217-229.
- CURTIS, A.S.G. (1961). Timing mechanics in the specific adhesion of cells. *Exp. Cell Res.* **8**, S107-S122.
- DAVIES, L.F., JOHNSTON, I.A. AND WAL, J.W. VAN DE (1995). Muscle fibres in rostral and caudal myotomes of the Atlantic cod (*Gadus morhua* L.) have different mechanical properties. *Physiol. Zool.* **68**, 673-697.
- EATON, R.C., BOMBARDIERE, R.A. AND MEYER, D.L. (1977). The Mauthner-initiated startle response in teleost fish. *J. Exp. Biol.* **66**, 65-85.
- EL-FIKY, N., HINTERLEITNER, S. AND WIESER, W. (1987). Differentiation of swimming muscles and gills, and development of anaerobic power in the larvae of Cyprinid fish (Pisces, Teleostei). *Zoomorph.* **107**, 126-132.
- FRITH, H.R. AND BLAKE, R.W. (1991). Mechanisms in the startle response in the northern pike, *Esox lucius*. *Can. J. Zool.* **69**, 2831-2839.
- FÜRST, D.O., OSBORNE, M., NAVE, R. AND WEBER, K. (1988). The organisation of titin filaments in the half-sarcomere revealed by monoclonal antibodies in immunoelectron microscopy: a map of ten nonrepetitive epitopes starting at the Z-line extends close to the M-line. *J. Cell. Biol.* **106**, 1563-1572.
- GRANZIER, H.L.M. AND WANG, K. (1993a). Gel electrophoresis of giant proteins: Solubilization and silver-staining of titin and nebulin from single muscle fibre segments. *Electrophoresis* **14**, 56-64.
- GRANZIER, H.L.M. AND WANG, K. (1993b). Passive tension and stiffness of vertebrate skeletal muscle and insect flight muscle: the contribution of weak crossbridges and elastic filaments. *Biophys. J.* **65**, 2141-2159.
- GRANZIER H.L.M., HELMES, M. AND TROMBITÁS, K. (1996). Nonuniform elasticity of titin in cardiac myocytes: a study using immunoelectron microscopy and cellular mechanics. *Biophys. J.* **70**, 430-442.
- GRILLNER, S. (1981). Control of locomotion in bipeds, tetrapods, and fish. In *Handbook of Physiology*, section 1, vol. II, Motor Control, part 2 (ed. V.B. Brooks), pp 1179-1236. Bethesda, MD, USA: American Physiological Society.

Chapter 1

- HARPER, D.G. AND BLAKE, R.W. (1990). Fast-start performance of rainbow trout *Salmo gairdneri* and northern pike *Esox lucius*. *J. Exp. Biol.* **150**, 321-342.
- HERTEL, H. (1966). *Structure, Form and Movement*. New York: Reinhold Publishing Corp. 251 pp.
- HINTERLEITNER, S., PLATZER, U. AND WIESER, W. (1987). Development of the activities of oxidative, glycolytic and muscle enzyme during early larval life in three families of freshwater fish. *J. Fish Biol.* **30**, 315-326.
- HOOGLAND, R. MORRIS, D. AND TINBERGEN, N. (1956). The spines of sticklebacks (*Gasterosteus* and *Pygosteus*) as a means of defence against predators (*Perca* and *Esox*). *Behaviour* **10**, 205-236.
- HOROWITS, R. (1992). Passive force generation and titin isoforms in mammalian skeletal muscle. *Biophys. J.* **61**, 392-398.
- HOROWITS, R., KEMPNER, E.S., BISHOP, M. AND PODOLSKY, R.J. (1986). A physiological role for titin and nebulin in skeletal muscle. *Nature* **323**, 160-163.
- JAYNE, B.C. AND LAUDER, G.V. (1993). Red and white muscle activity and kinematics of the escape response of the bluegill sunfish during swimming. *J. Comp. Physiol. A* **173**, 495-508.
- JAYNE, B.C. AND LAUDER, G.V. (1994). How swimming fish use slow and fast muscle fibers: implications for models of vertebrate muscle recruitment. *J. Comp. Physiol. A* **175**, 123-131.
- KIMMEL, C.B., EATON, R.C. AND POWELL, S.L. (1980). Decreased fast-start performance of zebrafish larvae lacking Mauthner neurons. *J. Comp. Physiol.* **140**, 343-351.
- LABBIT, S. AND KOLMERER, B. (1995). Titins: giant proteins in charge of muscle ultrastructure and elasticity. *Science* **270**, 293-296.
- MARUYAMA, K. (1986). Connectin an elastic filamentous protein of striated muscle. *Int. Rev. Cytol.* **104**, 81-114.
- MARUYAMA, K. (1994). Connectin, an elastic protein of striated muscle. *Biophys. Chem.* **50**, 73-85.
- MOSER, H.G. (1996). *The early stages of fishes in the California current region*. California Cooperative Oceanic Fisheries Investigations, Atlas no. 33. Kansas: Allen Press, Inc. 1505 pp.
- OSSE, J.W.M. (1990). Form changes in fish larvae in relation to changing demands of function. *Neth. J. Zool.* **40**, 362-385.
- OSSE, J.W.M. AND BOOGAART, J.G.M. VAN DEN (1997). Size of flatfish larvae at transformation, functional demands and historical constraints. *J. Sea Res.* **37**, 229-239.
- RAND, R.P. (1964). Mechanical properties of the red cell membrane. II. Viscoelastic breakdown of the membrane. *Biophys. J.* **4**, 303.
- TIDBALL, J.G. AND DANIEL, T.L. (1986). Myotendinous junctions of tonic muscle cells: structure and loading. *Cell Tiss. Res.* **245**, 315-322.
- ROME, L.C. AND SOSNICKI, A.A. (1991). Myofilament overlap in swimming carp. II. Sarcomere length changes during swimming. *Am. Physiol. Soc.* **260**, 289-296.
- SPIERTS, I.L.Y., AKSTER, H.A., VOS, I.H.C. AND OSSE, J.W.M. (1996). Local differences in myotendinous junctions in axial muscle fibres of carp (*Cyprinus carpio* L.). *J. Exp. Biol.* **199**, 825-833.
- TIDBALL, J.G. AND CHAN, M. (1989). Adhesive strength of single muscle cells to basement membrane at myotendinous junctions. *J. Appl. Physiol.* **67**, 1063-1069.
- TRINICK, J. (1991). Elastic filaments and giant proteins in muscle. *Curr. Opin. Cell. Biol.* **3**, 112-118.

- VAN LEEUWEN, J.L. (1995). The action of muscles in swimming fish. *Exp. Physiol.* **80**, 177-191.
- VAN LEEUWEN, J.L., LANKHEET, M.J.M., AKSTER, H.A. AND OSSE, J.W.M. (1990). Function of red axial muscles of carp (*Cyprinus carpio*): recruitment and normalised power output during swimming in different modes. *J. Zool.* **220**, 123-145.
- VERRETH, J.A.J. AND BIEMAN, J. DEN (1987). Quantitative feed requirements of African catfish (*Clarias gariepinus* Burchell) larvae fed with decapsulated cysts of *Artemia*. I. The effect of temperature and feeding level. *Aquaculture* **63**, 251-267.
- VERRETH, J.A.J., TORREBLE, E., SPAZIER, E., SLUISZEN, A. VAN DER, ROMBOUT, J.H.W.M., BOOMS, R. AND SEGNER, H. (1992). The development of a functional digestive system in the African catfish *Clarias gariepinus* (Burchell). *J. World Aquacult. Soc.* **23**, 286-298.
- WANG, K. (1985). Sarcomere associated cytoskeletal lattices in striated muscle. Review and hypothesis. In *Cell and Muscle Motility 6* (ed. J.W. Shay), pp 315-369. New York: Plenum Publ. Comp.
- WANG K., McCARTER R., WRIGHT J., BEVERLY J. AND RAMÍREZ-MITCHELL R. (1991). Regulation of skeletal muscle stiffness and elasticity by titin isoforms: a test of the segmental extension model of resting tension. *Proc. Natl. Acad. Sci. USA* **88**, 7101-7105.
- WANG K., McCARTER R., WRIGHT J., BEVERLY J. AND RAMÍREZ-MITCHELL R. (1993). Viscoelasticity of the sarcomere matrix of skeletal muscles. The titin-myosin composite is a dual-stage molecular spring. *Bioph. J.* **64**, 1161-1177.
- WARDLE, C.S., VIDELER, J.J. AND ALTRINGHAM, J.D. (1995). Review. Tuning in to fish swimming waves: body form, swimming mode and muscle function. *J. Exp. Biol.* **198**, 1629-1636.
- WEBB, P.W. (1975). Acceleration performance of rainbow trout *Salmo gairdneri* and green sunfish *Lepomis cyanellus*. *J. Exp. Biol.* **63**, 451-465.
- WEBB, P.W. (1976). The effect of size on the fast-start performance of rainbow trout *Salmo gairdneri*, and a consideration of piscivorous predator-prey interactions. *J. Exp. Biol.* **65**, 157-177.
- WEBB, P.W. (1978a). Effects of temperature on fast-start performance of rainbow trout, *Salmo gairdneri*. *J. Fish. Res. Bd Can.* **35**, 1417-1422.
- WEBB, P.W. (1978b). Fast-start performance and body form in seven species of teleost fish. *J. Exp. Biol.* **74**, 211-226.
- WEBB, P.W. AND BLAKE, R.W. (1985). Swimming. In *Functional Vertebrate Morphology* (ed. M. Hildebrand, D.M. Bramble, K. Liem and D.B. Wake), pp 110-128. Cambridge: Harvard University Press.
- WEIHS, D. (1973). The mechanism of rapid starting of slender fish. *Biorheology* **10**, 343-350.

2

Swimming

Jan W.M. Osse and Igor L.Y. Spierts

Experimental Zoology Group, Wageningen Institute of Animal Sciences (WIAS), Wageningen
Agricultural University, Marijkeweg 40, 6709 PG Wageningen;
The Netherlands

To be published in: a German textbook on fish for students (one chapter).

**'In einem Bächlein helle,
Da schoss in froher Eil,
Die launige Forelle,
Vorüber wie ein Pfeil'
(Christian F.D. Schubart
1739–1791).**

CONTENTS

- 2.1. Introduction**
- 2.2. The construction of a fish's body**
- 2.3. Muscles for swimming**
- 2.4. Fins and buoyancy**
- 2.5. Water in motion**
- 2.6. Swimming modes**
- 2.7. Propulsion, power and drag**
- 2.8. The generation of thrust**
- 2.9. Form of the tail fin**
- 2.10. Energetics**
- 2.11. How are the body undulations, seen during swimming, produced?**
- 2.12. Swimming adaptations in different fish species**
- 2.13. Swimming in fish larvae**

2.1. INTRODUCTION

Many modes of swimming tuned to ecology and body-plan are found in animals. Rowing is found in big water beetles with legs used as oars possessing a paddle like broadening at their end. Also ducks swimming at the surface perform rowing movements but this type of swimming is not very common.

Penguins however clumsy, when walking on land, are masters in speed and manoeuvrability when observed under water. Their wings at first sight appear to be used as subsurface oars. This would mean that the forward thrust generated is based on resistance (on pushing against the water). However the upstroke of the fin, working as a hydrofoil produces a downward force with an anterior component. The downstroke also produces a lift force, this time directed upwards and forward. The beating of the wings in swimming penguins thus is a system for generating lift forces just as in flying birds. The main difference is that penguins, being nearly weightless when submerged, mainly produce a forward thrust, whereas the main force provided by bird wings is a vertical one to keep the animal in the air.

Jet propulsion as found in jelly fish and squids consists of accelerating a certain amount of water. The reaction force provides the thrust, the direction of motion can be chosen by aiming the flow from the funnel. The jet propulsion in squids can be considered as an exaggerated form of the ventilation movement of the gills in their mantle cavity. Jelly fish as well as squids can also move by passing waves of contraction along their body edge or fins. Such undulatory movements providing thrust are by far the most common mode of swimming found in a seemingly endless variety of fish.

Form and construction of fish as primary aquatic vertebrates reflect the demands of swimming. Swimming is required to find food, to escape from predators, to execute the rituals of social behaviour and spawning and is essential for migratory species. In the course of more than 500 million years of fish evolution many types evolved and became extinct. The recent approximately 25.000 species (Nelson, 1994) show in body form, in position, size and type of movement of paired and unpaired fins a variety from fast swimming extremely streamlined mackerels and tuna's to the motionless in ambush lying stonefish or anglers. The most common type of swimming consists of travelling waves of bending with increasing amplitude towards the tail as found in the majority of fish (Fig. 1). Other fish are passing waves of contraction along continuous dorsal fins as found in *Amia* (bowfin), or anal fins as seen in *Electrophorus* (electric-eel) and *Gymnotus* (knife-eel). Also swimming with only the pectoral fins (e.g. *Coris formosa*, a wrasse, Geerlink, 1983), with dorsal and anal fins (sea horses, *Hippocampus*) or with only sculling motions of the tail (*Ostracion tidoe*, boxfish) are met. Other combinations of fin motions for specific actions are found in e.g. the threespined-stickleback using its pectorals to ventilate the eggs in the nest and in the highly specialised trunkfish (*Tetraodontidae*) showing vibrations in dorsal and anal fins in combination with undulations passing over the fin rays of the pectorals. In the complex environment of the coral reef they so can turn, move up- and downward and change the direction of motion in a tiny fraction of space. Manoeuvrability, and not cheap fast swimming is their mode of life.

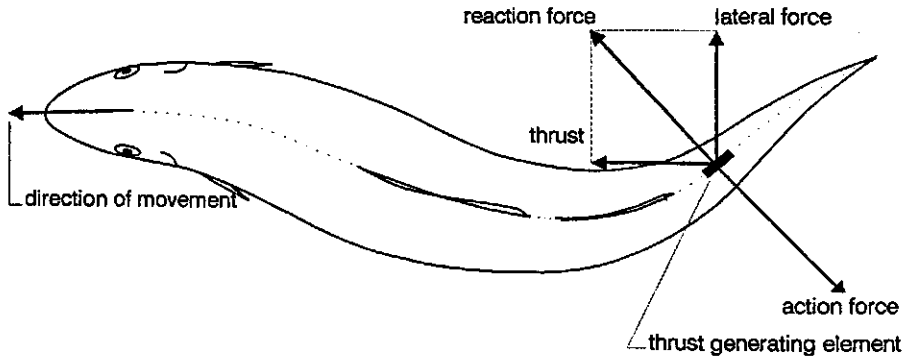


Fig. 1. Drawing of a swimming cod (*Gadus morhua*, $L=42$ cm). The box drawn in the tail represents an element for thrust generation. Swimming is made possible through co-operation of all thrust generating elements. During swimming the body curvature of the fish changes continuously. The tail moves to the right and hence the reaction force of the water on the fish is pointed to the left. The thrust generated by an element at the tail base is bigger than the thrust generated by elements close to the head, because the angle between the element and the direction of movement is larger in the tail region.

Swimming only looks simple e.g. when looking at a trout from a bridge effortlessly gliding through the water. In fact, as in any other field of biomechanics, only a combination of hydrodynamics including measurements of flow parameters and the analysis of movement leads to an understanding of thrust generation. Such combined data sets also provide insight in the construction of fish, as well as awe for their elegance of swimming and turning. The interactions between the changing body form of the fish and the yielding water is governed by the equations of continuity and of motion (Navier-Stokes, Childress, 1981) in which the important physical properties of water, density and viscosity, are included. Central problems are: how are fish built, what are the properties of their skeleton and muscles; how do they move and generate thrust; what resistance do they meet; and how is this drag related to body form, skin surface, scales and position and size of the paired and unpaired fins. Such information, including also a paragraph about hydrodynamics, is required to be able to recognise and designate specialists and generalists among fish, to understand the specific features of fish larvae and to grasp the energy efficiency of the swimming motion in fish. Swimming is the most important item in the energy budget of the every day life of fish and economic use of possibilities through structural, functional and behavioural adaptations is therefore of the utmost importance. In the following paragraphs the above suit of items will be followed.

2.2. THE CONSTRUCTION OF A FISH'S BODY

Seen from above fish are very similar, nearly all are spindle-shaped, widest slightly behind the pectoral girdle and tapering towards the tail. Both characters reflect streamline and flexibility that fish need for swimming. The important differences between species and between different size-classes of one species become apparent when the lateral views are considered (Fig. 2). Here fish of different super orders of teleosts show considerable variation in body form, size and positions of the paired and unpaired fins, headlength/bodylength ratio and form and size of the tailfin (cf. Fig. 33 and paragraph 2.12).

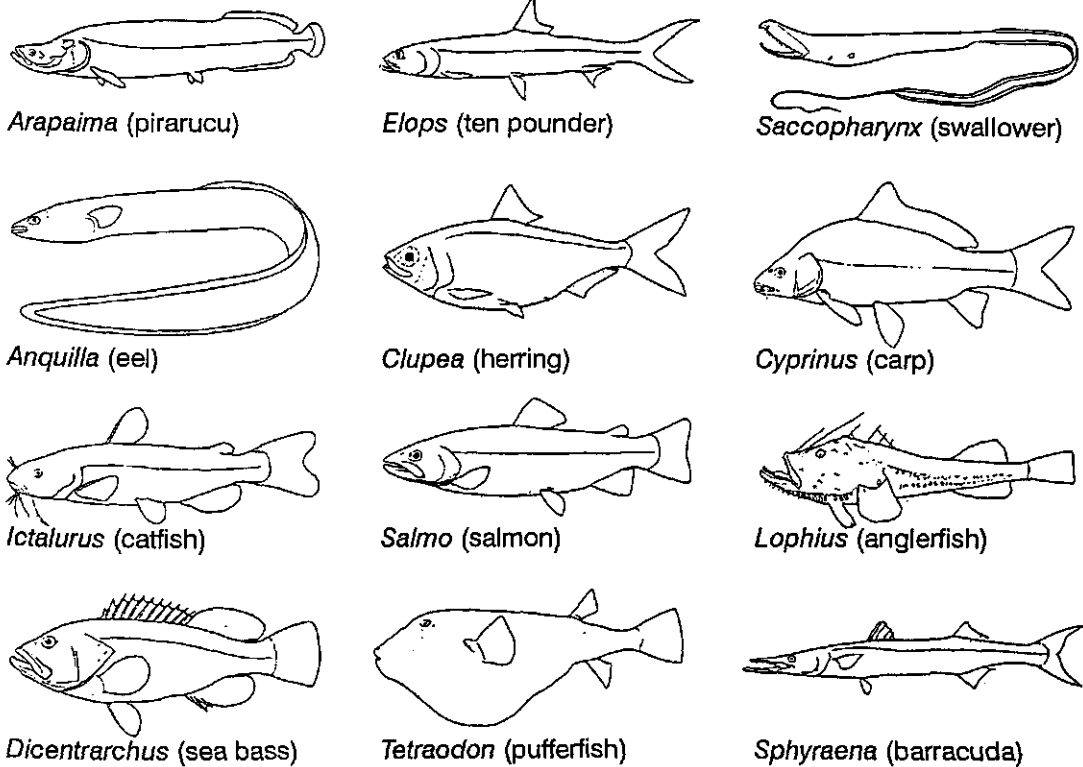


Fig. 2. A variety of teleost fish. Large differences exist in body shape and position and size of the fins. Drawings derived from Nelson (1994).

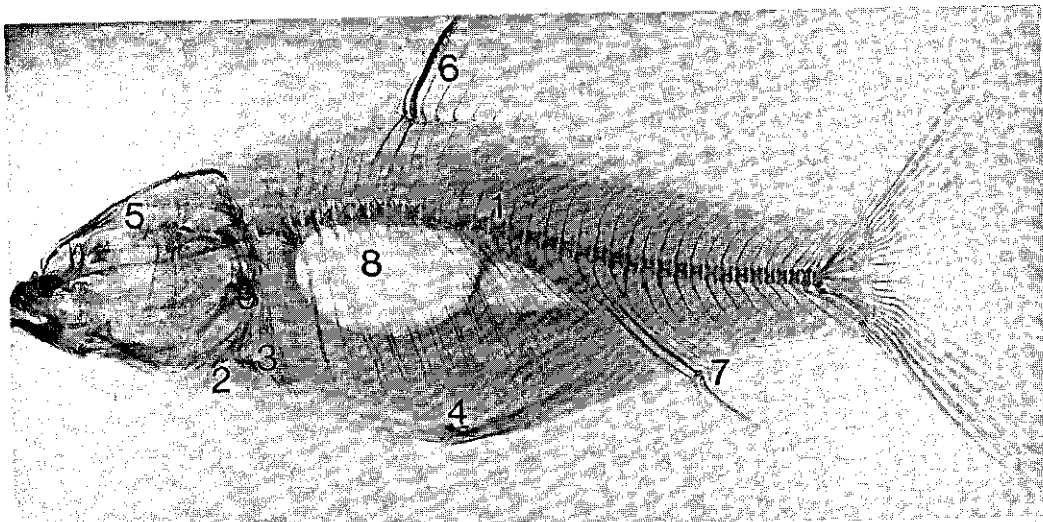


Fig. 3. Radiograph of a carp (*Cyprinus carpio* L.): 1, vertebral column; 2, pectoral girdle; 3, pectoral fin; 4, pelvic fin; 5, skull; 6, dorsal fin; 7, tail fin; 8, swimbladder; 9, pharyngeal jaws. The swimbladder consists of two parts.

The radiograph of Fig. 3 shows a frequently seen construction of the skull, the pectoral and pelvic girdle, the skeleton of the body axis and the position and structure of the paired and unpaired fins. The swimming bladder, here consisting of two parts, is clearly visible. The skeleton of the head, consisting of the cranium, jaws, hyoid- and gill arches, part of the opercular bones form, with the pectoral girdle, the stiff bow during swimming. The head as a unit can rotate upwards with the anterior vertebrae as a pivot point. The vertebrae form a laterally very flexible, nearly incompressible body axis through which the thrust force, mainly provided by the tail during swimming, is transmitted to the anterior-most point of the fish. The flexibility in the vertical plane is considerably smaller. Their dorsal neural and ventral haemal arches contribute little to the stiffness. During swimming the length of the body axis is constant except for compression of the intervertebral cartilage. Contractions of the body muscle produce the typical lateral undulations seen in swimming fish. Generally teleost have more than 30 vertebrae with ligamentous interconnections (Symmons, 1979). Species with more than twice this number (approximately 70 in the tarpon, *Megalops*) do not show greater flexibility. The vertebrae are mostly biconcave, with funnel shaped anterior and posterior depressions filled with fibrous connective tissue. The whole system develops during ontogeny from the continuous notochord and the bases of neural and haemal arches. Measurements of the mechanical properties of the backbone of a subcarangiform swimmer such as the Norfolk spot (*Leiostomus xanthurus*) and of a thunniform swimmer such as the skipjack tuna (*Katsuwonus pelamis*) showed that the latter has three distinct regions of different flexibility in bending while the former is uniform in bending properties all along its length. Another interesting detail is that hysteresis in lateral bending is so high that it is unlikely that the elasticity of the backbone contributes to the swimming ability.

Morphologically trunk and caudal vertebrae are distinct, the latter bearing haemal arches at their ventral sides.

The trunk muscles are segmentally arranged and consist of complexly folded myomeres, muscle segments, separated by collagenous myosepts. Myosepts have the form of a three dimensional horizontally lying W with the open side pointing cranially (Fig. 4A,B). The central anterior cone is attached at the anterior edge of a centre and the myosept runs caudally. Myosepts are built from layers of connective tissue and contain networks of collagen fibres in which discrete strengthened bundles are found. They are thin, even in fish of 25 cm hardly thicker than 0.1 mm. A strong medial vertical sheet of connective tissue, *septum verticale*, separates the muscles of both sides of the body. Mostly a horizontal septum, *septum horizontale*, is present separating the body muscles in a dorsal epaxial and a ventral hypaxial part. Dorsal ribs are sometimes found in the horizontal septum while ventral ribs, surrounding the abdominal cavity reinforce the side walls of the body cavity. Ribs develop at the sites where the myosepts intersect with the horizontal septum and/or peritoneum in the wall of the body cavity. Here the hypaxial layer of the body muscles is mostly thin. The myosepts are connected with both septa as well as with the skin.

The skin is in nearly all fish species thick and solid, more than ten times thicker as the myosepts. It consists of a thin epidermis mostly loaded with mucus cells (overlying the scales if present) and a dermis consisting of three layers. The stratum compactum shows two major directions of collagen fibres (Fig. 4C). The scales, each in a separate pocket, are anchored in the dermis. During cruising at moderate velocities the shear forces exerted by the water sliding along the skin constitute a weak mechanical load and therefore do not provide an explanation for the strength of the skin. A hypothesis about the possible function of the skin in the transmission of muscle forces to the tail during swimming will be discussed later (paragraph 2.11).

The body cavity surrounded by the peritoneum houses the digestive, reproductive and excretory systems as well as the swimbladder, when present. Its wall is strengthened by the previously mentioned ribs. The abdominal cavity tapers towards the anus. The part of the body caudal from the anus is the tail, mostly bearing a prominent tail fin.

2.3. MUSCLES FOR SWIMMING

Muscle fibre trajectories

Fish locomotor muscle, the axial musculature, is segmented. The myomeres are derived from the embryonic myotomes. During growth the originally rectangular myomeres acquire their complex adult form (Fig. 4A,B). Three types of muscle fibres, white, pink and red can be distinguished (Fig. 5). The lateral-most red fibres run parallel to the body axis. The inner fibre system (white fibres) is arranged in a complex pattern.

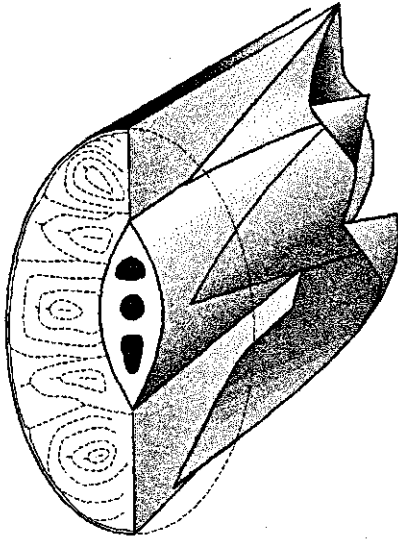


fig. 4a: Cartilaginous fish

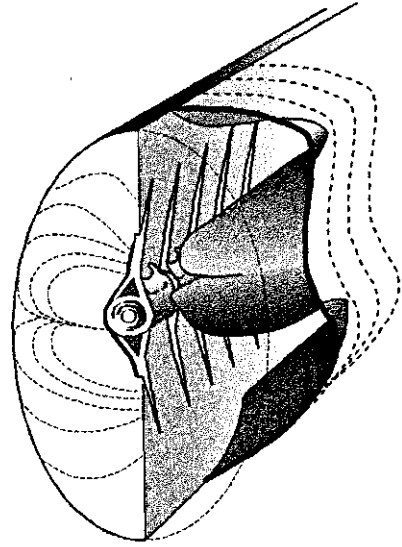


fig. 4b: Bony fish

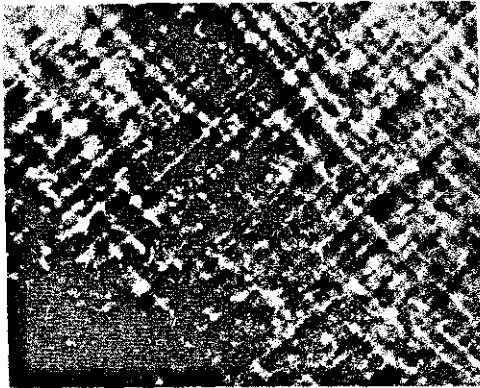


fig. 4c: Skin

Fig. 4. Diagram of myomeres and myosepts in the tail of a cartilaginous fish (A) (*Squalus acanthias*) and a teleost; (B) (*Cyprinus carpio* L.). Note the complex folding of the myosepts (three cones pointing anteriorly, 2 posteriorly). Accepting the functional demand that all muscle fibres equally contribute in developing power for swimming, a folded construction of the myosepts (to enable the required course of the muscle fibre trajectories) is the only solution. See text for further explanation. Fig. A modified after van der Stelt. (C) Crossing bundles of collagen fibres in the stratum compactum of the dermis of a cichlid fish, (*Tilapia sarotherodon*).

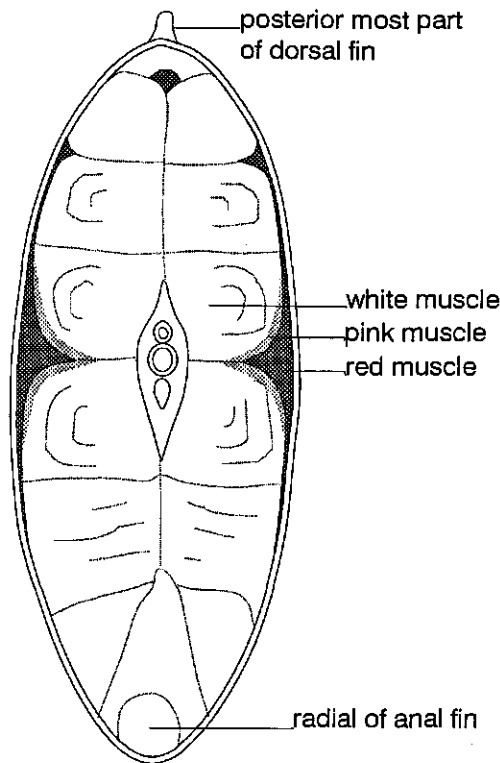


Fig. 5. Cross-section through the tail of a carp of a fish, showing the location of white, pink and red muscles.

The architecture of the white muscle system of fish with its complex W-shaped overlapping myotomes is only partly understood. Alexander (1969) defined a fibre trajectory as the imaginary curved line along the length of the fish giving in every point the direction of the muscle fibres. Such curves run at both sides from the head through a myotome, the neighbouring myosept and the next myotome onwards to the tail. These trajectories appear to be helices as shown in Fig. 6A-C and thus are nowhere parallel with the fish axis. If this were the case the direction of the force would be optimal for bending the fish body. The underlying deeper fibres also parallel with the fish outer surface would however have to contract and thus thicken against the inward directed force provided by that superficial sheet. Another effect of such a construction would be that muscle fibres close to the axis could hardly shorten during the bending of the body because the axis of the body is incompressible and therefore such fibres would hardly or not contribute to the work done on the water during swimming. Alexander (1969), Kashin and Smoljaninov (1969a,b) and van der Stelt (1968) suggest that the peculiar helical arrangement of the white fibre trajectories allow all fibres to contribute equally to the power delivered during swimming for the bending of the body.

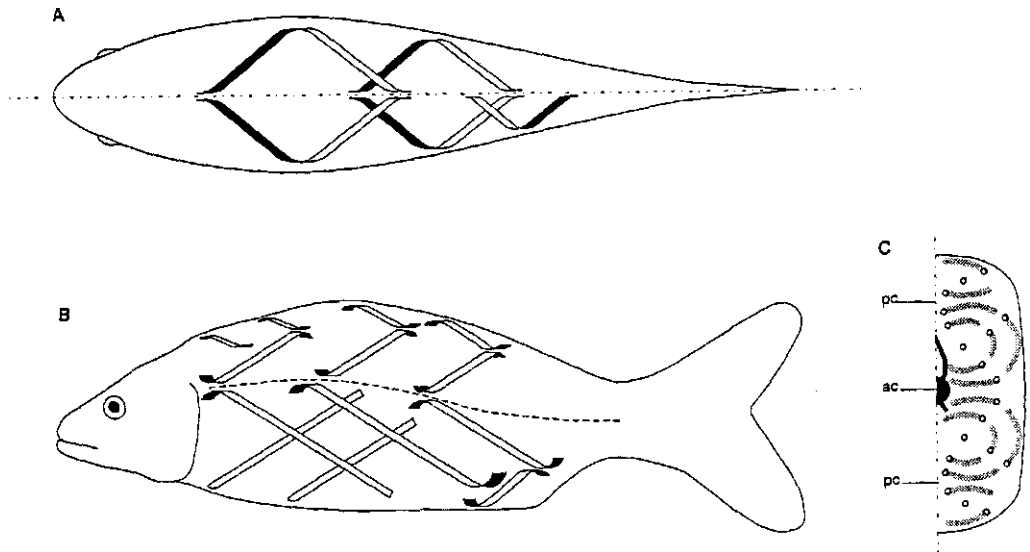


Fig. 6. Muscle fibre trajectories in a teleost fish. (A) Dorsal view; (B) Lateral view; (C). Thick transverse slice across a teleost showing the orientation of myotomal muscle fibres (pc, posterior cone; ac, anterior cone of the myotomes). Four bundles of muscle fibre trajectories can be recognised in half of the body: two in the epaxial part (e) and two in the hypaxial part (h). The helices shown were obtained by following successive muscle fibres between myosepts as if they were continuous along the fish body. In one bundle trajectories run like concentric helices. This white fibre arrangement enables an equal shortening whether the fibre is close to the skin or close to the backbone and therefore all muscle fibres can provide an equal share in the work. Red muscle fibres run almost parallel to the body axis, directly beneath the skin. These fibres do not have a helical orientation. Modified after Alexander (1969).

This helical arrangement, in which the inner fibres make different angles with the body axis than the outer ones also allows the sarcomeres of all white fibres to contract to the same extent during muscle shortening. To cause body curvatures similar to those due to white fibre contraction, sarcomeres of red fibres must shorten over a considerable larger distance. In most cases the red fibres, however, form only a thin mid-laterally lying layer used for slow continuous swimming and generally responsible for gentle body undulation.

Types of muscle fibres

The three main fibre types (Fig. 5, Table 1) white, pink and red, differ considerably in contractile and metabolic properties (van Raamsdonk 1978). White fibres have a high contraction velocity and therefore can produce a high power output (power is the product of force and velocity and is expressed in Watts). They however can deliver such power only for a short period of time (10 to 60 seconds). During contraction no oxygen is used, glycogen is anaerobically broken down into lactic acid. White fibres therefore fatigue fast and require a long time to recover. The lateral red fibres contract approximately three times slower than white fibres, have an aerobic metabolism, are practically infatigable and therefore suitable for continuous function. Their energy (ATP) is produced by aerobic burning of lipids. This very economic way to produce ATP from food substances in combination with their endurance make this system very suitable for the production of thrust during quiet swimming. Although in a generalised teleost the red muscles form less than 10 % and the white together with the pink fibres more than 90 % of the total muscle mass, the white muscle is only used during fast escapes from predators, sudden approaches to prey or during aggressive behaviour. In these short but vital periods their high contraction velocity and power output is of crucial importance for survival.

Table 1. Properties of red and white fibre types. Pink or intermediate fibres resemble white fibres in most respects but have higher endurance. ATP, adenosine-tri-fosphate. SDH, succinate dehydrogenase.

Properties	Red fibres	White fibres
Colour	red	white
Contraction velocity	slow	fast
Myosin-ATPase activity	low	high
SDH activity	high	low
ATP production	oxidative	glycolytic
Type of metabolism	aerobic	anaerobic
Number mitochondria	large	small
Number capillaries	large	small
Myoglobin content	high	low
Glycogen content	low	high
Fibre diameter	small	large
Stress (force/unit area in cross-section)	small	high
Endurance	good	bad

The properties of the pink fibres are intermediate between white and red. Several different types of such intermediate fibres have been described (Akster and Osse, 1978; Akster, 1983; Akster 1985). Intermediate fibres generally are situated between the red and the white fibre zones (Fig. 5). Fibre

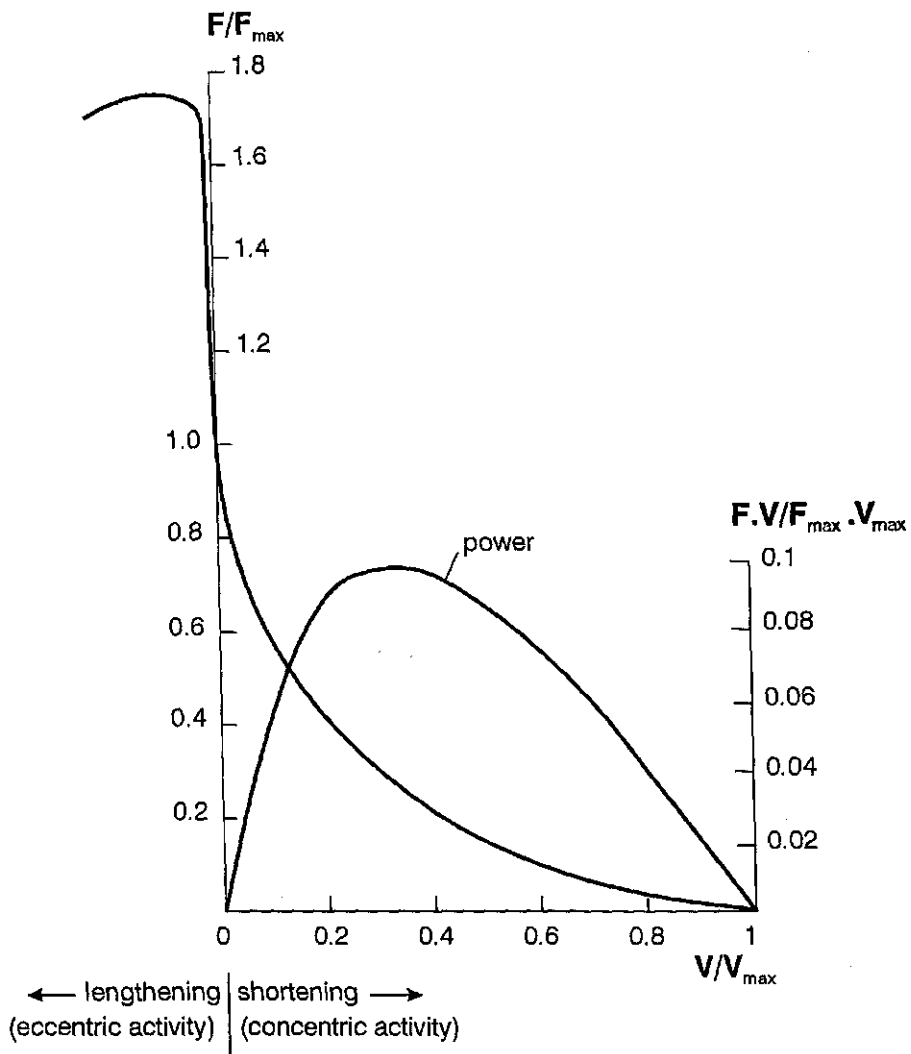


Fig. 7. Force-velocity relationship (relative to the maximum force and maximum velocity) and the direct power output of a muscle. F , force; F_{max} , maximum (isometric) force; V , velocity; V_{max} , maximum velocity. Power = force-velocity ($F V$). Isometric contraction: the muscle develops tension, but does not shorten, no (external) work is being done. Isotonic contraction: the muscle shortens with a load that remains constant, maximum velocity with zero load. The power output ($F V$) is maximal at approximately 30 % of V_{max} . Very high forces are generated in an active muscle during lengthening (eccentric activity).

types are generally classified based on the myosin ATPase isotype in their sarcomeres and also on their metabolism. The isotype of myosin ATPase is decisive for the maximal contraction velocity of the fibre and therefore an important factor in power output. Force velocity curves (Fig. 7) show that power output is maximal at approximately $0.3 V_{\max}$, the maximal contraction velocity of a muscle fibre. Fast myosin ATPase means a high ATP consumption. Optimal use of muscle and the need to function in a certain range of temperatures require the presence of a variety of muscle fibres subtypes (Alexander and Goldspink, 1977), differing in myosin ATPase. For practical reasons all these fibres are grouped in three main types: red, pink (intermediate) and white.

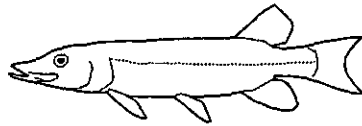
Within fibre types differences in detailed properties may exist. Tension development in active fibres depends on V/V_{\max} , the ratio between the actual contraction velocity and the maximal (unloaded) contraction velocity of the fibre (Hill, 1938), and eccentric activity (being stretched when active and hence negative contraction velocity) results in tensions higher than those during concentric activity (shortening when active). Therefore, in addition to the medial-lateral difference in muscle fibre types, there are also antero-posterior differences in muscle function between fibres of the same type in the body of a swimming fish. Computer models (van Leeuwen *et al.*, 1990; van Leeuwen, 1995) based on electromyography and motion analysis of free swimming carp (*Cyprinus carpio* L.) predicted that, during continuous and intermittent swimming, muscle fibres in the tail region (together with the connective tissue) would play an important role in the transmission of force produced by more anterior muscle fibres. The posterior fibres have a longer phase of eccentric activity than the anterior fibres (van Leeuwen *et al.*, 1990; van Leeuwen, 1995). As a result, these posterior fibres will develop greater forces (cf. Fig. 7) than the anterior fibres, which was confirmed by simulation experiments of Davies *et al.* (1995).

The arrangements of fibre types differ greatly between different fish species. In Fig. 8 cross-sections of the bodies of a pike (*Esox*), a white bream (*Blicca*) and a salmon (*Salmo*) are shown. Note that the three different fibre types appear also in completely different proportions, reflecting the life history strategy of the species. Ambush hunters like the pike have nearly exclusively white fibres, cruisers like the white bream have a lateral section of red fibres and stayers have a high proportion of red fibres and centrally many pink fibres.

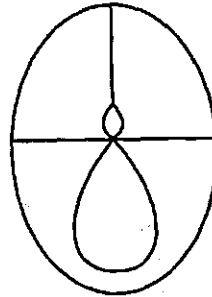
White and red muscle zones generally also show a mosaic pattern of fibre diameters. This is caused by the presence of small, young fibres between larger, more mature fibres. In contrast to birds and mammals, where formation of new muscle fibres generally stops around the time of birth or hatching, the recruitment of fibres in fish continues well into the adult stage.

Muscle function is very dependent on body temperature and the temperature of the surrounding water. Almost all fish operate with a body temperature that generally differs little from the water outside due to the loss of body heat in gill circulation. Some fish however are able to run their red muscles above the temperature of the water outside. In these fish special features of the vascular system exist in which warm venous blood, leaving the red muscle portion of the myotomes, pass close to the entering cool oxygenated blood in special parallel networks of arteries and veins (the *retia mirabilia*). In this way heat is exchanged to the arteries supplying these muscles and the muscle can retain an elevated temperature. A heat transfer efficiency of approximately 98 % was measured in the

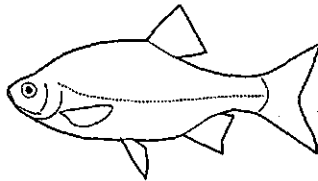
A Sprinters



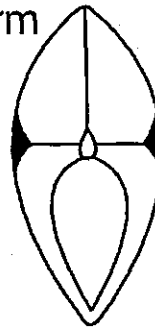
Esox (pike)



B Intermediate form



Rutilus (rudd)



C Stayers



Salmo (salmon)

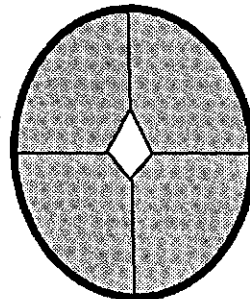


Fig. 8. Simplified cross-section of the axial muscles of three fish with different life styles. (A) Ambush hunters (pike): have almost exclusively white muscles; (B) Intermediate form, cruiser (white bream): have a lateral section of red muscles. These fish show very diverse swimming activities in time; (C) Stayers (salmon): have a high proportion of red fibres and centrally pink fibres. These fish swim continuously at a moderate speed. Red fibres are dark, stippled areas indicate pink fibres interspersed between white fibres. Note that the relative share of red fibres increases from anterior to posterior: when comparing fish species it is therefore necessary to use similar cross-sections. Modified after Boddeke *et al.* (1959).

retia of albacore (*Thunnus alalunga*) The arrangement of these countercurrent retia is seen in Fig. 9. The heat loss in the gills is reduced and locally in the body muscle body heat is accumulated such that here muscle is contracting at temperatures up to 10 °C above ambient water temperature (Bone *et al.* 1995). This means that the power output will be two to three times higher, providing these fish with a considerable ecological advantage as predators.

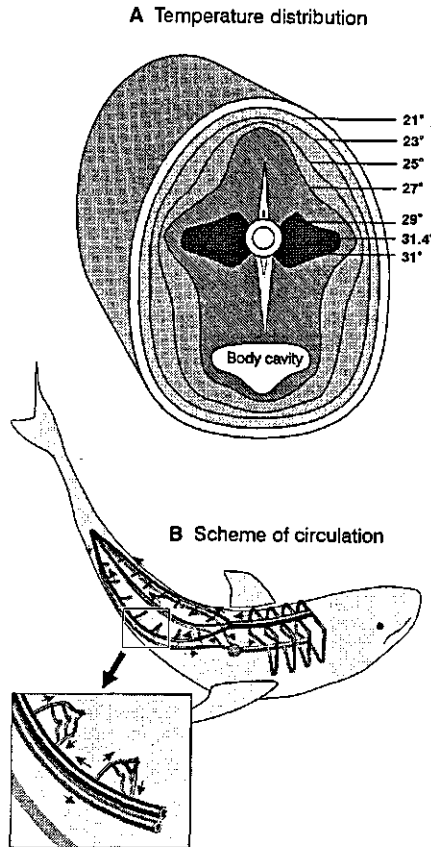


Fig. 9. Organisation and function of the retial thermoregulation system in large active fish. (A) The bluefin tuna (*Thunnus thynnus*) maintains internal temperatures much higher than the surrounding water (the different layers are the swimming muscles cut in transverse section). The temperatures shown were recorded for a tuna in 19.3 °C water. Modified after Carey and Teal (1966, 1969); (B) The great white shark (*Carcharodon carcharias*) has, like the tuna, a counter current heat exchanger in its swimming muscles that reduces the loss of metabolic heat. When blood passes through the gills all fish lose some heat to the surrounding water, however in contrast to exothermic fish, endothermic species have a relatively small diameter dorsal aorta carrying little blood from the gills to the core of the body. Instead most of the blood of the gills is conveyed via large arteries just under the skin, keeping cool blood away from the body core. In the enlargement the counter current flow, retaining heat in the muscles, is shown. A network of small vessels carrying cool blood inward from the skin arteries is paralleled by small veins carrying warm blood outward from the inner body. Modified after Campell (1996).

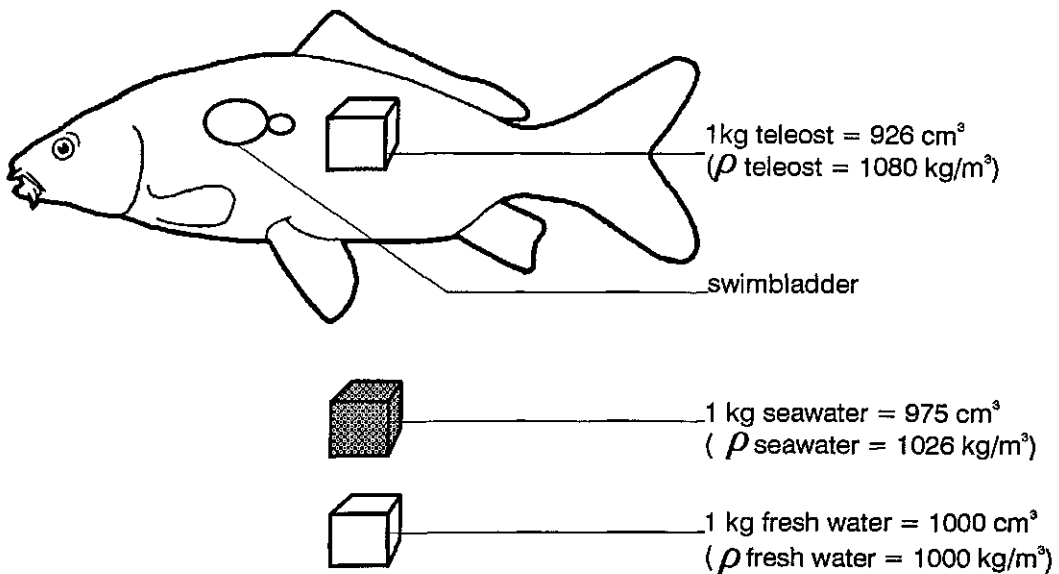
2.4. FINS AND BUOYANCY

Fish have median unpaired and paired fins. Unpaired fins are the dorsal fin (one or more), the anal fin and the tail fin. The paired fins are the pectoral and pelvic fins. Median fins with their broad surfaces are important to stabilise the body against roll (around their long axis) during locomotion. They also reduce sideslip which can be caused by occasionally occurring high uni-lateral forces. The pectoral and pelvic fins also are used for stabilising but are the important devices for steering and braking. Yaw, turning about a vertical axis in a horizontal plane, and pitch motions, turning about a transverse axis in a vertical plane, are required to reach a particular spot. A laterally projecting pectoral fin will cause a moving fish to turn to that side. Fins may have a great many of other functions e.g. positioned at an angle to the flow, they can act as hydrofoils to produce lift. Coloured fins may send signals to conspecifics, fins with strong anterior spines sometimes provided with locking mechanisms (many catfish, *Siluroidea*) reduce predation by increasing the effective size of the prey, especially when spines occur in the pectorals as well as in the dorsal fin. In sticklebacks the pectorals are used to ventilate the nest with eggs. The beating heterocercal tail typical for sharks produces thrust as well as lift forces which tend to cause a downward pitching movement of the head around the centre of gravity. The widely spread pectorals lying anterior to the centre of gravity and also providing lift forces can counteract these movements and thereby regulate the direction of motion and the depth of these fish in the water mass.

The density of water varies with temperature and is at 4° C 1000 kg m⁻³ for fresh water and 1026 kg m⁻³ for sea water. The density of water is not only very constant, but also in the same order of magnitude as the density of fish tissues and those of other aquatic organisms. Small adjustments of density e.g. by volume changes of swimbladders may cause neutral buoyancy.

Cartilaginous fish lack swimbladders or lungs. Their higher density (e.g. spiny dogfish, *Squalus acanthias*; 1075 kg m⁻³) and therefore tendency to sink is not only compensated by the lift forces mentioned above, but also by the presence of a fatty substance (wax esters), squalene in the liver (in some forms up to 1/4 of the total body weight) with a density of 870–880 kg m⁻³. In this way these fish can maintain their position at a certain depth without the need of permanent swimming. Many pelagic teleost fish such as sword fish, mackerels and some tunas are also negatively buoyant so they must swim constantly to produce lift forces. Most teleosts, however, possess a gas filled swimbladder which make them neutrally buoyant so they can effortlessly maintain a chosen position in the water column (Fig. 10). During diving in fish the increased water pressure (100 kPa per 10 meters water column, 1 atmosphere) will compress the gas in the bladder thereby increasing the average density of the fish and thus speed up the sinking. Primitive teleosts like eels and herrings, anchovies, minnows and salmons retain the ontogenetic connection between gut and swimbladder (physostomes); more advanced teleosts have lost the pneumatic duct (physoclists). In the latter volume regulation of the swimbladder during descent requires the secretion of gas into the bladder. In many teleosts such a gas gland, possessing a rete mirabile performs this secretion, a remarkable feat because at e.g. 500 meters depth in the sea the gas pressure in the bladder will be approximately 50 atmospheres. During ascend in the water column physoclists open a muscular valve located dorsally on the swimbladder, the ovale. A capillary bed lying there absorbs the gasses of the bladder,

previously retained in the elsewhere impermeable wall of the bladder, due to their higher than ambient partial pressure.



Contents swimbladder: 49 cm³ of gas → neutral buoyancy in **seawater**
 74 cm³ of gas → neutral buoyancy in **fresh water**

Fig. 10. Buoyancy in fish with a swimbladder occurs when the volume of 1 kg teleost equals the volume of 1 kg water. As 1 kg teleost has a smaller volume (926 cm³) than 1 kg seawater (975 cm³) buoyancy only occurs when the swimbladder contains 49 cm³ of gas (with a neglectable addition to the weight). A similar calculation can be made for fish swimming in fresh water. The densities of the fish and the water are shown between brackets. So swim bladders in fresh water fish tend to be larger than in marine fish. Data from Alexander (1975).

2.5. WATER IN MOTION

Hydrodynamic interactions between fish and water determine to a large extent the movements of fish in water. Streamlined bodies offering low drag are especially important when fish are moving at high velocities and for extended periods of time.

Water can be considered as an incompressible fluid and its density is assumed to be constant. It follows that a specified volume of water has always the same mass (continuity condition). If water flows in a tube of varying cross-sectional area, the volume entering the tube in a certain period of time must equal the volume that flows out of the tube in that same time interval. The debit, the volume of water per unit of time, is the same at any point in the tube. Using the continuity condition it is possible to calculate the relation between the flow velocities in three mutually perpendicular directions. Knowledge of local flow velocities is important in determining the pressure (force per unit of area, $\text{N m}^{-2} = \text{Pa}$). The density of water varies little between 0 and 25 °C viscosity decreases in this range with 50 %.

Water flow is the result of forces exerted on it or caused by accumulated kinetic or potential energy. Here, Newton's second law of motion ($F = m a$) is relevant, but its application to water is complex. When, due to movements, a spatial pattern of velocities and accelerations of water particles is established, the water flow can be visualised by streamlines. A streamline is a curve indicating at each point the direction in which the water moves. A water flow is called steady, given a particular value of the debit, when the streamlines do not change in time. When the flow pattern changes continuously in time due to local accelerations and decelerations varying in time, the flow is called unsteady. For example, although water in a tube travels faster when the tube is locally more narrow, the flow is called steady because the change in velocity is constant and always located at the same point along the tube (provided other conditions are kept constant). The velocity of the flow is constant but not the same in each part of the tube. However, if the flow rate is altered in time e.g. by repeatedly opening and closing the tap, the flow pattern of streamlines continuously changes and the flow is unsteady.

The importance of unsteady flow (turbulence) is determined by a frequency parameter σ (sigma) which is a measure of the amount of change in time. The frequency parameter σ is the product of the radial frequency, the characteristic length and the reciprocal of the characteristic velocity. Turbulence is already substantial if σ equals one. The contribution of unsteady flow on an overall flow pattern increases with an increase in the number of changes in the flow pattern per second. In swimming fish σ may attain values of 8 and higher, even during continuous steady swimming, resulting in a strong unsteady component. In such situations, exact calculations of pressure, velocity and the transfer of energy from the fish to the moving water becomes close to impossible. Hence in the literature of swimming many different ways to approximate energy costs and losses are found.

Frictional (viscous) forces and inertial forces dominate in water in motion. The relationship between the two forces is expressed by a dimensionless parameter, the Reynolds number (Re):

$$\text{Re} = \frac{\rho \cdot u \cdot L}{\eta}$$

where ρ (rho) is the density of the fluid, u is the average fluid velocity, L is a characteristic length of the moving object, and η (eta) is the dynamic viscosity (Pa s). The kinematic viscosity η/ρ is nearly a constant, has a value of approximately 10^{-6} and is expressed in $\text{m}^2 \text{s}^{-1}$. The inertial forces are represented by the numerator and the frictional forces by the denominator. Frictional forces dominate the flow if the Reynolds number is small (small u , L , or both): layers of fluid with different velocities move slowly past each other and the flow will be laminar (Fig. 11A). At Reynolds numbers exceeding 10^2 – 10^3 , the laminar flow will be reduced to a thin boundary layer concentrated around the moving object (Fig. 11B). A steep gradient in water velocity will develop over a short distance in the thin boundary layer, because the inner layer of this thin boundary layer at the fish surface is travelling

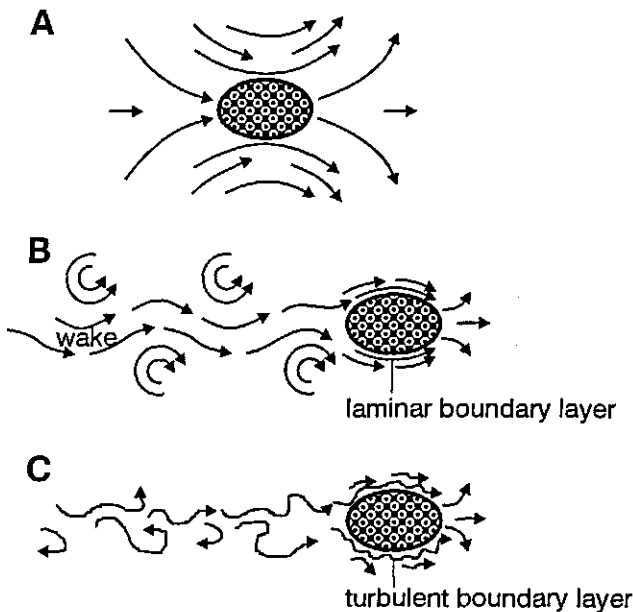
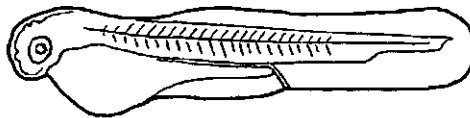


Fig. 11. Scheme of a moving body in a fluid. The arrows indicate the movements of the fluid caused by the moving body. (A) Re number < 1 ; (B) Re number between 10^2 and 10^6 ; (C) Re number $> 10^6$; at these high Re numbers the laminar boundary layer becomes turbulent.

with the speed of the fish while the water outside this layer is not moving at all. The energy that is needed to move layers of adjacent water relative to each other is one of the main sources of drag during swimming, the so called friction drag. A second important source of drag during swimming is the acceleration of water in forward and lateral direction, pressure drag, especially by the head (resulting in high pressures on the snout). At Reynolds numbers above 10^5 – 10^6 the boundary layer will not anymore be closely applied to the fish's body but it will peel off the body and produce a continuous series of lateral vortices (rotating masses of water) which cause a considerable increase in drag (Fig. 11C). The flow is now turbulent and no longer laminar.

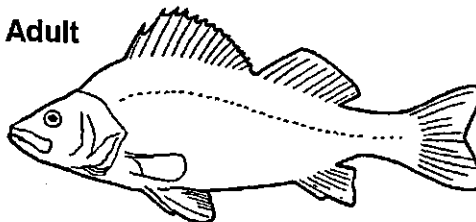
When viscosity forces dominate the flow at low Reynolds numbers ($Re < 1$), a streamlined body is not important because a moving object will be surrounded by a thick boundary layer, a mass of water outside but moving with the object. Therefore small animals like protista have totally different demands upon their bodyform than large fast swimming fish. Small fish larvae also experience large frictional forces due to their small size and low absolute velocity (Fig. 12 and paragraph 2.13). It has been calculated that during suction feeding in such larvae essentially 60 % of the energy of the created suction flow is lost in overcoming frictional forces (Drost and van den Boogaart, 1986). The value of the Reynolds number determines to a large extent the flow pattern that will be created around a moving object in water. It must be kept in mind however that, because the Reynolds number changes with the velocity (u), it is strictly speaking not permitted to apply the Reynolds number in situations of unsteady flow.

Larvae



length: 5 mm, velocity: 3 BL/s
 $Re = 0.005 \times 0.015 \times 10^9 = 75$

Adult



length: 200 mm, velocity: 2 BL/s
 $Re = 0.2 \times 0.4 \times 10^9 = 80000$

Fig. 12. Comparison of Re numbers of a larval and an adult perch (*Perca fluviatilis*). Re number is calculated from length ($m s^{-1}$), velocity ($m s^{-1}$) divided by the kinematic viscosity. The value of this is taken to be $10^{-6} m^2 s$. Kinematic viscosity is dynamic viscosity (pascal-second) divided by density (mass per unit volume). Note the median finfold and the yolk sac in the larva. A streamlined body as in adult fish is of little importance in tiny fish larvae because of the large influence of frictional forces.

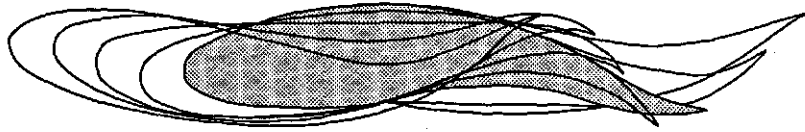
The law of conservation of momentum holds for swimming fish and the water surrounding them. The momentum transferred to the water during swimming equals the sum of the products of mass and velocity of all moving water particles. When a backward momentum is transferred to the water, the fish is given forward propulsion. The rate at which the fish transfers momentum to the water determines the generation of thrust. Acceleration of the fish during take off requires the transfer of a large momentum in backward direction to the water. This is most effectively realised by giving a large volume of water (with mass m) a small velocity (v). In this way the momentum ($m v$) is large and the energy costs of the fish, $1/2 m v^2$ are reduced compared to a motion with small mass and high velocity. Efficient propulsion following this principle is realised by the production of vortices with a large diameter and a small vorticity (velocity of rotation of the water) in the wake of the fish.

2.6. SWIMMING MODES

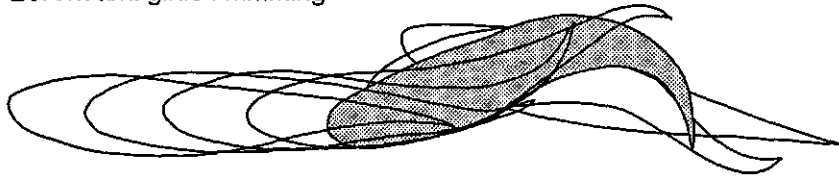
Movements of swimming fish have been studied by many scientists (a.o. Gray, 1933; Bainbridge, 1958; Webb and Weihs, 1983; Videler and Hess, 1984; van Leeuwen, 1995). It is possible to distinguish: forward swimming with uniform speed (continuous swimming; steady straight swimming), intermittent swimming (burst-and-coast swimming, also called kick and glide swimming), turning and forward accelerating during fast starts. Examples of movements associated with the different modes of swimming are given in Fig. 13.

Although continuous swimming at uniform velocities along a straight path is rather uncommon in fish, it is a good starting point for the analysis of swimming motions. During continuous swimming, lateral waves of body curvature run from head to tail along the body axis. A pattern generator activating the musculature in the proper time and to the proper action is postulated to lie in the rostral part of the spinal cord. The amplitude of the lateral movement of the body decreases slightly from the snout to approximately the centre of gravity of the fish and then increases sharply towards the tail (Fig. 14). The average lateral velocity of the body is therefore largest at the position of the tail fin. As a result of this pattern of movement, water is accelerated along the entire length of the body. Due to the rigidity of the head of the fish, lateral curvature is not present in the head region. Fig. 15 shows drawings of the outline of the body of a 42 cm cod (*Gadus morhua*) during continuous straight swimming. The drawings were drawn from film images recorded from a position above the fish at 200 frames per second. Each fourth frame of the stroke of the tail fin is drawn. The first image is at the left, the last image at the right. The time shift between two images is 20 ms (the horizontal axis in Fig. 15 represents time). The fish moves forward with a velocity (u) of 0.7 m s^{-1} with respect to the background represented by two black dots for each image. Note that in half of the period of body curvature ($1/2 T$) the tail position has shifted from an extreme left position to an extreme right position. The backward speed of the propulsion wave (v) is 0.9 m s^{-1} .

A. Continuous swimming (carp)



B. Kick and glide swimming



C. Start

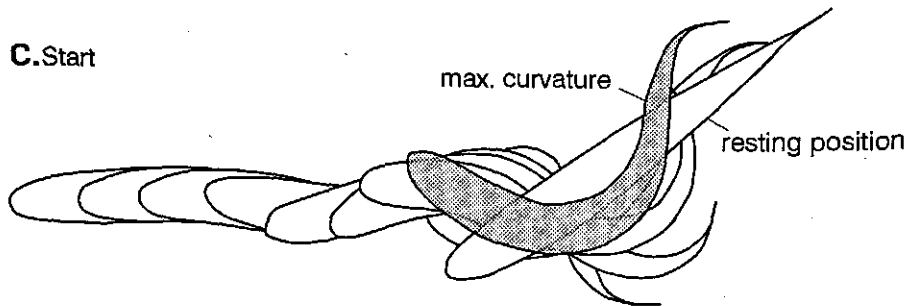


Fig. 13. Dorsal view of different swimming types (pictures redrawn from fast film, earth bound frame). (A) Continuous swimming of a carp: the snouttip shows little lateral movements. At the centre of gravity of the fish body the amplitude is minimal, at the tail fin the amplitude is maximal. After van Leeuwen *et al.* (1990). Fish length 15,6 cm; (B) Kick and glide swimming of a carp: after the gliding period (with a straightened body) a new acceleration sets in by means of several body undulations, also the direction of movement may change. Initially the body curvature is bigger in kick and glide swimming than in continuous swimming. The carp uses this intermittent swimming mode frequently. Modified after van Leeuwen *et al.* (1990). Fish length 13.0 cm; (C) Fast start of a trout: during the start extreme body curvatures occur. After several tail beats a situation comparable to continuous swimming is reached. From position 1 to position 3 in approximately 0.033s. From position 3 to position 6 is approximately 0.05s. Bodylength 29 cm. Modified after Hertel (1966).

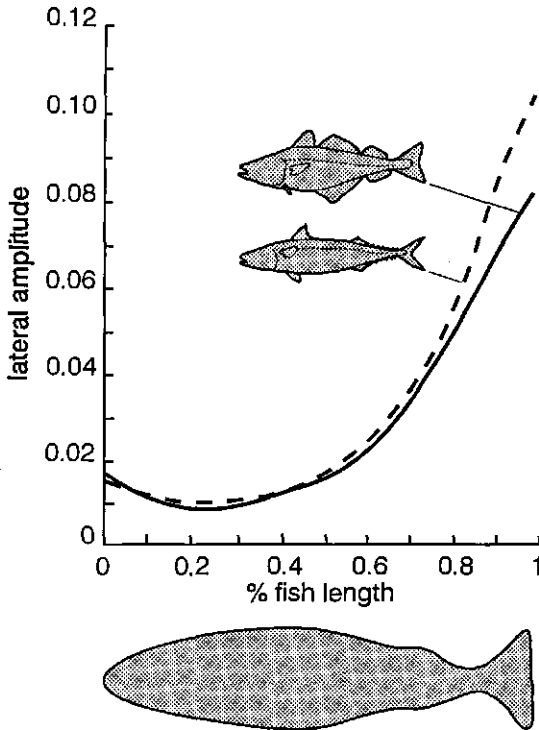


Fig. 14. The amplitude of the lateral movement during continuous swimming of a saithe (*Pollachius virens*) (solid lines) and a mackerel (*Scomber scombrus*) (broken lines). The amplitude is given as a fraction of the bodylength. The movements of saithe and mackerel differ little, except for the tail region where the mackerel reaches the highest values for amplitude. After Videler and Hess (1984).

Broken lines in Fig. 15 connect the maximum lateral body curvatures at the left (L) and right (R) side of the fish. The horizontal distance between two adjacent broken lines is equal to half of the period of the wave of body curvature ($1/2 T$). The vertical distance between two broken lines is equal to half of the wavelength of the body wave ($1/2 \lambda_{\text{body}} = 1/2 \lambda_b$). Note that with respect to the fixed environment (the black dots) the fish has covered the indicated half stride length in this half wave period.

The volume of water that is accelerated (added or virtual mass) per unit of bodylength is determined by the height and width of the fish body. An example of the virtual mass of a saithe (*Pollachius virens*) is shown in Fig. 16.

The forward velocity (u) of fish is expressed in m s^{-1} . When comparing the speed of fish of different size, forward velocity (U) is usually expressed in bodylength per second ($BL \text{ s}^{-1}$). In comparative studies of swimming movements the specific swimming velocity (U^*) is calculated as

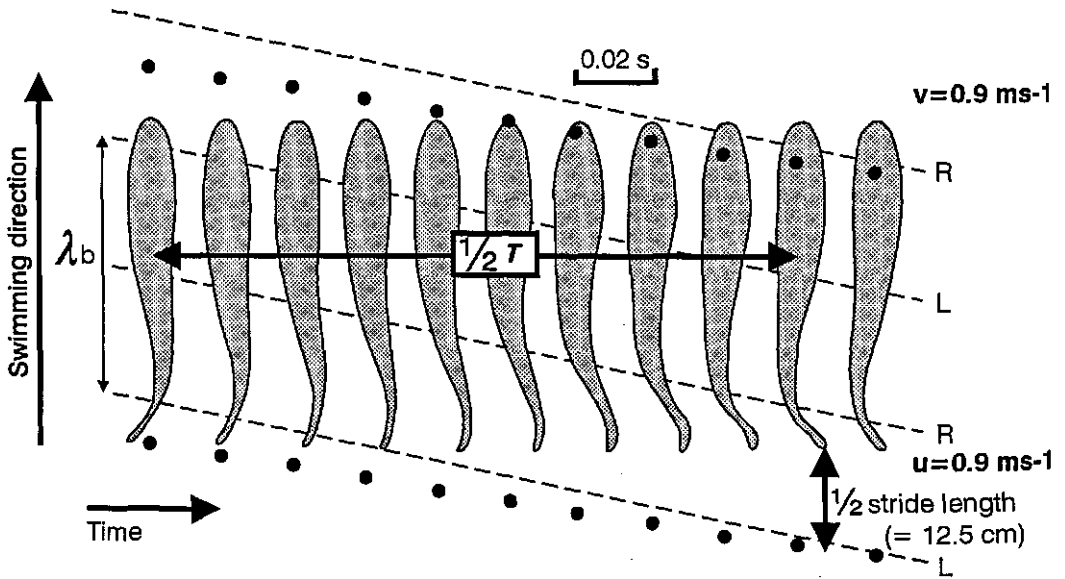


Fig. 15. A swimming cod viewed from above. Ten pictures constitute one half of a complete tail beat. Fish are drawn in an earthbound frame. The black dots are fixed points in the background. u is the forward velocity of the fish (m s^{-1}), v is the backward speed of the propulsive wave over the body, the length of one complete body wave, is 32.4 cm. In half a tail beat (picture 1–10) the fish covers the distance indicated as $1/2$ of the stride length. Each species has its own typical stride length. Generally speaking, high speed are the result of a high repetition rate of a approximately similar motion. Modified after Wardle and Videler (1980).

$U^* = BL/T$ (T is the period of the wave of body curvature; $1/T$ is frequency of strokes of the tail fin i.e. the number of complete (left and right) beats per second). The specific swimming velocity U^* differs among fish with different body forms. Larger fish beat their tails more slowly than small ones, but if account is taken of this by including fish size (Fig. 17), we see that the fish moves forwards for the same fraction of bodylength for each tail beat. In mackerel (*Scomber scombrus*) $U^* = 0.83 BL/T$, in saithe (*Pollachius virens*) $U^* = 0.8 BL/T$, in cod (*Gadus morhua*) $U^* = 0.62$, and in eel (*Anguilla*) U^* is only $0.55 BL/T$. In human beings swimming with 'web-feet' $U^* = 0.5 BL/T$ (Videler, 1985). In mackerel, cod, saithe, trout and goldfish, U^* varied only to a small extent over large ranges of absolute swimming speeds (Bainbridge, 1958; Videler and Hess, 1984). In all these fish the absolute swimming speed is proportional to the frequency of the tail fin strokes but this linearity only holds for frequencies above 5 Hz. In that realm the fish do not change their swimming mode importantly when travelling at higher swimming speeds, they just increase the number of beats per second. At

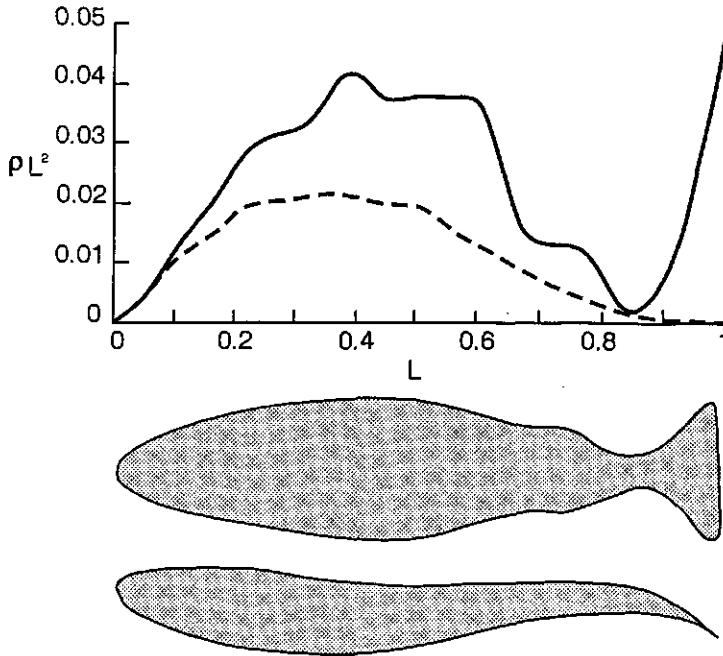


Fig. 16. Distribution of body mass (broken line) and virtual mass of water (solid line) for saithe. The X-axis represents the fraction of the bodylength (L) and the Y-axis (ρL^2) represents added mass (ρ^2) per unit of bodylength (BL). In the tail region the body mass is small whereas the virtual mass of water is increasing. Fluctuations in the kinetic energy of the body itself are therefore small in this region but energy is transferred to the water very efficiently. Modified after Hess and Videler (1984).

frequencies lower than 5 Hz demands of stability steering and equilibrium require adjustments in unpaired and paired fins, increasing the drag and reducing the distance covered per tail beat i.e. 'stride' length. It is clear that the frequency of beating is limited by the activation, contraction and release time characteristic for the type of muscle fibre involved. In dace the limit is reached at a frequency of beating of 25 Hz (Fig. 17). In fish larvae higher frequencies (40–50 Hz) for short periods of time (less than 1 second) are observed. Table 2 shows the swimming speed of some selected fish species.

In intermittent 'burst-and-coast' swimming, a swimming period of body oscillations is followed by a coast phase. During coasting the fish keeps its body motionless and straight, while pressing its fins against its body to minimise drag.

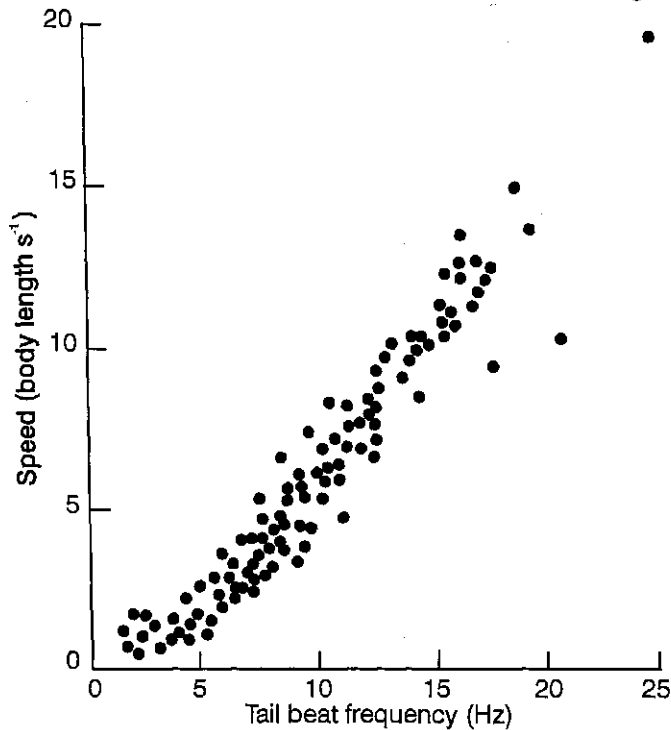


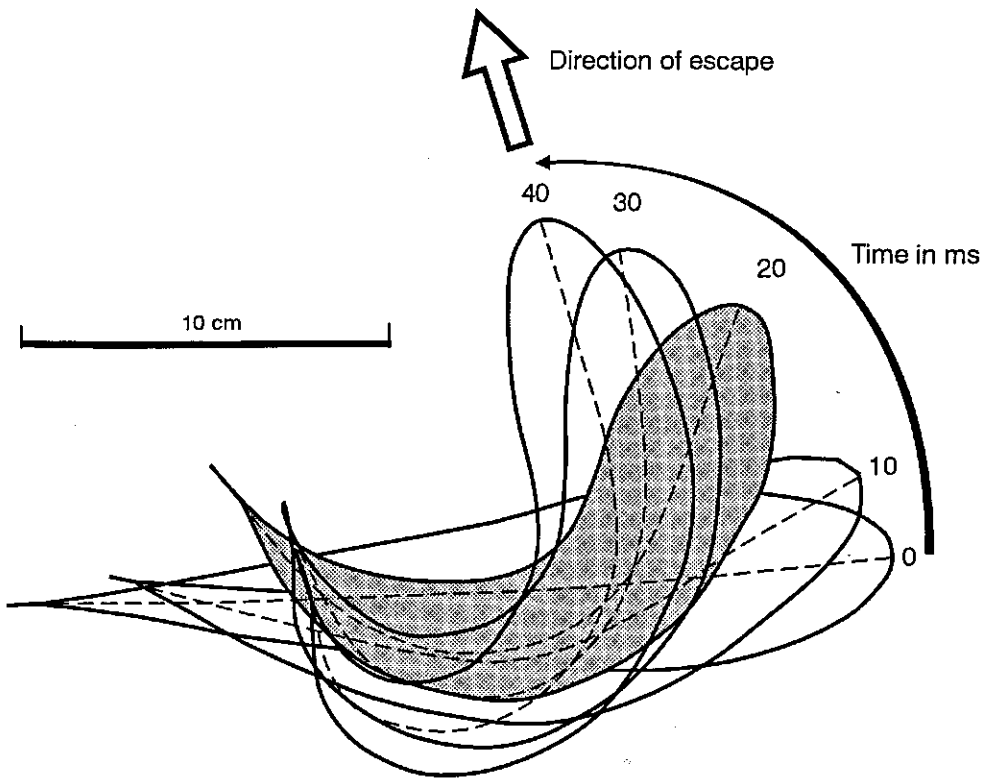
Fig. 17. Relation between tail beat frequency and relative swimming speed in dace (*Leucis cus*) of different sizes. Above a tail beat frequency of 5 Hz the relative swimming speed is directly proportional to tail beat frequency. Note that the larger, older fish are near the graph's origin. Frequencies larger than 25 Hz are only found in larval fish. Modified after Bainbridge (1958).

Table 2. Maximum and cruising speed of some selected fish species.

Fish species	Bodylength (<i>BL</i>) (cm)	Maximum speed (<i>BL s</i> ⁻¹)	Cruising speed (<i>BL s</i> ⁻¹)
Tuna	76	20	2.5–12
Mackerel	30	13	6
Cod	40	8	3
Saithe	20	10	4
Salmon	50	8	?–3
Perch	11.5	12.6 (1 s)	–
Pike Perch	43	4.2	–
Carp	35	8.2	–
Pike	30	10.5	1.5–4
Surf perch	15	3–8.5 (tail)	0–2.5 (pectoral fins)
Knife-eel	15	–	0–2.5 (pelvic fin)
Roach	22	5	–
Ruffe	10.5	12.7 (1 s)	–

Extreme body curvatures (cf. Fig. 13) are sometimes observed during a tight turn of manoeuvring fish. The fish body must meet many conflicting demands: rigid during coasting, flexible and powerful during acceleration, and flexible in extreme curvatures during quick, tight turns. Few studies have addressed turning in fish (but see Weihs, 1972). There is no doubt that the positions and movements of pectoral fins and pelvic fins are important during these activities.

Fast starts of fish are brief, sudden accelerations used during predator-prey encounters or for escaping predators (Fig. 18), and have attracted a lot of attention of fish biologists (among others Weihs, 1973; Webb, 1976; Domenici and Blake, 1997, review article). Two main types of fast-starts



Escape response of an adult carp; C-start

Fig. 18. Part of an escape response of an adult carp (*Cyprinus carpio* L.), 25 cm TL, filmed at 200 frames per second. Every second picture is shown. The dashed outline represents the maximum curvature of the fish. After 100 ms (not shown) a total angle of turn of 155° is reached.

are recognised, C-starts and S-starts (respectively Figs 19 and 20) in which the fish is bent into a 'C' or 'S' shape at the end of the first contraction of the lateral musculature. C-starts are mainly used by fish to avoid predators and imply large angles of turn, whereas S-starts are used by predators attacking prey and show displacement in line with the original body axis. In this latter start the S-shape probably reduces lateral movement of the head which is important in aiming at a prey during a fast attack. C-starts are initiated by a strong curvature of the body and a small arc of rotation of the

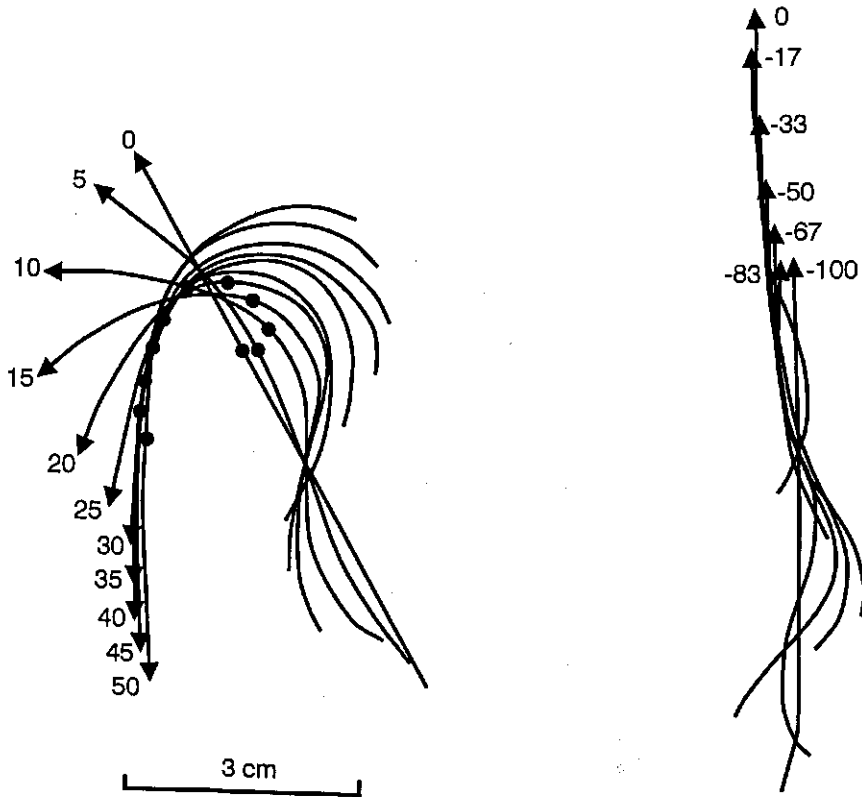


fig. 19

Small fish can turn nearly 180° in a C-start escape

fig. 20

20 cm

Fig. 19. Single-bend C-start in angelfish (*Pterophyllum eimekei*), the total fish length is 7.6 cm. Times between tracings are in milliseconds from the first detectable movement. The midline and centre of mass (filled circles) of the fish when stretched straight are shown. The head is indicated by the arrowhead. Modified after Domenici and Blake (1991).

Fig. 20. Example of an S-start. Pike (*Esox* sp.), total length is 21.7 cm, attacking a prey. Times between tracings are in milliseconds, measured backwards from a reference time of predator-prey contact. The head is indicated by the arrowhead. Note that the movement is in the same direction of the original position of the body. Modified after Webb and Skadsen (1980).

centre of gravity. The fish's final direction of escape seems hardly a matter of interest and is thus very useful as an escape motion due to its unpredictability. During normal swimming the waves of contraction of the successive segments originate from a central pattern generator found in the anterior spinal cord. How are the fish's muscles activated during these extremely fast escape and attack movements? C-starts are usually mediated by the Mauthner neurones and associated networks (Eaton *et al.*, 1991). Little however is known about the mechanisms controlling S-starts (Fig. 21), although Mauthner neurones can be active during the terminal phase of prey capture in goldfish (Canfield and Rose, 1993).

FAST STARTS

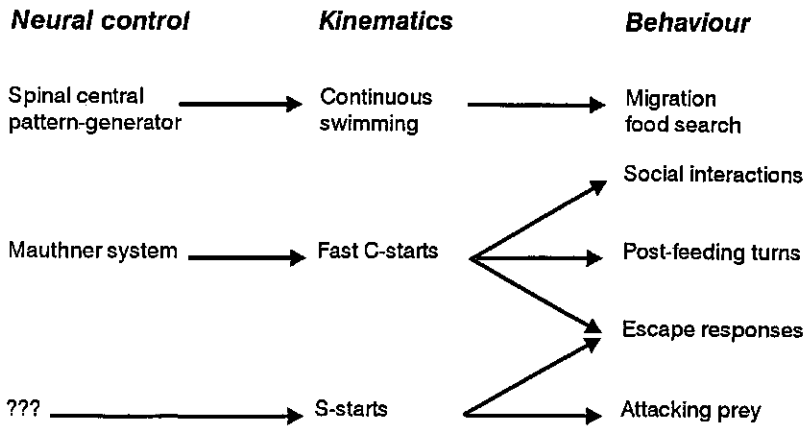
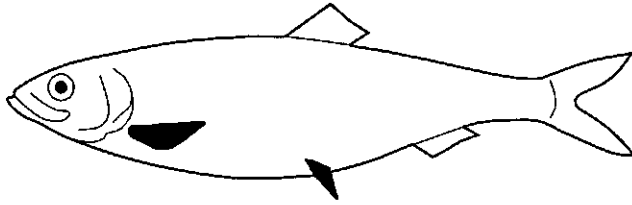


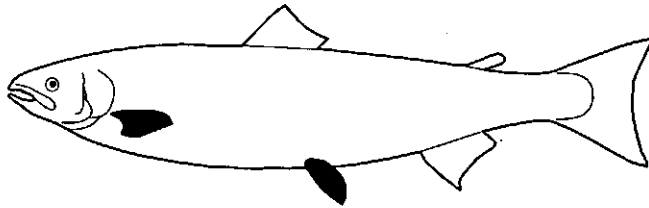
Fig. 21. Diagram relating the neural control, kinematics and behaviour. Higher centres (brain stem) can modify normal swimming actions. The question marks indicate that the neural commands driving S-starts are unknown. Various sources, a.o. Domenici and Blake (1997).

Pectoral fins, pelvic fins and median fins are important during swimming, steering and backing in fish (Fig. 22). Pectoral fins in teleosts are sometimes used in great variety of other functions, as propulsors, in benthic and terrestrial locomotion, for flying, attachment to the substratum, digging, defence, camouflage and even copulation (Bertin, 1958). In some fish groups pectoral fins contribute to propulsion. Straightforward swimming with pectoral fins takes place by undulations of the fin rays (Diodontiform mode) or by means of bilateral symmetric beating movements of these fins (Labriform mode, Breder, 1926; Lindsey, 1978). Skates and rays such as eagle rays (*Myliobatinae*) and large manta and devil rays (*Mobulinae*) use their large pectoral fins to fly underwater.

A Herring (*Clupea harengus*)



B Trout (*Salmo trutta*)



C Bass (*Dicentrarchus labrax*)

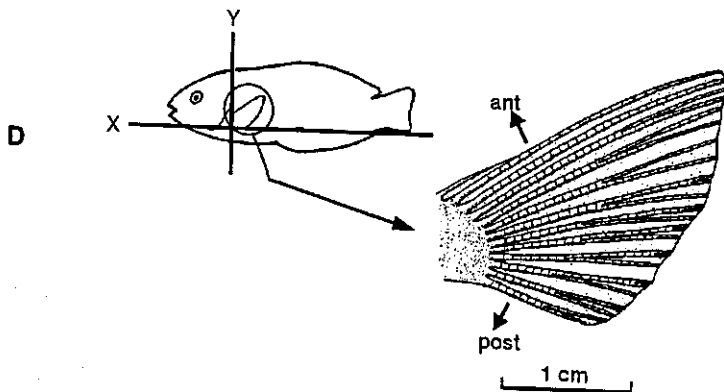
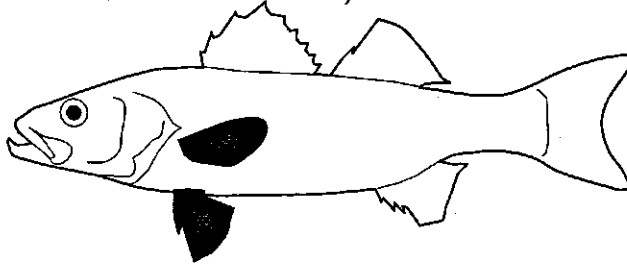


Fig. 22. Primitive teleosts have their pectorals in a low ventral position and pelvics also ventrally just in front of the anus (A,B). Perciforms (C) generally have a half way the body flank position of the pectorals and direct under them the pelvics, obtaining a far anterior position. A pectoral propulsor *Coris formosa*, a Labrid fish, is depicted in D. A functional interpretation of fin size and position is largely unknown. Modified after Nelson (1994) and Geerlink (1986).

2.7. PROPULSION, POWER AND DRAG

Direct push off of the fish body against the water results in propulsion. This way to obtain thrust is important in long cylindrical fish with continuous dorsal and anal fins and without a large tail fin (e.g. eel, *Anguilla anguilla*). Contraction waves with a large amplitude run along the body from head to tail.

In fish like cod, salmon and mackerel the body curvature has a much smaller amplitude; the largest excursion typically is found at the tail blade. The central question is how the lateral undulation of body and tail contribute to the backward momentum transferred to the water. Two mechanisms underlying the exchange of momentum are distinguished. A swimming fish, with its laminar boundary layer, coasts through a tunnel created by the forward moving head. Outside the tunnel the water is at rest. Because the lateral waves of body curvature travel at a larger speed than the forward movement of the fish these waves increasingly accelerate a mass of water in backward direction at both sides of the fish body. This moving water is found in the tunnel between the fish body and the motionless water surrounding the tunnel. The speed and mass of the moving water increase from head to tail due to the growing amplitude of the body waves and most energy is transferred to the water by the trailing edge of the tail fin. In this way undulations of the body, contractions of the anterior myotomes, may contribute to the propulsive forces. A second possible mechanism in which the contraction forces of the anterior myotomes can be transferred to the tail blade is through the leathery part of the skin acting as a tendon.

Lighthill's (1971) 'slender body' theory describes in detail how power (work per unit of time) is transmitted by the fish to the water. The power generated by the fish is used to overcome the drag of the water (P_d), to transfer momentum to the water (P_w) and to give the fish body a forward acceleration (P_a). The total power (P_{tot}) spend by the fish equals the sum of $P_d + P_w + P_a$. The power generated by the fish is spend efficiently if the useful power ($P_d + P_a$) has a large share in the total power P_{tot} . The hydrodynamic efficiency (Froude efficiency; $(P_d + P_a)/P_{tot}$) is high in most fish reaching values of 0.7–0.95. The hydrodynamic efficiency of humans during swimming is 0.3–0.4 and of a boat is 0.45. Such low efficiencies are due to moving at the water–air interface and the concomitant high drag. The economic use of the produced power clearly illustrates how well fish are adapted to swimming.

The drag (D), the resistive force that fish need to overcome during swimming is, within certain limits of the Reynolds number, given by the equation:

$$D = 1/2 \rho u^2 A C_D$$

where ρ is density, u is forward velocity of the fish, A is the effective cross-sectional area of the fish in the direction of movement, and C_D is a dimensionless number called the drag coefficient. The value of the drag coefficient depends on the shape of the fish body and the nature of its outer surface. Inspection of the drag equation immediately shows that the power required to overcome drag during swimming with a constant velocity u is proportional with u^3 , because power is the product of force

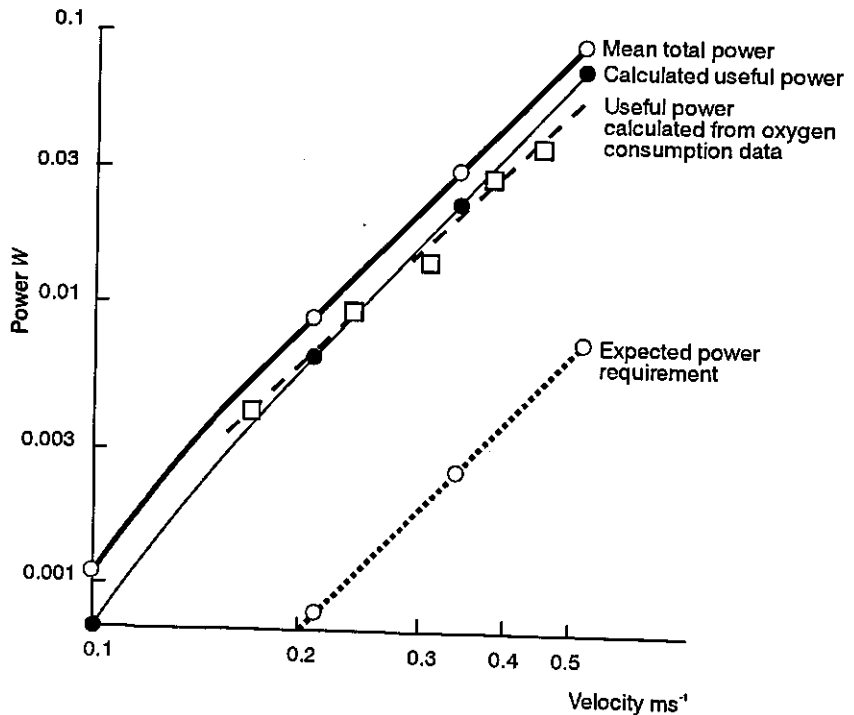


Fig. 23. The relationship between power and speed in a straight swimming trout (*Salmo gairdneri*) of 28 cm TL, weighing 220 g. The expected power requirement for a stiff body is also indicated. In the double logarithmic plot power increases with speed^{2.67}, which is close to expected value of 3. The considerable difference between required (7–9 times higher) and expected power has mostly been attributed to the effect of lateral undulation, increasing the drag considerably. Modified after Alexander (1978).

(proportional with u^2) and displacement per unit of time (speed, u). To double swimming speed a fish must generate 8 times its power previously used to overcome the drag.

Fig. 23 shows the relationship between generated power and swimming speed in rainbow trout (*Salmo gairdneri*). The drag of a fish during lateral undulations is 3 to 5 times higher than the drag when it is kept stiff and rigid. The formula shows that A increases importantly in that case. During coasting, intermittent 'burst-and-coast' (kick and glide) swimming it is energetically advantageous to combine short periods of movements with approximately equally long periods of gliding, utilising the obtained impulse moment to glide on seemingly effortless with a rigid body. Such swimming is easily observed in aquarium fish. It is an energy saving strategy of aquatic locomotion.

The maximum swimming speed of fish is only achieved when the white muscles generate the highest possible power. However, the white muscle fibres become rapidly exhausted. In two minutes

a trout consumes 50 % of its glycogen store in its active white muscles. In plaice exhausted by chasing them for two minutes (*Pleuronectes*) it took eight hours before the glycogen level in the white muscles reached 70 % of its original value (Wardle and Videler, 1980). Fish only generate their maximum power during short bursts of activity, in an attack or during escape movements. Such movements are a matter of life or death for both predators and prey. Finally, the question arises how fish apparently can afford to build up, maintain and carry approximately 90 % of their muscle mass when only using it now and then for just a few seconds. The answer may lie in the near weightlessness of a submerged fish, the need for a streamlined body which can efficiently be filled with useful muscle tissue with low basic metabolic rate.

2.8. THE GENERATION OF THRUST

Two processes in fish swimming are inextricably linked: (1) the generation of thrust by the fish body, and (2) the creation of a distinct wake in the water (see Childress, 1981 and Webb and Blake, 1985).

In order to overcome drag during continuous swimming fish must generate forward thrust, transported to the snouttip of the fish through the axial skeleton. Although fish generally are only slightly more dense than the water in which they swim they generally also have to generate a small lift force, being the difference between buoyancy and sinking forces. How does a fish accomplish this?

Thrust

Let us assume a semi-static mechanism of force production in which the fish body is stiff with only a flapping tail fin moving with a constant amplitude (Fig. 24A) When we consider the force of the tail fin acting on the water (= action force) and the force of the water acting on the fish (= reaction force) it is clear that this latter force provides the thrust. When the tail fin is moving away from the fully stretched position (Fig. 24B) the net reaction force is directed backwards, when the tail fin is moving towards the fully stretched position (Fig. 24C) the net reaction force is directed forward. In other words, during a complete beating cycle of the tail the fish would move alternately forwards and backwards, resulting in no motion at all. If we call the angle between the tail fin with the direction of motion α and the distance between the tail fin tip and the direction of motion d , then a graph of α and d during a tailbeat shows that α and d always are in the same phase, resulting in no net thrust.

A little more complex but more realistic picture (Fig. 25) emerges when we study a series of static positions but now include the undulation of the tail of the fish, so tail plus tail fin. Fig. 25A demonstrates one half tail beat and shows how the reaction force of the water now always maintains a forward component of thrust. Fig. 25B shows that by including the undulating of the tail, α and d now are constantly in a counterphase. The above semi-static picture might explain how in carangiform swimming a variable thrust force is maintained during undulation of tail and tail fin.

It is important to realise that thrust production during fish swimming cannot be adequately described by a sequence of static positions of the tail fin as done in Figs 24 and 25. The actual factors

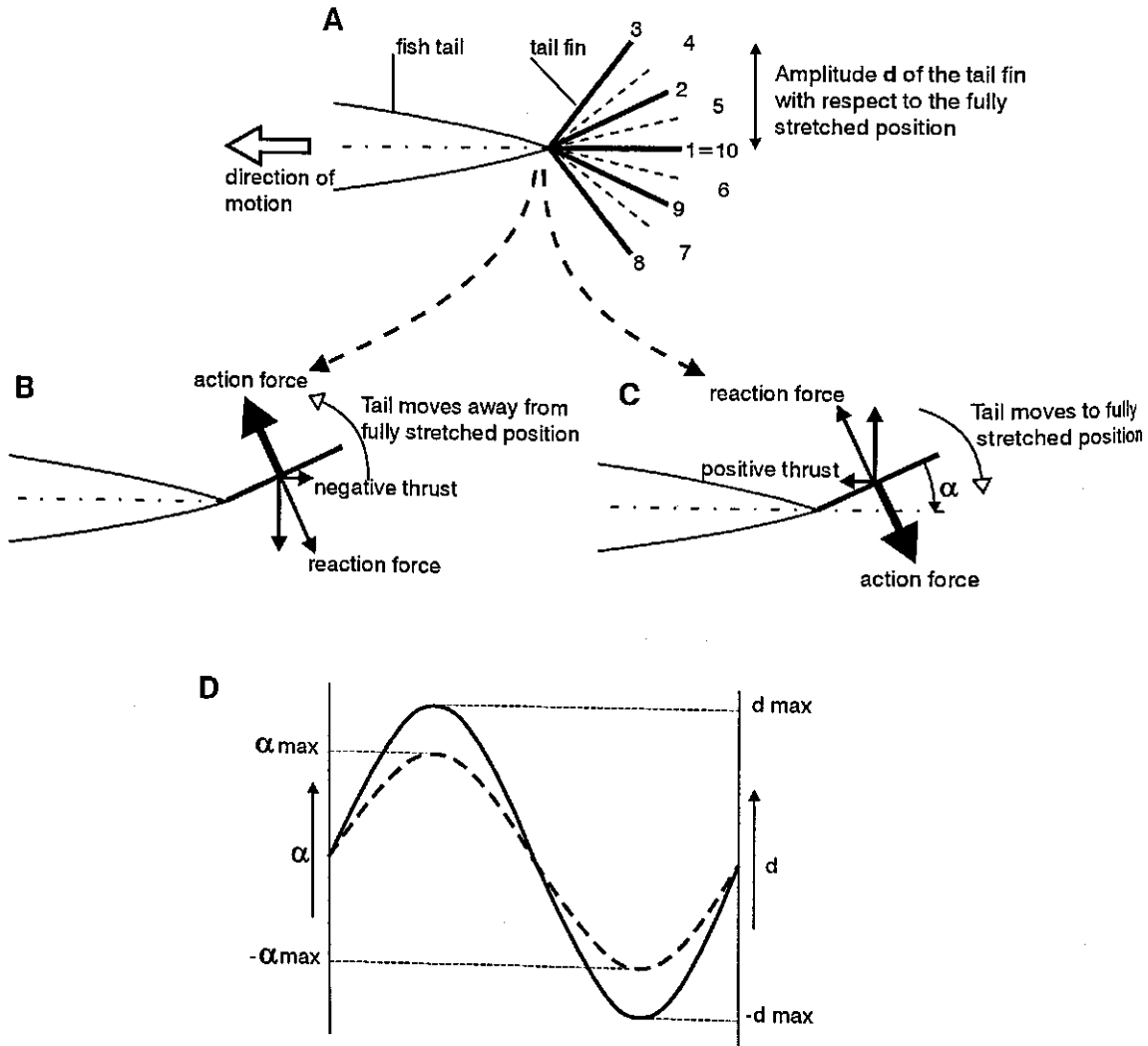


Fig. 24. Semi-static mechanism of thrust production in which the fish body and tail are taken to be stiff with only a flapping tail fin moving from the right to the left with a constant amplitude. (A) Numbers 1–10 indicate the sequence of positions of the tail fin. Amplitude (d) of the tail fin with respect to the direction of motion; (B) The net reaction force of the water dissolved into components shows the negative thrust (= reaction force) when the tail moves away from the fully stretched position; (C) When the tail moves towards the fully stretched position the net reaction force is directed forward and its component in the direction of motion provides a positive thrust. This suggests that only a flapping tail fin is ineffective for thrust production (simplified because unsteady effects are not included); (D) The angle of attack of the tail fin (α , the angle of attack lies between the tail fin and the direction of motion) differs with the same phase as the amplitude of the tail beat (d). In this situation there is no phase difference between α and d , resulting in no net thrust. Both angle α and amplitude d are indicated as percentages of their maximum value.

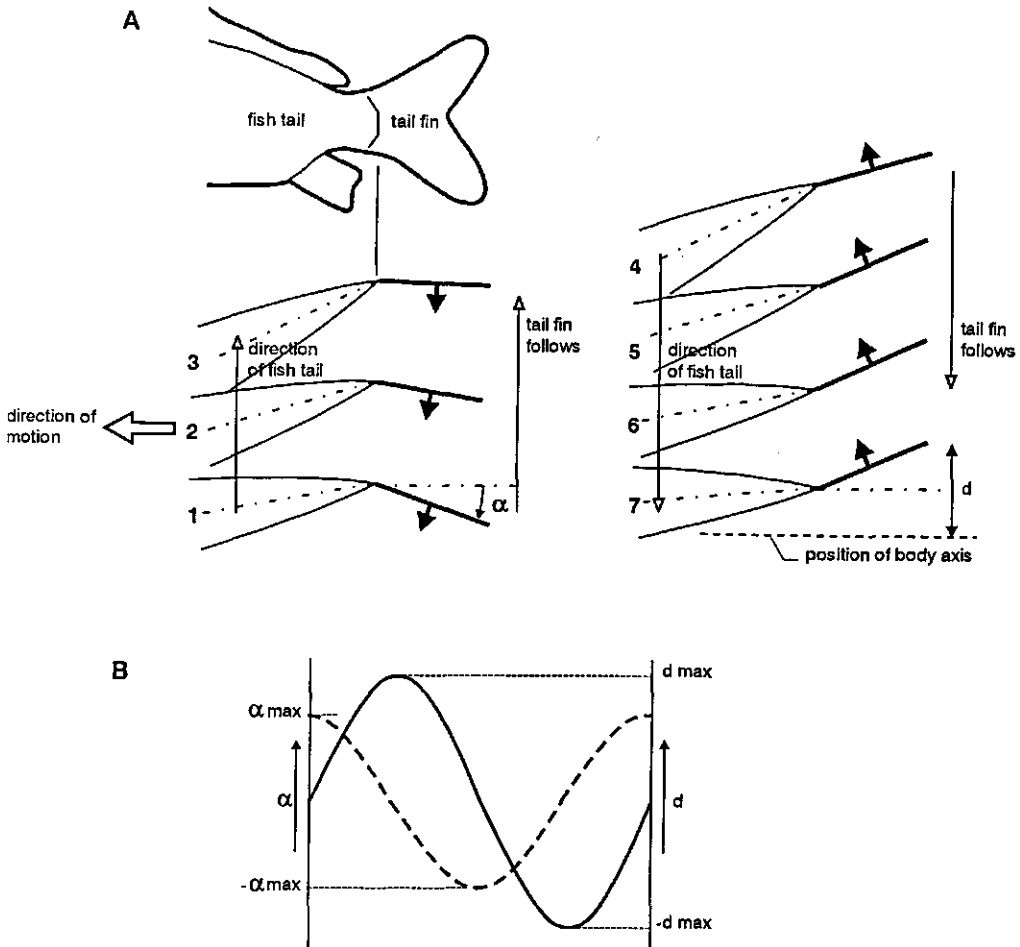


Fig. 25. More realistic mechanism of thrust production in which a phase difference exists between angle α of the tail fin and amplitude d of the tail beat. (A) The subsequent positions (1-7, half a tail beat) of the fish tail and its tail fin during the movement are shown. Angle α and amplitude d are shown with respect to the direction of motion. The fish tail moves and in time the tail fin follows this movement. The small black arrows indicate the direction of the reaction force of the water on the fish. Now this force is always directed forward, resulting in variable forward thrust; (B) Amplitude d of the fish tail and angle α of the tail fin are in counterphase. When amplitude d is maximal, angle α is small or zero and vice versa. In this way the reaction force of the water on the fish generates a variable forward thrust and the fish moves forward. Note that this is just a semi-static visualisation of how thrust is generated.

involved and how they interact to produce thrust are extremely complex to formulate. However, for the present purpose we must consider the importance of the dynamics of the swimming motion i.e. the variations in velocity and angles of attack (Daniel, 1984; Dickinson, 1996). Many fish swim by undulation of a posterior tail fin in which the tail moves a few chords lengths at a high angle of attack, stops, rotates slightly, and repeats the motion in the opposite direction. During this type of swimming the velocity and angle of attack of the biofoil (tail fin) changes. The tail fin has the highest velocity when it crosses the direction of motion, the angle of attack varies from nearly zero to approximately 20° . This creates an unsteady mechanism of thrust generation (Dickinson, 1996; Videler, 1993; Webb, 1975).

The creation of a wake in the water

To understand the mechanism a detailed knowledge of the flow pattern around the fish is needed. During each tail beat a force acting normal to its surface generates a vortex ring (rotating masses of water) in the water which is left behind (Fig. 26A). At the end of every stroke, the tail deposits the old vortex ring into the wake, reverses direction, and develops circulation in the other direction. Thus, each complete stroke cycle will produce a pair of vortex rings moving obliquely backwards in opposite directions (Fig. 26B). After several undulatory cycles, the wake will consist of a series of rings that continue to translate through the fluid under their own induced velocity, thus spreading the wake laterally (Dickinson, 1996). Fig. 26C gives an artist impression of a probable jet flow generated by the vortices behind a swimming tuna. The vortices, being the result of frictional- and inertial forces, determine the propulsive force of the fish. It is important to keep the energy costs of the production of such vortices as low as possible. As these costs are proportional to the square of the strength of the vortex (velocity of flow) divided by the square root of the surface of the vortex ring (its surface in a sideview) it is efficient to produce vortices with a large surface and a low rotation velocity. This is realised by fast swimming fish using a high narrow tail fin with a high aspect ratio (see later).

2.9. FORM OF THE TAIL FIN

In fish that are able to produce extremely large accelerations we intuitively expect a large surface of the tail blade to increase the mass of the accelerated water (see paragraph 2.5). The pike (*Esox lucius*) is an example of a fish with such a large surface area of the tail and tail fin. However, a large surface area of the tail blade is not observed in fish that are swimming fast over long distances (a high continuous swimming speed). In these fish it is important to minimise drag by reducing the surface area of the body and fins. It seems appropriate to mention here that the drag formula used earlier (paragraph 2.7) uses the effective cross-sectional area of the fish (A) and a drag coefficient C_d . Other ways to calculate drag is to use the wetted body surface S instead of A and to it belongs another drag coefficient C_s . It is clear that in a certain situation the value of the drag is a constant, whatever method you apply to calculate it. Fast long-distance swimmers are characterised by tail fins with a high

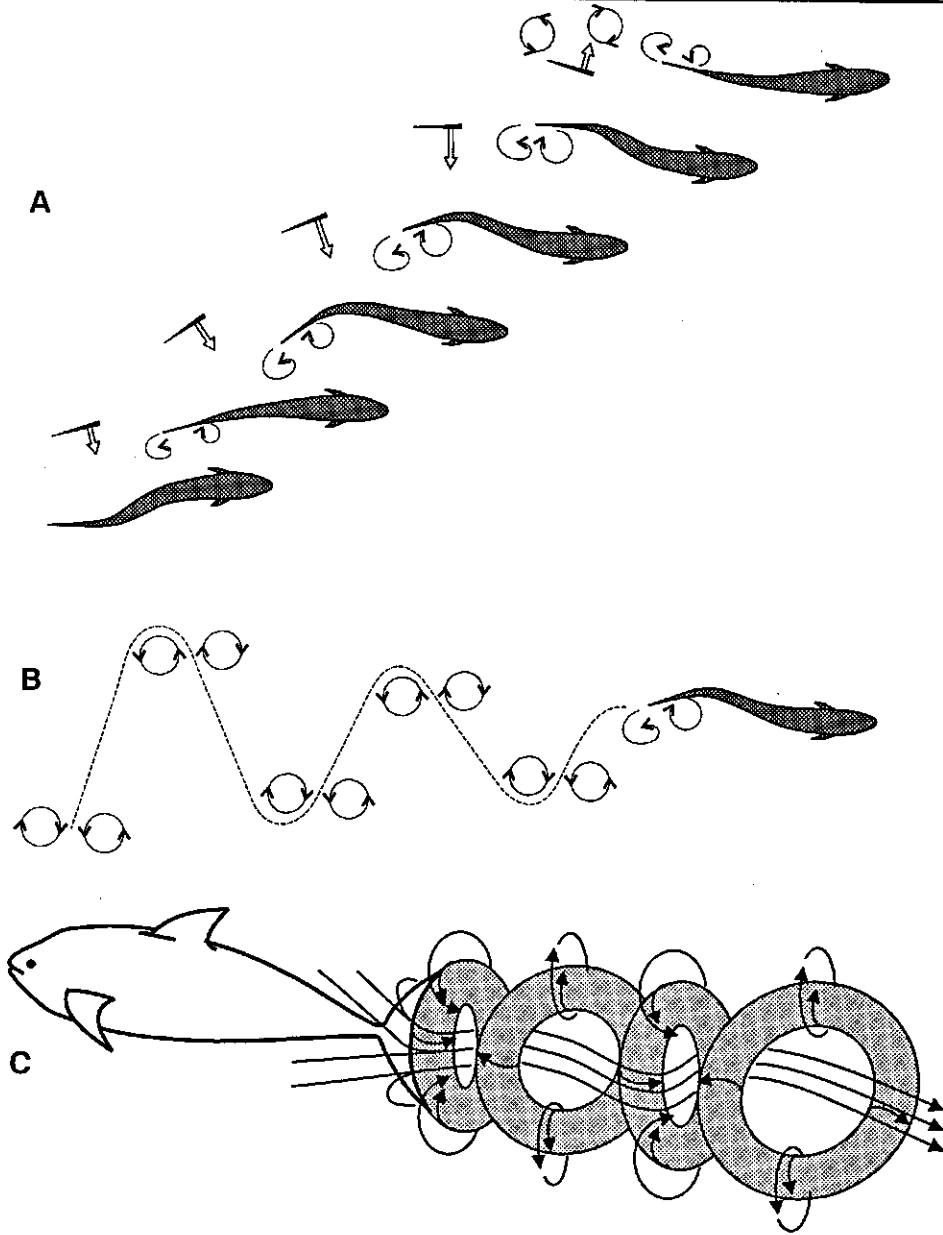


Fig. 26. Drawings of vortices in the wake behind a fish swimming with a beating tail. (A) The sequences start at the bottom and move to the right. Each lateral stroke of the tail creates a single vortex loop, seen in cross-section as a pair of starting and stopping vortices. The direction of the total circulatory force is indicated by the biofoil outline drawn to the left of each figure. Modified after Dickinson (1996); (B) After many stroke cycles the fish creates a wake of alternating vortex pairs, each moving laterally under their own induced velocity. Modified after Dickinson (1996); (C) Artist impression of flow through vortex loops during tail beats of a tuna. Modified after Lighthill (1971).

'aspect ratio', which is the square of the height (or span) of the fin divided by the surface area. The mackerel, a fast continuous swimmer, has a rounded body and the highest aspect ratio (Fig. 27). The vortices produced by the tail fin of a mackerel are efficient with a large surface area and small power, resulting in small velocities of the water in the vortices (e.g. Rayner, 1985). In this way, the energy needed for their generation their is kept minimal. The pike, an ambush hunter, has a huge caudal surface. It strikes a prey with a couple of high amplitude tail beats, accelerating a high mass of water thereby gaining a considerable speed in a fraction of a second. The white bream is a slow cruising benthic feeding Cyprinid. A discussion of the large variation in tail shapes, of which some are shown in Fig. 2, is outside the scope of this chapter. The characteristic asymmetric (heterocercal) tail fin of sharks was mentioned before.

2.10. ENERGETICS

The cost of swimming in fish, expressed in ml O₂ per hour-unit of weight, or in J kg⁻¹ m⁻¹, at the most efficient (i.e. optimum) speed is lower than for flying or running. Walking (or running) is the most expensive way of transport of animals. This result is at first view surprising because water is 800 times more dense than air and the drag at a given speed will be increased in a similar manner. Two factors must be considered here: (1) aquatic locomotion mostly is at relatively low speed (a 20 cm fish swimming 2.5 BL s⁻¹ travels at less than 2 km h⁻¹!); and (2) neutral buoyancy considerably reduces the cost of transport. Birds must generating lift forces, terrestrial locomotion requires muscles being active to lift the centre of gravity as well to control its drop. Most of these costs of transport are spent to keep the bird airborne, or for terrestrial animals to compensate the effects of gravity.

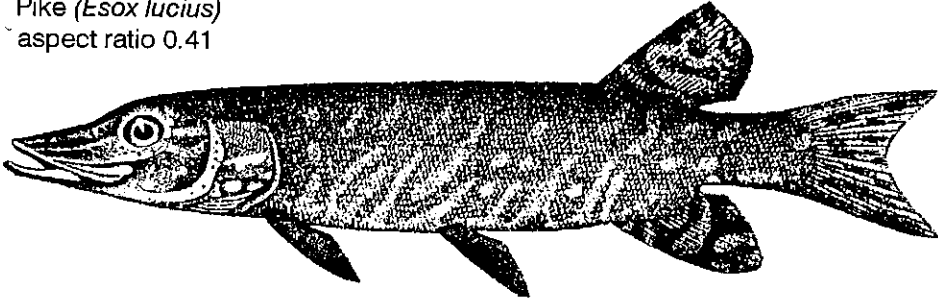
Energy required for sustained activity must be derived from aerobic metabolic activity. The difference between active and standard metabolic rate is called the scope for activity. It increases with temperature, the optimum temperature range is very different for cold adapted and tropical fish due to different activities of the myosin ATPase found in these different species. Many other factors like pH, toxicants, pressure etc., are important in determining this scope. External form, shape, surface structure and probable mucus determine the value of the drag coefficient and therefore the thrust required. The relation between the gross cost of transport (GCOT measured in J kg⁻¹ m⁻¹) of fish and swimming speed is given by Brett (1964) in an exponential function:

$$\log Q_{02} = \log Q_s + \alpha u$$

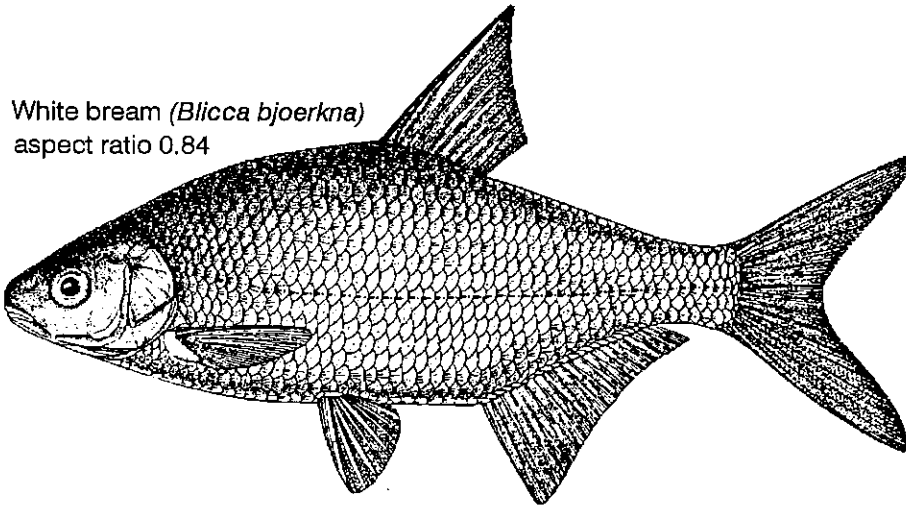
$$Q_{02} = Q_s e^{\alpha u},$$

where Q_{02} is the total metabolic rate, Q_s is the standard metabolic rate and α is the regression coefficient.

A Pike (*Esox lucius*)
aspect ratio 0.41



B White bream (*Blicca bjoerkna*)
aspect ratio 0.84



C Mackerel (*Scomber scombrus*)
aspect ratio 1.22

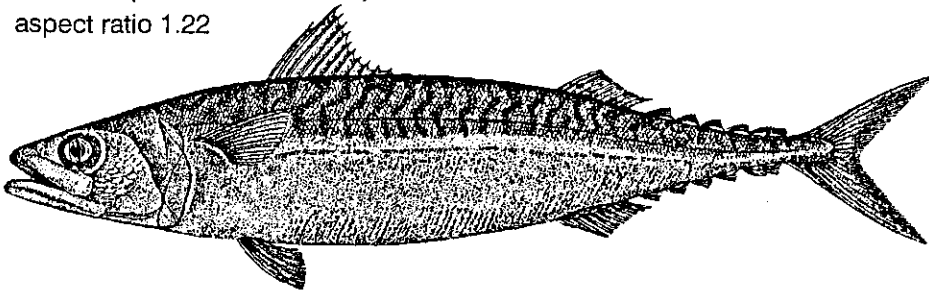


Fig. 27. Aspect ratio of several tail fins. (A) pike (*Esox lucius*); (B) white bream *Blicca bjoerkna*; (C) mackerel (*Scomber scombrus*). See text for further explanation. Drawings after Nijssen and de Groot (1987).

Based on data (Brett, 1964) from the sockeye salmon (*Oncorhynchus nerka*, Fig. 28). Fig. 28 shows, in arbitrary units, the U-shape of the relation between GCOT and speed. The choice of the exponent largely determines how apparent the U-shape will be. At low speed the contribution of the standard metabolism to the GCOT is relatively large, at moderate speed this fraction (per meter covered) is much smaller while at really high speeds the active metabolism becomes the dominant factor. Fish thus have optimal, fuel economic, speeds which we expect to reflect its mode of life and type of food and habitat. In this way the explanation of a particular fish in a specific biotope can be derived from detailed knowledge of form-structure relations.

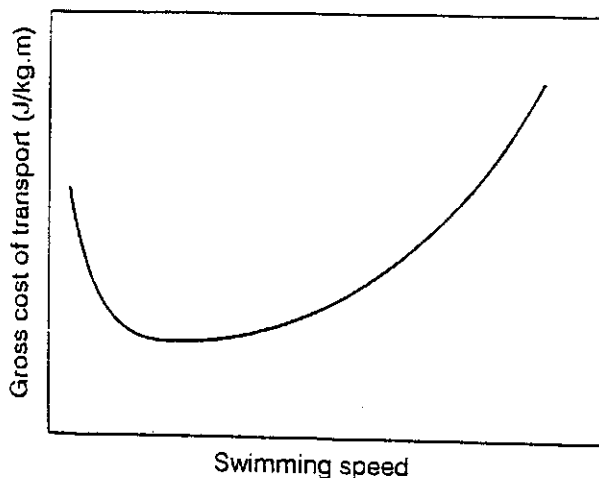


Fig. 28. The relation between the gross cost of transport in a sockeye salmon (*Oncorhynchus nerka*) and the swimming speed. The graph here is based on data from Brett (1964) and given for a value 1 for α . Modified after Webb (1993).

Fig. 29 demonstrates the effect of size in the cost of transport. In general the transport costs per unit weight decrease in big animals, although such a relationship does not always exist.

Next to an aerobic metabolism fish also have an anaerobic energy system. Both may be high in active fish or both may be low in sluggish species but also an inverse relationship has been found. In sedentary species, e.g. mudminnow (*Umbra limi*), the lactate production may be twice as high than in an active species. Our present knowledge on the relation between mode of life and metabolism in fish species is still largely incomplete.

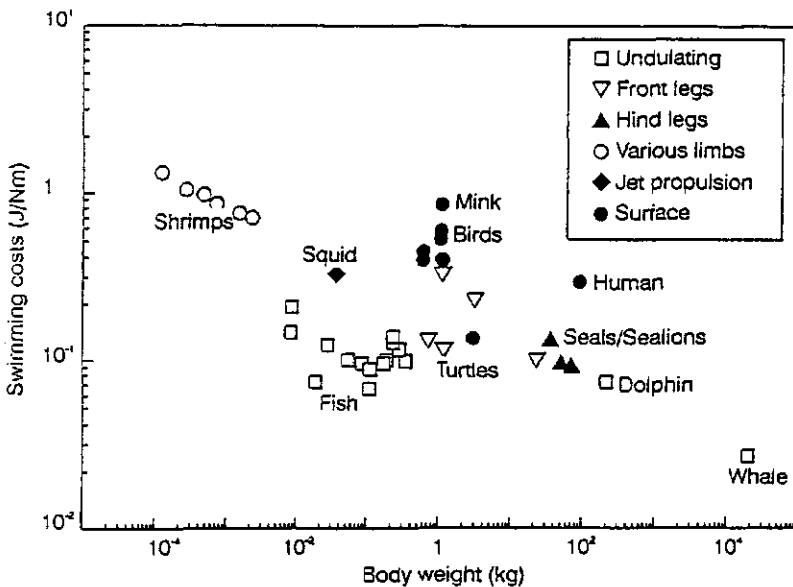


Fig. 29. Cost of swimming (J/Nm) in relation to body mass of different types of animals. Note that fish occupy the most cost effective swimmers. Modified after Videler (1992).

2.11. HOW ARE THE BODY UNDULATIONS, SEEN DURING SWIMMING, PRODUCED?

A continuously swimming fish needs a thrust to equal its drag. To produce this the fish continuously bends its body and tail to right and left side (Fig. 15). The propulsive force needs not to be constant during oscillation cycles but the fish must be able to maintain a certain average level of thrust generation during swimming cycles.

In the trunk of a fish body, from head to just behind the anus, mainly positive work is done by the muscles ($W = F \Delta V$, Fig. 7). The muscles shorten ($\Delta V =$ positive) while supplying power, and the bending momentum and body curvature are almost in phase. The tail lags behind in movement, here the generation of the bending moment and the resulting curvature differ in phase. The large surface area of the tail blade creates this delay. This means that when the contraction of the body muscles arrives at the tail the tail fin continues to move away from the generated bending moment. In this part of the body *negative* work is done because the muscles and tendons supply power while being stretched ($\Delta V =$ negative). Here, energy is absorbed, stored in the tendons as elastic (potential) energy and released during the subsequent half beat of the tail fin (van Leeuwen *et al.*, 1990; van Leeuwen, 1995). Blight (1977) demonstrated in a model study that even one-sided contractions of the body musculature can produce a wave form of the body (Fig. 13) because of the interaction between

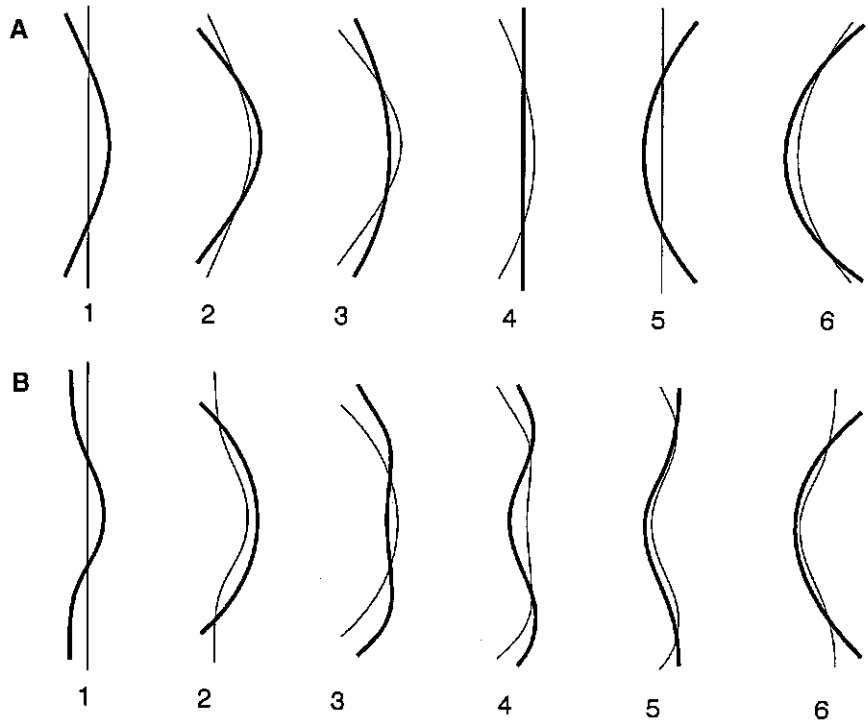


Fig. 30. Model of a fish represented by a stiff homogenous bar being bent to left and right. The previous position of the bar is drawn with a thin line in every next drawing. (A) Moving in air: the stiffness of the bar dominates its form changes: in each cycle two straight-line positions occur; (B) Moving in water: now resistive forces from the interacting between bar and water dominate the movements. Starting form a straight-line position no further straight-line positions occur but an undulatory movement develops, depending on the structure and movements of the model. Modified after Blight (1977).

fish and water (Fig. 30). This suggestion of Blight (1977) has been confirmed by calculations of Hess and Videler (1984) who observed this pattern of movement in the saithe (*Pollachius virens*). In the eel (*Anguilla anguilla*) a delay in the generation of power is observed between the anterior and posterior side of the body. The undulations seen in the fish body during swimming thus are the result of the generation of power by the body musculature, its elastic properties and hydrodynamic interaction between fish and water.

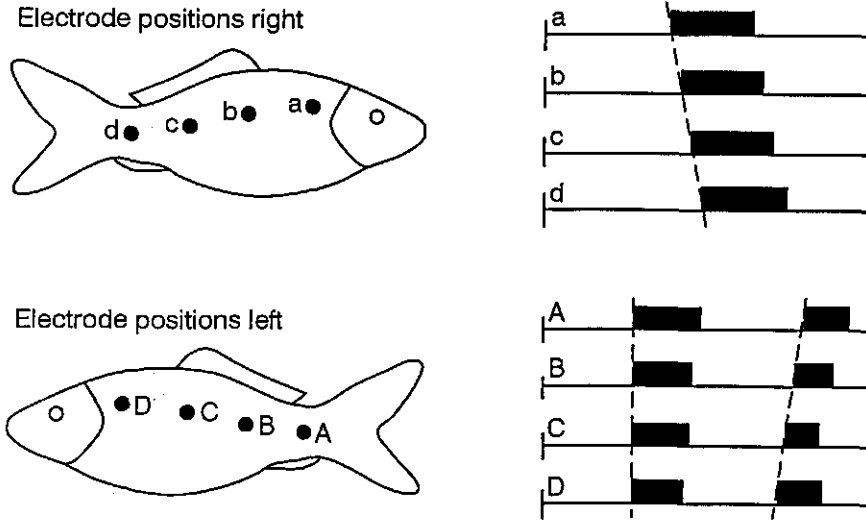


Fig. 31. Time of muscle activity measured at 8 positions in a carp during the start of a swimming period. During the start synchronous activity occurs along the complete length of the body. Later waves of contracting muscles alternating between left and right side are observed. Modified after van Leeuwen *et al.* (1990).

Both synchronous and delayed activity of body muscles during swimming have been recorded in free swimming fish. Electric activity of body muscles was recorded using 50 μm diameter wire implanted at eight locations along the fish body. During starting synchronous activation of the muscles on the left side of the body is recorded. (Fig. 31). So some evidence supports the theory of Blight (1977). Thereafter we observe a wave of contraction of body muscles from anterior to posterior alternating between left and right side of the body. So the body undulations are the results of waves of contraction passing along the length of the body.

How is the power, created by the body muscles, transferred to the tail? Although the greater part of the body muscle mass used in swimming is situated between head and tail, a disproportionate part of the swimming power is transferred by the tail fin to the water. The transfer of energy in the fish body was studied by Hess and Videler (1984). In their analysis of the generation and transfer of power, the fish is conceived as composed of a series of slices from head to tail (Fig. 32A), where each slice is regarded as a separate element. The sum of the forces and moments (the product of force and its distance to the centre of rotation) working on each element is determined (Fig. 32B). The power generated by an element may increase its own kinetic energy, be transferred to the water or transported anteriorly or posteriorly along the body (Fig. 32C). As mentioned above this transfer differs between body and tail.

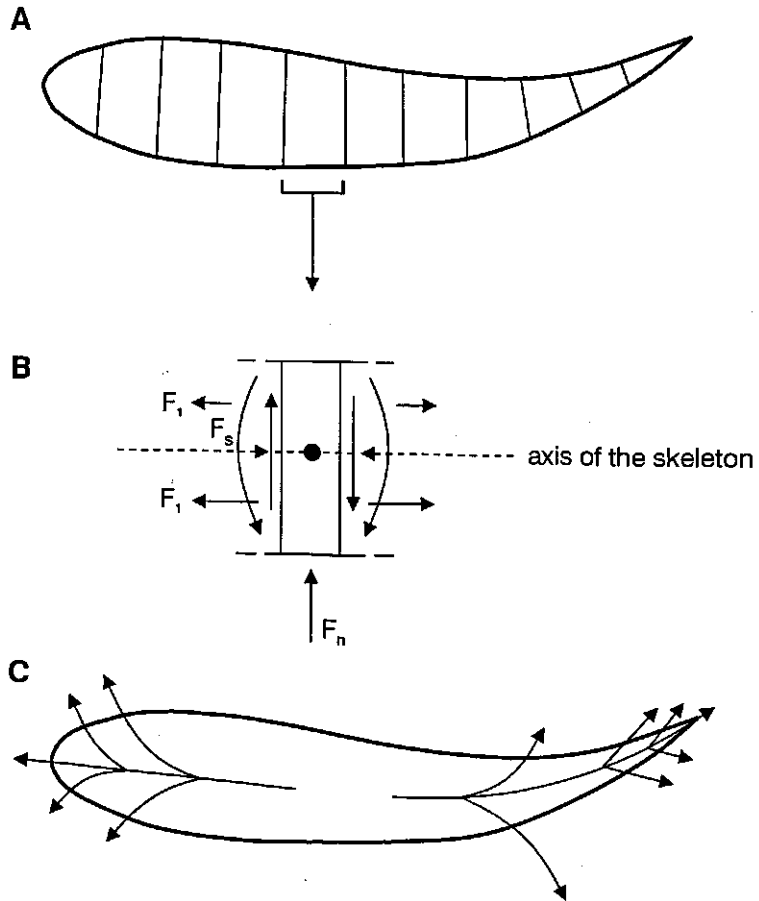


Fig. 32. Analysis of the bending moments and power transports within a fish body. (A) The fish body is divided in a series of elements (final elements method). For the actual calculations much more and much smaller elements are used; (B) Forces and moments working on one element. F_s , sliding forces exerted by preceding and following elements; F_1 , longitudinal forces (different at both sides of the medial plane); F_n , compressive force resisted by the vertebral column; F_1 and F_s forces exert moments, depicted by the curved arrow. The total bending moment is the sum of the individual moments; (C) Schematic representation of the direction of power transport.

Muscles in fish differ in two aspects from those in terrestrial animals. In the limbs of terrestrial animals muscles shorten by contraction and in this way supply rotating couples upon systems of levers. In the tail of fish active muscles are stretched and the resulting high force, exceeding that of isometric contraction, brakes the tail blade and moves it back.

The thickening of the limb muscles results in a bulging (swelling) of the skin without any further mechanical effect (except on the vascular supply). Muscle contraction during bending movements of fish also results in local thickening of the body. At these locations, muscles exert forces in a transverse direction on the skin. Collagenous fibres run criss-cross in the skin (Fig. 4C). At the flanks of the fish near its middle portion, the myosepts are also attached directly to the skin (e.g. in the cod, *Gadus morhua*). Several authors (Videler, 1975; Wainwright *et al.*, 1976) have suggested that in tightening the network of collagenous fibres in the skin by the transverse forces, power is transferred through the skin to the tail region. Whether this system really contributes to the transfer of power is unknown. It is also unknown whether the tensile strength of the skin increases in the direction of the tail fin, a property we would expect if transfer of power to a narrowing section of the skin is important.

2.12. SWIMMING ADAPTATIONS IN DIFFERENT FISH SPECIES

Webb (1984a,b) divided fish after their body shape, fin form and swimming movements into three types of extreme specialists and a large number of intermediate, more generalist types. When the specialists are placed at the corners of a triangle (Fig. 33) other, more generalist, species may be positioned inside the triangle. Most fish species do not belong to one of the three specialist types, but instead display features derived from more than one of these type. The three specialist groups are: (1) fish constructed for fast continuous swimming like the extremely streamlined, spindle-shaped tunas (*Thunnus*), (2) specialists for bursts of high acceleration like the pike (*Esox lucius*) and (3) short-bodied, laterally-flattened manoeuvring specialists like butterfly-fish (*Chaetodon*).

Tuna have extremely smoothed streamlined bodies with the thickest part at approximately one fourth to one third of its length, a narrow caudal peduncle, and a high and narrow tail fin (with a high aspect ratio). The fins that are not used during fast continuous swimming fit neatly into special slots and grooves of the body wall, thereby preventing surface irregularities. During swimming the body is kept stiff with minimal lateral movements. This importantly reduces the drag. Oscillating lateral motions are restricted to the tail where the narrow caudal peduncle reduces the lateral component of the force exerted on the water (and thus the amplitude of the lateral movement of the body). The spindle-shaped body has a minimal drag coefficient C_D (Hertel, 1966). Lateral movements of the body are further reduced by concentrating the main part of the body mass just behind the head. While the small surface area of the tail blade reduces frictional forces, its large height increases the efficiency of propulsion (high diameter, low vorticity and vortices in the wake). In tuna, specialisation for fast cruising has a negative effect on the manoeuvrability of the fish: only 10–15 % of the prey fish in view are captured (Webb, 1984a,b). Tuna follow over long distances, large schools of herring-like fish.

Pike, scorpion fish and to a lesser extent sculpins are specialists in acceleration. They remain more or less stationary in the water, lying in ambush between stones or vegetation until a potential prey occurs within striking distance. The large acceleration during the strike results from the high backward acceleration given to a large mass of water. It is caused by a few high amplitude (powerful)

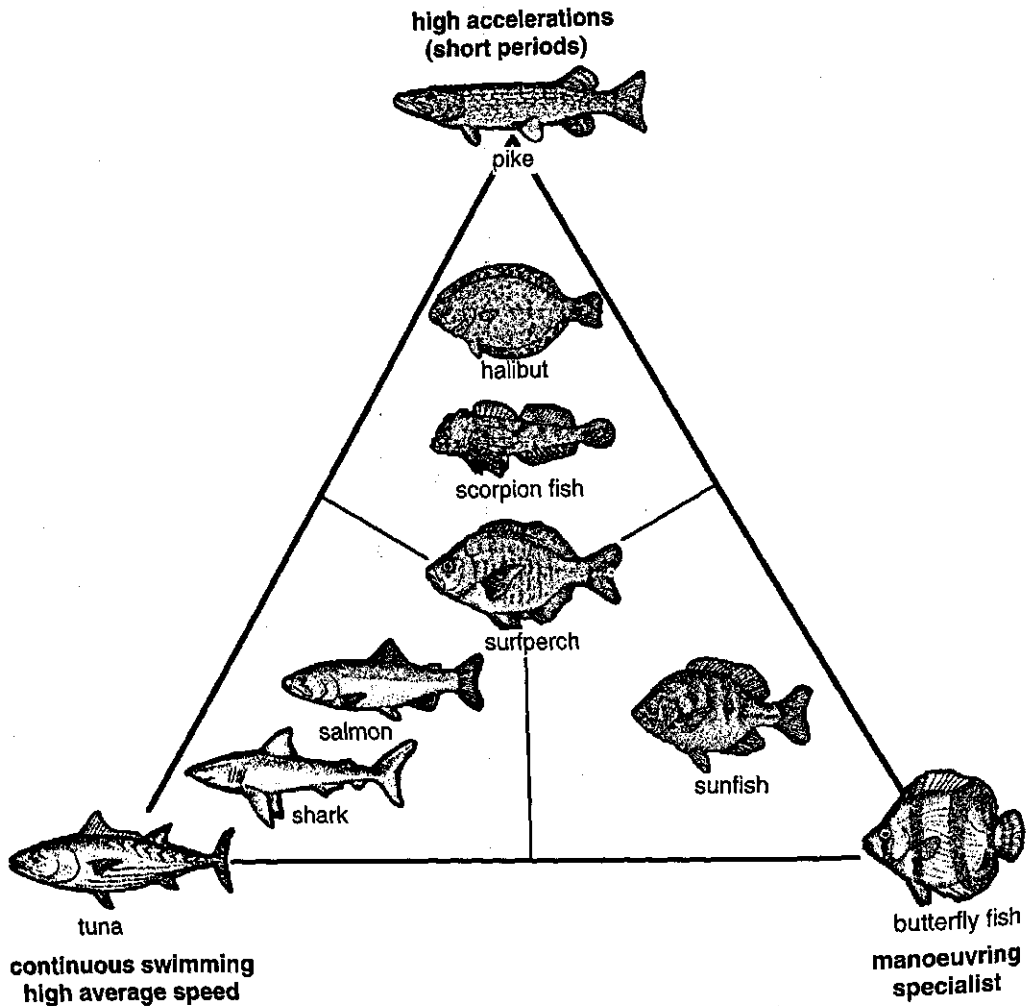


Fig. 33. Classification of swimming types with specialists on the corners and the more generalistic species in the middle. Structural requirements for the three specialist swimming types can not be combined in one fish's body. The extremely streamlined tuna (left) is a fast continuous swimmer, the pike (top) a very fast ambush hunter and the butterfly fish (right), a precisely manoeuvring coralfish. Good swimmers, also with lateral undulations, are shown down left. Down right is the sun fish, using besides its tail also its fins, and from the top to the centre fish are shown that are less and less pure ambush hunters. The surf perch (Fam. *Embiotocidae*, *Periformes*) is considered to be an all-rounder, its construction has elements of the three specialists. Modified after Webb (1984b).

beats of body and tail. Its large tail fin and the closely associated dorsal and anal fins (positioned extremely rearward close to the caudal fin) provide a large surface area. The whole white muscle mass is involved in this fast attack and constitutes more than 60 % of the total body mass. Such a large mass of muscles is characteristic for pike, but not found in sculpins. During continuous swimming of pike a large friction drag would develop as a result of the large surface area of the tail and its associated fins. However, during the short period of acceleration (e.g. 100 ms), friction drag is initially still relatively low, because it takes some time before a friction boundary layer is formed. The long flexible body, necessary to produce the first big beats of the tail during acceleration, decreases the ability of the fish for turning and subtle manoeuvring.

The third group of specialists, the manoeuvring experts, occur in many varieties and large numbers in eel-grass beds and coral reefs. Precise manoeuvring is necessary in aiming at small prey hidden between the coral branches (e.g. polychaetes). Continuous fast swimming is hardly observed in these fish, but the complex structure of their habitat offers plenty of hiding places enabling them to escape from their predators. The manoeuvring specialists have a short, manoeuvrable body often with oscillating propulsive pectoral fins positioned near the centre of gravity of the body. In this way the pectoral fins are able to produce (rather small) forces in any direction, allowing subtle manoeuvring movements. The big median fins with numerous fin rays, each one provided with erector, depressor and inclinor muscles, enable subtle forward and backward undulations of those fins as well as rotations. Vertical movements are produced by tail fin undulations. In some species, the pectoral fins are used as rowing oars: during the propulsive stroke the fins beat backward with a higher speed than the forward velocity of the fish and during the back stroke they are kept in a horizontal position. A very different type of propulsive stroke is found in butterflyfish (*Chaetodon*) and wrasse (*Coris formosa*, Fig. 22D). Here, the pectoral fin is moved down and forwards at an oblique angle in a transverse plane perpendicular to the swimming direction. In the back stroke the fin is moved up and backwards to its starting position. This beating hydrofoil provides thrust. The downward stroke of the pectoral fins of *Chaetodon* generates a lifting force directed forwards at an oblique angle. Propulsion results from the forward component of the lifting force, but also the backward stroke generates a propulsive force. The small base of attachment of the pectoral fins allows for the great flexibility needed in the complex fin stroke; the rounded distal part of the fin reduces the water flow across the moving fin.

Less specialised fish are placed within the triangle formed by the three extreme types (Fig. 33). The generalist species do not trade manoeuvrability for fast, low cost swimming, nor streamline for a small turning circle. The surface area of their tail fin does not produce large friction drag during periods of continuous swimming.

It is clear that it is not possible to combine the very different requirements for fast continuous swimming, high instantaneous acceleration, and precise manoeuvring in one fish. This is known as the compromise principle of functional morphology. Most fish species show a mixture of the different characteristics of the super specialists, adapted to the environment in which they live. The choice of these three extremes has the advantage that the required construction features are to some degree contrary. Videler (1993) distinguishes more types but also that approach is not solving the problem to attribute a swimming type to each of the 25.000 species of fish. It is clear that the biomechanical

approach followed in the present chapter is needed to clarify the complex relationship between the way fish live and the body form associated with swimming but details about the way of life are indispensable.

2.13. SWIMMING OF FISH LARVAE

Fish larvae may be as small as 1.2 mm total length (*TL*) but are generally at hatching between 3 and 6 mm *TL*. The *Re* number of a cruising fish larvae at e.g. 3 bodylength $s^{-1} = 3 \times 10^{-3} \times 9 \times 10^{-3} \times 10^6 = 27$ (cf. paragraph 2.5), which is well within the viscous regime. Swimming at these *Re* values thus suggest an important drag due to a relatively large mass of water moving with the larvae. At such *Re* values streamline is not important, because advantages of a streamlined body are mainly based on inertial forces and not on viscous forces. The natural history of fish larvae shows that their streamline indeed seems not of much concern. Fish larvae around 5 mm swim in a kind of anguilliform motion (Fig. 34). This changes at higher speed, larger size, or both rapidly into a sub-carangiform motion that consists of undulations of increasing amplitude towards the tail starting at approximately half bodylength. Fig. 34 clearly shows the anguilliform curvature of the body in the initial tail beats. It also demonstrates that at the end of the movements, when the animal's body is again fully stretched the gliding with the acquired impulse is very, very small, only 1/3 of one bodylength in 280 ms. This is the effect of the low *Re* number. The primordial or median fin fold found in all small fish larvae, bearing numerous tiny collagen-like fin rays (called actinotrichia), most probably is an adaptation to early swimming in a low *Re* regime.

The change in body curvature during swimming in larvae of the carp from 4.8 mm to 23.6 mm *TL* (Fig. 35) shows the transition from anguilliform swimming to carangiform. In the latter thrust is mainly generated at the tail blade. The morphological development of the tail fin leading to ossified fin rays is closely synchronised with this change from anguilliform like to carangiform swimming. In the latter the reactive forces of the water on the moving tail are transmitted to the body axis by the now stiff lepidotrichia of the tail.

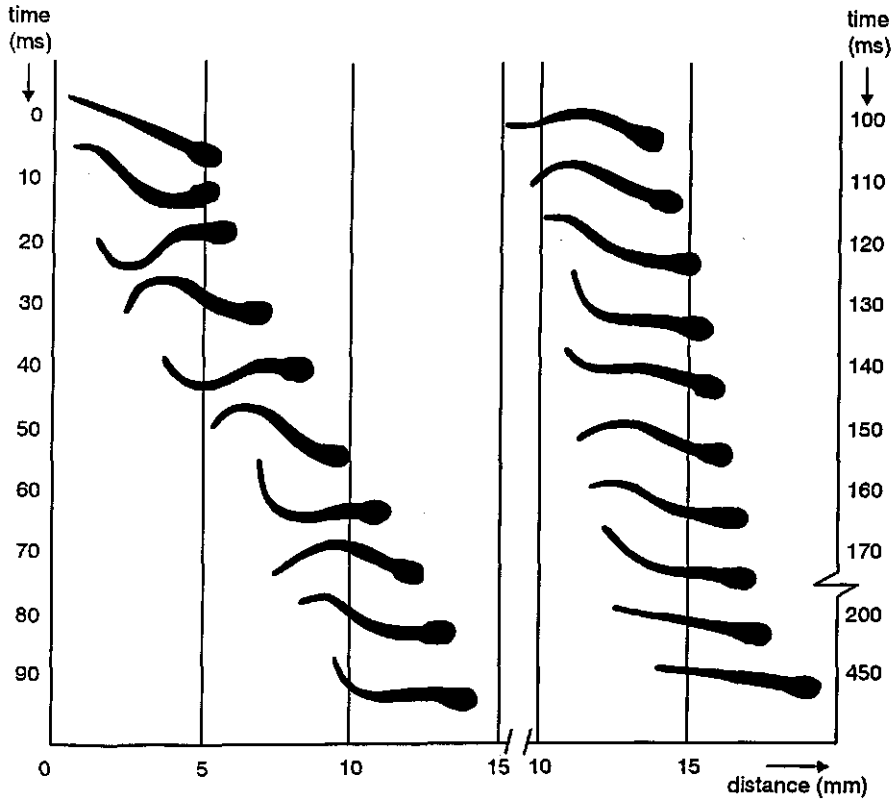


Fig. 34. Burst swimming of carp larvae, 5.45 mm TL. Note the anguilliform (eel-like) early swimming strokes. In 200 ms approximately three bodylength are covered, a swimming speed of approximately 15 bodylength s^{-1} is reached. Gliding is hardly effective at this size and speed. In 250 ms the animal glides with the obtained speed less than $1/3$ bodylength. Modified after Osse and Drost (1989).

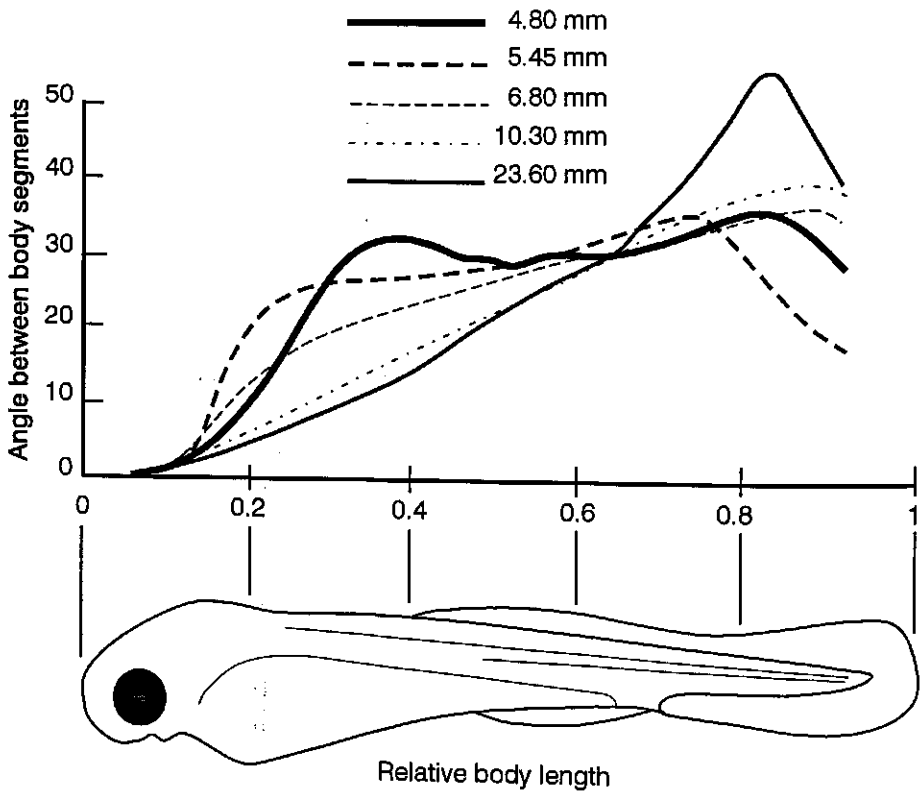


Fig. 35. Averages maximum angles of body curvature over whole spontaneous swimming bouts in larvae and juveniles of five size classes of carp. The body axis is divided into 12 segments of equal length and the angles between these segments are depicted. Note how the form of the swimming motion changes with body size. The fish larva shown beneath the graph has a total length of 5.45 mm. Modified after Osse (1990).

REFERENCES

- AKSTER, H.A. AND OSSE, J.W.M. (1978). Muscle fibre types in head muscles of the perch *Perca fluviatilis* (L.), Teleostei. *Neth. J. Zool.* **28**, 94–110.
- AKSTER, H.A. (1983). A comparative study of fibre type characteristics and terminal innervation in head and axial muscle of the carp (*Cyprinus carpio* L.): a histochemical and electron-microscopical study. *Neth. J. Zool.* **33**, 164–188.
- AKSTER, H.A. (1985). Morphometry of muscle fibre types in the carp (*Cyprinus carpio* L.). Relations between structural and contractile characteristics. *Cell Tissue Res.* **241**, 193–201.
- ALEXANDER, R. MCN. (1969). Orientation of muscle fibres in the myomeres of fish. *J. Mar. Biol. Assoc. UK* **49**: 263–290.
- ALEXANDER, R. MCN. (1975). *The chordates*, pp. 142–154. London: Cambridge University Press.
- ALEXANDER, R. MCN. (1978). *Fish swimming: size and shape related to energy consumption*. Proc. of the Zodiac Symposium on Adaptation, pp. 44–47. Wageningen: Pudoc Wageningen.
- ALEXANDER, R. MCN. AND GOLDSPIK G. (1977). *Mechanics and energetics of animal locomotion*, pp. 18–22. London: Chapman and Hall.
- BAINBRIDGE, R. (1958). The speed of swimming as related to size and to the frequency and amplitude of tail beat. *J. Exp. Biol.* **40**, 23–56.
- BERTIN, L. (1958). Modifications des nageoires. In *Traité de Zoologie*, tome XIII (ed. P.P. Grassé), pp. 710–747. Paris: Masson et Cie.
- BLIGHT, A.R. (1977). The muscular control of vertebrate swimming movements. *Biol. Rev.* **52**, 181–218.
- BODDEKE, R., SLIJPER, E.J. AND STELT, A. VAN DER (1959). *Histological characteristics of the body musculature of fish in connection with their mode of life*, Proceedings, Series C, Vol. LXII, pp. 576–588. Koninklijke Nederlandse Akademie van Wetenschappen.
- BONE, Q., MARSHALL, N.B. AND BLAXTER, J.H.S. (1995). *Biology of fish*, second edition. London: Chapman and Hall, 332 pp.
- BREder, C.M. (1926). The locomotion of fish. *Zoologica* (NY) **4**, 159–297.
- BRETT, J.R. (1964). The respiratory metabolism and swimming performance of young sockeye salmon. *J. Fish. Res. Bd. Can.* **21**, 1183.
- CANFIELD, J.G. AND ROSE, G.J. (1993). Activation of Mauthner neurons during prey capture. *J. Comp. Physiol. A* **172**, 611–618.
- CAMPBELL, N.A. (1996). *Biology*, fourth edition. New York: The Benjamin/Cummings Publishing Company, Inc. 1206 pp.
- CAREY, F.G. AND TEAL, J.M. (1966). Heat conservation in tuna fish muscle. *Proc. Nat. Acad. Sci. U.S.A.* **56**, 1464–1469.
- CAREY, F.G. AND TEAL, J.M. (1969). Regulation of body temperature by the bluefin tuna. *Comp. Biochem. Physiol.* **28**, 205–213.
- CHILDRESS, S. (1981). *Mechanics of swimming and flying*. Cambridge: Cambridge University Press. 155 pp.
- DANIEL, T.L. (1984). Unsteady aspects of aquatic locomotion. *Amer. Zool.* **24**, 121–134.

- DAVIES, L.F., JOHNSTON, I.A. AND WAL, J.W. VAN DE (1995). Muscle fibres in rostral and caudal myotomes of the Atlantic cod (*Gadus morhua* L.) have different mechanical properties. *Physiol. Zool.* **68**, 673–697.
- DICKINSON, M.H. (1996). Unsteady mechanisms of force generation in aquatic and aerial locomotion. *Amer. Zool.* **36**, 537–554.
- DOMENICI, P. AND BLAKE, R.W. (1991). The kinematics and performance of the escape response in the angelfish (*Pterophyllum eimekei*). *J. Exp. Biol.* **156**, 187–205.
- DOMENICI, P. AND BLAKE, R.W. (1997). Review. The kinematics and performance of fish fast-start swimming. *J. Exp. Biol.* **200**, 1165–1178.
- DROST, M.R. AND BOOGAART, J.G.M. VAN DEN (1986). The energetics of feeding strikes in larval carp, *Cyprinus carpio* L. *J. Fish Biol.* **29**, 371–379.
- EATON, R.C., NISSANOV, J. AND DIDOMENICO, R. (1991). The role of the Mauthner cell in sensorimotor integration by the brainstem escape network. *Brain Behav. Evol.* **37**, 272–285.
- GEERLINK, P.J. (1983). Pectoral fin kinematics of *Coris formosa* (Teleostei, Labridae). *Neth. J. Zool.* **33**, 515–531.
- GEERLINK, P.J. (1986). *Pectoral fins, aspects of propulsion and breaking in Teleost fish*, Thesis. Groningen: University of Groningen. 154 pp.
- GRAY, J. (1933). Studies in animal locomotion I. The movement of fish with special reference to the eel. *J. Exp. Biol.* **10**, 88–104.
- HERTEL, H. (1966). *Structure, form and movement*. New York: Reinhold. 251 pp.
- HESS, F. AND VIDELER, J.J. (1984). Fast continuous swimming of saithe (*Pollachius virens*): A dynamic analysis of bending movements and muscle power. *J. Exp. Biol.* **109**, 229–251.
- HILL, A.V. (1938). The heat of shortening and the dynamic constants of muscle. *Proc. R. Soc. Lond. B* **126**, 136–195.
- KASHIN, S.M. AND SMOLYANINOV, V.V. (1969a). Concerning the geometry of fish trunk muscles. *J. Ichthyol.* (Engl. Transl. Vopr. Ikhti.) **9**, 923–925.
- KASHIN S.M. AND SMOLYANINOV V.V. (1969b). On the question of the geometrical arrangement of body muscles in fish. *J. Ichthyol.* (Engl. Transl. Vopr. Ikhti.) **9**, 1139–1142.
- LIGHTHILL, M.J. (1971). Large-amplitude elongated-body theory of fish locomotion. *Proc. R. Soc. Lond.* **179B**, 125–138.
- LINDSEY, C.C. (1978). Form, function and locomotory habitats in fish. In *Fish Physiology*, vol. VII (ed. W.S. Hoar and D.J. Randall), pp. 1–100. London: Academic Press.
- NELSON, J.S. (1994). *Fish of the world*, third edition. New York: John Wiley and Sons. 600 pp.
- NIJSSSEN, H. AND GROOT, S.J. DE (1987). *De vissen van Nederland*. Utrecht: Stichting Uitgeverij van de Koninklijke Nederlandse Natuurhistorische Vereniging. 224 pp.
- OSSE, J.W.M. (1990). Form changes in fish larvae in relation to demands of function. *Neth. J. Zool.* **40**, 362–385.
- OSSE, J.W.M. AND DROST, M.R. (1989). Hydrodynamics and mechanics of fish larvae. *Pol. Arch. Hydrobiol.* **36**, 455–465.
- RAYNER, J.M.V. (1985). Vorticity and propulsion mechanics in swimming and flying vertebrates. In *Principles of construction in fossil and recent reptiles*, Konzepte SFB 230 Heft 4, pp. 89–118.

- SYMMONS, S. (1979). Notochordal and elastic components of the axial skeleton of fish and their function in locomotion. *J. Zool. Lond.* **189**, 157–206.
- VAN DER STELT, A. (1968). *Spijrmecanica en myotoombouw bij vissen*, Thesis. Amsterdam: University of Amsterdam. 94 pp.
- VAN LEEUWEN, J.L. (1995). Review article: The action of muscles in swimming fish. *Exp. Physiol.* **80**, 177–191.
- VAN LEEUWEN, J.L., LANKHEET, M.J.M., AKSTER, H.A. AND OSSE, J.W.M. (1990). Function of red axial muscles of carp (*Cyprinus carpio* L.) recruitment and normalised power output during swimming in different modes. *J. Zool. Lond.* **220**, 123–145.
- VAN RAAMSDONK, W. (1978). *De ontwikkeling van de rompmusculatuur van Brachydanio rerio (de zebravis)*, Thesis. Amsterdam: University of Amsterdam. 125 pp.
- VIDELER, J.J. (1975). On the interrelationships between morphology and movement in the tail of the Cichlid fish *Tilapia nilotica* (L.). *Neth. J. Zool.* **25**, 143–154.
- VIDELER, J.J. (1985). Fish swimming movements: a study of one element of behaviour. *Neth. J. Zool.* **35**, 170–185.
- VIDELER, J.J. (1992). Wateraap of geboren verdrinker? Vergelijking van zwemprestaties van mens en dier. In *Biologie, Mechanica en Sport*, Biologische Raad Reeks, KNAW (ed. J.W.M. Osse, G.J. van Ingen Schenau, P. Voogt and C.M. van den Heuvel), pp. 107–130. Amsterdam.
- VIDELER, J.J. (1993). *Fish swimming*. London: Chapman and Hall. 260 pp.
- VIDELER, J.J. AND HESS, F. (1984) Fast continuous swimming of two pelagic predators, saithe (*Pollachius virens*) and mackerel (*Scomber scombrus*): a kinematic analysis. *J. Exp. Biol.* **109**, 209–228.
- WAINWRIGHT, S.A., BIGGS, W.D., CURRY, J.D. AND GOSLINE, J.M. (1976). *Mechanical design in organisms*. London: Edward Arnold. 423 pp.
- WARDLE, C.S. AND VIDELER, J.J. (1980). Fish swimming. In *Aspects of Animal Movement* (ed. H.Y. Elder and E.R. Trueman), pp. 125–150. Cambridge: Cambridge University Press.
- WEBB, P.W. (1975). Hydrodynamics and energetics of fish propulsion. *Bull. Fish. Bd. Can.* **190**, 1–158.
- WEBB, P.W. (1976). The effect of size on the fast–start performance of rainbow trout, *Salmo gairdneri*, and a consideration of piscivorous predator–prey interactions. *J. Exp. Biol.* **65**, 157–177.
- WEBB, P.W. (1984a). Bodyform, locomotion and foraging in aquatic vertebrates. *Am. Zool.* **24**, 107–120.
- WEBB, P.W. (1984b). Form and function in fish swimming. *Sc. American* **251**, 58–68.
- WEBB, P.W. (1993). Swimming. In *The Physiology of Fishes*. Marine Science Series (ed. D.H. Evans), pp. 47–73. London: CRC Press.
- WEBB, P.W. AND SKADSEN J.M. (1980). Strike tactics of *Esox*. *Can. J. Zool.* **58**, 1462–1469.
- WEBB, P.W. AND WEIHS, D. (1983). *Fish biomechanics*. New York: Praeger. 398 pp.
- WEBB, P.W. AND BLAKE, R.W. (1985). Swimming. In *Functional Vertebrate Morphology* (ed. M. Hildebrand, D.M. Bramble, K.F. Liem and D.B. Wake), pp. 110–128. Cambridge: Belknap Press.
- WEIHS, D. (1972). A hydrodynamical analysis of fish turning manoeuvres. *Proc. R. Soc. Lond. B* **182**, 59–72.
- WEIHS, D. (1973). The mechanism of rapid starting of slender fish. *Biorheology* **10**, 343–350.

3 Muscle growth and swimming in larvae of *Clarias gariepinus* (Burchell)

Hendrica A. Akster¹, Johan A.J. Verreth², Igor L.Y. Spierts¹, Thomas Berbner²,
Meike Schmidbauer² and Jan W.M. Osse¹

¹Experimental Zoology Group, Wageningen Institute of Animal Sciences (WIAS), Wageningen
Agricultural University, P.O. Box 338, 6700 AH Wageningen;

²Fish Culture and Fisheries Group, Wageningen Institute of Animal Sciences
(WIAS), Wageningen Agricultural University, P.O. Box 338, 6700 AH Wageningen;
The Netherlands

Published in: ICES marine Science Symposia (1995) 201: 45-50
Reproduced with permission of The ICES marine Science Symposia.

SUMMARY

This study describes the muscle fibre type distribution and the swimming activity in early stages of *Clarias gariepinus* (Burchell). It also describes the influence of different diets on muscle fibre numbers and muscle fibre diameters of *Clarias* larvae. Yolk-sac larvae of *Clarias* have a superficial monolayer of red muscle fibres that surrounds inner 'white' muscle. At approximately 11 mm length (larvae fed for 3 days on *Artemia*), an adult-like fibre type distribution begins to appear. One day after hatching, the larvae (approximately 5 mm total length) show nearly continuous stationary activity interrupted by slow swimming (velocity 2.4 ± 0.9 bodylength per second ($BL s^{-1}$)). This activity is probably powered by the superficial red fibres. Stimulation of the larvae results in burst-swimming with an initial velocity of at least $17 BL s^{-1}$, which is probably powered by the inner white fibres. After yolk-sac absorption the time spent in stationary activity and swimming decreases. From the start of feeding, a group of larvae was fed with *Artemia* and another group with dry food. Larvae fed for 3 days on *Artemia* and larvae fed for 5 days on dry food have similar length, similar white muscle fibre sizes, and similar white muscle fibre numbers. This indicates that muscle development is related to the length of the larvae, rather than to age.

INTRODUCTION

Production of fish meat is production of fish muscle. The ultimate size of a fish and the velocity of growth are related to the number of muscle fibres present in young fish (Weatherley, 1990). The relation between muscle fibre pattern (number and size distribution) and fish length is largely genetically determined; in post-larval stages it is unaffected by differences in food availability and temperature (Weatherley, 1990). However, in fish embryos, muscle fibre number was influenced by differences in rearing temperature (Stickland *et al.*, 1988; Viera and Johnston, 1992). In the present study, we investigated if early (from the start of feeding) differences in food quality affected the muscle fibre pattern. We compared muscle fibre numbers and diameters of the 'white' muscle of fast-growing *Clarias* larvae fed with *Artemia* and slow-growing *Clarias* larvae fed with dry food.

We also investigated the relation between muscle development and swimming in *Artemia*-fed *Clarias*. Muscle development is one of the early necessities in fish larvae. When the yolk is absorbed, muscle development should be sufficiently advanced to enable the larvae to search for prey and to catch it and to escape predators. Axial muscle of fish larvae differs from that of adult fish. Adult fish have a triangular red zone at the level of the horizontal septum separated by a pink or intermediate zone from the white bulk of the muscle mass (Johnston *et al.*, 1977). Yolk-sac larvae have an inner 'white' muscle mass surrounded by a superficial red monolayer (Fig. 1). Both fibre types have an aerobic metabolism (El-Fiky *et al.*, 1987), but their myosin ATPase differs (van Raamsdonk *et al.*, 1980; Scapolo *et al.*, 1988). Myosin ATPase of both types of larval muscle differs from that of adults (Scapolo *et al.*, 1988). During the free-swimming larval stage the adult patterns of muscle fibre type distribution and the differences in metabolism between the red aerobic fibres and the white anaerobic fibres develop (Hinterleitner *et al.*, 1987). This occurs probably in relation to gill development (Batty,

1984; El-Fiky *et al.*, 1987) and to a size-dependent difference in swimming. For small larvae that swim at a relatively low velocity, the viscosity forces of the water are dominant, while for the longer and faster juveniles and adults the inertial forces are more important (Batty, 1984; Osse, 1990).

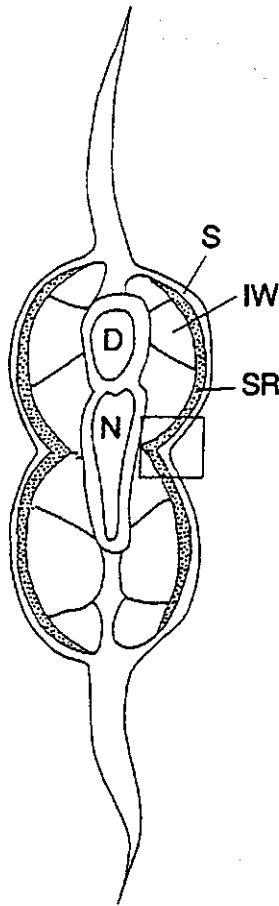


Fig. 1. Scheme of a cross-section through the tail of a *Clarias* yolk-sac larva. S, skin; IW, inner 'white' muscle; SR, superficial red layer; D, dorsal chord; N, notochord; rectangle: area shown in Fig. 2A-D.

MATERIALS AND METHODS

Histochemical and histological data were obtained from several batches of larvae, produced over a period of 2 years. No differences were noticed in data obtained from different batches. For the feeding experiment, larvae of a single batch were used. Swimming speed was also measured using larvae from a single batch. Each batch of larvae was obtained through artificial reproduction of one male and two females, selected randomly from a large pool or broodstock fish kept under standard conditions (Richter *et al.*, 1995) at the experimental hatchery 'De Haar Vissen' at Wageningen Agricultural University. The fertilized eggs were pooled and the larvae reared according to standard procedure (Verreth and Den Bieman, 1987; Verreth *et al.*, 1992). At 30 °C *Clarias gariepinus* hatches 24 hours after fertilization and yolk-sac absorption lasts 48 hours. Just prior to yolk-sac absorption the fish were transferred to 27.5 °C. Feeding level ($FL=0.3$) corresponded to a near satiation level. According to Verreth and Den Bieman (1987), both this temperature and this feeding level belong to the optimal rearing conditions for larval *Clarias gariepinus*.

Muscle growth and development were studied in cross sections through the anal region. For reactions on succinate dehydrogenase (SDH) activity (Nachlas *et al.*, 1957) and myosin ATPase (Akster and Osse, 1987) tissue was frozen in liquid freon, cooled in liquid nitrogen and sectioned at -20 °C. Antisera against adult carp red and pink muscle were a gift from Dr. W. van Raamsdonk, University of Amsterdam. Reaction procedure was according to van Raamsdonk *et al.* (1980). Results for all histochemical reactions were obtained from at least three fish.

The number of white fibres in one half of the epaxial musculature was counted in 1µm thick sections of larvae fixed in Karnovsky's reagent, postfixed in osmium tetroxide and embedded in Epon. The sections were stained with Weigert's Eisenhaematoxylin (Romeis, 1968) and paraphenylenediamin (1 % aqueous solution). Counts were made at the start of feeding (day 0; 48 hours after hatching), in larvae fed for 3 days and for 5 days with *Artemia*, in larvae fed for 5 days with dry food and in larvae that were starved for 5 days (three fish per group). In each fish the cross-sectional area of approximately 35 white muscle fibres in a sample zone extending from medial to lateral at the level of the neural tube was measured with a digitizing tablet. These data were recalculated to fibre diameters (mean ± S.D., not corrected for shrinkage). Significance of differences was calculated with an approximate t-test for unequal variances (Sokal and Rohlf, 1969).

Swimming behaviour was studied using video films of 25 frames per second (temperature, 27.6-26.1 °C; oxygen content of the water 85-69 %).

RESULTS

Histochemistry

At hatching, SDH activity is high in both the superficial red layer and the inner muscle mass. At 48 hours after hatching (total length (*TL*) approximately 7 mm) only the superficial red fibres have a relatively high SDH activity; in the white fibres the SDH activity has decreased. The superficial red

muscle reacts more strongly with an antibody against red muscle of adult carp than the white zone (Fig. 2A,B).

At approximately 11 mm length (larvae fed for 3 days with *Artemia*) a V-shaped red zone emerges along the horizontal septum and a single layer of pink fibres appears between the red and white zones (Fig. 2C,D). These pink fibres react more strongly with an antibody against pink muscle of adult carp than do other muscle zones. The pH stability of the myosin ATPase of these larval red, pink, and white fibres still differs from the adult pattern (Fig. 2E,F).

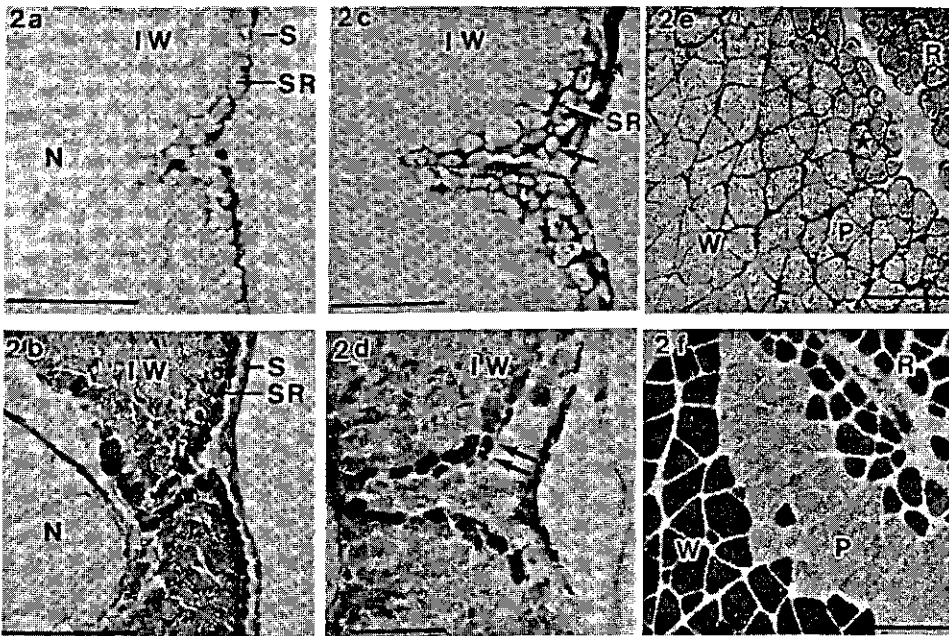


Fig. 2. Histochemical reactions on cross-sections through the axial muscle at the anal region; calibration bar 50 μm . (A,C,E) SDH activity; (B) Reactivity to anti-red antiserum; (D,F) Myosin ATPase activity after alkaline pre-incubation (2 min at pH 10.2); (A,B) Late yolk-sac larva (length 6 mm); the superficial red layer (SR) reacts more strongly with an antibody against carp red muscle than the inner 'white' muscle mass (IW); S, skin; N, notochord; (C,D) Free-swimming larva, length 12 mm. The first fibres of a triangular red zone (C, arrow) are present lateral to the superficial red layer (SR). Between the superficial red layer and the inner 'white' (IW) fibres a single layer of pink fibres (D, arrows) is present. The myosin ATPase of these fibres is more resistant to alkaline pre-incubation (stains darker) than that of the red and 'white' fibres; (E,F) Muscle of adult, serial sections, the asterisk indicates the same (red) fibre. The myosin ATPase of adult red (R) and white (W) fibres is more resistant to alkaline pre-incubation than that in 'red' and 'white' fibres of the 12 mm larva. The myosin ATPase of pink (P) fibres is less resistant than that in the pink fibres of the larva (compare with D).

Muscle growth

After 5 days feeding, *Clarias* fed on *Artemia* were larger than *Clarias* fed with dry food (28.7 and 13.5 mg, respectively) and they showed a better survival. The inner, white muscle, zone of *Artemia*-fed *Clarias* contained more muscle fibres than that of larvae fed with dry food (595 ± 3 and 358 ± 50 fibres, respectively, $P < 0.001$) and the muscle fibres had larger diameters (34 ± 6 μm respectively, $P < 0.001$). Larvae fed for 5 days with dry food were similar in length to larvae fed for 3 days with *Artemia*. This similarity in length was accompanied by a similarity in fibre number (fig. 3A) and in fibre size (Fig. 3B). The development of the red zone was also similar in both groups. At this size, the monolayer of red fibres was acquiring additional fibres along the horizontal septum, resulting in a double layer of red fibres at this location.

In starved larvae, the fibre number had significantly ($P < 0.01$) decreased from 205 ± 9 to 154 ± 22 fibres (Fig. 3A). No significant decrease in fibre diameter (7.7 ± 1 μm and 7.5 ± 0.3 μm) was found.

Swimming behaviour

A few hours after hatching the larvae aggregated in a corner of the basin, where they showed almost continuous tail beat activity. One day after hatching (at approximately 5mm TL) over 90 % of the time was spent in stationary activity with a tail beat frequency of 3-5 Hz. Approximately 6-8 % of the time was spent in swimming excursions with a velocity of 2.4 ± 0.9 bodylengths per second ($BL s^{-1}$, $N=20$; tail beat frequency approximately 8 Hz). The rest of the time, no movement was noticed. Stimulation (touching with a probe) resulted in burst-swimming with an initial velocity of at least $17 BL s^{-1}$. At the end of the yolk-sac stage (3 days after hatching, 8.5 mm TL), the larvae no longer showed stationary activity. They spent approximately 50 % of their time in routine swimming (velocity $2.4 \pm 0.3 BL s^{-1}$), the rest of the time they were inactive. In older larvae, swimming activity decreased. At 6 days after hatching (10.5 mm TL), approximately 30 % of the time was spent swimming. Larvae of 49 mm TL spend less than 5 % of their time swimming.

DISCUSSION

Muscle fibre types and swimming

In larvae of *Clarias gariepinus* the beginning of the transition in muscle composition from the early larval inner white and superficial red muscle zones to an adult-like pattern occurs in the free swimming larvae, as has also been described for other fish species (van Raamsdonk *et al.*, 1987; Proctor *et al.*, 1980; Batty, 1984; El-Fiky *et al.*, 1987). In herring and in Cyprinids this transition has been correlated to the development of gill respiration (Batty, 1984; El-Fiky *et al.*, 1987). In *Clarias* larvae, too, development of the gill lamella begins early in the free-swimming larval stage (H. Segner, pers. comm.). In yolk-sac larvae and in early free-swimming larvae, when gill development is still insufficient, the muscles rely for oxygen supply on diffusion through the body surface. This and the

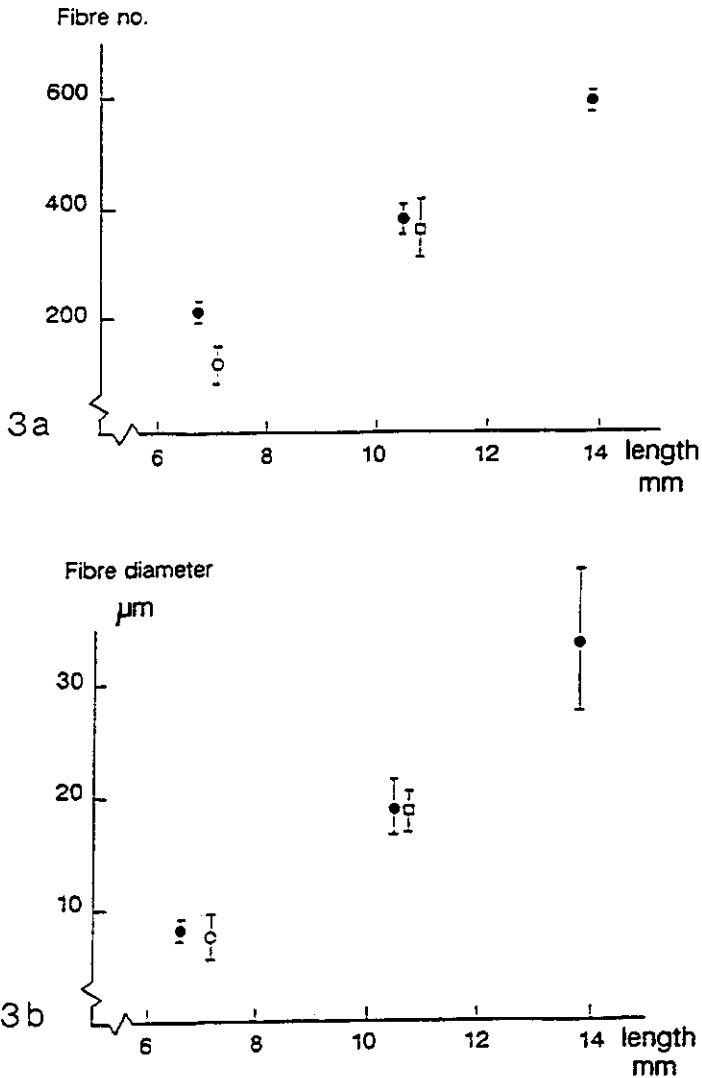


Fig. 3. Muscle fibre numbers (A) and muscle fibre diameters (B) from the white zone of larvae fed for 0, 3, and 5 days with *Artemia* (closed symbols), larvae fed for 5 days with dry food (open rectangle), and larvae starved for 5 days (open circle). Means \pm S.D., $N=3$. Both fibre number (A) and fibre diameter (B) increase linearly with increasing length of the larva. Larvae fed for 5 days with dry food and day larvae fed for 3 days with *Artemia* have similar lengths, similar mean fibre sizes, and similar fibre numbers. In starving larvae, the fibre number decreases.

high activity of respiratory mitochondrial enzymes present in these fibres suggest a respiratory role for the superficial red muscle layer (El-Fiky *et al.*, 1987). El-Fiky *et al.* (1987) propose that respiration is

the main function of these larval muscle fibres and that their role in swimming is negligible. Yolk-sac larvae of *Clarias gariepinus* show almost continuous tail beats, interrupted by slow swimming ($2.4 \pm 0.9 BL s^{-1}$). When stimulated, these larvae show burst-swimming with speeds of over $17 BL s^{-1}$. The very different swimming speeds shown by *Clarias* larvae must be powered by different muscle fibre types with different myosin ATPase isoenzymes (Rome *et al.*, 1988). Therefore, it is highly probable that the stationary tail beats and the slow swimming are powered by the superficial red layer (that contains a myosin which has antigenic determinants in common with slow red adult muscle). The rapid burst-swimming is probably powered by the larger inner 'white' muscle mass.

Almost continuous tail-beating followed by haphazard swimming is also seen in yolk-sac larvae of *Clarias gariepinus* in their natural habitat (Bruton, 1979). It is likely that these tail beats are respiratory movements. Increase in swimming activity at the end of the yolk-sac stage is also described for larvae of other fish species (Nag and Nursall, 1972; Proctor *et al.*, 1980; Batty, 1984). The decrease in swimming activity in the free swimming larvae of *Clarias gariepinus* may be related to the development of the gills and the decrease in relative importance of the red fibre zone.

Fibre number and fibre size

In the inner white muscle zone of growing larvae, fibre number (Fig. 3A) and fibre diameter (Fig. 3B) increased linearly with increasing length of the larvae. This shows that muscle of free-swimming *Clarias* larvae grows by the addition of fibres (hyperplasia) as well as by the growth of existing fibres (hypertrophy). Larvae fed for 3 days with *Artemia* and larvae fed for 5 days with dry food are similar in length. They also have a similar fibre type distribution and similar fibre diameters and fibre numbers in the inner white zone. This indicates that muscle growth is related to larval length rather than to age. This is in contrast to data on gut development in larvae of *Clarias gariepinus* (Verreth *et al.*, 1992), but it agrees with the finding of Weatherley (1990) that, in young fish, muscle growth is length dependent. It also concurs with data of Higgins and Thorpe (1990), who found that in juvenile Atlantic salmon (*Salmo salar*) smaller than 6.5 cm fork length, fibre number and fibre size are related to fish length. In larger juveniles, only fibre number is length-related. The relation between muscle growth and fish length is not unexpected, since the Reynolds number, too, the ration between inertial and viscous forces acting on swimming fish larvae, is length-dependent (Batty, 1984; Osse, 1990).

Muscle cellularity can be influenced by external circumstances, mainly temperature (Stickland *et al.*, 1988); Viera and Johnston, 1992). the present study indicates that, although inadequate feeding of larvae (dry food) influences growth rate and survival, it does not influence the muscle fibre pattern. it is likely that the growth potential of the muscle is not affected by the inadequate feeding.

ACKNOWLEDGMENTS

We thank Dr. W. van Raamsdonk, University of Amsterdam, for supplying the antisera and W.J.A. Valen and K. Boekhorst for their help in preparing the illustrations. The collaboration of T. Berbner and of M. Schmidbauer was made possible through Erasmus grants from the Commission of the European Community.

REFERENCES

- AKSTER, H.A. AND OSSE, J.W.M. (1978). Muscle fibre types in head muscles of the perch *Perca fluviatilis* (L), Teleostei. A histochemical and electromyographical study. *Neth. J. Zool.* **28**, 94-110.
- BATTY, R.S. (1984). Development of swimming movements and musculature of larval herring (*Clupea harengus*). *J. Exp. Biol.* **110**, 217-229.
- BRUTON, M.N. (1979). Breeding of *Clarias gariepinus*. *Trans. Zool. Soc. Lond.* **35**, 7-44.
- EL-FIKY, N., HINTERLEITNER, S. AND WIESER, W. (1987). Differentiation of swimming muscles and gills and development of anaerobic power in the larvae of cyprinid fish (Pisces, Teleostei). *Zoomorph.* **107**, 126-132.
- HIGGINS, P.J. AND THORPE, J.E. (1990). Hyperplasia and hypertrophy in the growth of skeletal muscle in juvenile Atlantic salmon *Salmo salar* L. *J. Fish Biol.* **37**, 505-519.
- HINTERLEITNER, S., PLATZER, U. AND WIESER W. (1987). Development of the activities of oxidative, glycolytic and muscle enzymes during early larval life in three families of freshwater fish. *J. Fish Biol.* **30**, 315-326.
- JOHNSTON, I.A., DAVISON, W. AND GOLDSPIK, G. (1977). Energy metabolism of carp swimming muscles. *J. Comp. Physiol.* **114**, 203-216.
- NACHLAS, M.M., TSOU, K.-C., SOUZA, E. DE, CHENG, C.-S. AND SELIGMAN, A.M. (1957). Cytochemical demonstration of succinic dehydrogenase by the use of a new p-nitrophenyl substituted ditetrazole. *J. Histochem. Cytochem.* **5**, 420-436.
- NAG, A.C. AND NURSALL, J.R. (1972). Histogenesis of white and red muscle fibres of trunk muscles of a fish *Salmo gairdneri*. *Cytobios.* **6**, 227-246.
- OSSE, J.W.M. (1990). Form changes in fish larvae in relation to changing demands of function. *Neth. J. Zool.* **40**, 362-385.
- PROCTOR, C., MOSSE, P.R.L. AND HUDSON, R.C.L. (1980). A histochemical and ultrastructural study of the development of the propulsive musculature of the brown trout, *Salmo trutta* L., in relation to its swimming behaviour. *J. Fish Biol.* **16**, 309-329.
- RICHTER, C.J.J., EDING, E.J., VERRETH, J.A.J. AND FLEUREN, W.L.G. (1995). African catfish *Clarias gariepinus*. In *Broodstock Management and Egg and Larval Quality* (ed. N.R. Bromage and R.J. Roberts), pp. 242-276. Oxford, London: Blackwell Science.
- ROME, L.C., FUNKE, R.P., ALEXANDER, R. MCN., LUTZ, G., ALDRIDGE, H., SCOTT, F. AND FREADMAN, M. (1988). Why animals have different muscle fibre types. *Nature* **335**: 824-827.
- ROMEIS, B. (1968). *Mikroskopische Technik*, 16e edition. München: Oldenbourg Verlag. 757 pp.

Chapter 3

- SCAPOLO, P.A., VEGETTI, A., MASCARELLO, F. AND ROMANELLO, M.G. (1988). Developmental transitions of myosin isoforms and organisation of the lateral muscle in the teleost *Dicentrarchus labrax* (L.). *Anat. Embryol.* **178**, 287-295.
- SOKAL, R.R. AND ROHLF, F.J. (1981). *Biometry*, second edition. New York: W.H. Freeman and Company. 859 pp.
- STICKLAND, N.C., WHITE, R.N., MESCALL, P.E., CROOK, A.R. AND THORPE, J.E. (1988). The effect of temperature on myogenesis in embryonic development of the Atlantic salmon (*Salmo salar* L.). *Anat. Embryol.* **178**, 253-257.
- VAN RAAMSDONK, W., POOL, C.W. AND KRONNIE, G. TE (1987). Differentiation of muscle fibre types in the teleost *Brachydanio rerio*. *Anat. Embryol.* **153**, 137-155.
- VAN RAAMSDONK, W., KRONNIE, G. TE, POOL, C.W. AND LAARSE, W. VAN DE (1980). An immune histochemical and enzymic characterization of the muscle fibres in myotomal muscle of the teleost *Brachydanio rerio*, Hamilton-Buchanan. *Acta Histochem.* **67**, 200-216.
- VERRETH, J.A.J. AND BIEMAN, J. DEN (1987). Quantitative feed requirements of African catfish (*Clarias gariepinus* Burchell) larvae fed with decapsulated cysts of *Artemia*. I. The effect of temperature and feeding level. *Aquaculture* **63**, 251-267.
- VERRETH, J.A.J., TORREELE, E., SPAZIER, E., SLUISZEN, A. VAN DER, ROMBOUT, J.H.W.M., BOOMS, R. AND SEGNER, H. (1992). The development of a functional digestive system in the African catfish *Clarias gariepinus* (Burchell). *J. World Aquacult. Soc.* **23**, 286-298.
- VIERA, V.L.A. AND JOHNSTON, I.A. (1992). Influence of temperature on muscle-fibre development in larvae of the herring *Clupea harengus*. *Mar. Biol.* **112**, 333-341.
- WEATHERLEY, A.H. (1990). Approaches to understanding fish growth. *Trans. Am. Fish. Soc.* **119**, 662-672.

4

Local differences in myotendinous junctions in axial muscle fibres of carp (*Cyprinus carpio* L.)

Igor L.Y. Spierts, Hendrica A. Akster, Ingrid H.C. Vos and Jan W.M. Osse

Experimental Zoology Group, Wageningen Institute of Animal Sciences (WIAS), Wageningen
Agricultural University, Marijkeweg 40, 6709 PG Wageningen;
The Netherlands

Published in: The Journal of Experimental Biology (1996) **199**: 825-833

Reproduced with permission of The Journal of Experimental Biology, Company of Biologists, LTD.

SUMMARY

We studied the myotendinous junction of anterior and posterior red and white axial muscle fibres of carp using stereology. In posterior axial muscle fibres of swimming fish, stress (load on the myotendinous junction) must be higher than in anterior fibres as posterior fibres have a longer phase of eccentric activity. As we expect the magnitude of the load on the junction to be reflected in its structure, we compared the interfacial ratio, the ratio between the area of the junctional sarcolemma and the cross sectional fibre area, of these muscle fibres. This ratio differed significantly between the investigated groups, with red fibres and posterior fibres having the larger ratios. The higher interfacial ratio of posterior myotendinous junctions is in accordance with the proposition mentioned above. The difference between myotendinous junctions of red and white fibres is probably related to a difference in the duration of the load on the junction.

INTRODUCTION

At the myotendinous junction (MTJ), forces generated or transmitted by the myofibrils are transferred to the collagen fibres of the tendon. The muscle fibre and the tendon interdigitate, which results in an amplification of the interfacial membrane area and in a reduction in local stress (force per unit area). The interdigitation of muscle and tendon also results in a shift from tensile load to shear load. Angle α between the muscle fibre membrane and the direction of the force applied to the joint (transmitted by the actin filaments) is indicative of the amount of shear loading; a smaller value of α indicates more loading in shear (Lubkin, 1957; Tidball 1983). Joints loaded in shear are commonly found to be much stronger than those loaded in tension (Bikerman, 1968) and a smaller value of α is assumed to result in a stronger MTJ (Tidball, 1983; Tidball and Daniel, 1986). The magnitude of the load on the MTJ is expected to influence the amplification of the interfacial membrane area and angle α . Decrease of the load on the muscle, caused by disuse (Tidball, 1983; Kannus *et al.*, 1992) or by space-flight (Tidball and Quan, 1992), indeed resulted in an increase in the value of angle α (Tidball, 1983) or in a decrease of the membrane amplification (Tidball and Quan, 1992; Kannus *et al.*, 1992). Tidball and Daniel (1986) considered that the duration of the load may also significantly influence the demands imposed upon the junction. This assumption is based on the viscoelastic properties of the junction and the fluid nature of the membrane.

Membrane amplification at the MTJ showed no consistent relation to 'muscle fibre type characteristics' (tonic versus phasic and slow twitch versus fast twitch, Trotter *et al.*, 1985a,b; Tidball and Daniel, 1986; Trotter and Baca, 1987; Kannus *et al.*, 1992; Trotter, 1993). However, 'fibre type' denotes a combination of muscle fibre properties, and fibres of the same type may differ in the type of activity (see below). In vitro, most muscles experience cyclic alternations of contraction and lengthening. Tension development (loading of the MTJ) depends on V/V_{\max} , the ratio between the actual contraction velocity and the maximal (unloaded) contraction velocity of the fibre (Hill, 1938). and eccentric activity (negative contraction velocity) results in tensions higher than those during concentric activity.

Axial muscles of fish contain spatially separated muscle zones that differ in activity pattern. A laterally situated strip of red muscle is used for slow continuous activity. The bulk of the musculature, which consists of white muscle fibres, is used for short powerful bursts of activity (Hudson, 1973; Johnston *et al.*, 1974, 1975; Akster and Osse, 1978; Bone, 1978; Proctor *et al.*, 1980; Rome *et al.*, 1988; Altringham and Johnston, 1990a,b; van Leeuwen *et al.*, 1990).

In addition to the medial-lateral difference in fibre types, there are also antero-posterior differences in muscle function between fibres of the same type in the body of a swimming fish. Computer models (van Leeuwen *et al.*, 1990; van Leeuwen, 1995) based on electromyographic and motion analysis of carp (*Cyprinus carpio* L.) predicted that, during continuous and intermittent swimming, muscle fibres in the tail region (together with the connective tissue) would play an important role in the transmission of force produced by more anterior muscle fibres. The posterior fibres have a longer phase of eccentric activity than the anterior fibres (van Leeuwen *et al.*, 1990; van Leeuwen, 1995). As a result these posterior fibres will develop greater forces than anterior fibres. This expectation was confirmed by simulation experiments (Davies *et al.*, 1995). We expect that greater forces in posterior fibres will be accompanied by a greater membrane amplification at the MTJ.

The MTJ of the common carp shows a general resemblance in morphology (Akster *et al.*, 1995) to the MTJs previously characterised in a wide variety of vertebrates from hagfish to mammals, including teleosts (Hanak and Böck, 1971; Korneliussen, 1973; Schattenberg, 1973; Trotter *et al.*, 1981, 1983a,b, 1985a,b; Trotter and Baca, 1987; Trotter, 1990, 1993; Tidball, 1983, 1984; Tidball and Daniel, 1986; Tidball and Quan, 1992; Ishikawa *et al.*, 1983; Eisenberg and Milton, 1984; Bremner and Hallett, 1985; Hallett and Bremner, 1988).

In this study we investigated the MTJs of both anterior and posterior axial white and red muscle fibres of the common carp, by means of stereology (Eisenberg and Milton, 1984) to determine if the published differences in loading of these fibres are accompanied by differences in the structure of the MTJ.

MATERIALS AND METHODS

Three common carp (*Cyprinus carpio* L.) of 19-24 cm standard length, bred in the laboratory at 23 °C, and fed on commercial fish food (trouvit pellets; Trouw and Co. Putten), were used.

The fish were killed with an overdose (0.2 %) of tricaine methane sulphonate (Sandoz). A piece of skin was removed and Karnovsky's fixative (1965) was injected into the axial muscle. After fixation *in situ* at room temperature for approximately 15 min, small pieces of red and white axial muscle (approximately 10 mm X 5 mm X 3 mm) were dissected from the tail region near the anus (posterior) and from the body region immediately rostral to the fourth ray of the dorsal fin (anterior, Fig. 1). When superficial white axial muscle was dissected, care was taken to avoid red and pink muscle layers. Fixation was continued for approximately 90 min in fresh Karnovsky's fixative. The muscle tissue was rinsed in 0.1 % cacodylate buffer, pH 7.3.

MTJs were prepared for scanning electron microscopy as described by Trotter and Baca (1987). For transmission electron microscopy, the muscle tissue was postfixed in 1 % osmium tetroxide,

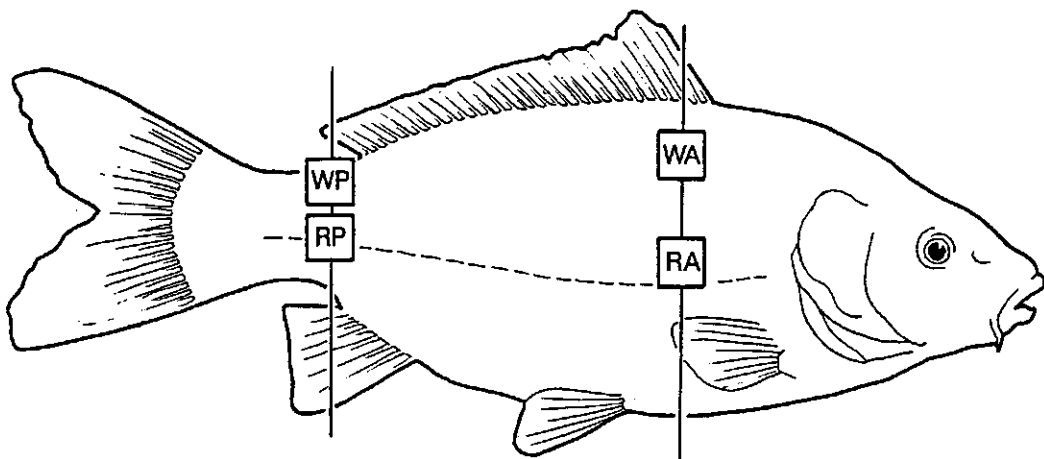


Fig. 1. Position of the muscle sample sites on the common carp *Cyprinus carpio*, indicated by rectangles. W, white muscle; R, red muscle; A, anterior; P, posterior.

followed by 1 % uranyl acetate, dehydrated in graded alcohols and propylene oxide, and embedded in an epon mixture.

Sampling procedure

Four sample sites (anterior and posterior red and anterior and posterior white) and six fibres per sample site were examined for each of the three fish. Two or three blocks of tissue were taken from each sample site. Ultrathin longitudinal sections were made from each block using a diamond knife on a Reichert-Jung Ultracut E ultramicrotome. The ultrathin sections were stained with uranyl acetate and lead citrate.

Owing to the orientation of axial muscle fibres of fish in oblique fibre trajectories (Alexander, 1969) slight differences in the direction of the muscle fibres occur at the sample sites. Transmission electron micrographs were made of the MTJs of the first two (or three, depending on the number of blocks obtained from the sample site) truly longitudinally sectioned fibres that were identified under a Phillips EM 201C electron microscope. Sections were considered to be longitudinal when thick filaments could be traced over the entire length of an A-band. Deformation by fixation was considered to be minimal when the angle between the filaments and the Z-line was approximately 90°. The beginning of the MTJ was defined as the middle of the location where the membrane on both sides of the fibre profile was not parallel for at least two sarcomeres lengths.

For random morphometric sampling, the micrograph area, indicated on the image screen of the microscope, was used as a sample area. A micrograph (X 25 500) was made of every fourth area of the interfacial membrane and used for subsequent morphometric analysis. For each fibre, the starting point for sampling was obtained using a sampling scheme containing twelve different starting points (the first, second, third and fourth frames from the left side, the right side and the middle of the MTJ of the fibre). This resulted in 3-5 micrographs per fibre and approximately 24 micrographs per sample site from each fish.

Lower-magnification micrographs (X 2400) of every fibre were used to measure the diameter of the fibre profile, d_f , and the length of the MTJ (L_{mj} , the distance between the last Z-line before the beginning of the taper and the tip of the taper). The diameter of the fibre profile was measured at a location where the membrane on both sides of the fibre profile was parallel.

Morphometry

Sectioning muscle fibres with a diameter D_f produces a population of fibre profiles with a mean diameter \bar{d}_f . Only a small part of the profile is cut through the real diameter, D_f . The mean fibre diameter, \bar{d}_f , measured from the electron micrographs, is an undervaluation of the real fibre diameter, D_f . For circular fibres, randomly sampled in longitudinal sections, the real fibre diameter can be calculated (Weibel and Bolender, 1973) by:

$$D_f = (4/\pi) \bar{d}_f \quad (1)$$

Amplification of the membrane area at MTJs is defined as the interfacial ratio (IFR), the ratio of the interfacial membrane area (S_m) to the cross-sectional area of the fibre (S_c), where:

$$\text{IFR} = S_m/S_c. \quad (2)$$

This ratio was calculated using stereological methods (Merz, 1967; Weibel and Bolender, 1973; Aherne and Dunnill, 1982 and Royet, 1991) with a 2 cm semicircular test grid placed on the micrograph. The method was adjusted to muscle fibres by Eisenberg and Milton (1984). The membrane area per unit volume (S_m/V) was calculated from the number of intersections (I_m) between the interfacial membrane of the fibre and the test grid. The fibre cross sectional area was obtained from the projected length of the interfacial membrane on the plane of the last Z-disc before the beginning of the taper (Tidball, 1983). The cross-sectional area per unit volume (S_c/V) is calculated from the number of intersections (I_c) between this projection and the test grid.

Muscle is highly anisotropic, it has a high degree of orientation. This means that projections of the membrane on a plane perpendicular to the fibre axis and on a plane parallel to the fibre axis are not equal (as they would be in a purely isotropic system). DeHoff and Rhines (1968) called this type of anisotropy linear. For every specific geometry with a known degree of orientation an appropriate

constant is necessary to relate the boundary length seen in the micrographs to a surface area in the real tissue. Some specific constants have been derived and are reviewed by Eisenberg (1983).

The stereological equations relating the area of interfacial membrane per unit volume (S_m/V) to the number of intersections between the membrane and the line length of the test grid (I_m/L) for an isotropic orientation of the membrane are (Eisenberg, 1983):

$$S_{\text{isotropic}}/V = 2I_m/L, \quad (3)$$

for an anisotropic orientation of the membrane:

$$S_{\text{anisotropic}}/V = (\pi^2/4)I_m/L. \quad (4)$$

For the fibre cross section the equation is:

$$S_c/V = (\pi/2)I_c/L. \quad (5)$$

The percentage anisotropy ($\%_{\text{anisotropy}}$) of the interfacial membrane was determined in every second fibre from the number of intersections with the parallel (I_{\parallel}) and perpendicular (I_{\perp}) lines of a 1 cm X 1 cm test grid. Orientation of the grid lines was parallel and perpendicular to the fibre axis. According to DeHoff and Rhines (1968) and to Eisenberg and Milton (1984):

$$\%_{\text{anisotropy}} = 100(I_{\perp} - I_{\parallel}) / (0.273I_{\parallel} + I_{\perp}). \quad (6)$$

Using equations (2-6), and f_{isotr} and f_{anisotr} for, respectively, the fractional isotropy and anisotropy of the membrane, the IFR is given by:

$$\text{IFR} = \frac{[2f_{\text{isotr}} + (\pi^2/4)f_{\text{anisotr}}]Im}{(\pi/2)I_c}. \quad (7)$$

We determined two IFR values, IFR_{em} (entire membrane IFR) and IFR_{am} (attachment membrane IFR). For IFR_{em} , the surface of the entire interfacial membrane (S_{em}) was considered. Only caveolae were excluded; they were treated as if the membrane continued over their mouth without interruption. For IFR_{am} , only that part of the surface of the membrane where actin filaments attached to the membrane (S_{am}) was considered. The presence of actin filaments along the membrane or a thickened cell-membrane (a clearly visible lamina densa and a thick glycocalyx with a descending gradient in the

direction of the lamina densa) were the criteria used to assess this portion of the interfacial membrane. In case of doubt the cell-membrane was always considered to be attachment membrane.

Statistics

All data measured in this study appeared to be normally distributed (Shapiro and Wilk, 1965). Statistical analyses of the measured differences in L_{mj} , D_f , IFR_{em} and IFR_{am} were performed using analysis of variance (ANOVA). Statements of statistical significance are based on $P \leq 0.05$, unless specified otherwise (Sokal and Rohlf, 1981; Rohlf and Sokal, 1981).

RESULTS

Shape of the MTJs

Red and white fibres differ in the type of membrane folding at the MTJ. Red fibres attach mainly perpendicular to the fascial plane of the tendon (myosept) and their MTJs have large finger-like extensions (Figs 2 and 3). White fibres attach at an angle to the fascial plane of the tendon and their MTJs have more, but smaller, finger-like extensions (Figs 4-6).

White fibres have a significantly larger mean fibre diameter ($44.58 \pm 13.74 \mu\text{m}$) than red fibres ($32.38 \pm 10.62 \mu\text{m}$, $P=0.0001$) and posterior fibres have a significantly larger mean fibre diameter ($41.29 \pm 12.28 \mu\text{m}$) than anterior fibres ($35.67 \pm 14.47 \mu\text{m}$, $P=0.045$) (Table 1). These values are corrected for the underestimation caused by measuring diameter profiles in thin sections (see Materials and Methods), but not for shrinkage. L_{mj} , the length of the tapering fibre end, is significantly greater in white than in red fibres (Table 1). L_{mj} is not corrected for the underestimation caused by measuring this variable from thin sections through a tapering fibre end, so that values including this variable are relative, not absolute. L_{mj} divided by D_f gives a rough impression of the general shape of the fibre end (Table 1). This ratio is not significantly different between anterior and posterior fibres, indicating that the general shape of the MTJ anteriorly and posteriorly is comparable. White fibre MTJs are thick-set ($L_{mj}/D_f=1.07 \pm 0.17$) compared to the more slender red fibre MTJs ($L_{mj}/D_f=1.32 \pm 0.31$, $P=0.0001$).

Stereological analysis of the MTJs

IFR_{em} (entire membrane IFR) and IFR_{am} (attachment membrane IFR), were calculated by means of morphometry. No significant differences between individual fish were found on the IFR values. The values for IFR_{am} are consistently 85-90 % of the values for the corresponding IFR_{em} (Table 2). IFR_{em} and IFR_{am} show similar significant differences for muscle type, muscle location and combined effects; therefore we will limit the description to IFR_{em} .

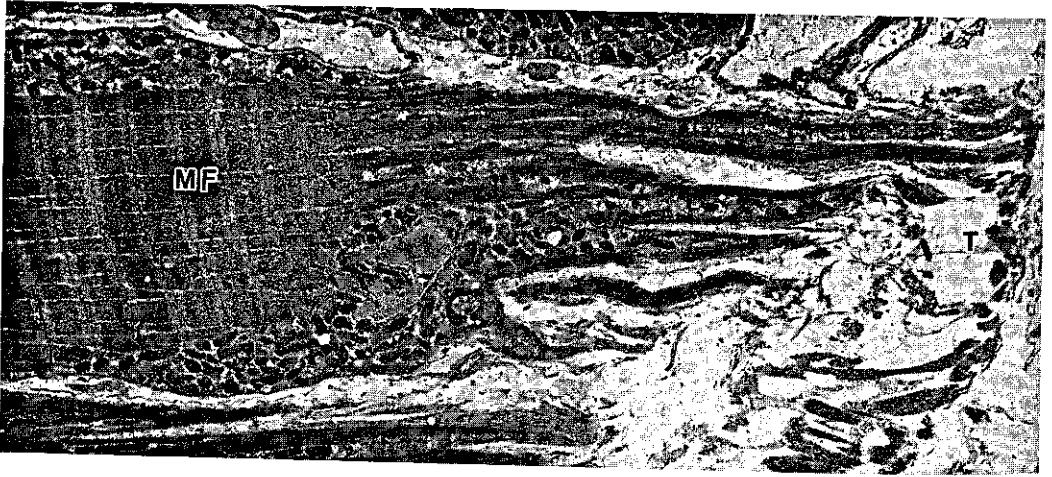


Fig. 2. Transmission electron micrograph of a longitudinally sectioned myotendinous junction (MTJ) of a red axial muscle fibre. Long bundles of actin filaments connect the myofibrils (MF) with the interfacial membrane. Long finger-like protrusions extend into the tendon (T). X 2400.

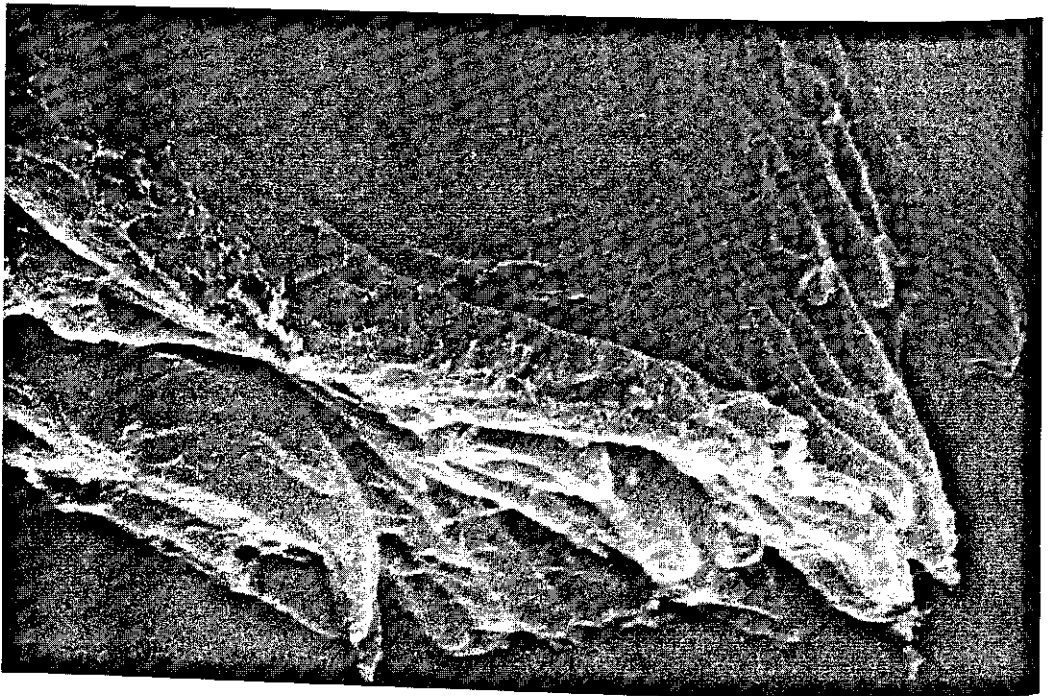


Fig. 3. Scanning electron micrograph of a red axial muscle fibre. Note the large finger-like extensions. X 7300.

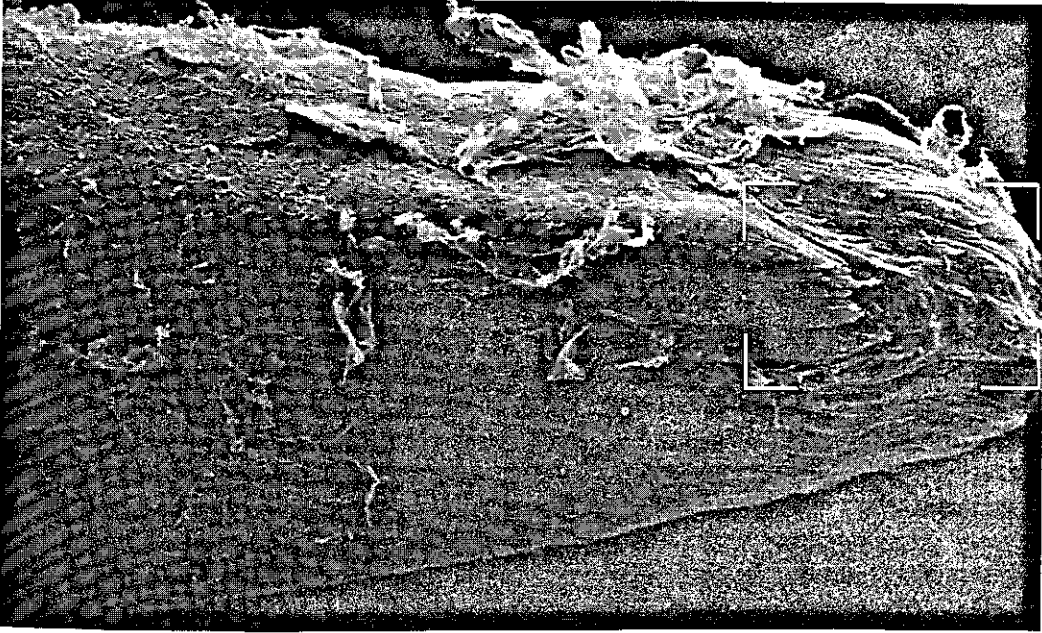


Fig. 4. Scanning electron micrograph of a white axial muscle fibre. The asymmetrical taper indicates that the fibre attaches at an angle to the fascial plane of the tendon. X 2100. The marked area is also shown in Fig. 5.

The muscle type effect is very large ($P=0.0001$). For red muscle fibres (36 fibres) the mean IFR_{em} is 8.20 ± 1.71 ; for white fibres (36 fibres), it is 6.29 ± 1.34 . A significant difference in IFR_{em} was also found for posteriorly (7.76 ± 1.77 , 36 fibres) and anteriorly (6.73 ± 1.68 , 36 fibres) situated fibres ($P=0.0048$). The combined effects of muscle type and muscle location led to the following set of declining mean IFR_{em} values (18 fibres): red posterior: 8.77 ± 1.70 ; red anterior: 7.63 ± 1.63 ; white posterior: 6.75 ± 1.24 and white anterior: 5.83 ± 1.34 (Table 2).

The percentage of membrane area in the MTJ with an anisotropic orientation was significantly higher in red muscle tissue ($68.19\pm 7.44\%$, 18 fibres) than in white muscle tissue ($63.66\pm 3.98\%$, 18 fibres, $P=0.021$). It did not differ significantly between posterior muscle tissue ($66.42\pm 6.77\%$, 18 fibres) and anterior muscle tissue ($65.42\pm 5.92\%$, 18 fibres).



Fig. 5. Detail of Fig. 4 at the same magnification (X 7300) as that of the red axial muscle fibre in Fig. 3. The finger-like extensions of the white fibre are smaller and more numerous than those of the red fibre.

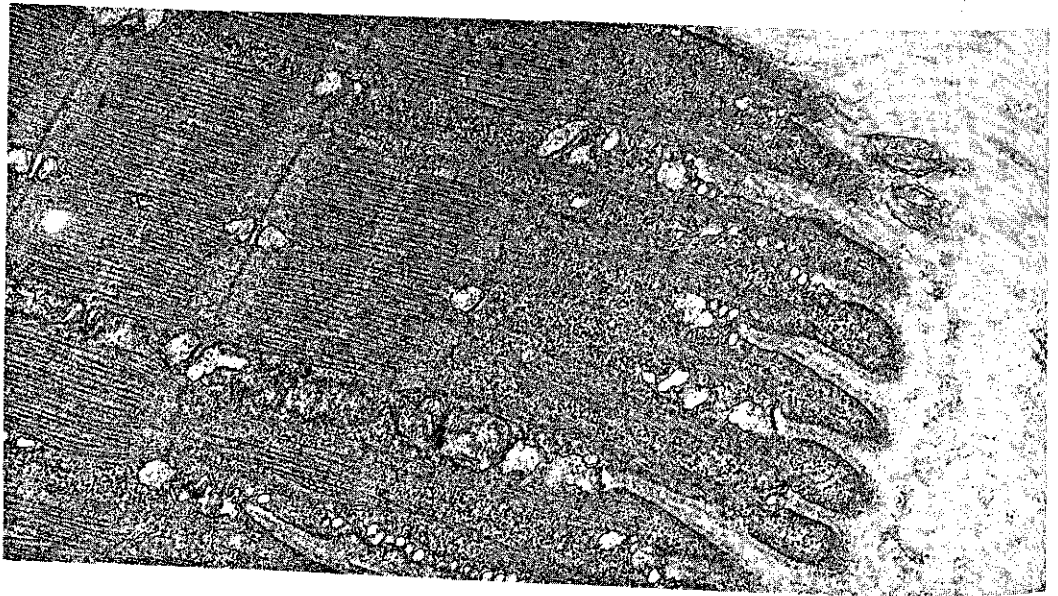


Fig. 6. Transmission electron micrograph of a longitudinal sectioned myotendinous junction (MTJ) of a white axial muscle fibre. Note the shallow finger-like extensions. MF, myofibrils; T, tendon. X 18 500.

Table 1. Morphometric values of the myotendinous junctions. Data of all muscle types and locations combined. Within each section of a column (mutually distinguished by blank lines), groups indicated with different letters (a,b,c) differ significantly ($P \leq 0.05$); *N*, number of fibres measured. Values are mean \pm S.D. MTJ, myotendinous junction.

Type	Fibre Diameter, D_f (μm)	Length of MTJ, L_{mtj} (μm)	L_{mtj}/D_f
Red, anterior ($N=18$)	30.10 \pm 10.63 ^a	38.63 \pm 10.17 ^a	1.35 \pm 0.29 ^a
Red, posterior ($N=18$)	34.66 \pm 10.10 ^{a,b}	42.32 \pm 6.64 ^{a,b}	1.30 \pm 0.32 ^a
White, anterior ($N=18$)	41.25 \pm 15.61 ^{b,c}	45.32 \pm 15.73 ^{a,b}	1.13 \pm 0.17 ^b
White, posterior ($N=18$)	47.92 \pm 10.56 ^c	48.88 \pm 13.06 ^b	1.02 \pm 0.15 ^b
Anterior, total ($N=36$)	35.67 \pm 14.47 ^a	41.98 \pm 13.66 ^a	1.24 \pm 0.26 ^a
Posterior, total ($N=36$)	41.29 \pm 12.28 ^b	45.60 \pm 10.87 ^a	1.16 \pm 0.28 ^a
Red, total ($N=36$)	32.38 \pm 10.62 ^a	40.47 \pm 8.79 ^a	1.32 \pm 0.31 ^a
White, total ($N=36$)	44.58 \pm 13.74 ^b	47.10 \pm 14.57 ^b	1.07 \pm 0.17 ^b

DISCUSSION

Shape of the MTJs

Red and white fibres differ in the angle of attachment to the tendon and in the general shape of the MTJ, expressed as the ratio L_{mtj}/D_f . These differences are in accordance with the difference in orientation of red and white axial muscle fibres of fish. White axial muscle fibres are situated in helical fibre trajectories, red fibres lie more parallel to the body axis (Alexander, 1969). In addition, there was an, as yet unexplained, difference in the size of the finger-like extensions (compare Figs 3 and 5). Red and white fibres also differ in the orientation of the interfacial membrane. The percentage of anisotropically orientated interfacial membrane in white fibres of carp (63.66 %) is close to the percentage of anisotropy found in white fibres of the sartorius of frog *Rana temporaria* (approximately 60 %; Eisenberg and Milton, 1984). Red fibres have a higher percentage anisotropy (68.19 %). The attachment of red fibres, which is almost perpendicular to the fascial plane of the tendon, and the greater slenderness of their junctions probably contribute to this higher anisotropy.

No significant differences in the ratio L_{mtj}/D_f were found between anterior and posterior fibres (Table 1).

Quantification procedure

The amplification of the membrane area was estimated with a stereological method (Weibel and Bolender, 1973; Weibel, 1979) that was adapted to the degree of anisotropy of the muscle tissue (Eisenberg and Milton, 1984). This method is reliable, efficient and precise compared with other

Table 2. The calculated interfacial ratios of the myotendinous junctions and the percentages anisotropy of the muscle tissue. Within each section of a column (mutually distinguished by blank lines), groups indicated with different letters (a,b,c) differ significantly ($P \leq 0.05$); N , number of fibres measured for calculating the interfacial ratios (IFRs); half of these amounts were used for calculating the percentage anisotropy. Values are mean \pm S.D.

Type	Entire membrane IFR _{em}	Attachment membrane IFR _{am}	IFR _{am} /IFR _{em} (%)	Anisotropy of tissue (%)
Red, anterior ($N=18$)	7.63 \pm 1.63 ^a	6.77 \pm 1.50 ^a	88.87	64.89 \pm 8.32 ^a
Red, posterior ($N=18$)	8.77 \pm 1.70 ^b	7.93 \pm 1.75 ^b	90.42	71.49 \pm 5.54 ^b
White, anterior ($N=18$)	5.83 \pm 1.34 ^c	4.95 \pm 1.38 ^c	84.91	65.96 \pm 3.02 ^a
White, posterior ($N=18$)	6.75 \pm 1.24 ^{a,c}	5.9 \pm 1.18 ^{a,c}	87.70	61.35 \pm 3.81 ^a
Anterior, total ($N=36$)	6.73 \pm 1.68 ^a	5.70 \pm 1.65 ^a	84.47	65.4 \pm 5.92 ^a
Posterior, total ($N=36$)	7.76 \pm 1.77 ^b	6.92 \pm 1.77 ^b	89.18	66.42 \pm 6.77 ^a
Red, total ($N=36$)	8.20 \pm 1.71 ^a	7.35 \pm 1.77 ^a	89.63	68.19 \pm 7.44 ^a
White, total ($N=36$)	6.29 \pm 1.34 ^b	5.43 \pm 1.34 ^b	86.33	63.66 \pm 3.98 ^b

methods (Weibel and Bolender, 1973; Royet, 1991) and it requires no presuppositions about the shape of the MTJ. This is important as red and white fibres differ in shape of the MTJ as well as in the angle of attachment of the fibres to the fascial plane of the tendon. Results obtained using this method are comparable with results obtained using other methods (Trotter, 1993).

We determined the IFR_{em} (entire membrane IFR, without caveolae) and the IFR_{am} (attachment membrane IFR) and obtained similar results for both. The IFR_{am} values were 85-90 % of the IFR_{em} values for the different locations and muscle types, and for individual muscle fibres. This indicates that the criteria used to distinguish the attachment membrane were consistently applied. It also indicates that IFR_{em} can be used as accurately as IFR_{am}, which is more difficult to define, to compare amplifications of membrane areas.

We found that the membrane amplification at the MTJ differs significantly between anterior and posterior fibres and between red and white fibres; posterior fibres and red fibres having larger amplifications (Table 2).

Force transmission at the MTJs

According to the models of van Leeuwen *et al.* (1990) and van Leeuwen (1995), the posterior axial muscle fibres of carp experience a longer phase of eccentric activity than the more anterior fibres, resulting in a negative contraction speed and work output and, hence, in larger forces in the posterior fibres. These predictions were corroborated by simulation experiments with cod *Gadus morhua*. When activation patterns and cycle frequencies, as observed *in vivo*, were imposed on isolated bundles of superficial cod white axial muscle fibres, posterior fibres developed higher forces than anterior fibres (Davies *et al.*, 1995). Posterior muscle fibres are slower than anterior fibres (Rome *et*

al., 1993; Altringham *et al.*, 1993; Davies *et al.*, 1995). Anterior and posterior fibres also differ in duty cycle (the proportion of the tail-beat cycle during which the muscle shows electromyographic activity), relaxation time and shortening inactivation time (Rome *et al.*, 1993). But simulation experiments show that the resulting patterns of force duration are similar for anterior and posterior fibres (Rome *et al.*, 1993; Altringham *et al.*, 1993). Thus, the higher amplification of the membrane area in posterior fibres (Table 2) is indeed related to a larger load on the junction.

The difference in IFR between red and white fibres is less easily explained. Although in carp head muscle the measured maximal isometric stress is similar in red and white muscle, 120 kN m^{-2} and 110 kN m^{-2} , respectively (Granzier *et al.*, 1983), in axial muscle it is smaller in red fibres than in white fibres (64 kN m^{-2} and 209 kN m^{-2} , respectively, at $23 \text{ }^{\circ}\text{C}$; Johnston *et al.*, 1985). As these values are not corrected for the differences in the volume percentages of connective tissue, capillaries and mitochondria between red and white muscle, the difference in net stress between red and white axial muscle must be smaller. However, it seems unlikely that net maximal isometric stress is higher in red fibres than in white fibres.

Other factors that can be expected to influence the structure of the MTJ are (1) a high contraction velocity, (2) a large strain and (3) a long duration of the load on the junction. Contraction velocity is lower in red fibres than in white fibres (Rome *et al.*, 1988). Strain can reach high values in red fibres (Rome and Sosnicki, 1991), but such large strains occur at high tail-beat frequencies when red fibres have a high V/V_{max} ratio (Rome and Sosnicki, 1991) and consequently a very low force production (van Leeuwen *et al.*, 1990). Also, Tidball and Chan (1989) found in mechanical experiments on MTJs of single muscle fibres from frog (*Rana pipiens*) semitendinosus muscle that failure of the MTJ was independent of strain and of strain rate. Therefore we do not expect the differences in IFR found in this study to be related to differences in strain. It is more likely that the large strain fluctuations in red fibres (Rome and Sosnicki, 1991) will impose high demands on the series elastic elements (titin filaments, Wang *et al.*, 1991) of these fibres. The third factor, the duration of the load on the junction, is longer in red than in white fibres; red fibres are active at lower tail-beat frequencies (longer cycle times) than white fibres and for longer periods. Tidball and Daniel (1986) proposed that the degree of membrane folding at the MTJ depends on the magnitude and on the duration of the load on the junction. Curtis (1961) and Rand (1964) have shown that the mechanical behaviour of cell membranes is dependent on loading time. At a certain shear load (caused by applying either a large load for a short time or a small load for a longer time), the behaviour of a cell membrane changes from elastic to viscous. This leads to non-reversible structural rearrangement. The cell can survive such a load by reducing the stress on the membrane through an amplification of the membrane area. The greater IFR value of MTJs of red muscle fibres of the carp may be related to the longer duration of the load on the junction in this fibre type. As muscle fibres probably transmit part of the developed force by their lateral surface (Street, 1983; Trotter, 1993), it is also possible that this lateral transmission is more important in white than in red fibres. However, we have no other observations that support this suggestion.

The IFR_{am} values vary from approximately 5 (anterior white fibres) to approximately 8 (posterior red fibres). These values are lower than IFR values of mouse, chicken, snake and frog, summarised by Trotter (1993). The IFR_{am} values for these species (also determined using the method of Eisenberg

and Milton, 1984) are between approximately 9 (plantaris of adult mouse; Trotter and Baca, 1987) and 16 (sartorius of frog; Eisenberg and Milton, 1984). As far as we know, no other quantitative data reporting the amplification of the membrane area in fish have yet been published. Hallett and Bremner (1988) described the invaginations in MTJs of hoki (*Macruronus novaezelandiae*) as being shallow, which agrees with the low IFR values we found in carp.

The low IFR in the MTJ of axial muscle of carp suggest that, in these myomeric muscles, load on the MTJ is less intense or shorter-lasting than in the muscles that have been investigated in other vertebrates.

ACKNOWLEDGEMENTS

We thank Dr. J.L. van Leeuwen for his valuable comment on the manuscript and Ms. J.J. Taverne and Ms. A. Clerx for skilled technical help with the electron microscopy. We also thank Mr. J.W. van de Wal for supplying the scanning electron micrographs and mr. W.A. Valen for help in preparing the illustrations.

REFERENCES

- AHERNE, W.A. AND DUNNILL, M.S. (1982). *Morphometry*, 205 pp. London: E. Arnold Ltd.
- AKSTER, H.A. AND OSSE, J.W.M. (1978). Muscle fibres in head muscles of the perch *Percha fluviatilis* (L), Teleostei. A histochemical and electromyographical study. *Neth. J. Zool.* **28**, 94-110.
- AKSTER, H.A., WAL, J.W. VAN DE AND VEENENDAAL, T. (1995). Interaction of force transmission and sarcomere assembly at the muscle-tendon junctions of carp (*Cyprinus carpio*): ultrastructure and distribution of titin (connectin) and α actinin. *Cell. Tissue Res.* **281**, 517-524.
- ALEXANDER, R. MCN. (1969). The orientation of muscle fibres in the myomeres of fishes. *J. Mar. Biol. Ass.* **49**, 263-290.
- ALTRINGHAM, J.D. AND JOHNSTON, I.A. (1990a). Modelling muscle power output in a swimming fish. *J. Exp. Biol.* **148**, 395-402.
- ALTRINGHAM, J.D. AND JOHNSTON, I.A. (1990b). Scaling effects in muscle function: power output of isolated fish muscle fibres performing oscillatory work. *J. Exp. Biol.* **151**, 453-467.
- ALTRINGHAM, J.D., WARDLE, C.S. AND SMITH, C.I. (1993). Myotomal muscle function at different locations in the body of a swimming fish. *J. Exp. Biol.* **182**, 191-206.
- BIKERMAN, J.J. (1968). Stresses in proper adhints. In *The science of adhesive joints*, second edition, pp. 192-263. New York, London: Academic Press.
- BONE, Q. (1978). Locomotor muscle. In *Fish Physiology*, vol. VII (ed. W.S. Hoar and D.J. Randall), pp. 361-424. New York: Academic Press.
- BREMNER, H.A. AND HALLETT, I.C. (1985). Muscle fiber-connective tissue junctions in the fish blue grenadier (*Macruronus novaezelandiae*). A scanning electron microscopy study. *J. Food Sc.* **50**, 975-980.

- CURTIS, A.S.G. (1961). Timing mechanics in the specific adhesion of cells. *Exp. Cell Res.* **8**, S107-S122.
- DAVIES, L.F., JOHNSTON, I.A. AND WAL, J.W. VAN DE (1995). Muscle fibres in rostral and caudal myotomes of the Atlantic cod (*Gadus morhua* L.) have different mechanical properties. *Physiol. Zool.* **68**, 673-697.
- DEHOFF, R.T. AND RHINES, F.N. (1968). *Quantitative microscopy*. New York: Mcgraw-Hill. 422 pp.
- EISENBERG, B.R. (1983). Quantitative ultrastructure of mammalian skeletal muscle. In *Handbook of Physiology*, section 10 (ed. L.D. Peachey and R.H. Adrian), pp. 73-112. Bethesda, MD: American Physiological Society.
- EISENBERG, B.R. AND MILTON, R.L. (1984). Muscle fibre termination at the tendon in the frog's sartorius: A stereological study. *Am. J. Anat.* **171**, 273-284.
- GRANZIER, H.L.M., WIERSMA, J., AKSTER, H.A. AND OSSE, J.W.M. (1983). Contractile properties of a white- and a red-fibre type of the m. hyohyoideus of the carp (*Cyprinus carpio* L.). *J. Comp. Physiol.* **149**, 441-449.
- HALLETT, I.C. AND BREMNER, H.A. (1988). Fine structure of the myocommata-muscle fibre junction in hoki (*Macruronus novaezelandiae*). *J. Sc. Food Agric.* **44**, 245-261.
- HANAK, H. AND BÖCK, P. (1971). Die Feinstruktur de Muskel-Sehnverbindung von Skelett- und Herzmuskel. *J. Ultrastruct. Res.* **36**, 68-85.
- HILL, A.V. (1938). The heat of shortening and the dynamic constants of muscle. *Proc. R. Soc. Lond. B* **126**, 136-195.
- HUDSON, R.C.L. (1973). On the function of the white muscles in teleosts at intermediate swimming speeds. *J. Exp. Biol.* **58**, 509-522.
- ISHIKAWA, H., SAWADA, H. AND YAMADA, E. (1983). Surface and internal morphology of skeletal muscle. In *Handbook of Physiology* (ed. L.D. Peachey and R.H. Adrian), pp. 1-21. Bethesda, MD: American Physiological Society.
- JOHNSTON, I.A., PATTERSON, S., WARD, P. AND GOLDSPIK, G. (1974). The histochemical demonstration of microfibrillar adenosine triphosphatase activity in fish muscle. *Can. J. Zool.* **52**, 871-877.
- JOHNSTON, I.A., SIDELL, B.D. AND DRIEDZIC, W.R. (1985). Force-velocity characteristics and metabolism of carp muscle fibres following temperature acclimation. *J. Exp. Biol.* **119**, 239-249.
- JOHNSTON, I.A., WARD, P. AND GOLDSPIK, G. (1975). Studies on the swimming musculature on the rainbow trout. I. Fibre types. *J. Fish. Biol.* **7**, 451-458.
- KANNUS, P., JOZSA, L., KVIST, M., LEHTO, M. AND JÄRVINEN, M. (1992). The effect of immobilisation on myotendinous junction: an ultrastructural, histochemical and immunohistochemical study. *Acta Physiol. Scand.* **144**, 387-394.
- KARNOVSKY, M.J. (1965). A formaldehyde glutaraldehyde fixative of high osmolality for use in electronmicroscopy. *J. Cell Biol.* **27**, 137A-138A.
- KORNELIUSSEN, H. (1973). Ultrastructure of myotendinous junctions in myxine and rat. Specializations between the plasma membrane and the lamina densa. *J. Anat. Entwickl. Gesch.* **142**, 91-101.
- LUBKIN, J.L. (1957). A theory of adhesive scarf joints. *J. Appl. Mech.* **24**, 255-260.

- MERZ, W.A. (1967). Die Streckenmessung an gerichteten Strukturen im Mikroskop und ihre Anwendung zur Bestimmung von Oberflächen-Volumen-Relationen im Knochengewebe. *Mikroskope* **22**, 132.
- PROCTOR, C., MOSSE, P.R.L. AND HUDSON, R.C.L. (1980). A histochemical and ultrastructural study of the development of the propulsive musculature of the brown trout, *Salmo trutta* L., in relation to its swimming behaviour. *J. Fish. Biol.* **16**, 309-329.
- RAND, R.P. (1964). Mechanical properties of the red cell membrane. II. Viscoelastic breakdown of the membrane. *Biophys. J.* **4**, 303.
- ROHLF, F.J. AND SOKAL, R.R. (1981). *Statistical tables*, second edition. New York: W.H. Freeman and Company. 219 pp.
- ROME, L.C., FUNKE, R.P., ALEXANDER, R. MCN., LUTZ, G., ALDRIDGE, H., SCOTT, F. AND FREADMAN, M. (1988). Why animals have different muscle fibre types. *Nature* **335**, 824-827.
- ROME, L.C. AND SOSNICKI, A.A. (1991). Myofilament overlap in swimming carp II. Sarcomere length changes during swimming. *Am. J. Physiol.* **260**, C289-C296.
- ROME, L.C., SWANK, D. AND CORDA, D. (1993). How fish power swimming. *Science* **261**, 340-343.
- ROYET, J.P. (1991). Stereology: A method for analysing images. *Prog. Neurobiol.* **37**, 433-474.
- SCHATTENBERG, P.J. (1973). Licht- und elektronenmikroskopische Untersuchungen über die Entstehung der Skelettmuskulatur von Fischen. *Z. Zellforsch. Mikrosk. Anat.* **143**, 569-586.
- SHAPIRO, S.S. AND WILK, M.B. (1965). An analysis of variance test for normality (complete samples). *Biometrika* **52**, 591-611.
- SOKAL, R.R. AND ROHLF, F.J. (1981). *Biometry*, second edition. New York: W.H. Freeman and Company. 859 pp.
- STREET, S.F. (1983). Lateral transmission of tension in frog myofibres: a myofibrillar network and transverse cytoskeletal connections are possible transmitters. *J. Cell. Physiol.* **114**, 346-364.
- TIDBALL, J.G. (1983). The geometry of actin filament-membrane associations can modify adhesive strength of the myotendinous junction. *Cell Motil.* **3**, 439-447.
- TIDBALL, J.G. (1984). Myotendinous junctions: morphological changes and mechanical failure associated with muscle cell atrophy. *Exp. Mol. Path.* **40**, 1-12.
- TIDBALL, J.G. AND CHAN, M. (1989). Adhesive strength of single muscle cells to basement membrane at myotendinous junctions. *J. Appl. Physiol.* **67**, 1063-1069.
- TIDBALL, J.G. AND DANIEL, T.L. (1986). Myotendinous junctions of tonic muscle cells: Structure and loading. *Cell Tissue Res.* **245**, 315-322.
- TIDBALL, J.G. AND QUAN, D.M. (1992). Reduction in myotendinous junction surface area of rats subjected to 4-day spaceflight. *J. Appl. Physiol.* **73**, 59-64.
- TROTTER, J.A. (1990). Interfiber tension transmission in series-fibered muscles of the cat hindlimb. *J. Morph.* **206**, 351-361.
- TROTTER, J.A. (1993). Functional morphology of force transmission in skeletal muscle: A brief review. *Acta Anat.* **146**, 205-222.
- TROTTER, J.A. AND BACA, J.M. (1987). The muscle-tendon junctions of fast and slow fibres in the garter snake: Ultrastructural and stereological analysis and comparison with other species. *J. Muscle Res. Cell Motil.* **8**, 517-526.

Myotendinous junctions in axial muscle of carp

- TROTTER, J.A., CORBETT, K. AND AVNER, B.P. (1981). Structure and function of the murine muscle-tendon junction. *Anat. Rec.* **201**, 293-302.
- TROTTER, J.A., EBERHARD, S. AND SAMORA, A. (1983a). Structural domains of the muscle-tendon junction. I. The internal lamina and the connecting domain. *Anat. Rec.* **207**, 573-591.
- TROTTER, J.A., EBERHARD, S. AND SAMORA, A. (1983b). Structural connections of the muscle-tendon junction. *Cell Motil.* **3**, 431-438.
- TROTTER, J.A., HSI, K., SAMORA, A. AND WOFYSY, C. (1985a). A morphometric analysis of the muscle-tendon junction. *Anat. Rec.* **213**, 213-226.
- TROTTER, J.A., SAMORA, A. AND BACA, J.M. (1985b). Three-dimensional structure of the murine muscle-tendon junction. *Anat. Rec.* **213**, 16-25.
- VAN LEEUWEN, J.L. (1995). Review article: The action of muscles in swimming fish. *Exp. Physiol.* **80**, 177-191.
- VAN LEEUWEN, J.L., LANKHEET, M.J.M., AKSTER, H.A. AND OSSE, J.W.M. (1990). Function of red axial muscles of carp (*Cyprinus carpio*) recruitment and normalised power output during swimming in different modes. *J. Zool., Lond.* **220**, 123-145.
- WANG, K., MCCARTER, R., WRIGHT, J., BEVERLY, J. AND RAMIREZ-MITCHELL, R. (1991). Regulation of skeletal muscle stiffness and elasticity by titin isoforms: a test of the segmental extension model of resting tension. *Proc. Nat. Acad. Sci. U.S.A.* **88**, 7101-7105.
- WEIBEL, E.R. (1979). *Stereological methods. Practical Methods for Biological Morphometry*, vol. 1, pp. 1-415. New York: Academic Press.
- WEIBEL, E.R. AND BOLENDER, R.P. (1973). Stereological techniques for electron microscopic morphometry. In *Principles and Techniques of Electron Microscopy. Biological Applications*, vol. 3 (ed. M.A. Hayat), pp. 237-297. New York: Van Nostrand Reinhold Company.

5

Expression of titin isoforms in red and white muscle fibres of carp (*Cyprinus carpio* L.) exposed to different sarcomere strains during swimming

Igor L.Y. Spierts², Hendrica A. Akster² and Henk L. Granzier¹

¹Department of Veterinary and Comparative Anatomy, Pharmacology and Physiology, Washington State University, Pullman, WA 99164-6520;

USA

²Experimental Zoology Group, Wageningen Institute of Animal Sciences (WIAS), Wageningen Agricultural University, Marijkeweg 40, 6709 PG Wageningen;
The Netherlands

SUMMARY

Titin (also known as connectin) is a striated-muscle-specific protein that spans the distance between the Z- and M-lines of the sarcomere. The elastic segment of the titin molecule in the I-band is thought to be responsible for developing passive tension and for maintaining the central position of thick filaments in contracting sarcomeres. Different muscle types express isoforms of titin that differ in their molecular mass. To help to elucidate the relation between the occurrence of titin isoforms and the functional properties of different fibre types, we investigated the presence of different titin isoforms in red and white fibres of the axial muscles of carp. Gel-electrophoresis of single fibres revealed that the molecular mass of titin was larger in red than in white fibres. Fibres from anterior and posterior axial muscles were also compared. For both white and red fibres the molecular mass of titin in posterior muscle fibres was larger than in anterior muscle fibres. Thus, the same fibre type can express different titin isoforms depending on its location along the body axis. The contribution of titin to passive tension and stiffness of red anterior and posterior fibres was also determined. Single fibres were skinned and the sarcomere length dependencies of passive tension and passive stiffness were determined. Measurements were made before and after extracting thin and thick filaments using relaxing solutions with $0.6 \text{ mol l}^{-1} \text{ KCl}$ and $1 \text{ mol l}^{-1} \text{ KI}$. Tension and stiffness measured before extraction were assumed to result from both titin and intermediate filaments, and tension after extraction from only intermediate filaments. Compared to mammalian skeletal muscle, intermediate-filaments developed high levels of tension and stiffness in both posterior and anterior fibres. The passive tension-sarcomere length curve of titin increased more steeply in red anterior fibres than in red posterior fibres and the curve reached a plateau at a shorter sarcomere length. Thus, the smaller titin isoform of anterior fibres results in more passive tension and stiffness for a given sarcomere strain. During continuous swimming, red fibres are exposed to larger changes in sarcomere strain than white fibres, and posterior fibres to larger changes in strain than anterior fibres. We propose that sarcomere strain is one of the functional parameters that modulates the expression of different titin isoforms in axial muscle fibres of carp.

INTRODUCTION

In recent decades good progress has been made in understanding the biochemical, structural and mechanical properties of different muscle fibre types (review: Schiaffino and Reggiani, 1996). Studies of fish muscle have contributed to this understanding (Granzier *et al.*, 1983; Akster *et al.*, 1985, 1989). The fish is a good animal model for the study of muscle function because different fibre types are separated anatomically. A lateral red zone contains slow fibres with good endurance that are used for slow continuous swimming (Hudson 1973; Johnston *et al.*, 1974, 1975; Bone 1978). This zone is separated by an intermediate (pink) zone from the bulk of the musculature that consists of white, fast and easily fatigued fibres used for short powerful bursts of activity (Rome *et al.*, 1988; Altringham and Johnston 1990a,b; van Leeuwen *et al.*, 1990). These muscle fibre types are characterised on their myosin isotype: red fibres contain a slow myosin isotype and white fibres

contain a fast myosin isotype (Johnston *et al.*, 1977; Akster 1983). In order to advance our understanding of muscle properties further, a better understanding of passive muscle elasticity is, however, still required.

Our understanding of the molecular basis of muscle elasticity has made progress as a result of the discovery of the protein titin. Titin is a giant protein that spans the distance from the Z-line to the M-line of the sarcomere (Wang, 1985; Maruyama 1986, 1994; Trinick, 1991). The I-band segment of titin consists of series-coupled immunoglobulin (Ig)-like domains, each containing approximately 100 residues, and an unique domain rich in proline (P), glutamate (E), lysine (K) and valine (V), referred to as the PEVK domain (Labeit and Kolmerer, 1995). This region is thought to function as a molecular spring that maintains the central position of the thick filaments in the sarcomere and develops passive tension upon sarcomere stretch (Horowitz *et al.*, 1986; Fürst *et al.*, 1988; Wang *et al.*, 1991, 1993; Granzier *et al.*, 1996).

It is now well established that the passive tension-sarcomere length relation of skeletal muscle fibres and cardiac myocytes contains the following phases: (1) an initial shallow phase, (2) a subsequent steep phase, and (3) at long lengths a plateau phase (Granzier *et al.*, 1996). Immunoelectron microscopy suggests that in slack sarcomeres the elastic segment of titin is in a 'super-folded' state (Trombitás *et al.*, 1995; Granzier *et al.*, 1996) and the above mentioned phases of the tension-sarcomere length relation have been explained as follows: (1) upon initial stretch of slack sarcomeres the elastic segment first straightens developing modest levels of passive tension in the process; (2) upon further stretch PEVK and Ig-like domains unfold, giving rise to high levels of passive tension; (3) at long sarcomere lengths an increase in the extensible segment of titin occurs by detachment of titin from its anchors in the A-band and passive tension attains a plateau, the yield-point (Wang *et al.*, 1991, 1993; Granzier *et al.*, 1996; Linke *et al.*, 1996).

Different muscles express size variants of titin (isoforms) that result from differential splicing in the elastic region of titin (Labeit and Kolmerer, 1995). By comparing several rabbit muscles, positive correlations were found between the size of the expressed titin isoform and the tension-sarcomere length relationship of passive fibres (Wang *et al.*, 1991; Horowitz, 1992). We reported previously that different head muscles of perch contain different titin isoforms and that they differ in their passive tension-sarcomere length relationships as well (Akster *et al.*, 1989; Granzier *et al.*, 1991). The existence of differences in muscle function along the body of swimming fish led us to investigate whether these differences are accompanied by differences in titin. We also investigated fibres from the same type that are exposed to different strain amplitudes during swimming. In steadily swimming fish, a wave of curvature travels from head to tail with an increasing amplitude. The curvature imposes rhythmic cycles with alternating phases of positive and negative strain on the muscle fibres and consequently on the sarcomeres, resulting in higher sarcomere strains in posterior fibres than in anterior fibres (Hess and Videler, 1984; Wardle *et al.*, 1995). In addition to these anterior-posterior differences, there is a medial-lateral difference in strain as well. Differences in the distance of the muscle to the body axis of the fish, and differences in fibre arrangement, result in a larger sarcomere strain during swimming in red than in white fibres (Rome *et al.*, 1988).

Using gel-electrophoresis we investigated the presence of titin isoforms in different fibre types and fibres exposed to differences in strain amplitude. Passive tension-sarcomere length curves and passive

stiffness-sarcomere length curves were also determined using mechanically skinned single fibres. Because it is known that at long sarcomere lengths passive tension and passive stiffness are derived from titin and intermediate filaments (IFs), we dissected the contribution of each using KCl/KI extractions (Wang *et al.*, 1991; Granzier and Wang, 1993a).

MATERIALS AND METHODS

Preparations

Five common carp (*Cyprinus carpio* L.; 34-65 cm fork length) were caught in the Snake River (Washington State, United States), and killed with a firm blow to the head. Fibre bundles of red and white axial muscle were quickly dissected from two locations along the body axis. The positions (indicated as percentages of the fork length) were measured from the tip of the snout: anterior between the first and fourth ray of the dorsal fin: 41.75 ± 1.26 % ($N=5$); posterior, 2-4 cm caudal to the anus: 79.88 ± 0.98 % ($N=5$). When superficial white axial muscle was dissected, care was taken to exclude other fibre types.

Fibre bundles were skinned for 60 min in relaxing solution containing (mmol l⁻¹): imidazole 40; EGTA 10; MgAc 6.4; NaATP 5.9; NaN₃ 5; K-propionate 80; creatine-phosphate 10; DTT 1; leupeptin: 0.04; PMSF 0.5 (pH 7.0; 20 °C) and that also contained 1 % (w/v) purified Triton X-100 (28314; Pierce Chemical). Bundles were subsequently washed twice with relaxing solution (as above), and either used immediately for single fibre dissection, or stored in 50 % glycerol in relaxing solution at -20 °C. Single fibres were mechanically skinned, as described in Granzier and Wang (1993a), in order to remove extracellular material (collagen).

Mechanics

The mechanical set-up was built around an inverted microscope (Nikon Diaphot TMD) equipped for phase-contrast microscopy and placed on top of a vibration isolation table (Micro-G, model 63-573, Technical Manufacturing). Fibres were attached at one end to a motor (model 6800, Cambridge Technology; step response 0.5 ms; RMS position noise: approximately 0.5 µm) and at the other end to a force transducer (AME 801E, Horton, Norway) with a strain gauge conditioning amplifier (model 2310, Measurement Group, Raleigh, N. C.) used at a bandwidth of DC-10 kHz. Peak-to-peak force noise was approximately 0.2 mg. The force transducer and motor were mounted to manipulators attached to the XY stage of the microscope. The chamber had a volume of approximately 300 µl, contained a small J-type thermocouple, and was temperature controlled at 20 °C.

To attach fibres to the transducers, fibres were wrapped around fine hooks that had been glued to the force transducer and motor. During wrapping, fibres were present in 50 % glycerol/relaxing solution, allowing us to work briefly outside the chamber and to add a small amount (< 0.1 µl) of glutaraldehyde (2 % in relaxing solution) to the wrapped fibre segment. Fibres were then quickly lowered into the chamber that was rapidly perfused with relaxing solution. Force and stiffness

developed by the intermediate filament system were studied by removing thin and thick filaments. Fibres were treated for 20 min with relaxing solution containing an additional 0.6 mmol l⁻¹ KCl, and then for 45 min with relaxing solution containing 1.0 mmol l⁻¹ KI (cf. Granzier and Wang, 1993a). Although the extraction resistant nature of Ifs is well established, at present we cannot exclude that this treatment removes some of the Ifs from fish muscle fibres.

Sarcomere length measurement

Sarcomere length was measured with laser-diffraction using a He-Ne laser beam focused to a diameter of approximately 250 µm. The diffraction pattern was collected with a bright-field objective (Nikon, ELWD plan 40/0.55); a telescope lens was focused on the back focal plane of the objective and the diffraction pattern was projected, after compression with a cylindrical lens, onto a photo-diode array (Reticon RL 256 C/17). The first-order diffraction peak position was obtained using a digital spot-position detector board installed in an IBM AT computer (cf. Granzier and Irving, 1995). This signal was converted to sarcomere length using a calibration curve that was established with the diffraction peaks of a 25 µm grating that was present in the chamber. Sarcomere-length noise (peak-to-peak) during slow ramp stretches was approximately 20 nm. Sarcomere length was measured in the middle region of the fibre.

Protocols

To obtain reproducible results, fibres were subjected to stretch-release cycles generated by a computer-controlled mechanics workstation that was designed to impose identical mechanical protocols. It contained 16-bit D/A and 16-bit A/D converters, which allowed very slow stretch rates to be imposed on the preparations and small amplitude signals to be sampled. All protocols were generated using an IBM AT (486 processor) computer and a D/A board (DT 2823; Data-translation) with 100 kHz throughput. Force, fibre length and sarcomere length were recorded using another acquisition board (DT 2823). The software for the protocols and for data acquisition was written using Asyst (Version 4.0; Asyst Software Technologies).

Fibres were stretched with a constant velocity (25 % in 180 s) to a predetermined amplitude and then released to the initial length with the same velocity. Fibre length, sarcomere length and tension were measured every 350 ms. Concurrently, dynamic stiffness was also measured using sinusoidal length perturbations. Every 350 ms the preparation was subjected to a 15-ms burst of sinusoidal length oscillations (2200 Hz; amplitude 0.1 % of cell length). Each burst consisted of 32 oscillations (generated digitally). The ensuing tension oscillations were sampled, and the tension amplitude determined, on-line, using FFT analysis. Stiffness was calculated as the ratio of the tension amplitude to strain amplitude, and the time course of stiffness was plotted. Mechanical results were obtained from fresh fibres used within 6 hours post-mortem.

Gel electrophoresis and gel staining

Fibre bundles were quick frozen in liquid N₂ and the tissue was pulverised to a fine powder using a mortar and pestle bathed in liquid N₂. The powder was rapidly added to a tenfold excess of 1.1X Solubilisation buffer (50 mmol l⁻¹ TRIS-Cl, 2 % SDS, 10 % glycerol, 80 mmol l⁻¹ DTT, 30 µl ml⁻¹ Pyronin Y, pH 6.8 at 25 °C) in a homogeniser that was present in a water bath of 80 °C. The sample was solubilised for 90 sec and then cooled down and analysed with SDS-PAGE using 2.4-12 % acrylamide gradient gels. To obtain a high molecular mass standard for comparison, we solubilised and co-electrophoresed samples from psoas and semitendinosus muscle from the rabbit. Gels were stained with Coomassie blue (five carp) as explained in Granzier and Wang (1993a). We also solubilised, electrophoresed, and silver-stained single fibre segments (three carp) using the methods explained in detail in Granzier and Wang (1993a). Gels were overrun 2.5 hours to increase resolution. The migration distances of carp and rabbit skeletal muscle proteins were determined using video densitometry and normalised to nebulin of rabbit semitendinosus muscle.

Statistics

The results of our studies will be given as the means ± S.E., unless indicated otherwise. Statements of significant differences were assigned to selected parameters, using the Student's *t*-test with $P \leq 0.05$.

RESULTS

Gel electrophoresis

Solubilised carp axial muscle proteins were electrophoresed on low-porosity gels that were stained with Coomassie blue when fibre bundles were used (Fig. 1A), or with silver in the case of single fibres (Fig. 1B). To have titin standards, carp samples were either electrophoresed side by side with rabbit psoas and rabbit semitendinosus muscle or mixed with the rabbit samples and co-electrophoresed. Carp titin consisted of a doublet, T1 and T2 (Fig. 1A,B). T2 is considered to be a degradation product of the parent molecule T1, a process that may occur during sample preparation (Wang, 1985). Considerable degradation is found in most skeletal muscles, with the exception of rabbit semitendinosus muscle which is known to be relatively insensitive to degradation (Wang *et al.*, 1991). T1 of carp axial muscle migrated further than T1 of semitendinosus muscle and psoas muscle (Fig. 1A,B and Table 1). It is also apparent that white axial muscle T1 migrates further than red axial muscle T1 (Fig. 1A,B and Table 1). Furthermore, T1 of both white and red anterior axial muscle had a higher mobility than that of posterior axial muscle (Table 1). This latter difference can be observed most clearly in the lanes where posterior and anterior samples were mixed (red fibres: Fig. 1A, lane 8; white fibres: Fig. 1A, lane 2 and 5 and Fig. 1B, lane 5). Results from carp that varied in size from 34-65 cm fork length were indistinguishable.

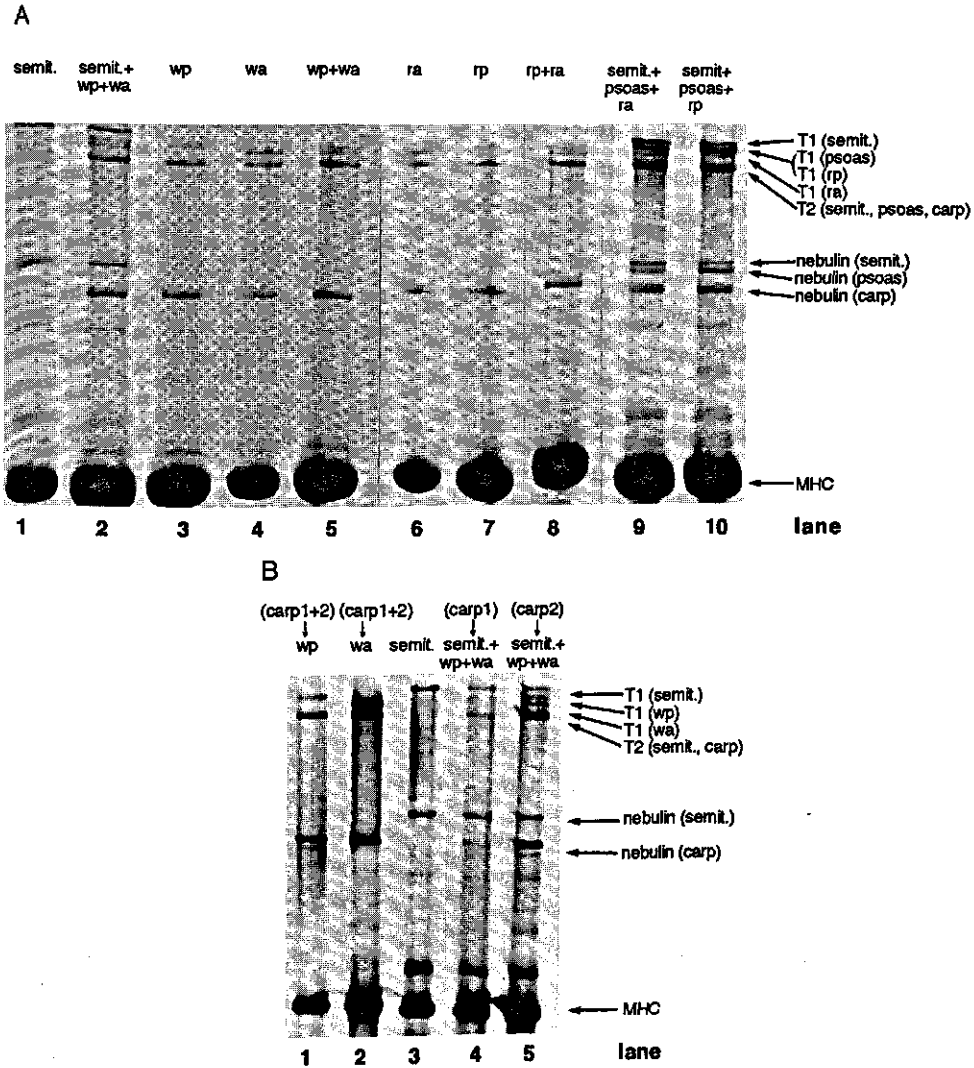


Fig. 1. (A) SDS-PAGE of fibre bundles. Carp axial muscle titin (r, red; w, white; a, anterior; p, posterior) consists of a doublet, T1 and T2. White muscle T1 migrates further than that of red muscle and anterior muscle T1 migrates further than that of posterior muscle (*lanes 3, 4, 6 and 7*), which can be observed most clearly in the lanes where anterior and posterior samples of one carp are mixed (*lanes 5 and 8*). Psoas and semitendinosus muscles from rabbit were used as high molecular mass standards, and titin of these muscles had a lower mobility than carp muscle T1 (*lanes 2, 9 and 10*). MHC, myosin heavy chain; (B) SDS-PAGE of single fibres. The difference in mobility between carp muscle T1 and rabbit semitendinosus titin (*lane 3*) is clearly visible when both samples are mixed (*lanes 4 and 5*). When carp muscle samples from carp that varied in size from 34 cm (carp 1) to 65 cm (carp 2) were mixed (*lanes 1 and 2*) and electrophoresed side by side (*lanes 4 and 5*) no differences in mobility were distinguished. See text for further details.

Unlike titin, nebulin of white and red fibres did not vary in mobility and neither did nebulin of anterior and posterior fibres (Fig. 1). This is consistent with the view that nebulin regulates thin filament length (Kruger *et al.*, 1991) and the finding that carp fibres obtained from different body locations shows no significant differences in thin filament length (van Leeuwen *et al.*, 1990; Sosnicki *et al.*, 1991). Furthermore, nebulin of carp fibres migrated much further than that of rabbit psoas muscle (Fig. 1), consistent with the much shorter thin filament length in carp muscle (approximately 0.95 μm ; van Leeuwen *et al.*, 1990; Sosnicki *et al.*, 1991) than in rabbit psoas muscle (approximately 1.1 μm ; Kruger *et al.*, 1991).

Table 1. Relative mobility of carp and rabbit skeletal muscle proteins. The migration distances were determined using video densitometry and normalised to nebulin of rabbit semitendinosus muscle, which was loaded in all lanes of the gels used to determine these migration distances.

Protein→ Muscle ↓		Titin T1	Titin T2	Nebulin
Rabbit	Semitendinosus	0.36		1.0
	Psoas	0.39	0.50	1.06
Carp	Red posterior	0.40		
	Red anterior	0.41		
	White posterior	0.42	0.49	1.15
	White anterior	0.43		

Passive tension and stiffness

The sarcomere slack length was determined in slightly buckled fibres that were perfused with relaxing solution. Slack sarcomere length of red fibres was $1.95 \pm 0.005 \mu\text{m}$ ($N=13$), and was significantly higher than that of white fibres ($1.92 \pm 0.004 \mu\text{m}$, $N=8$). No significant differences were found in slack sarcomere lengths of anterior and posterior fibres. Mechanical experiments were carried out on fibres dissected immediately post-mortem. White fibres could not be used in these studies because fibres were strongly interconnected by connective tissue, preventing us from isolating undamaged single fibres. Red fibres, on the other hand, were not as well interconnected, and posterior and anterior fibres could be dissected with relative ease. Therefore, reported mechanical results are from red fibres only. Red fibres were mechanically skinned and their mechanical properties measured in relaxing solution.

When fibres were stretched, passive tension of both anterior and posterior fibres increased initially modestly and then much more steeply with length, while a clear force plateau was often absent (Fig. 2A,C, curves marked 'total'). Because the titin-based plateau in the force-sarcomere length relation can be masked by the contribution of IFs to tension and stiffness (Granzier and Irving, 1995), we dissected the contribution of titin and IFs by removing thin and thick filaments using a KCl/KI treatment (see Materials and methods). This treatment extracts the anchor points for titin in the sarcomere and the ensuing decrease in tension and stiffness (curves marked 'KCl/KI sensitive') may be ascribed to titin, and the remaining tension and stiffness (curves marked 'KCl/KI insensitive') to

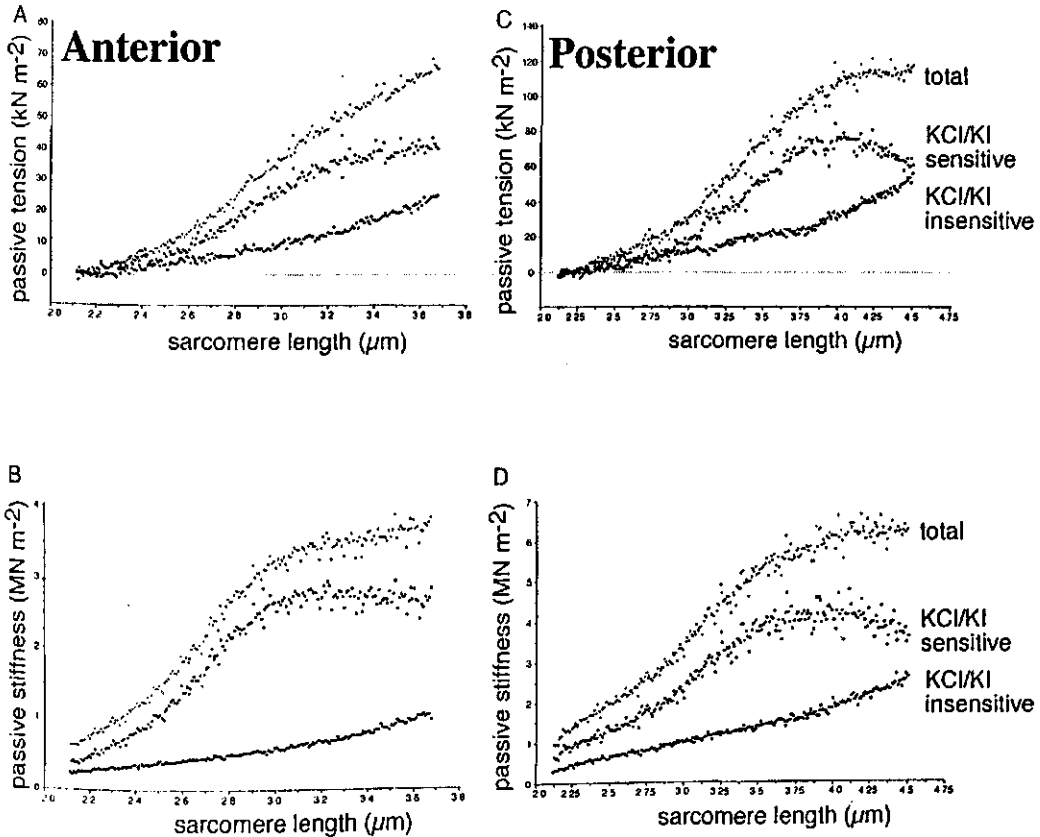


Fig. 2. (A,C) Passive tension-sarcomere length relations; (B,D) Passive stiffness-sarcomere length relations. Fibres were stretched with a constant velocity (25 % of slack length in 180 s) from their slack length to either a sarcomere length of approximately 3.7 μm (in A and B) or approximately 4.5 μm (in C and D), after which the fibre was released (25 % of slack length in 180 sec) back to the slack length. Stiffness was measured using brief bursts of 2200 Hz sinusoidal oscillations (see Materials and methods). First, the control curve was measured (curves marked *total*), after which the fibre was treated with KCl/KI (see Materials and methods), and the KCl/KI-insensitive component was then measured by stretching the fibre using the same velocity as before. By subtracting the KCl/KI-insensitive component from the total before treatment, the KCl/KI-sensitive tension and stiffness were obtained. See text for further details.

IFs (Granzier and Irving, 1995).

In both anterior and posterior fibres, IFs contributed considerably to tension (see Fig. 2, curves marked 'KCl/KI-insensitive'). In anterior fibres, for example, IFs contributed 35 % of the total tension at a sarcomere length of approximately 3.6 μm . IFs also contributed considerably to stiffness (Fig. 2B,D). However, their contribution to total stiffness was somewhat less than their contribution to total tension (Fig. 2). For example, in anterior fibres IFs contributed 24 % of the total stiffness at a sarcomere length of approximately 3.6 μm . The different IF contribution to total tension and stiffness results from mechanical differences between IFs and titin, specifically the lower stiffness to tension ratio of IFs. A similar observation has been made in cardiac myocytes (see Fig. 4 in Granzier and Irving, 1995).

The titin-based passive tension was obtained by subtracting the KCl/KI-insensitive tension from the total tension. Titin-based tension initially increased modestly with sarcomere length, then much more steeply, and finally levelled off to reach a plateau at a long sarcomere length (the yield-point). In anterior fibres the yield-point occurred at a significantly shorter sarcomere length ($3.17 \pm 0.03 \mu\text{m}$; $N=6$) than in posterior fibres ($3.79 \pm 0.04 \mu\text{m}$; $N=7$; Fig. 2A,C). Differences between anterior and posterior fibres were especially clear when results were normalised relative to the tension at the yield-point and after superimposing results (Fig. 3A). Normalised passive tension-sarcomere length curves revealed that the initial phase of modest tension rise extended to longer sarcomere length in posterior fibres (approximately 2.7 μm) than in anterior fibres (approximately 2.5 μm). Furthermore, the subsequent phase of the steep tension rise was less steep in posterior than in anterior fibres (Fig. 3A).

The titin-based stiffness-sarcomere length relation also contained a shallow and a steep phase, although the difference between the two phases was not as clear as for tension. Stiffness reached a maximum (yield-point) at a significantly shorter sarcomere length in anterior fibres ($3.05 \pm 0.04 \mu\text{m}$; $N=6$) than in posterior fibres ($3.65 \pm 0.03 \mu\text{m}$; $N=7$; Fig. 2B,C). When stiffness was expressed relative to the stiffness maximum, stiffness increased more steeply in anterior than posterior fibres (Fig. 3B). In both anterior and posterior fibres, the tension yield-point was reached at a sarcomere length that was approximately 0.2 μm longer than the passive stiffness yield-point (cf. 3A with 3B). Similar observations have been made in studies on rabbit skeletal muscle (Granzier and Wang, 1993b) and rat cardiac myocytes (Granzier and Irving, 1995).

DISCUSSION

We investigated the existence of different titin isoforms in red and white anterior and posterior axial muscle fibres of carp. It was found that red fibres express larger titin isoforms than white fibres and that posterior fibres express larger titin isoforms than anterior fibres. We also determined the passive tension- and passive stiffness-sarcomere length curves for red anterior and posterior fibres and dissected the contribution of titin and IFs to tension and stiffness. IFs contributed greatly to tension at sarcomere lengths where the titin yield-point is reached and masked the plateau of the titin-based passive tension-sarcomere length curve. Titin-based passive tension-sarcomere length curves revealed a yield-point which was reached at a shorter sarcomere length in anterior than in posterior fibres.

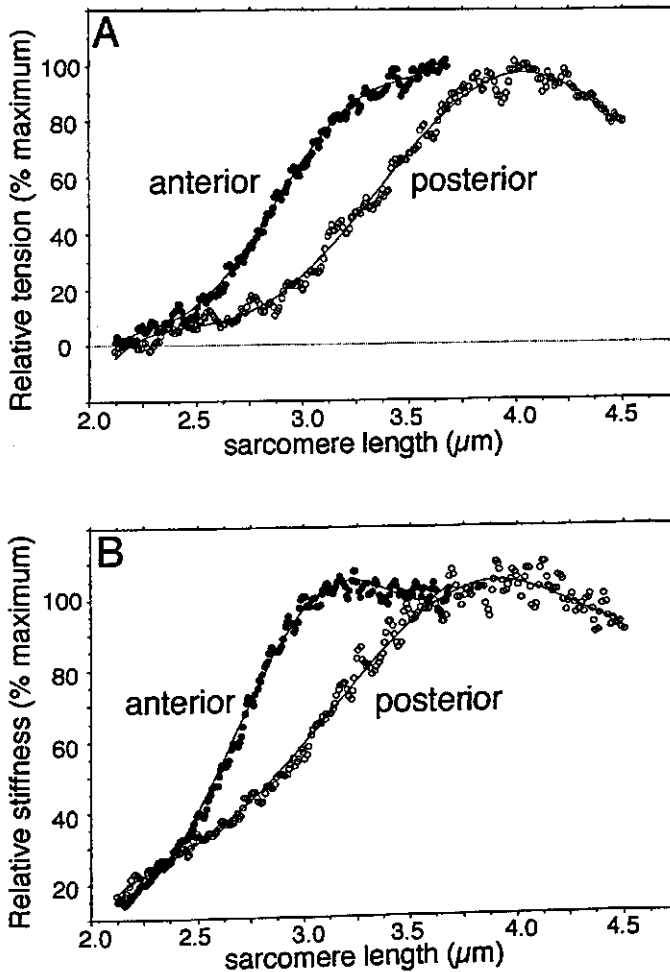


Fig. 3. (A) KCl/KI-sensitive tension-sarcomere length relations; (B) KCl/KI-sensitive stiffness-sarcomere length relations. Tension and stiffness were expressed relative to their respective maxima at their yield-points. In anterior fibres the tension and the stiffness increased steeper with sarcomere length than in posterior fibres, and tension and stiffness yield-points were reached at shorter sarcomere length than in posterior fibres. See text for further details.

Titin-based passive tension and stiffness

Differences in the molecular mass of titin result mainly from variation in the number of Ig-like domains and the number of amino acids in the PEVK region in the elastic I-band region of titin (Labeit and Kolmerer, 1995). Because red anterior muscle fibres of carp express a titin isoform that migrates further into SDS gels than that of red posterior fibres (Fig. 1 and Table 1), it is likely that the anterior

fibre titin contains a smaller number of Ig-like domains and/or a smaller number of PEVK residues. Thus, the elastic segment of titin is likely to be shorter in anterior fibres.

The difference in length of the elastic titin segment is predicted to result in differences in the tension-sarcomere length relation. In the recently proposed model of titin-based passive tension development (Granzier *et al.*, 1996) the low passive tension phase that occurs upon modest sarcomere stretch, results from straightening of the elastic segment, and a steep phase starts when the elastic segment is completely straight and molecular subdomains (Ig-like domains and PEVK domain) start to unfold. The shorter elastic segment of anterior fibres is thus predicted to result in a steep tension rise that starts at shorter sarcomere length than in posterior fibres. Our mechanical measurements indeed confirm this prediction (Fig. 3A). Furthermore, the titin yield-point, which in previous studies was found at sarcomere lengths where the elastic segment was stretched by a factor of three to four (Granzier and Wang, 1993b; Wang *et al.*, 1993; Granzier and Irving, 1995; Granzier *et al.*, 1996), is reached at a lower sarcomere length in anterior than in posterior fibres (Fig. 3). Thus, our mechanical results support the theory that the differences in electrophoretic mobility of the titin isoforms of red anterior and posterior fibres are related to differences in the size of the elastic I-band segment of titin.

Passive stiffness was measured by imposing on the fibres a sinusoidal length change with constant amplitude. As in rabbit skeletal muscle (Granzier and Wang, 1993b), stiffness of carp fibres reached a yield-point at a sarcomere length of approximately 0.2 μm shorter than where the tension yield-point was reached, and then declined with further sarcomere stretch (Figs 2 and 3). At sarcomere lengths beyond the stiffness yield-point, stiffness decreases while passive tension initially increases modestly and then, typically, attains a plateau. It has been proposed that at the stiffness yield-point passive tension is sufficiently high to detach titin from its anchors to the thick filaments, recruiting it thereby to the elastic titin pool (Wang *et al.*, 1991, 1993; Granzier and Wang, 1993b; Granzier and Irving, 1995). As a result of this recruitment, the constant amplitude of the sinusoid imposed on the fibre decreases in proportion to the length of the elastic I-band segment of titin. Therefore, stiffness can decrease with sarcomere stretch beyond the stiffness yield-point, despite an increase in strain of the elastic titin segment that is suggested by the modest increase in passive tension. The decrease in stiffness at long sarcomere lengths that we observed in carp fibres is thus a mechanical manifestation of the detachment of titin from its anchors in the A-band.

Intermediate filaments

It has been reported that passive tension of mammalian muscle fibres is not only derived from titin but also from IFs (Wang *et al.*, 1991, 1993; Granzier and Wang, 1993b). Our results on red fibres of carp (Fig. 2, curves marked 'KCI/KI-insensitive') are consistent with these earlier findings. Initially, IFs contribute little to passive tension of carp fibres, but at sarcomere lengths where the titin yield-point is reached their contribution is considerable and approaches a level that is similar to that of titin (Fig. 2). These findings deviate quantitatively from the results reported for rabbit psoas and semitendinosus muscle where at the yield-point the IFs contribute much less to tension than titin does (Wang *et al.*, 1993; Granzier and Wang, 1993b; Granzier *et al.*, 1996). Behaviour of the IFs in carp muscle shows some resemblance to that in rat myocytes (Granzier and Irving, 1995). In both muscle

types, IF-based tension is a larger proportion of the total passive tension, masking the plateau of the tension-sarcomere length relation of titin (Granzier and Irving, 1995). Cardiac muscle is known to contain larger amounts of desmin, the main protein of IFs in striated muscle, than skeletal muscle (Price, 1984). Results of the present study suggest that red axial muscle fibres of carp may also contain a relatively high content of desmin.

IFs in skeletal muscle form small bundles of short transverse filaments that connect adjacent myofibrils by forming transverse connections at the level of the Z-lines and M-lines, and continuous longitudinal filaments that connect the peripheries of successive Z-discs and ensheath the sarcomere (dos Remedios and Gilmour, 1978; Lazarides, 1982; Price and Sanger, 1983; Wang and Ramírez-Mitchell, 1983). Wang *et al.* (1993) proposed that the longitudinally oriented IFs in skeletal muscle function as a safety device, preventing damaged sarcomeres from being overstretched and torn apart during activation by adjacent undamaged sarcomeres. Torn sarcomeres would be disastrous as the severed myofibrils would considerably shorten during contraction ruling out any simple repair of the damaged areas. Our work implies that sarcomeres of carp fibres are more vulnerable to such damage than those of rabbit skeletal muscle. This may be related to a phase of eccentric activation that occurs during the rhythmic strain cycles of the swimming movements. During this phase of eccentric activation, which is longer in posterior than in anterior carp fibres, high demands are imposed on the stress-bearing structures (van Leeuwen *et al.*, 1990; van Leeuwen, 1995; Wardle *et al.*, 1995; Spierts *et al.*, 1996).

Titin and sarcomere strain

We found differences in titin between different fibre types (red and white) and within fibre types (anterior and posterior fibres of the same type). This suggests that sarcomere strain may be an important factor determining the titin isoform, and not the fibre type per se, which is generally based on the myosin isotypes present in the fibres. This notion is supported by our recent work in which we found that single fibres from human soleus muscle, which are exposed to the same sarcomere strain, express the same titin isoform, despite belonging to different fibre types (H.L.M. Granzier *et al.*, unpublished observations). It appears that physiological sarcomere strain amplitude and the expression of titin isoform are correlated.

In swimming fish sarcomere strain (for a given body curvature) is indeed larger in red fibres, which have a larger titin isoform than white fibres, due to differences in the distance between the sarcomere and the body axis and differences in fibre arrangement between both types (Rome *et al.*, 1988; Rome and Sosnicki, 1991). As yet the differences in titin isoform between anterior and posterior fibres can less easily be related to sarcomere strain. During steady swimming local curvature, and consequently sarcomere strain, increase from anterior to posterior, but differences are relatively small [approximately 3 % anterior and approximately 5 % posterior, relative to sarcomere slack length (Hess and Videler, 1984; Wardle *et al.*, 1995; Altringham *et al.*, 1993; Jayne and Lauder, 1995; Coughlin *et al.*, 1996)]. At the beginning of bursts of intermittent swimming strains are greatly amplified when larger body curvatures are attained. For this type of swimming, however, data are scarce and conflicting, attributing the largest strains to posterior fibres (up to 20 %; van Leeuwen *et al.*

al., 1990) as well as to anterior fibres (Rome and Sosnicki, 1991). This matter needs more investigation.

For the present we speculate that the presence of a larger titin isoform allows fibres to attain larger strain amplitudes without having to expend larger amounts of energy in stretching the elastic I-band segments of titin. In recent mechanical experiments on single titin molecules which were stretched and then released it was shown that force hysteresis is small if the stretch amplitude is modest and can be accommodated by straightening of the molecule and unfolding of the PEVK domain (Kellermayer *et al.*, 1997). If the stretch amplitude is higher, hysteresis is much enhanced due to unfolding/refolding processes of the Ig-like domains that take place during the stretch-release cycle. Thus, fibres that are exposed to large strains *in situ* can minimise energy loss by expressing a titin isoform that has a larger elastic segment. This allows larger strains to be imposed without substantial Ig-unfolding. Thus, in this view, titin isoform and sarcomere strain are correlated in order to minimise energy loss during cyclic loading of the muscle fibres.

ACKNOWLEDGEMENTS

We express our gratitude to Prof. Dr. J.W.M. Osse and Ir. H.L.M. Helmes for the valuable discussions and to Mrs. B. Stockman for superb technical assistance. This work was made possible by a Fulbright Scholarship for Graduate Study awarded by the Netherlands America Commission for Educational Exchange (NACEE, I.L.Y.S.), by the Netherlands Organisation for Scientific Research, Institution of Life Sciences, project 805-28.266 (NWO-SLW, I.L.Y.S.) and by a grant from the USA National Institute of Arthritis and Musculoskeletal and Skin Disease, AR42652 (to H.L.G.). All experiments performed in this study comply with the Principles of animal care, publication No. 86-23 revised 1985 of the National Institute of Health.

REFERENCES

- AKSTER, H.A. (1983). A comparative study of fibre type characteristics and terminal innervation in head and axial muscle of the carp (*Cyprinus carpio* L.): a histochemical and electron-microscopical study. *Neth. J. Zool.* **33**, 164-188.
- AKSTER, H.A., GRANZIER, H.L.M. AND KEURS, H.E.D.J. TER (1985). A comparison of quantitative ultrastructural and contractile characteristics of muscle fibre types of the perch, *Perca fluviatilis* L. *J. Comp. Physiol. B* **155**, 685-691.
- AKSTER, H.A., GRANZIER, H.L.M. AND FOCANT, B. (1989). Differences in I-band structure, sarcomere extensibility and electrophoresis of titin between two muscle fibre types of the perch (*Perca fluviatilis* L.). *J. Ultrastruct. Res. Mol. Struct. Res.* **102**, 109-121.
- ALTRINGHAM, J.D. AND JOHNSTON, I.A. (1990a). Modelling muscle power output in a swimming fish. *J. Exp. Biol.* **148**, 395-402.

- ALTRINGHAM, J.D. AND JOHNSTON, I.A. (1990b). Scaling effects in muscle function: power output of isolated fish muscle fibres performing oscillatory work. *J. Exp. Biol.* **151**, 453-467.
- ALTRINGHAM, J.D., WARDLE, C.S. AND SMITH, C.I. (1993). Myotomal muscle function at different locations in the body of a swimming fish. *J. Exp. Biol.* **182**, 191-206.
- BONE, Q. (1978). Locomotor muscle. In *Fish Physiology*, vol. VII. (ed. W.S. Hoar and D.J. Randall), pp. 361-424. New York: Academic Press.
- COUGHLIN, D.J., VALDES, L. AND ROME, L.C. (1996). Muscle length changes during swimming in scup: sonomicrometry verifies the anatomical high-speed cine technique. *J. Exp. Biol.* **199**, 459-463.
- DOS REMEDIOS, C.G. AND GILMOUR, D. (1978). Is there a third type of filament in striated muscles? *J. Biochem. (Tokyo)* **84**, 235-238.
- FÜRST, D.O., OSBORNE, M., NAVE, R. AND WEBER, K. (1988). The organisation of titin filaments in the half-sarcomere revealed by monoclonal antibodies in immunoelectron microscopy: a map of ten nonrepetitive epitopes starting at the Z-line extends close to the M-line. *J. Cell. Biol.* **106**, 1563-1572.
- GRANZIER, H.L.M. AND WANG, K. (1993a). Gel electrophoresis of giant proteins: Solubilization and silver-staining of titin and nebulin from single muscle fibre segments. *Electrophoresis* **14**, 56-64.
- GRANZIER, H.L.M. AND WANG, K. (1993b). Passive tension and stiffness of vertebrate skeletal muscle and insect flight muscle: the contribution of weak crossbridges and elastic filaments. *Biophys. J.* **65**, 2141-2159.
- GRANZIER, H.L.M. AND IRVING, T. (1995). Passive tension in cardiac muscle: the contribution of collagen, titin, microtubules and intermediate filaments. *Biophys. J.* **68**, 1027-1044.
- GRANZIER, H.L.M., HELMES, M. AND TROMBITÁS, K. (1996). Nonuniform elasticity of titin in cardiac myocytes: a study using immunoelectron microscopy and cellular mechanics. *Biophys. J.* **70**, 430-442.
- GRANZIER, H.L.M., WIERSMA, J., AKSTER, H.A. AND OSSE, J.W.M. (1983). Contractile properties of a white- and a red-fibre type of the M. Hyohyoideus of the carp (*Cyprinus carpio* L.). *J. Comp. Physiol.* **149**, 441-449.
- GRANZIER, H.L.M., AKSTER, H.A. AND KEURS, H.E.D.J. TER (1991). Effect of filament length on the force-sarcomere length relation of skeletal muscle. *Am. J. Physiol.* **260**, C1060-C1070.
- HESS, F. AND VIDELER, J.J. (1984). Fast continuous swimming of saithe (*Pollachius virens*): a dynamic analysis of bending moments and muscle power. *J. Exp. Biol.* **109**, 229-251.
- HOROWITS, R., KEMPNER, E.S., BISHER, M. AND PODOLSKY, R.J. (1986). A physiological role for titin and nebulin in skeletal muscle. *Nature (Lond.)* **323**, 160-163.
- HOROWITS, R. (1992). Passive force generation and titin isoforms in mammalian skeletal muscle. *Biophys. J.* **61**, 392-398.
- HUDSON, R.C.L. (1973). On the function of white muscles in teleosts at intermediate swimming speeds. *J. Exp. Biol.* **58**, 509-522.
- JAYNE, B.C. AND LAUDER, G.V. (1995). Red muscle motor patterns during steady swimming in largemouth bass: effects of speed and correlation's with axial kinematics. *J. Exp. Biol.* **198**, 1575-1587.

- JOHNSTON, I.A., PATTERSON, S., WARD, P., AND GOLDSPIK, G. (1974). The histochemical demonstration of microfibrillar adenosine triphosphatase activity in fish muscle. *Can. J. Zool.* **52**, 871-877.
- JOHNSTON, I.A., WARD, P. AND GOLDSPIK, G. (1975). Studies on the swimming musculature on the rainbow trout. I. Fibre types. *J. Fish. Biol.* **7**, 451-458.
- JOHNSTON, I.A., DAVISON, W. AND GOLDSPIK, G. (1977). Energy metabolism of carp swimming muscles. *J. Comp. Physiol. B* **114**, 203-216.
- KELLERMAYER, M.S.Z., SMITH, S.B., GRANZIER, H.L. AND BUSTAMANTA, C. (1997). Folding-unfolding transitions in single titin molecules characterised with laser tweezers. *Science* **276**, 112-116.
- KRUGER, M., WRIGHT, J. AND WANG, K. (1991). Nebulin as a length regulator of thin filaments of vertebrate skeletal muscles: correlation of thin filament length, nebulin size, and epitope profile. *J. Cell Biol.* **115**, 97-107.
- LABEIT, S. AND KOLMERER, B. (1995). Titins: giant proteins in charge of muscle ultrastructure and elasticity. *Science* **270**, 293-296.
- LAZARIDES, E. (1982). Intermediate filaments: a chemically heterogeneous, developmentally regulated class of proteins. *Annu. Rev. Biochem.* **51**, 219-250.
- LINKE, W.A., IVEMEYER, M., OLIVIERI, N., KOLMERER, B., RUEGG, J.C. AND LABEIT, S. (1996). Towards a molecular understanding of the elasticity of titin. *J. Mol. Biol.* **261**, 62-71.
- MARUYAMA, K. (1986). Connectin an elastic filamentous protein of striated muscle. *Int. Rev. Cytol.* **104**, 81-114.
- MARUYAMA, K. (1994). Connectin, an elastic protein of striated muscle. *Biophys. Chem.* **50**, 73-85.
- PRICE, M. (1984). Molecular analysis of intermediate filament cytoskeleton--a putative load bearing structure. *Am. J. Physiol.* **246**, H566-H572.
- PRICE, M.G. AND SANGER, J.W. (1983). Intermediate filaments in striated muscle. A review of structural studies in embryonic and adult skeletal and cardiac muscle. In *Cell and muscle motility*, vol. 3. (ed. R.M. Dowben and J.W. Shay), pp. 1-40. New York: Plenum Press.
- ROME, L.C. AND SOSNICKI, A.A. (1991). Myofilament overlap in swimming carp II. Sarcomere length changes during swimming. *Am. J. Physiol.* **260** (Cell Physiol 29), C289-C296.
- ROME, L.C., FUNKE, R.P., ALEXANDER, R. MCN., LUTZ, G., ALDRIDGE, H., SCOTT, F. AND FREADMAN, M. (1988). Why animals have different muscle fibre types. *Nature* **335**, 824-827.
- SCHIAFFINO, S. AND REGGIANI, C. (1996). Molecular diversity of myofibrillar proteins: gene regulation and functional significance. *Physiol. Rev.* **76**, 371-409.
- SOSNICKI, A.A., LOESSER, K.E. AND ROME, L.C. (1991). Myofilament overlap in swimming carp I. Myofilament lengths of red and white muscles. *Am. J. Physiol.* **260** (Cell Physiol 29), C283-C288.
- SPIERTS, I.L.Y., AKSTER, H.A., VOS, I.H.C. AND OSSE, J.W.M. (1996). Local differences in myotendinous junctions in axial muscle fibres of carp (*Cyprinus carpio* L.). *J. Exp. Biol.* **199**, 825-833.
- TRINICK, J. (1991). Elastic filaments and giant proteins in muscle. *Curr. Opin. Cell. Biol.* **3**, 112-118.
- TROMBITÁS, K., JIN, J.P. AND GRANZIER, H. (1995). The mechanically active domain of titin in cardiac muscle. *Circ. Research* **77**(4), 856-861.

- VAN LEEUWEN, J.L., LANKHEET, M.J.M., AKSTER, H.A. AND OSSE, J.W.M. (1990). Function of red axial muscles of carp (*Cyprinus carpio*): recruitment and normalised power output during swimming in different modes. *J. Zool.* **220**, 123-145.
- VAN LEEUWEN, J.L. (1995). The action of muscles in swimming fish. *Exp. Physiol.* **80**, 177-191.
- WANG, K. (1985). Sarcomere associated cytoskeletal lattices in striated muscle. Review and hypothesis. In *Cell and muscle motility 6* (ed. J.W. Shay), pp 315-369. New York: Plenum.
- WANG, K. AND RAMÍREZ-MITCHELL, R. (1983). A network of transverse and longitudinal intermediate filaments is associated with sarcomeres of adult vertebrate skeletal muscle. *J. Cell. Biol.* **96**, 562-570.
- WANG, K., MCCARTER, R., WRIGHT, J., BEVERLY, J. AND RAMÍREZ-MITCHELL, R. (1991). Regulation of skeletal muscle stiffness and elasticity by titin isoforms: a test of the segmental extension model of resting tension. *Proc. Natl. Acad. Sci. United States* **88**, 7101-7105.
- WANG, K., MCCARTER, R., WRIGHT, J., BEVERLY, J. AND RAMÍREZ-MITCHELL, R. (1993). Viscoelasticity of the sarcomere matrix of skeletal muscles. The titin-myosin composite is a dual-stage molecular spring. *Biophys. J.* **64**, 1161-1177.
- WARDLE, C.S., VIDELER, J.J. AND ALTRINGHAM J.D. (1995). Review. Tuning in to fish swimming waves: body form, swimming mode and muscle function. *J. Exp. Biol.* **198**, 1629-1636.

6

Kinematics and muscle dynamics of C- and S-starts of carp (*Cyprinus carpio* L.)

Igor L.Y. Spierts¹ and Johan L. van Leeuwen^{2,3}

¹Experimental Zoology Group, Wageningen Institute of Animal Sciences (WIAS), Wageningen
Agricultural University, Marijkeweg 40, 6709 PG Wageningen;

²Department of Physiology, Leiden University, Wassenaarseweg 62, PO Box 9604, NL-2300 RC
Leiden;

³Institute of Evolutionary and Ecological Sciences, Leiden University, Kaiserstraat 63, PO Box 9516,
NL-2300 RA Leiden;
The Netherlands

Published in: The Journal of Experimental Biology (1999) **202** (4): 393-406

Reproduced with permission of The Journal of Experimental Biology, Company of Biologists LTD.

SUMMARY

An analysis is presented of body curvature, acceleration and muscle strain during fast-starts in the common carp (*Cyprinus carpio* L.). C- and S-starts were filmed at 200 frames s^{-1} at 23 °C. Curvatures and accelerations of mid-body axes were calculated from digitised outlines. Maximum accelerations at 0.3 *FL* (fork length) from the snout were 54 $m s^{-2}$ for C-starts and 40 $m s^{-2}$ for S-starts. The total turning angle was approximately 150° in C-starts. This angle was 70° during escape S-starts, significantly larger than for predatory S-starts in other species. Sarcomere strains of axial muscle fibres were calculated at 0.4 and 0.8 *FL*. During C-starts, white muscle fibres were exposed to maximum sarcomere strains of up to approximately 16 %, and posterior fibres had similar strains to anterior fibres (red 27 %; white 16 %). During S-starts, however, maximum strains in anterior fibres (red 39 %; white 24 %) were more than twice those in posterior fibres (red 17 %; white 10 %). In a C-start, the fish made a large turning angle directed away from the stimulus by bending its tail strongly and thereby producing a large thrust. A larger anterior peak curvature of the fish during S-starts enabled the carp to control the direction of escape better than during C-starts, but with lower accelerations and smaller turning angles. During cyclic and intermittent swimming, red posterior fibres experienced the largest strains. Interestingly, previous studies have shown these fibres to have the lowest passive stiffness and the largest titin isoform, allowing them to attain large strain amplitudes with relatively low passive tensions.

INTRODUCTION

Fish generate fast-start swimming manoeuvres to avoid predators and to capture prey. Very high accelerations of the body (typically 30 $m s^{-2}$ or more, see Domenici and Blake, 1997) enable high swimming velocities to be attained in a short time. Three kinematic stages of fast-starts have been described: (1) a preparatory stroke; (2) a propulsive stroke; and (3) a subsequent variable behaviour (Weihs, 1973; Webb, 1976; Webb and Blake, 1985). For subcarangiform swimming (in teleosts), two major types of fast-start, generally referred to as C- and S-starts, have been distinguished (Hertel, 1966; Weihs, 1973; Eaton *et al.*, 1977; Webb, 1975, 1976, 1978a,b; Webb and Blake, 1985). During C-starts, the whole trunk curves in the same direction (Weihs, 1973; Webb, 1978a; Frith and Blake, 1991). These escape or startle responses are usually mediated by the Mauthner system (Eaton *et al.*, 1977; Kimmel *et al.*, 1980). C-starts have been subdivided into single- and double-bend types, depending on the presence of a second tail beat (Domenici and Blake, 1991; Kasapi *et al.*, 1993).

S-starts have been subdivided into those occurring during predatory attacks and escape responses. During predation starts, the turning angle of the body is small and the posterior region of the trunk curves more than the anterior portion (Hoogland *et al.*, 1956). S-shaped escape responses exist with considerable turning angles (generally smaller than in C-starts). Little is known about the neuronal mechanisms controlling S-starts.

Kinematic analyses of fast-starts of fish provide important information (e.g. curvature of the fish body and acceleration of the fish) for a functional analysis of the axial muscles that drive the

movements. The lateral curvature of the fish body can be used to derive the length changes of the sarcomeres. The tensile stresses of the sarcomeres are strain-dependent owing to length-dependent variations of (1) the overlap of thick and thin filaments (active contribution) and (2) the tension of titin (passive). Titin, a giant highly elastic muscle protein, is a stabilising structure that spans the distance between the Z- and M-lines of the sarcomere and contributes importantly to passive tension (Fig. 1). The titin segment in the A-band region of the sarcomere is ignored in this figure for clarity's sake. Titin also helps to maintain the central position of thick filaments in contracting sarcomeres (Wang, 1985; Maruyama, 1986, 1994; Wang *et al.*, 1991, 1993; Fürst *et al.*, 1988; Granzier *et al.*, 1996).

So far, very few studies have investigated the strain waves during intermittent swimming, turning manoeuvres and fast-starts. Van Leeuwen *et al.* (1990) recorded high-speed film of carp (*Cyprinus carpio*) during cyclic and kick-and-glide swimming, simultaneously with electromyographic recordings of the slow muscle fibres at eight positions along the trunk. The strain and strain rate of the slow fibres were determined (using curvature data) and used to calculate the force and power output of the muscle fibres. For kick-and-glide swimming, van Leeuwen *et al.* (1990) found that intermediate and fast muscle fibres are required to drive the movements.

Rome *et al.* (1988) examined strain rate amplitudes of fast and slow fibres during fast-starts in carp (*Cyprinus carpio*). These data were compared with experimentally obtained values for maximum shortening speed, and they suggested that fast fibres operated at strain rates close to optimum values for maximum power output.

Johnston *et al.* (1995) investigated instantaneous muscle strain and power output during a fast-start in the short-horned sculpin (*Myoxocephalus scorpius*). Predation fast-starts were filmed, and muscle strains were calculated for dorsal fast muscle using the lateral body curvature and the fibre orientation. The maximum peak-to-peak ranges of the muscle strain at 15 °C during the first tail beat were largest (approximately 0.19) at 0.52 *TL* (where *TL* is the total length of the fish measured from the snout) and smallest (approximately 0.15) at 0.77 *TL*. At 0.32 *TL*, the muscle strain range was 0.16. Furthermore, fibres at 0.52 *TL* and 0.77 *TL* on the same side of the body were initially stretched by the contralateral bending of the fish body, thus receiving a pre-stretch prior to shortening.

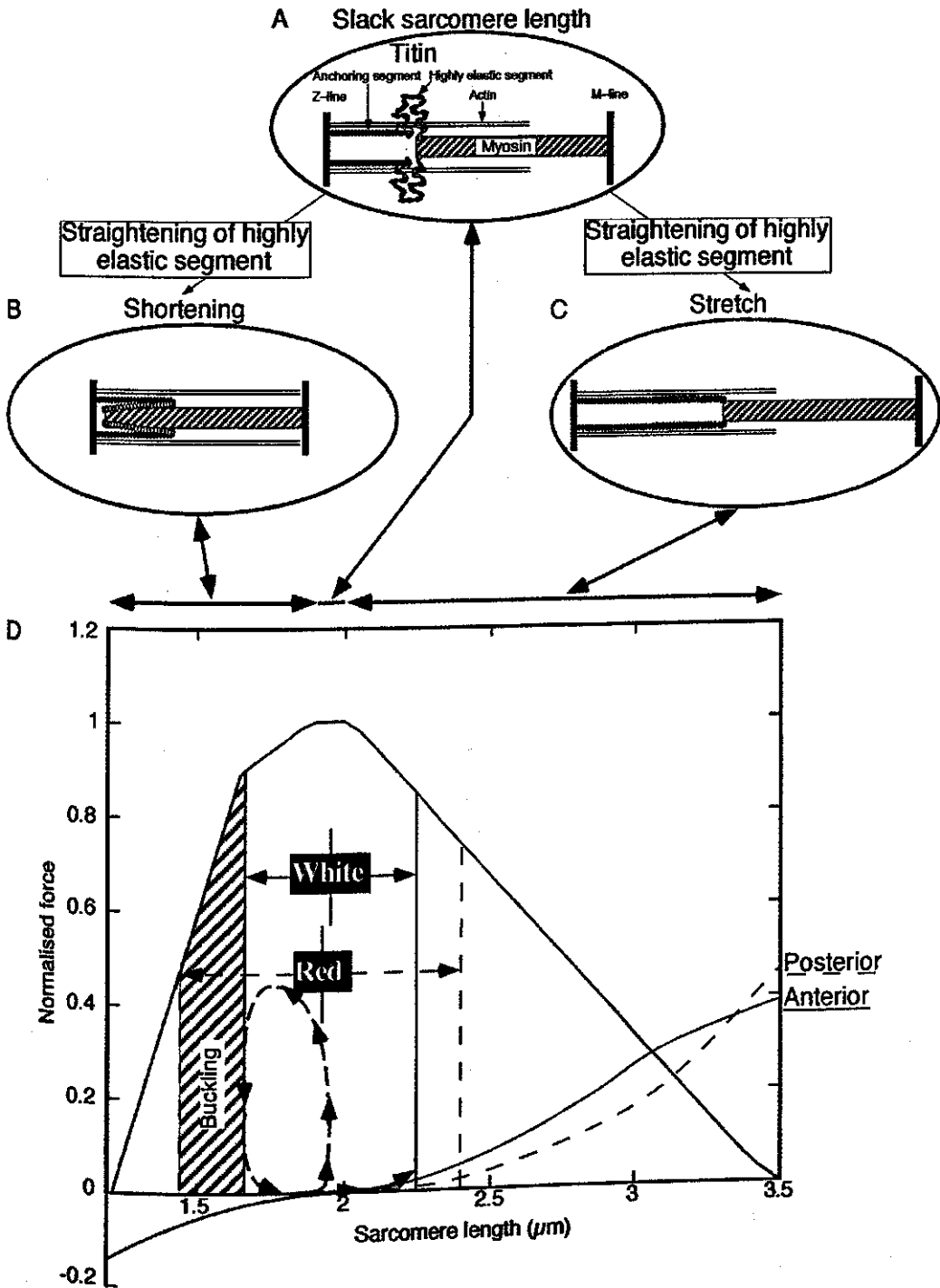
The present study examines fast-starts in carp. First, we will quantify the kinematic profiles of C- and S-starts by measuring and calculating (1) turning angles of the anterior part of the body, (2) accelerations at 0.3 *FL*, and (3) lateral body curvature as a function of position and time. Second, the curvature data and measured muscle fibre orientations are used to calculate strain variations of anterior and posterior red and white axial muscle fibres. Finally, sarcomere strains are used to interpret known structural features of the sarcomeres (which vary with fibre type and position along the trunk), such as the dimensions of titin and myofilaments.

MATERIALS AND METHODS

Swimming experiments

Eight specimens of common carp (*Cyprinus carpio* L.), 22.5-27.5 cm in fork length (*FL*), bred in the laboratory at 23 °C and fed on commercial fish food (Trouvit pellets; Trouw and Co. Putten) were used. High-speed motion films were made to determine sarcomere length changes (muscle strain) during fast swimming at 0.4 and 0.8 *FL* (measured from the snout) in red and white axial muscle fibres of carp. Swimming events of the fish were filmed from a dorsal viewpoint in a tank (90 cm long, 45 cm wide and 45 cm deep) using a Teledyne DBM 54 16 mm high-speed ciné camera at 200 frames s⁻¹. The camera was positioned 2 m above the tank, and a Nikon 28 mm lens was used to capture images of the complete tank. Films (Kodak double-X negative, 250 ASA) were taken with continuous light from seven Hama video lights so as to obtain sharp silhouettes of the swimming fish (power input of 5.2 kW). Water temperature was 23 °C, and warming of the aquarium by the filming lights was negligible because of the short lighting periods. Fast swimming responses, C- and S-starts and an intermediate swimming mode (I-swimming), were elicited by a sudden sound wave in the tank created by a blow to the laboratory floor adjacent to the tank or by tapping the side of the tank with a hard rubber mallet.

Fig. 1. Hypothesised mechanism of passive tension generation by titin (schematic). The titin segment in the A-band region of the sarcomere is ignored in this figure for clarity's sake. The I-band segment of titin consists of two subsegments: a stiff anchoring segment attached to the Z-line (coloured blue) and a highly elastic segment, connecting the anchoring segment to the myosin filaments (coloured red). (A) Slack sarcomere. The highly elastic titin segment is highly folded; (B) Sarcomere shortened below the slack length. The highly elastic segment of titin straightens and passive tension develops (see corresponding green curve in D); (C) Sarcomere stretch. The highly elastic segment of titin again straightens and passive tension develops (see corresponding red curves in D); (D) Force-sarcomere length curve for carp red and white muscles. The lengths of the actin and myosin filaments are 1.82 µm and 1.58 µm, respectively. The passive tension *versus* sarcomere length curves for carp red anterior and posterior fibres upon stretching (red curves) and shortening (green curve), derived from data of Spierts *et al.* (1997), are also shown and are expressed relative to a maximum active tension of approximately 150 kPa. The mean maximum sarcomere length excursions of red (25.1 %) and white (14.7 %) axial muscle fibres during fast-starts are indicated by dashed and solid lines, respectively. The blue dashed line indicates a hypothetical work loop for the white muscles that primarily power fast-starts and generate approximately 50% maximum tension. During (passive) muscle lengthening the work loop 'follows' the matching passive tension *versus* sarcomere length curve (not indicated for white muscles; see text for further details). Red fibres are not able to keep up with the high shortening velocity of white fibres and therefore tend to buckle at the concave side of the fish body (see hatched area). A-C are based on Granzier *et al.* (1996).⇒



Calculation of accelerations and muscle fibre strain

Films were analysed by projecting them onto sheets of A3 paper through a flat glass plate. Projected outlines of the fish during fast-starts and cyclic swimming were traced onto the paper at 5 ms intervals and digitised relative to fixed reference points, using an x,y -data-tablet (Calcomp 9100). For each side of the body, approximately 100 points were used. The points were distributed non-equidistantly. The shortest distances were used for the strongest curvatures of the outline. The estimated maximum error of the digitising process was 0.5 mm, which is approximately 0.002 % of the fork length of the fish.

For successive frames, a longitudinal axis of the fish during the swimming event was calculated from its digitised outlines, using the methods of van Leeuwen *et al.* (1990) and Johnston *et al.* (1995). The axis was divided into a number (typically 20-35) of straight-line segments before its shape was calculated. The mathematical segment length D_s was reduced linearly down the trunk of the fish:

$$\Delta s = \frac{(FL - s)s_1 + ss_2}{FL}, \quad (1)$$

where FL is the fork length of the fish (determined independently for the fish in a straight position), s is the distance of the most rostral point of the segment along the axis from the snout, s_1 is the length of the most rostral segment, and s_2 is a second prescribed length ($s_2 < s_1$). The variable segment length improved the stability of the applied algorithm while approaching the actual curvatures as closely as possible by allowing enough flexibility. The largest segment length chosen was in the head region, which is very stiff, allowing practically no curvature (typically $s_1 \approx 0.1 FL$) and the smallest segment length was in the tail region where curvature is largest (typically $s_1 \approx 0.025 FL$). The chosen segment lengths corresponded approximately to the anatomical length of the carp segments (skull, vertebrae and finray segments, respectively). Every axis was calculated starting at the anteriormost visible point of the body (determined manually). The orientation of each new axis segment was found iteratively by assuming that the left and right projected fish areas were equal (van Leeuwen *et al.*, 1990). This assumption was supported by the results of radiography of free-swimming fish (van Leeuwen *et al.*, 1990). The axis calculation ended at the posteriormost visible point of the body (i.e. the fork point of the tail blade, also determined manually).

The number of initial segments was allowed to vary from frame to frame (generally, the highest numbers of segments were used for the strongest curvatures). The 'raw' data were therefore interpolated so as to obtain 31 points for each calculated axis. The axes were subsequently smoothed as a function of position down the trunk using natural cubic B -spline functions (spline function package; Woltring, 1986). A natural spline function can be defined as a piecewise polynomial function between and outside selected knot positions s_j on the abscissa (reflecting, for the positional smoothing, the distances along the axis to the anterior snout point). A B -spline (e.g. de Boor, 1978) of degree q consists of $q + 1$ polynomial pieces that join at q inner knots. Derivatives up to order $q-1$

are continuous at the joining points. On a basis of B -splines $\{B_j(s): j = 1, \dots, n\}$, a fitted spline curve \hat{w} to data (s_j, w_j) is the linear combination:

$$\hat{w} = \sum_{j=1}^n \hat{a} B_j(s, q), \quad (2)$$

where \hat{a} are the spline coefficients. The spline coefficients can be manipulated using the so-called regularisation or smoothing parameter (Woltring, 1986). For smoothing of the axes, appropriate values were chosen for the smoothing parameter (the higher the smoothing factor, the more 'straight' the curve approximation becomes) in such a way that: (1) the fish axis was kept as straight as possible in the head region, (2) unrealistic small-scale fluctuations (i.e. with a length in the order of a few anatomical segments of the fish) in the curvature were eliminated, and (3) the fundamental characteristics of the wave of lateral curvature were preserved (i.e. over-smoothing was avoided). A more objective smoothing criterion, such as the minimisation of the generalised cross-validation (GCV, for details, see Woltring, 1986) function, could not be used for the positional smoothing because of correlated errors in neighbouring points. This would lead to too small a smoothing parameter. The smoothed axes (x_p, y_p) were described in parametric form by $x_p = F(s, t)$ and $y_p = G(s, t)$, where t is time, and F and G are functions. Owing to inaccuracies in the digitising process (see above), small errors were introduced that varied from frame to frame, such as very small undesired rigid body displacements and rotations. Functions x_p and y_p were therefore smoothed as a function of time using quintic natural B -spline functions and the GCV criterion as described by Woltring (1986). The GCV criterion was used because the mean squared error in the data was not known *a priori*. The GCV criterion should be used cautiously because it leads to under-smoothing if too small a number of knots is used for a given knot density (our data sets contained several hundreds of points, far more than the minimum number of 40 suggested in Woltring, 1986, which was evaluated to be too low). This last smoothing step had only a minor effect on the data set. The calculated axes (using the smoothed 31 points per frame) were used to calculate the turning rates (degrees ms^{-1}) of the midline of the anterior part of the body (snout to estimated centre of mass at 0.3 FL) throughout a C- and an S-start. We also calculated the accelerations (derived as the rate of change of the velocity magnitude in time) of some carp at 0.3 FL during C- and S-starts.

The absolute curvature k was calculated using the F and G functions introduced above in the following formula (Lipschutz, 1969):

$$k = \frac{\sqrt{\left(\frac{d^2 F}{ds^2}\right)^2 + \left(\frac{d^2 G}{ds^2}\right)^2}}{\left(\frac{dF}{ds}\right)^2 + \left(\frac{dG}{ds}\right)^2}. \quad (3)$$

The fork length divided by the local radius of the curvature R gave the normalised curvature (FL/R), which is defined as positive for curvature to the right and as negative for curvature to the left.

For reasons similar to those given for the accelerations, the curvatures obtained from the $x_p(s,t)$ and $y_p(s,t)$ data were finally smoothed as a function of time using the GCV criterion. In calculating the strain, the observed thickening at the concave side of the body, the thinning at the convex side, and the position and orientation of the muscle fibres were taken into account. It was assumed that the fibres were at their resting length when the trunk was straight. The strain ϵ_{paq} in a direction parallel to the axis, at an instantaneous distance d from the median plane, was calculated as (van Leeuwen *et al.*, 1990):

$$\epsilon_{paq} = -\frac{d}{R} \quad (4)$$

for the concave side of the body, and

$$\epsilon_{paq} = \frac{d}{R} \quad (5)$$

for the convex side of the body, where $R = 1/k$ is the local radius of curvature. Similarly, the strain ϵ_{ppq} perpendicular to the axis, at an instantaneous distance d from the median plane, was calculated as (van Leeuwen *et al.*, 1990):

$$\epsilon_{ppq} = \frac{R}{\sqrt{(R-2d_0)R}} - 1 \quad (6)$$

for the concave side of the body, and

$$\epsilon_{ppq} = \frac{R}{\sqrt{(R+2d_0)R}} - 1 \quad (7)$$

for the convex side of the body, where d_0 is the corresponding (initial) distance along the straight axis. Finally, the strain of red and white muscle fibres were calculated using:

$$\epsilon_p = l^2 \epsilon_{ppq} + n^2 \epsilon_{paq}, \quad (8)$$

where l and n are the direction cosines of the muscle fibres in the perpendicular and the parallel direction, respectively.

Eight fish were used for the strain calculations and, for every fish, C-starts, S-starts and a fast-swimming mode intermediate between these two forms (I-swimming) were filmed and digitised. In total, we used 24 filmed scenes of fast-starts. Using equations 4-7, the maximum sarcomere strains were calculated for red and white muscle fibres at 0.4 and 0.8 FL for all fast-starts examined. For

every type of fast-start a mean maximum sarcomere strain was calculated for each muscle type and location (i.e. mean of 8 maximum values, 1 per filmed scene).

We also examined mean sarcomere strains during cyclic swimming of each carp. All computer programs were written for the Macintosh family of computers, using Think Pascal 4.0.2 (Symantec Corp.) or Mac FORTRAN II (Absoft Corp.) as programming languages. The two-dimensional-curvature data were interpolated using the cubic interpolation routine available in the Transform plotting package (Fortner Research LLC). The interpolated data were represented as contour plots.

The calculations did not compensate for possible buckling effects that are likely to occur in the red fibres during fast-starts. Unrealistically low negative sarcomere strains for red muscles were therefore obtained occasionally (see Results and Discussion). Only positive strains of the sarcomere (of both the left and right side of the body during a filmed scene) were included in the statistical analysis.

Muscle fibre orientation and sarcomere length measurements

The red and white muscle fibre position and orientation were measured using the method described by Alexander (1969). The skin of the fish was removed from one side of the body to reveal the musculature, and incisions were made using a sharp razor blade at the mid-point of the red (1-2 mm deep) and dorsal white muscle (3-4 mm deep) at points 0.4 and 0.8 *FL* along the body (Fig. 2). The angles, measured with respect to the median and frontal plane of the fish, were used to correct strain calculations for the orientation of red and white fibres.

Red and white muscle fibres at 0.4 *FL* and 0.8 *FL* along the trunk of a carp were prepared for electron microscopy as described by Akster (1985). The length of the actin filament and the myosin filament were measured. We used the cross striation in the I-band (caused by the 38.5 nm periodicity of the troponin complexes on the actin filament; Page and Huxley, 1963) to correct for the combined effects of uncertainties in the microscopic magnification and shrinkage. In this way, the natural length of the filaments could be accurately determined. In addition, our filament length measurements and derived sarcomere resting length were supported by single-fibre laser diffraction length measurements and force measurements (Spierts *et al.*, 1997).

Statistics

The maximum strain data calculated in this study (relative values) appeared to be normally distributed (Shapiro and Wilk, 1965). The differences in sarcomere strain we found between red and white anterior and posterior muscle fibres during different swimming modes were analysed statistically using a univariate analysis of variance procedure (ANOVA; SAS 6.11, SAS Institute Inc., Cary, USA), *t*-tests and least significant difference (LSD) of means (Sokal and Rohlf, 1981). Individual fish were taken as a random factor with four test positions of sarcomeres. Statements of statistical significance are based on $P \leq 0.05$ unless specified otherwise (Sokal and Rohlf, 1981; Rohlf and Sokal, 1981). Values are presented as means \pm S.D.

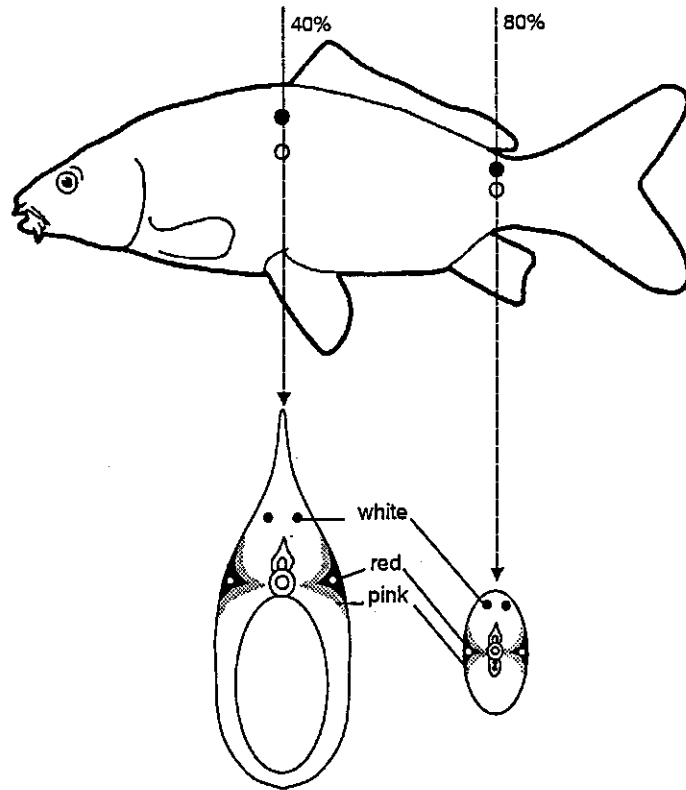


Fig. 2. Schematic drawing showing the positions used for calculating the muscle fibre strain in red and white muscle tissue on the left and right side of the fish body at 0.4 and 0.8 *FL*, where *FL* is fork length. The positions for white and red muscle tissue are indicated by filled and open circles, respectively.

RESULTS

The ranges of muscle fibre angles measured with respect to the median planes were 4-6° at 0.4 *FL* and 6-8° at 0.8 *FL* for red muscle fibres, and 20-27° at 0.4 *FL* and 12-17° at 0.8 *FL* for white muscle fibres. The ranges of angles measured with respect to the frontal plane were 8-10° at 0.4 *FL* and 2-5° at 0.8 *FL* for red muscle fibres, and 14-16° at 0.4 *FL* and 29-31° at 0.8 *FL* for white muscle fibres. The mean sarcomere lengths of red fibres, $1.95 \pm 0.0032 \mu\text{m}$, and of white fibres, $1.92 \pm 0.0036 \mu\text{m}$, differed significantly ($N=36$). The length of the actin filament was $1.82 \pm 0.028 \mu\text{m}$ ($N=12$) and the length of the myosin filament was $1.58 \pm 0.041 \mu\text{m}$ ($N=12$). As values varied very little along the trunk, no significant differences were found between anterior and posterior fibres.

Three types of fast-starts were distinguished: a typical C-start or startle response, an S-start and an intermediate fast-swimming mode (I-swimming). The statistical analysis did not reveal significant differences between individual fish.

Swimming responses of carp after introducing a sound wave into the tank

C-start

C-starts of carp occurred very suddenly and rapidly and involved large turning angles. Fig. 3 is an example of a single-bend C-start showing the calculated central axis of an adult carp (Fig. 3A) and the turning rate of the anterior body midline (Fig. 3B). Only stage 1 could be recognised, which is typical for a single-bend C-start because no change in turning direction occurs. Stage 1 started at $t=0$ ms, when the carp was in a resting position, and ended at $t=100$ ms when the turning rate had decreased to zero. The maximum turning rate was 4° ms^{-1} . After 100 ms, a total turning angle of 155° had been reached. Fig. 3C shows a contour plot of the body curvature during this C-start. The horizontal axis represents the normalised position along the body axis (0, tip of snout; 1, fork of tail fin), the ordinate shows the time, and the contours in the plot show the normalised curvature FL/R (R , local radius of curvature). The largest curvatures occurred between 0.5 and 0.8 FL . The body bent mainly to the right side during this start, although between 0 and 20 ms a very small curvature to the left was calculated for the tail region. At approximately 0.6 FL , the maximum curvature (inner small contour in the dark area) was reached approximately 25 ms after starting from an almost straight position. The contours show that the position of peak curvature along the trunk travelled at fairly constant speed from 0.5 to 0.72 FL (approximately $5 FL \text{ s}^{-1}$). Between 0.72 and 0.85 FL (peduncle region) the speed of the position of peak curvature was much higher, and the speed dropped again in the most posterior region.

Fig. 4A,B shows two typical examples of the acceleration of the fish axis at 0.3 FL during a C-start. Fig. 4A is from the same start as shown in Fig. 3. In the first 20 ms of a C-start, large accelerations of up to 54 m s^{-2} were achieved. The acceleration during a C-start showed at least two peaks. The first main peak almost coincided with the moment of maximum turning rate (Fig. 3B), just before the moment of maximum curvature. The timing of peaks 1 and 2 (Fig. 4A) is indicated by dashed horizontal lines in Fig. 3C.

The curvatures of the fish (Fig. 5A-C) clearly showed that both head and tail region curved extensively in the same direction during the C-start, resulting in large sarcomere strains anteriorly as well as posteriorly. In Fig. 5A, the carp started from a straight position. In Fig. 5B,C the fast-start began while the fish was swimming slowly. In these latter cases, the fast-start was preceded by a short preparatory stroke (see the first 10-15 ms) due to the preceding swimming motion. During this stroke, the fish body bent slightly after which the large C-shape developed in opposite direction. Fish often performed double-bend C-starts, which consisted of two stages (e.g. Fig. 5A-C). During stage 1, the carp bent extensively to one side, followed by a smaller bend to the opposite side, stage 2.

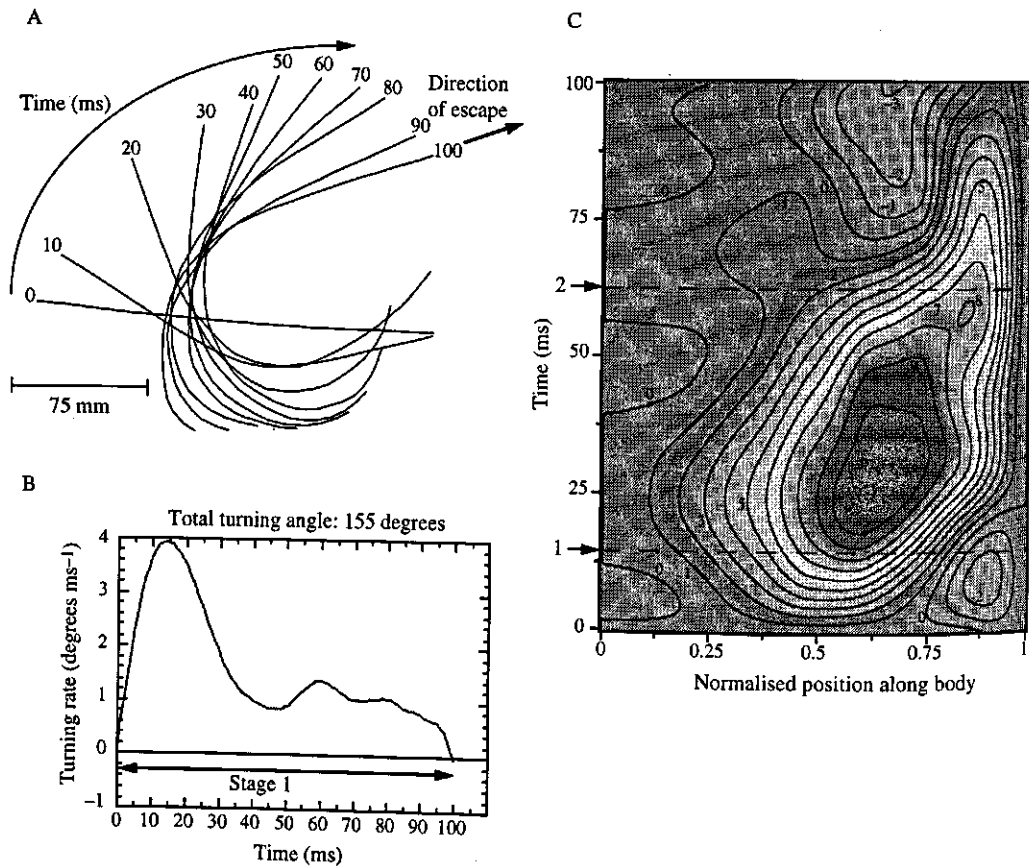


Fig. 3. Single-bend C-start of an adult carp. (A) The central axis of the fish (plotted using the 31 points derived per calculated axis) during a single-bend C-start, shown every 10 ms. Times between tracings are in milliseconds from the first detectable movement; (B) The turning rate of the anterior body midline (snout to estimated centre of mass at 0.3 FL, where FL is fork length) during this C-start. The single-bend C-start consisted of stage 1 only; (C) Contour plot of the body curvature during this C-start. The horizontal axis represents the body axis of the fish expressed as normalised FL (0, tip of snout; 1, fork of tail fin), the ordinate shows the time, and the contours in the plot show the normalised curvature FL/R (where R is the local radius of curvature). Curvature was positive for bending to the right and negative for bending to the left. The dashed horizontal reference lines numbered 1 and 2 indicate the peaks in acceleration of the fish axis at 0.3 FL during this C-start, shown in Fig. 4A.

In the absence of electromyographic (EMG) recordings, stages 1 and 2 of a fast-start were defined using the turning rate (Figs 3B and 6B). Stages 1 and 2 were delimited by the changes in the turning direction of the anterior body midline (after Domenici and Blake, 1991, 1993b; Kasapi *et al.*, 1993).

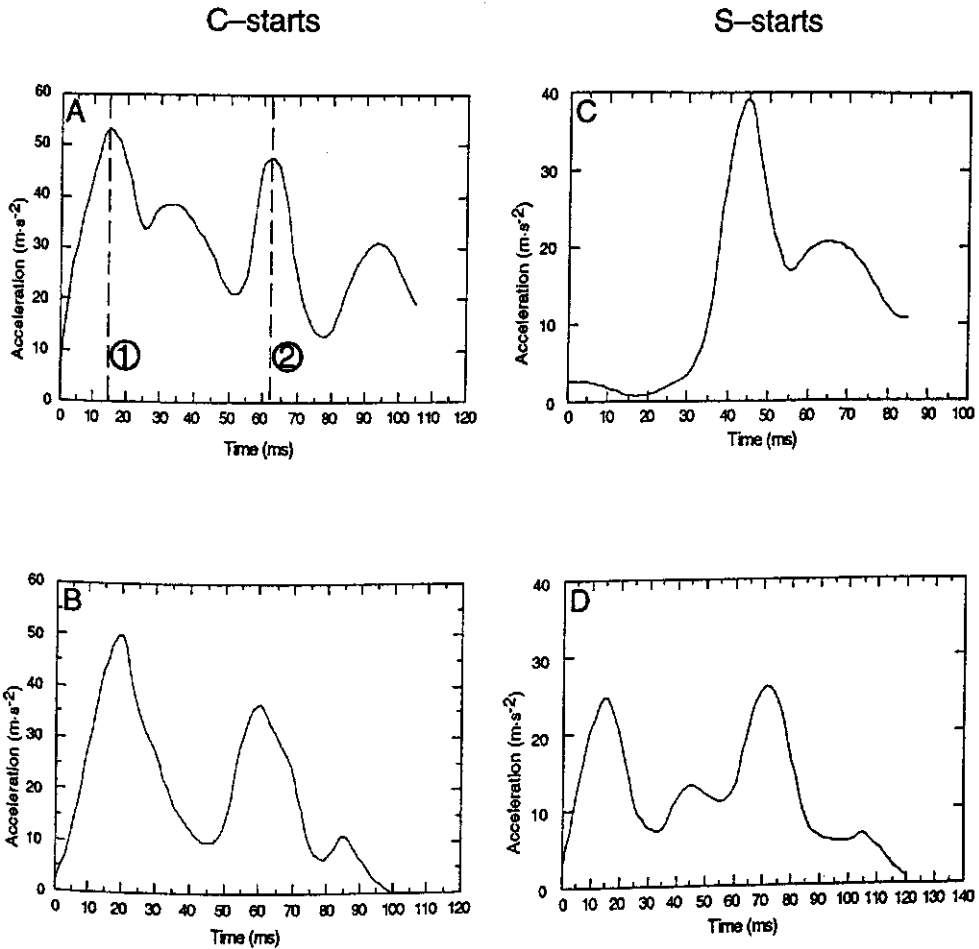


Fig. 4. Typical examples of acceleration (derived from velocity data) of the fish axis at 0.3 *FL*, where *FL* is fork length, during fast-starts; (A,B) C-starts. A represents the same start shown in Fig. 3. The timings of the two peaks of acceleration in A, labelled 1 and 2, are indicated by the dashed horizontal lines in Fig. 3C; (C,D) S-starts. C shows a slow start followed by a large acceleration.

The double-bend C-starts investigated lasted approximately 50-100 ms (the sum of stage 1 and 2). When carp performed C-starts, the maximum curvature on one side of the body (anteriorly, posteriorly or both) was always reached within 10-25 ms after starting from a straight body position. During this period of maximum curvature, maximum sarcomere strains were reached on the convex side of the fish body (see Figs 7A-C, 8A-C). Anterior and posterior maximum curvatures were reached with a time difference up to approximately 5 ms (Fig. 5A-C).

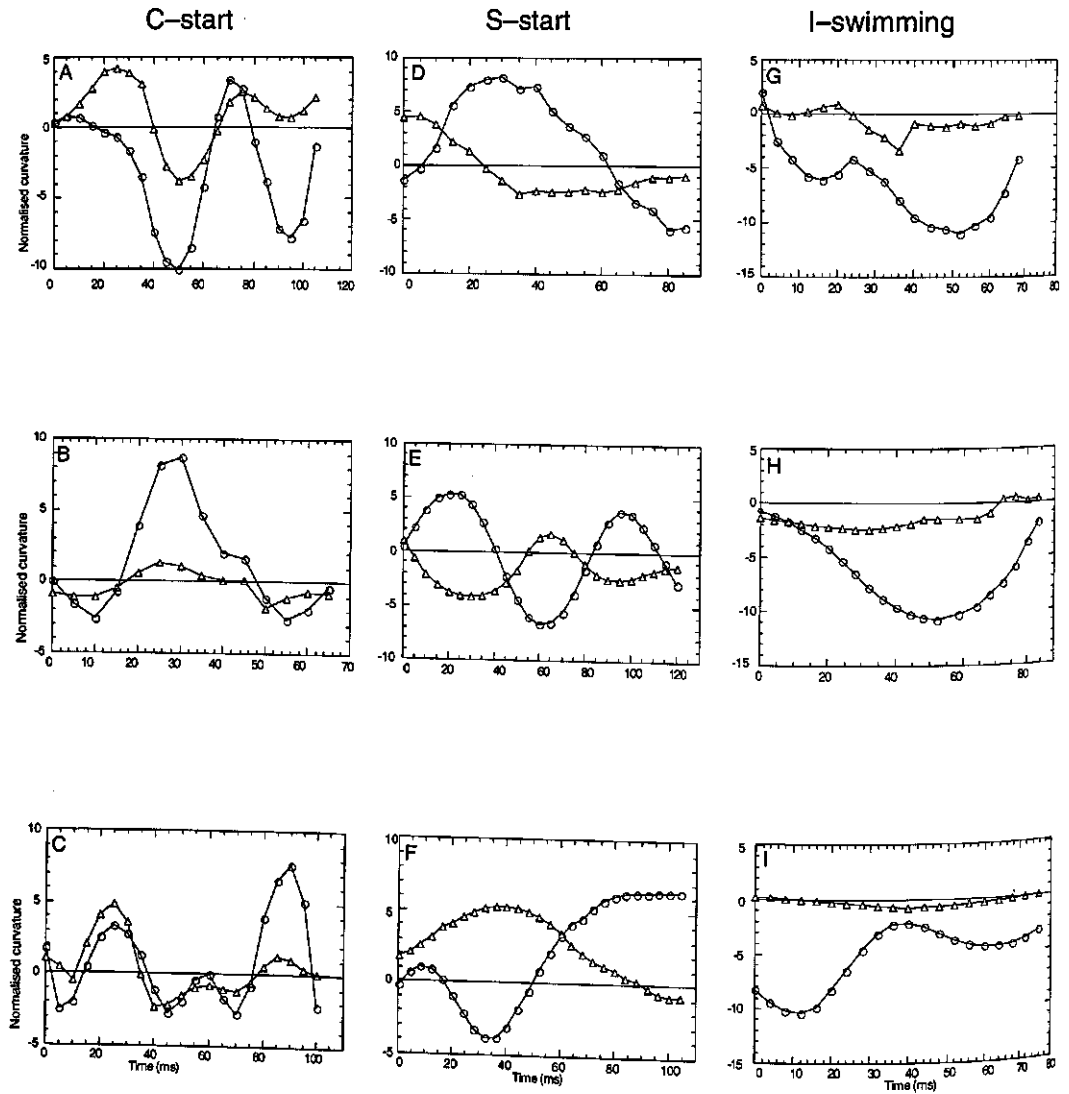


Fig. 5. Normalised curvature FL/R (where FL is fork length and R is local radius of curvature) of anterior (triangles) ($0.4 FL$) and posterior (circles) ($0.8 FL$) regions of the fish body during fast-starts. Curvature was positive for bending to the right and negative for bending to the left. When both anterior and posterior curvatures are zero, the fish is lying in a straight position; (A-C) C-starts; (D-F) S-start escape responses; (G-I) Intermediate fast-swimming movements (I-swimming). The sarcomere strains of fast-starts are shown in Figs 7 and 8, respectively.

S-start

Fig. 6 is an example of an S-start showing the central axis of an adult carp (Fig. 6A) and the turning rates of the anterior body midline (Fig. 6B). In stage 1, the carp started from a straight position and bent into a large S-shape with turning rates up to approximately $1.5^\circ \text{ ms}^{-1}$. At $t=60 \text{ ms}$, the turning rate became negative and stage 1 was followed by stage 2, in which the fish adopted an opposite S-shape. Stage 2 lasted until approximately $t=88 \text{ ms}$ when a further reversal of turning direction occurred and stage 3 (variable behaviour) followed. At 140 ms , the total turning angle was 72° . Fig. 6C shows a contour plot of the body curvature during this S-start. The contour plot shows that at each instant positive and negative curvatures were present down the trunk, which is typical for an S-start. The largest curvature occurred at 0.5 FL (dark area) and was reached approximately 50 ms after the initial straight position. The contours show that the position of maximum curvature along the trunk travelled at fairly constant speed from 0.35 to 0.7 FL (approximately 10 FL s^{-1}). In contrast to the C-start of Fig. 3, the speed decreased gradually posteriorly from 0.7 FL . These were typical S-starts because the largest curvatures occurred approximately half-way along the trunk (resulting in large anterior sarcomere strains, see below). S-starts of carp occurred at lower accelerations (Fig. 4) than in C-starts with displacements that were more in line with the body axis. Fig. 4C,D show two typical examples of the acceleration of the fish at 0.3 FL during S-starts. In the S-start shown in Fig. 4C, the fish began the movement slowly, after which large accelerations occurred (peak close to 40 m s^{-2}). The peaks in the acceleration curve (in Fig. 4C at $t=45 \text{ ms}$ and in Fig. 4D at 15 ms and 70 ms) coincided with moments at which the tail fin had a high lateral velocity (approximately $3\text{--}4 \text{ m s}^{-1}$) and was at a considerable angle (approximately $70\text{--}90^\circ$) relative to the direction of movement (i.e. favourable conditions for generating thrust).

The normalised curvatures plotted in Fig. 5D,F are for fish that began the S-start while swimming slowly, whereas in Fig. 5E the fish was in a straight position at the beginning of the start. The S-starts investigated lasted slightly longer (stages 1 + 2) than the C-starts, and lower turning rates were achieved. The time carp required to reach maximum curvature from a straight position (with large strains, see Figs 7D-F and 8D-F) was longer and more variable than in the C-starts.

I-swimming

During I-swimming, the body curvatures were largest in the posterior region of the trunk. In this region, curvature amplitudes were similar to those of the C- and the S-start (see Fig. 5G-I). Hence, much larger sarcomere strains occurred posteriorly than anteriorly (see Figs 7G-I and 8G-I).

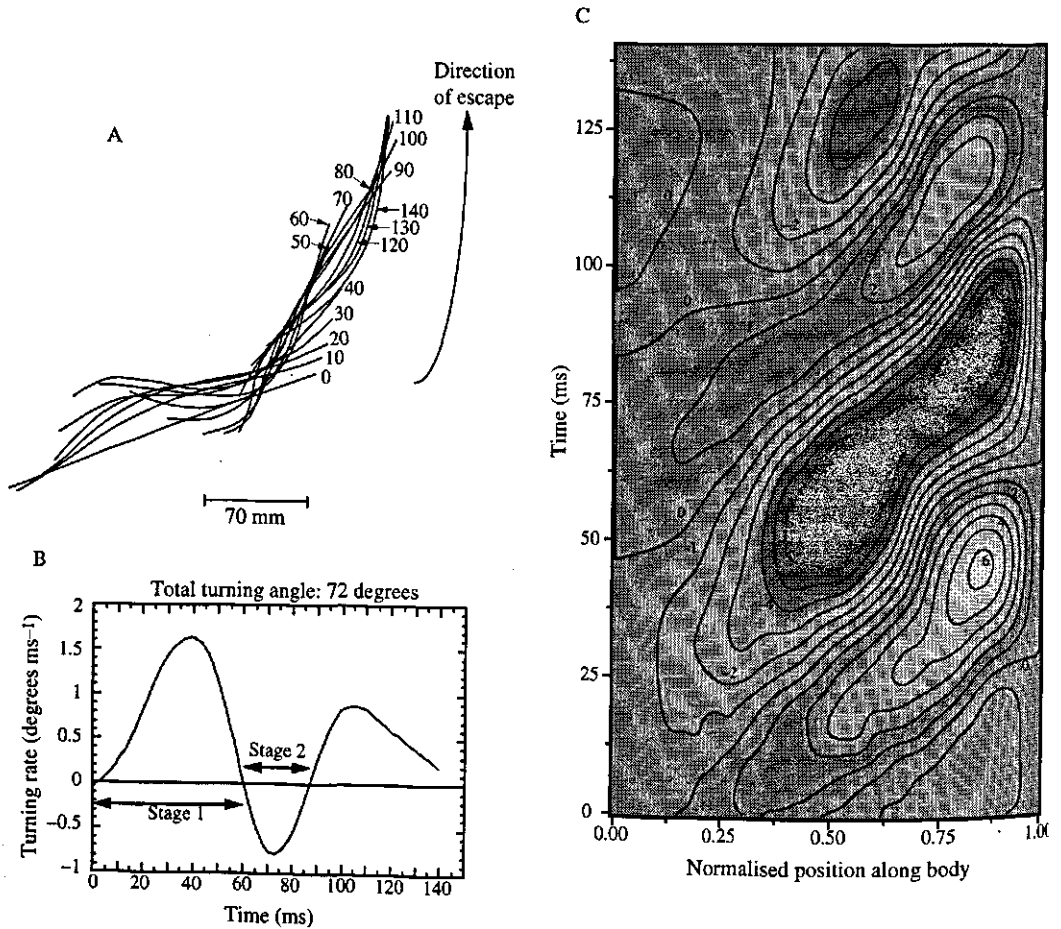


Fig. 6. S-start of an adult carp; (A) The central axis of the fish (plotted using the 31 points derived per calculated axis) during an S-start are shown every 10 ms. Times between tracings are in milliseconds from the first detectable movement; (B) The turning rate of the anterior body midline (snout to estimated centre of mass at 0.3 FL, where FL is fork length) during this S-start. The stages of the start are indicated; (C) Contour plot of the body curvature during this S-start. The horizontal axis represents the body axis of the fish expressed as normalised FL (0, tip of snout; 1, fork of tail fin), the ordinate shows the time, and the contours in the plot show the normalised curvature FL/R (where R is local radius of curvature). Curvature was positive for bending to the right and negative for bending to the left.

Strain variations in muscle fibres

Antero-posterior and red-white differences

Table 1 presents results from a statistical comparison of the maximum sarcomere strain at the convex side of the fish body. There was a large and significant difference ($P=0.0002$) between the maximum strains in red fibres (0.251 ± 0.126 , $N=48$) and white fibres (0.147 ± 0.074 , $N=48$). Strains for anterior fibres sampled at $0.4 FL$, which is close to 'mid-body', did not differ significantly from those for posterior fibres ($0.8 FL$).

Table 1. Mean maximum sarcomere strain during fast-starts. Within each section of a column (separated by spaces), different letters (a,b,c) indicate a significant difference ($P\leq 0.05$). N , total number of muscle tissue sections used for determining the mean maximum sarcomere strains (eight fish). Values are means \pm S.D. C, C-start; S, S-start; I, intermediate fast-swimming movements.

Muscle fibre type	N	Mean maximum sarcomere strain
Red, total	48	0.251 ± 0.126^a
White, total	48	0.147 ± 0.074^b
Anterior, total	48	0.209 ± 0.138^a
Posterior, total	48	0.201 ± 0.082^a
C, red anterior	8	0.272 ± 0.211^a
C, red posterior	8	0.275 ± 0.120^a
C, white anterior	8	0.163 ± 0.142^a
C, white posterior	8	0.168 ± 0.079^a
S, red anterior	8	0.389 ± 0.019^a
S, red posterior	8	0.171 ± 0.008^{bc}
S, white anterior	8	0.240 ± 0.017^b
S, white posterior	8	0.097 ± 0.004^c
I, red anterior	8	0.130 ± 0.057^a
I, red posterior	8	0.307 ± 0.053^b
I, white anterior	8	0.076 ± 0.033^a
I, white posterior	8	0.177 ± 0.032^a

C-start

Figs 7A-C and 8A-C show the sarcomere strain of red and white anterior and posterior muscle fibres at the left and right side of the fish body, respectively, during typical C-starts. No significant differences ($N=8$) in maximum sarcomere strain were found between red anterior (0.272 ± 0.211), red posterior (0.275 ± 0.120), white anterior (0.163 ± 0.142) and white posterior (0.168 ± 0.079 , Table 1) fibres. Based on the curvature data shown in Fig. 5A-C we conclude that in C-starts the maximum curvature does not consistently occur in the posterior or anterior half of the body, unlike S-starts and I-swimming.

S-start

Figs 7D-F and 8D-F show the sarcomere strain of the different muscle fibre types on the left and right side of the fish body, respectively, during S-starts. Red anterior (0.389 ± 0.019 , $N=8$) and white anterior (0.240 ± 0.017) fibres had significantly larger maximum strains than red posterior (0.171 ± 0.008) and white posterior (0.097 ± 0.004 ; Table 1) fibres, respectively. In general, during S-starts, red fibres had significantly larger maximum strains (0.280 ± 0.118 , $N=16$) than white fibres (0.167 ± 0.077 , $N=16$).

I-swimming

In Figs 7G-I and 8G-I, the sarcomere strain is shown during I-swimming on the left and right side of the fish body, respectively. During this swimming mode, only red posterior fibres were exposed to significantly larger maximum strains (0.307 ± 0.053 , $N=8$) than all other muscle fibres (see Table 1). No significant differences in maximum strain were found between red and white fibres.

Comparison of different fast-starts

The maximum sarcomere strain of anterior fibres ($N=16$) was significantly larger during S-starts (0.315 ± 0.081) and C-starts (0.215 ± 0.16) than during I-swimming (0.103 ± 0.052). Posterior fibres were subjected to significantly larger maximum strains in I-swimming (0.242 ± 0.080) than in S-starts (0.134 ± 0.040).

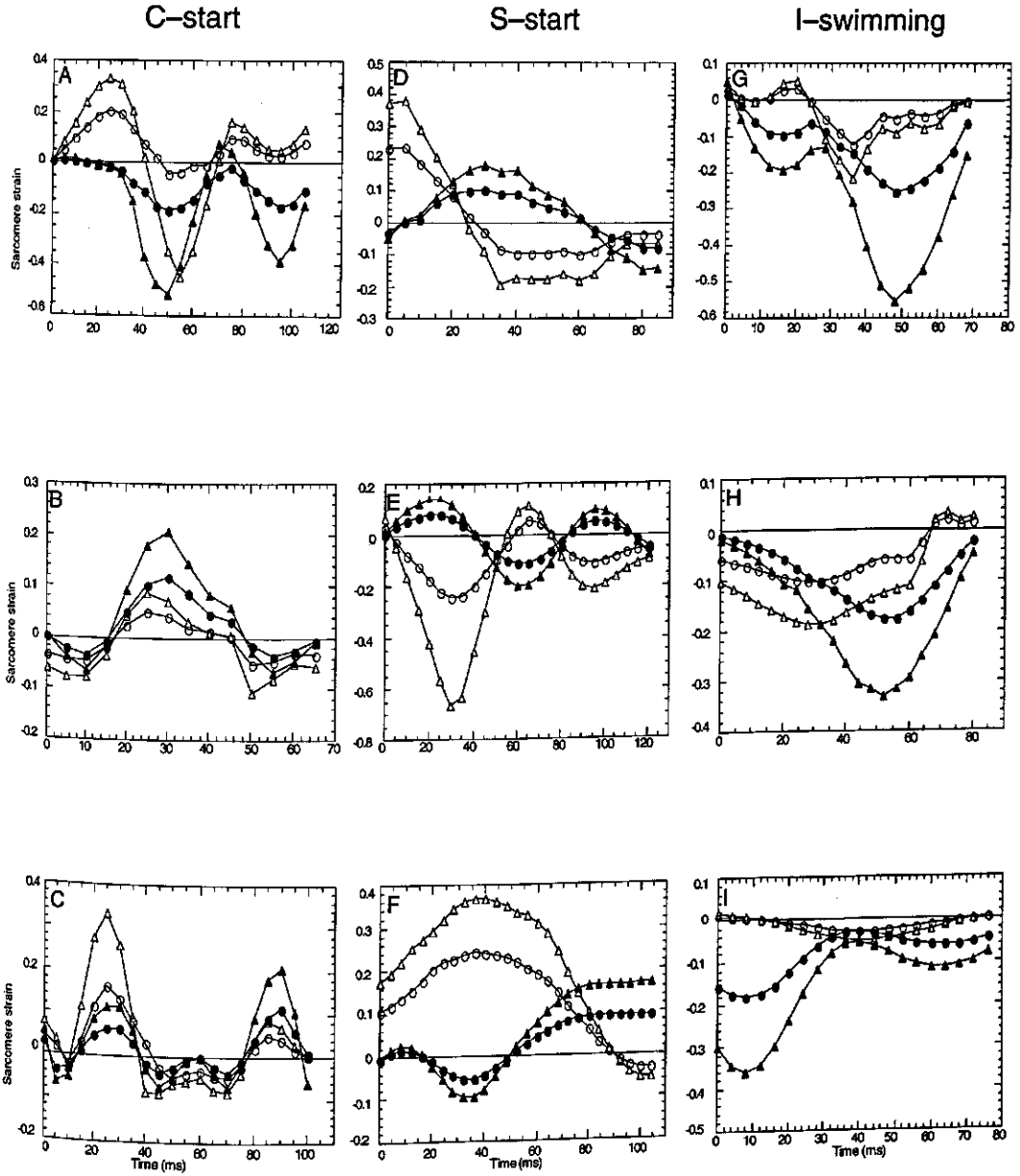


Fig. 7. Sarcomere strain of red (triangles) and white (circles) anterior (open symbols) and posterior (filled symbols) muscle fibres on the left side of the fish body during fast-starts. Positive strains indicate muscle fibre lengthening; negative strains indicate muscle fibre shortening; (A-C) C-starts; (D-F) S-start muscle fibre lengthening; (G-I) Intermediate fast-swimming movements (I-swimming).

DISCUSSION

Fast swimming movements of carp

Defining S-starts of carp

Predation S-starts are characterised by a variable S-shape of the fish axis, with the largest curvature and sarcomere strains located posteriorly and a small turning angle of the body. The (inclined) tail moves almost perpendicularly to the anterior axis of the fish (Hoogland *et al.*, 1956). In escape S-starts, the largest sarcomere strains occur anteriorly and turning angles are generally larger. Webb (1976) reported such escape S-starts in large rainbow trout (*Oncorhynchus mykiss*) but with relatively small turning angles.

Comparing different fast-starts

The fast-starts investigated in the present study resulted from escape responses to the same stimulus. Why do carp respond to the same stimulus with a C-start in one case and with an S-start or I-swimming in other situations? It is interesting that the highest maximum strains were recorded for S-starts. It is thought that C-starts are initiated by the Mauthner system, but little is known about the mechanisms controlling S-starts. Depending on the stimulus, there is great variation in turning angle relative to the initial orientation of the fish (Domenici and Blake, 1993a). The maximum curvature of the anterior trunk during escape S-starts of carp in the present study was strikingly large compared with predation S-starts of other species (during which larger posterior curvatures occur) and was associated with fairly big turning angles (approximately 60-80°). Based on these observations, it is expected that the final swimming direction can be determined least accurately in C-starts and most accurately in predation S-starts (in which precision of aiming is of vital importance). Escape S-starts seem to have an intermediate position in this respect.

During I-swimming, the largest curvatures and muscle strains occurred posteriorly, similar to the reported pattern for predation fast-starts. I-swimming is not a real fast-start but may occur just before or just after an actual fast-start.

The duration of C-starts is size-dependent (Domenici and Blake, 1993b) and linearly related to turning angle (Domenici and Blake, 1991; Domenici and Batty, 1994). C- and S-starts differ in their duration. Swimming performance is also influenced by water temperature and bodylength. In the present study, double-bend C-starts were performed slightly more quickly (50-100 ms) than S-starts or I-swimming. Fast-starts of rainbow trout with similar body sizes (20.4-29.6 cm TL) to our carp but at 15 °C had durations of 78-96 ms (Webb, 1976), whereas a duration of 115 ms was found for the fast-start of pike (*Esox sp.*, 21.7 cm TL, 15 °C; Webb, 1978b). Given the large variation in results from previous studies on fast-starts, direct comparison between the performance of different species requires the use of more similar experimental designs.

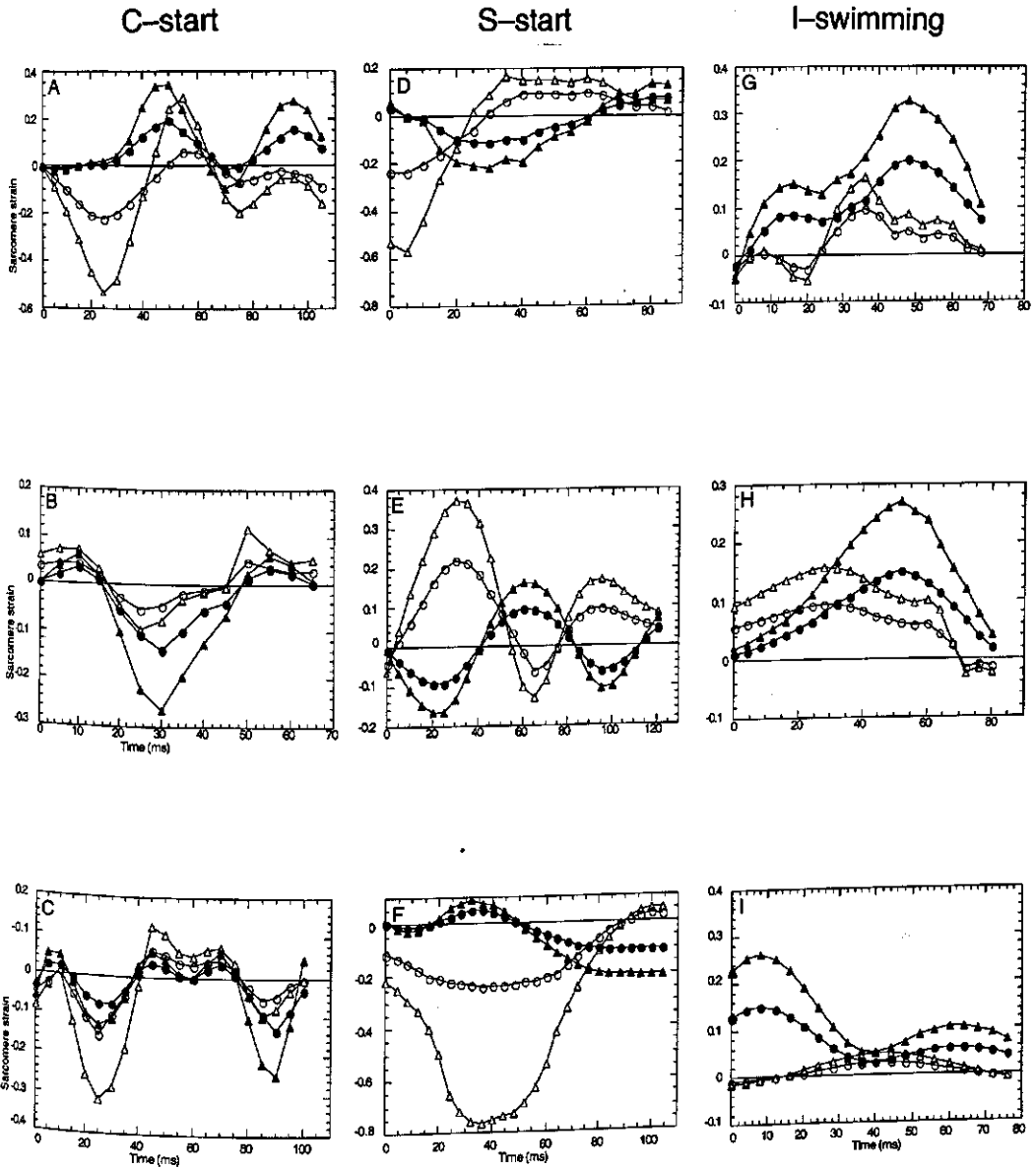


Fig. 8. Sarcomere strain of red (triangles) and white (circles) anterior (open symbols) and posterior (filled symbols) muscle fibres on the right side of the fish body during fast-starts. Positive strains indicate muscle fibre lengthening; negative strains indicate muscle fibre shortening; (A-C) C-starts; (D-F) S-start escape responses; (G-I) Intermediate fast-swimming movements (I-swimming).

Accelerations of the fish at 0.3 FL during fast-starts

The accelerations at 0.3 FL were larger during C-starts than during S-starts. The trough between the two main acceleration peaks observed during C-starts (Fig. 4A) was probably caused by rotation around the fish centre of mass at 0.3 FL, as bending caused the head and tail to move with large accelerations. During S-starts, maximum accelerations coincided with a tail fin movement of high lateral velocity and at a considerable angle to the anterior axis of the fish, conditions for which a large thrust will be produced. Reported maximum accelerations during fast-starts vary greatly between different studies (reviewed by Domenici and Blake, 1997). When comparing accelerations during fast-starts from different fish species, factors such as fish size, water temperature and filming rate must be considered. The study of Harper and Blake (1990) is most appropriate for comparison with the present data because of their similar experimental conditions. In that study, overall mean maximum accelerations of $59.7 \pm 8.3 \text{ m s}^{-2}$ (mean ± 2 S.E.M. $N=30$) were reported for fast-starting rainbow trout (*Oncorhynchus mykiss*, 31.6 ± 2 cm FL, mean ± 2 S.E.M.), and much higher single maximum accelerations (96 m s^{-2}) compared to those in the present study (approximately 54 m s^{-2} for C-starts and 40 m s^{-2} for S-starts).

Sarcomere strains during different fast-starts

It is assumed that the strains of red muscle fibres depend on (1) the distance between the fibre and the backbone of the fish and (2) the instantaneous local curvature of the body during swimming. This is supported by a study of Coughlin *et al.* (1996) who compared calculated and measured strain in scup (*Stenotomus chrysops*). Strain variations of white fibres are, due to their helical fibre paths, not only dependent on their distance to the body axis but also on their orientation. Red fibres are consequently exposed to larger strains, as was found in the present study (e.g. 25.1 % for red fibres and 14.7 % for white fibres). Strains determined by Rome and Sosnicki (1991) in rigor muscle of carp (*Cyprinus carpio*, at 0.38 and 0.68 TL) that were bent into extreme curvatures similar to those found during C-starts also showed larger maximum strain values in red than in white fibres. They found the highest sarcomere strains in red anterior fibres (up to 25 %, compared with 16.5 % for red posterior fibres) which they attributed to the relatively large distance between these fibres and the body axis. In the present study, maximum strains of red anterior and posterior fibres during C-starts were similar, at approximately 27 %. Rome *et al.* (1988) obtained a maximum shortening velocity (V_{\max}) of $4.65 \pm 0.55 L \text{ s}^{-1}$ (where L is length, mean \pm S.E.M. $N=5$) for red muscle fibres and $12.88 \pm 0.5 L \text{ s}^{-1}$ for skinned white fibres ($N=6$) both at 15°C . Since our experiments were carried out at a higher temperature (23°C) we expect somewhat higher values than those obtained by Rome *et al.* (1988): approximately $5.5 L \text{ s}^{-1}$ for red muscle fibres and $15 L \text{ s}^{-1}$ for white muscle fibres. Owing to the low V_{\max} of red fibres compared with the fast white fibres, red fibres are not able to equal the high shortening velocity of white fibres during very rapid fast-starts and therefore will tend to buckle on the concave side of the fish body. This confirms earlier suggestions by Rome *et al.* (1988) and Rome and Sosnicki (1991). The negative sarcomere strains of red fibres shown in Figs 7 and 8 were not corrected for these buckling effects, but reflect the shortening these fibres would need to undergo

to avoid buckling. White posterior fibres experienced similar strains (16.8 %) to white anterior fibres (16.3 %) during C-starts. Rome and Sosnicki (1991) found that white posterior fibres experienced larger strains than white anterior fibres (anterior: 6.1 %, posterior: 10.7 %) but with lower values than in our study. The carp we investigated were larger (22.5-27.5 cm *FL*) than those of Rome and Sosnicki (1991) (10-20 cm *TL*). The sarcomere strains we found in anterior fibres during S-starts were more than twice as large as in posterior fibres for both red and white muscle fibres (Table 1), due to the larger anterior curvature that occurs in S-starts relative to C-starts.

The maximum strain rate we calculated was less than approximately 10.5 s^{-1} for white fibres and 35 s^{-1} for red fibres.

Sarcomere strain in relation to titin isoforms

Sarcomere strain variations during cyclic swimming are smaller for white fibres than for red fibres (Rome *et al.*, 1988; van Leeuwen *et al.*, 1990; Rome and Sosnicki, 1991). Van Leeuwen *et al.* (1990) and van Leeuwen (1992) calculated strains of approximately 1.5-2 % and 5 % for white and red axial muscle fibres, respectively, of *Cyprinus carpio* during cyclic swimming. Posterior fibres experienced larger sarcomere strains than did anterior fibres during cyclic swimming (van Leeuwen, 1995). Van Leeuwen *et al.* (1990) found that during cyclic swimming anterior fibres were mainly concentrically active, within a limited length range, whereas fibres in the caudal peduncle were active for a longer period while being stretched. At the level of the anus, the concentric and eccentric activation periods were approximately equal. Rome and Sosnicki (1991) determined strains in rigor muscle of carp with body postures similar to those of cyclic swimming. They found strains of 2.9 % anteriorly (at 0.38 *TL*) and 5.7 % posteriorly (at 0.68 *TL*). For intermittent swimming, large strains (up to 20 %) were calculated for posterior fibres of carp (van Leeuwen *et al.*, 1990; see also van Leeuwen, 1992, for a correction). For cyclic swimming we found that the combined effects of muscle fibre type and muscle location led to the following set of declining mean sarcomere strains ($N=8$): red posterior 0.051 ± 0.023 ; white posterior 0.028 ± 0.013 ; red anterior 0.02 ± 0.022 ; white anterior 0.012 ± 0.012 . The observed variation in strain corresponds well with previously reported differences in molecular mass of the huge, highly elastic, muscle protein titin: red and posterior fibres of carp possessed larger titin isoforms as compared to white and anterior fibres (Spierts *et al.*, 1997). The increased molecular mass of titin correlates with an increase in the length of the highly elastic segment of titin (I-band segment). The position of titin in a slack sarcomere is illustrated in Fig. 1A. Titin acts as a dual spring resisting both negative (Fig. 1B and the green curve in Fig. 1D) and positive (Fig. 1C and the red curves in Fig. 1D) sarcomere strain. Differences in the length of the highly elastic titin segment are reflected in differences in the passive tension *versus* sarcomere length relationship of skinned muscle fibres (Granzier *et al.*, 1996). When red fibres are gradually stretched at a constant velocity from resting length to twice this length, the passive tension *versus* sarcomere length curve increased more steeply in fibres with small titin isoforms (anterior fibres) than in fibres with larger titin isoforms (posterior fibres). The passive tension *versus* sarcomere length curves for carp red anterior and posterior fibres upon stretching and shortening, derived from Spierts *et al.* (1997), are shown in Fig. 1D as the red and green curves, respectively, expressed relative to a maximum active tension of

approximately 150 kPa. The smaller titin isoform in anterior fibres results in more passive tension for a given sarcomere strain. Spierts *et al.* (1997) hypothesised that sarcomere strain is one of the functional variables that modulates the expression of different titin isoforms in axial muscle fibres of carp thus reducing energy loss during cyclic loading of the muscle fibres. In carp the fibres that experience the largest sarcomere strains during cyclic and intermittent swimming are those reported to have the largest titin isoforms, allowing these fibres to attain large strain amplitudes with relatively low tensions.

Fig. 1D shows the mean maximum sarcomere length excursions of red (25.1 %, dashed lines) and white (14.7 %, solid lines) muscle fibres of carp during fast-starts in a normalised force *versus* sarcomere length curve. The blue dashed line indicates a hypothetical work loop for the white muscles that power the fast-start (see also the work loops in Fig. 4 of Johnston *et al.*, 1995). The white muscle fibres start to shorten at slack length (1.95 μm) to approximately 1.66 μm and generate approximately 45-50 % maximum tension. During (passive) muscle lengthening the work loop 'follows' the matching passive tension *versus* sarcomere length curve (not indicated for white muscles in Fig. 1D). If the fast-starts were powered by red muscles these fibres need to shorten to approximately 1.44 μm , a sarcomere length at which the tension generated is very low and the fibres might be damaged. Red fibres however are not able to match the high shortening velocity of white fibres and are protected from being damaged by buckling on the concave side of the fish body (shaded area in Fig. 1D).

The largest loading of titin probably occurs during fast-starts in red fibres at approximately 0.4 *FL* at the point at which the largest strains occur and at which the smallest titin isoforms are found. To quantify the passive tension required to stretch red anterior fibres maximally during S-starts we compared our strain value of 39 % with the passive tension of carp red anterior fibres derived from a passive tension *versus* sarcomere length curve (Fig. 2A in Spierts *et al.*, 1997). The passive tension necessary for a strain of 39 % in these fibres is 20 kPa (Spierts *et al.*, 1997). Of this 20 kPa, the titin-based passive tension is 14 kPa whereas the intermediate filament-based passive tension is 6 kPa. This passive tension during stretching is considerable compared to the maximum active tension that can be generated by carp red muscles (which is low due to the buckling described above) when these fibres actively participate in power generation during fast-starts. The passive tension of red fibres during shortening, on the other hand, is much smaller, also due to this buckling. Further research is required to quantify the energetic consequences of these features of muscle.

ACKNOWLEDGEMENTS

We thank Dr H.A. Akster and Professor Dr J.W.M. Osse for useful discussions and comments on the manuscript. We also thank an anonymous referee for a detailed report that helped to improve this paper. This research was supported by the Life Sciences Foundation (SLW), which is subsidised by the Netherlands Organisation for Scientific Research (NWO).

REFERENCES

- AKSTER, H.A. (1985). Morphometry of muscle fibre types in the carp (*Cyprinus carpio* L.): relationships between structural and contractile characteristics. *Cell Tissue Res.* **241**, 193–201.
- ALEXANDER, R. MCN. (1969). The orientation of muscle fibres in the myomeres of fishes. *J. Mar. Biol. Ass.* **49**, 263–290.
- COUGHLIN, D.J., VALDES L. AND ROME L.C. (1996). Muscle length changes during swimming in scup: sonomicrometry verifies the anatomical high-speed cine technique. *J. Exp. Biol.* **199**, 459–463.
- DE BOOR, C. (1978). *A Practical Guide to Splines*. Berlin: Springer.
- DOMENICI, P. AND BATTY, R.S. (1994). Escape manoeuvres of schooling *Clupea harengus*. *J. Fish Biol.* **45**, (Suppl. A): 97–110.
- DOMENICI, P. AND BLAKE, R.W. (1991). The kinematics and performance of the escape response in the angelfish (*Pterophyllum eimekei*). *J. Exp. Biol.* **156**, 187–205.
- DOMENICI, P. AND BLAKE, R.W. (1993a). Escape trajectories in angelfish (*Pterophyllum eimekei*). *J. Exp. Biol.* **177**, 253–272.
- DOMENICI, P. AND BLAKE, R.W. (1993b). The effect of size on the kinematics and performance of angelfish (*Pterophyllum eimekei*) escape responses. *Can. J. Zool.* **71**, 2319–2326.
- DOMENICI, P. AND BLAKE, R.W. (1997). Review: The kinematics and performance of fish fast-start swimming. *J. Exp. Biol.* **200**, 1165–1178.
- EATON, R.C., BOMBARDIERE, R.A. AND MEYER, D.L. (1977). The Mauthner-initiated startle response in teleost fish. *J. Exp. Biol.* **66**, 65–85.
- FRITH, H.R. AND BLAKE, R.W. (1991). Mechanisms in the startle response in the northern pike, *Esox lucius*. *Can. J. Zool.* **69**, 2831–2839.
- FÜRST, D.O., OSBORNE M., NAVE R. AND WEBER K. (1988). The organisation of titin filaments in the half-sarcomere revealed by monoclonal antibodies in immunoelectron microscopy: a map of ten nonrepetitive epitopes starting at the Z-line extends close to the M-line. *J. Cell. Biol.* **106**, 1563–1572.
- GRANZIER H.L.M., HELMES M. AND TROMBITÁS K. (1996). Nonuniform elasticity of titin in cardiac myocytes: a study using immunoelectron microscopy and cellular mechanics. *Bioph. J.* **70**, 430–442.
- HARPER, D.G. AND BLAKE, R.W. (1990). Fast-start performance of rainbow trout *Salmo gairdneri* and northern pike *Esox lucius*. *J. Exp. Biol.* **150**, 321–342.
- HERTEL, H. (1966). *Structure, form and movement*. New York: Reinhold Publishing Corp. 251 pp.
- HOOGLAND, R. MORRIS, D. AND TINBERGEN, N. (1956). The spines of sticklebacks (*Gasterosteus* and *Pygosteus*) as a means of defence against predators (*Perca* and *Esox*). *Behaviour* **10**, 205–236.
- JOHNSTON, I.A., LEEUWEN, J.L. VAN, DAVIES, M.L.F. AND BEDDOW, T. (1995). How fish power predation fast-starts. *J. Exp. Biol.* **198**, 1851–1861.
- KASAPI, M.A., DOMENICI P., BLAKE, R.W. AND HARPER, D. (1993). The kinematics and performance of escape responses of the knifefish *Xenomystus nigri*. *Can. J. Zool.* **71**, 189–195.
- KIMMEL, C.B., EATON, R.C. AND POWELL, S.L. (1980). Decreased fast-start performance of zebrafish larvae lacking Mauthner neurons. *J. Comp. Physiol.* **140**, 343–351.

- LIPSCHUTZ, M.M. (1969). *Theory and Problems of Differential Geometry. Schaum's Outline Series.* New York: McGraw-Hill. 269 pp.
- MARUYAMA, K. (1986). Connectin an elastic filamentous protein of striated muscle. *Int. Rev. Cytol.* **104**, 81-114.
- MARUYAMA, K. (1994). Connectin, an elastic protein of striated muscle. *Biophys. Chem.* **50**, 73-85.
- PAGE, S.G. AND HUXLEY, H.E. (1963). Filament lengths in striated muscle. *J. Cell Biol.* **19**, 369-390.
- ROHLF, F.J. AND SOKAL, R.R. (1981). *Statistical Tables*, second edition. New York: W.H. Freeman and Company. 219 pp.
- ROME, L.C., FUNKE, R.P., ALEXANDER, R. MCN., LUTZ, G., ALDRIDGE, H., SCOTT, F. AND FREADMAN, M. (1988). Why animals have different muscle fibre types. *Nature* **335**, 824-827.
- ROME, L.C. AND SOSNICKI, A.A. (1991). Myofilament overlap in swimming carp II. Sarcomere length changes during swimming. *Am. Physiol. Soc.* **260**, 289-296.
- SHAPIRO S.S. AND WILK, M.B. (1965). An analysis of variance test for normality (complete samples). *Biometrika* **52**, 591-611.
- SOKAL, R.R. AND ROHLF, F.J. (1981). *Biometry*, second edition. New York: W.H. Freeman and Company. 859 pp.
- SPIERTS, I.L.Y., AKSTER H.A. AND GRANZIER, H.L. (1997). Expression of titin isoforms in red and white muscle fibres of carp (*Cyprinus carpio* L.) exposed to different sarcomere strains during swimming. *J. Comp. Physiol. B.*, **167** 543-551.
- VAN LEEUWEN, J.L. (1992). Muscle function in locomotion. In *Mechanics of animal locomotion* (ed. R. MCN. ALEXANDER), *Advances in Comparative and Environmental Physiology*, vol. 11. pp. 191-250. Heidelberg: Springer-Verlag.
- VAN LEEUWEN, J.L. (1995). The action of muscles in swimming fish. *Exp. Physiol.* **80**, 177-191.
- VAN LEEUWEN, J.L., LANKHEET, M.J.M., AKSTER, H.A. AND OSSE, J.W.M. (1990). Function of red axial muscles of carp (*Cyprinus carpio*): recruitment and normalised power output during swimming in different modes. *J. Zool.* **220**, 123-145.
- WANG K. (1985). Sarcomere associated cytoskeletal lattices in striated muscle. Review and hypothesis. In *Cell and Muscle Motility 6* (ed. J.W. Shay), pp 315-369. New York: Plenum Publ. Company.
- WANG K., McCARTER R., WRIGHT J., BEVERLY J. AND RAMÍREZ-MITCHELL R. (1991). Regulation of skeletal muscle stiffness and elasticity by titin isoforms: a test of the segmental extension model of resting tension. *Proc. Natl. Acad. Sci. USA* **88**, 7101-7105.
- WANG K., McCARTER R., WRIGHT J., BEVERLY J. AND RAMÍREZ-MITCHELL R. (1993). Viscoelasticity of the sarcomere matrix of skeletal muscles. The titin-myosin composite is a dual-stage molecular spring. *Bioph. J.* **64**, 1161-1177.
- WEBB, P.W. (1975). Acceleration performance of rainbow trout *Salmo gairdneri* and green sunfish *Lepomis cyanellus*. *J. Exp. Biol.* **63**, 451-465.
- WEBB, P.W. (1976). The effect of size on the fast-start performance of rainbow trout *Salmo gairdneri*, and a consideration of piscivorous predator-prey interactions. *J. Exp. Biol.* **65**, 157-177.
- WEBB, P.W. (1978a). Effects of temperature on fast-start performance of rainbow trout, *Salmo gairdneri*. *J. Fish. Res. Board Can.* **35**, 1417-1422.

- WEBB, P.W. (1978b). Fast-start performance and body form in seven species of teleost fish. *J. Exp. Biol.* **74**, 211–226.
- WEBB, P.W. AND BLAKE, R.W. (1985). Swimming. In *Functional vertebrate morphology* (ed. M. Hildebrand, D.M. Bramble, K. Liem and D.B. Wake), pp 110–128. Cambridge: Harvard University Press.
- WEIHS, D. (1973). The mechanism of rapid starting of slender fish. *Biorheology* **10**, 343–350.
- WOLTRING, H. (1986). A Fortran package for generalised, cross-validatory spline smoothing and differentiation. *Adv. Engng Software* **8**, 104–113.

7 How carp (*Cyprinus carpio* L.) activate the trunk muscles during C-and S-starts

Igor L.Y. Spierts¹, Johan L. van Leeuwen^{2,3}, Arie Terlouw¹ and Jan W.M. Osse¹

¹Experimental Zoology Group, Wageningen Institute of Animal Sciences (WIAS), Wageningen Agricultural University, Marijkeweg 40, 6709 PG Wageningen;

²Department of Physiology, Leiden University, Wassenaarseweg 62, PO Box 9604, NL-2300 RC Leiden;

³Institute of Evolutionary and Ecological Sciences, Leiden University, Kaiserstraat 63, PO Box 9516, NL-2300 RA Leiden;
The Netherlands

SUMMARY

We quantified body curvature, acceleration and muscle strain with synchronised electromyograms (EMGs) from red and white axial muscle of carp (*Cyprinus carpio* L.) during C- and S-starts. Fast-starts were filmed at 500 frames s⁻¹ at 23 °C. Body curvatures and accelerations were calculated from digitised outlines. Maximum accelerations at 0.3 *FL* (fork length) were approximately 70 m s⁻² for C-starts and approximately 40 m s⁻² for S-starts. In all fast-starts red and white muscle were simultaneously active at a given longitudinal location, whereas only red muscle were active during continuous swimming. Our findings corresponded with the 'additive' model of fibre recruitment, which suggests that as power output and speed of movement increase white fibres are sequentially recruited in addition to red fibres. Our results also showed that red and white muscle at a given longitudinal location were not necessarily active synchronously and could be uncoupled. This uncoupling took place during escape S-starts of carp and we suggest that in this way mechanically sub-optimal patterns of force generation can be avoided. During C-starts the uncoupling seemed hardly present. The antero-posterior delay in EMG onset was virtually absent during the first tail beat of C-starts (less than 1 ms), requiring very high conduction velocities of the Mauthner system and thus making a very fast escape possible. During S-starts a delay was clearly present which might be connected to the different neural patterns controlling these starts. In S-starts and in stage 1 of C-starts the EMGs generally showed posterior propagation, resulting in longer durations of posterior EMGs. These findings confirmed earlier studies of intermittent swimming and escape responses of fish. Both anterior and posterior muscle fibres were active whilst lengthening at certain moments during C- and S-starts, thus initially absorbing power, which might work advantageous for the transmission of force from the fish to the water.

INTRODUCTION

In a previous paper (Spierts and van Leeuwen, 1999) C- and S-starts of carp were studied with respect to the turning angle of the anterior body part, timing of accelerations at 0.3 *FL* and especially sarcomere strains of red and white muscle fibres at maximal bending. The probable relation between titin isoform, a highly elastic muscle protein, and muscle strain provided an example of structure-function relations over different ranges of study. Further study of the relations between locomotory muscles and fast-starts require additional synchronously recorded data, the electrical activity of the involved muscle parts. Intriguing questions arise when the presumed maximal performance of a fish, a C-start or an S-start in approximately 100-150 ms, is studied. Are white and red muscles always and synchronously activated? If so, is it conceivable that both fibre types contribute to the fast bending of the body? Is the delay between electrical and mechanical events constant and apparent from the recorded events, and, what is the mechanical effect of muscle activities on body curvatures and sarcomere strains during fast-starts? Such problems are very complex and not easily answered because variable distribution of muscle activity is found along the body axis. Furthermore, strains of fibres in a muscle segment of a swimming fish are not only determined by muscle activity patterns but

also by the forces exerted on this particular segment of surrounding segments and the effects of the water. The mechanical effect (in time and magnitude) of muscle activity during swimming is actually the summation of all these contributions.

Associated with these patterns of contraction are the patterns of motor activity. Are all muscles along the body axis synchronously activated during C-starts, and is the Mauthner system the only possible explanation for such fast actions? Is the slower S-start also initiated by the Mauthner system, modified or suppressed in the anterior body segments? What is the influence of initial velocity on a subsequent C- or S-start and is this possible effect reflected in the fast-start?

Escape responses consist of three kinematic stages: (1) a preparatory stroke (ipsilateral muscle activity), (2) a propulsive stroke (contralateral muscle activity), and (3) subsequent variable behaviour (Weihs, 1973; Webb, 1976; Webb and Blake, 1985). C-starts are usually mediated by the Mauthner system (Eaton *et al.*, 1977; Kimmel *et al.*, 1980) and have been subdivided into single- and double-bend types, depending on the presence of a second tail beat (Domenici and Blake, 1991; Kasapi *et al.*, 1993). S-starts, named after the S-shape of the fish body, have been subdivided in predatory attacks and escape responses. In a predatory attack, the posterior region of the body curves more than the anterior region and only a small angle of turn of the body is present (Hoogland *et al.*, 1956). During S-shaped escape responses considerable angles of turn occur, although smaller than during C-starts. Little is known about the neuronal mechanisms controlling S-starts. Simultaneous recordings of electrical and mechanical events are required to explain the bending patterns during these fast responses. High speed recordings of motion and multi-channel EMGs provide the data. Jayne and Lauder (1993) investigated red and white muscle activity and kinematics of escape responses of the bluegill sunfish (*Lepomis macrochirus*) and found that the onset of ipsilateral muscle activity was synchronous at different positions along the trunk. This had previously been reported by Kashin *et al.* (1979) in the escape response of carp (*Cyprinus carpio* L.). The onset and offset of contralateral muscle activity was asynchronous at different longitudinal locations, the EMG signal occurring earlier anteriorly. As the onset of contralateral muscle activity occurred only 3-6 ms after the offset of the ipsilateral muscle activity at any given position along the trunk, the offset of stage 1 and the onset of stage 2 were considered to be synchronous (Jayne and Lauder, 1993).

In several studies on cyclic swimming fish, the duration of the EMG decreased in the posterior direction (van Leeuwen *et al.*, 1990; Jayne and Lauder, 1993; Wardle and Videler, 1993). During intermittent swimming of carp (van Leeuwen, 1992) and in the escape response of the blue gill sunfish (Jayne and Lauder, 1993) however an increase in the duration of the EMG was observed in the posterior direction. Van Leeuwen *et al.* (1990) took high-speed films of carp (*Cyprinus carpio*) during cyclic and during kick-and-glide swimming, in synchrony with electromyography of red muscle fibres at eight positions along the trunk. The strain and strain rate of red muscle fibres were determined (using curvature data) and used to calculate force and power output of the muscle fibres. Van Leeuwen *et al.* (1990) suggested that red muscle fibres may not work optimally at every location along the trunk. Anteriorly fibres were mainly concentrically active, within a limited length range. Posteriorly fibres were longer active while being stretched. At the level of the anus, the concentric and eccentric activations were equal. The experimental and theoretical results of van Leeuwen *et al.* (1990) were later supported by findings of Altringham *et al.* (1993) on saithe (*Pollachius virens*). Johnston *et*

al. (1995) investigated instantaneous muscle strain and power output during a fast-start of the short-horned sculpin (*Myoxocephalus scorpius* L.). Fast-starts, elicited by prey capture, were filmed and muscle strains were calculated for dorsal fast muscle using the lateral body curvature and the fibre orientation. At 15 °C maximum muscle strain ranges during the first tail-beat, peak-to-peak were largest at 0.52 *TL* (approximately 0.19, where *TL* is the total length) and smallest at 0.77 *TL* (approximately 0.15). Furthermore, fibres at 0.52 *TL* and 0.77 *TL* at the same body side were initially stretched by the contralateral bending of the fish body, thus receiving a pre-stretch prior to shortening.

Earlier investigations on carp fast-start performance did not compare C-starts with escape S-starts, starts that are hypothesised to be innervated differently. The present study gives, in combination with the study of Spierts and van Leeuwen (1999), a detailed report and comparison of the relations between strain variations in red and white muscle, EMGs, and the final body movements in these two types of fast-starts. Special attention is paid to the presence, magnitude, and function of the delay in EMGs between anterior and posterior positions along the trunk and to differences occurring between the two differently innervated fast-starts. The duration of EMGs will be correlated with the maxima of the undulatory waves to determine the contribution of red muscles to fast-starts. These findings will contribute to a better understanding of the antero-posterior differentiation of locomotory muscles, especially because we expect a considerable advantage for fish survival when constructions are optimised to escape from predators.

MATERIALS AND METHODS

Swimming recordings

Three carp (*Cyprinus carpio* L., 22.5-23.5 cm fork length, *FL*), bred in the laboratory at 23 °C and fed on commercial fish food (Trouvit pellets; Trouw and Co. Putten) were used. High-speed motion films were made to determine sarcomere length changes (muscle strain) and muscle fibre activities during fast swimming at 0.4 and 0.8 *FL* (measured from the snout) in red and white axial muscle fibres of carp. For every fish three C-starts with no initial swimming speed ('type 1 C-start'), three C-starts with an initial speed ('type 2 C-start') and three S-starts were filmed. In total, we used 27 filmed scenes of fast-starts. Swimming events were filmed from a dorsal viewpoint in a tank (90 cm long, 45 cm wide and 45 cm deep) using a high speed video camera at 500 frames s⁻¹ (NAC colour High Speed Video system HSV 1000 FRS with a Super-VHS video tape recorder type V-306; Reinka B.V., Breda). The camera was positioned 2 meters above the tank and a Nikon 28 mm lens was used to capture images of the complete tank. Films (KODAK double-X negative, 250 ASA) were taken with continuous light from seven Hama video lights to obtain sharp silhouettes of the swimming fish (power input of 5.2 kW). Water temperature was 23 °C, warming of the aquarium by the filming lights was negligible due to the short lighting periods. Fast swimming responses, C- and S-starts, were elicited by a sudden sound wave in the tank created by a blow to the laboratory floor adjacent to the tank or by tapping the side of the tank with a hard rubber mallet.

Calculation of muscle fibre strain and accelerations

Films were analysed by printing the outlines of fish during fast-starts onto A3-paper sheets at 2 ms intervals. The outlines were digitised relative to fixed reference points, using an x,y-data-tablet (Calcomp 9100). For each side of the body, approximately 100 points were used. The points were distributed non-equidistantly. The shortest distances were used for the strongest curvatures of the outline. The estimated maximum error of the digitising process was 0.5 mm, which is approximately 0.002 % of the fork length of the carp. For successive frames, a longitudinal axis of the fish during the swimming event was calculated from its digitised outlines and the absolute curvature was determined, using equations 1-3 from Spierts and van Leeuwen (1999). We also calculated the accelerations (derived as the rate of change of the velocity magnitude in time) of some carp at 0.3 *FL* during C- and S-starts. Axis data were smoothed as a function of position down the trunk and curvature data were, for reasons similar to those for the accelerations, smoothed as a function of time, following van Leeuwen *et al.* (1990). The fork length (*FL*) divided by the local radius of the curvature (*R*) gave the normalised curvature (*FL/R*) and was defined as positive for curvature to the right and as negative for curvature to the left.

Calculation of the sarcomere strain of red and white muscle fibres at 0.4 and 0.8 *FL* during C- and S-starts was performed using equations 4-7 from van Leeuwen *et al.* (1990). These formulae describe the observed thickening at the concave side of the body and the thinning at the convex side. In the calculation, it was assumed that when the trunk was straight the fibres were at their resting length. We assumed a maximum shortening velocity (V_{max}) of approximately $5.5 L s^{-1}$ (where *L* is lengths) for red muscle fibres and $15 L s^{-1}$ for white muscle fibres (Spierts and van Leeuwen, 1999). The calculations did not compensate for possible buckling effects that are likely to occur in red fibres during fast-starts. Unrealistically low negative sarcomere strains of red muscle fibres were therefore obtained occasionally and not included in the results.

Muscle fibre position and orientation and sarcomere length data of red and white axial muscle fibres at 0.4 and 0.8 *FL* of carp were obtained from Spierts and van Leeuwen (1999). The angles, measured with respect to the median and frontal plane of the fish, were used to correct strain calculations for the orientation of red and white fibres.

Electromyography

Simultaneously with filming the fast-starts EMGs of red and white axial muscle fibres (at 0.4 *FL* and 0.8 *FL*) were recorded continuously with a differential technique. Fish were anaesthetised with a solution of 150 mg per litre MS 222 (Sandoz, Basel) and 6 pairs of insulated copper wire electrodes (Povin D, 50 μ m diameter; Pope, Venlo, the Netherlands) were inserted with a modified fork-tipped hypodermic needle (Osse *et al.*, 1972). At the left side of the fish body, both red (1-2 mm deep) and white muscle fibre activity (near the dorsal fin, 3-4 mm deep) was measured. At the right side only red muscle fibre activity was measured (see Fig. 1A). The distance between the two-bared electrode tips was approximately 2-3 mm in each muscle. The positions of the electrodes were checked before the actual experiment by short stimulation (Square waves, 50 Hz, 0.5-2.5 V) and after the experiment

in lateral X-ray photographs (see Fig. 1B). The fish were killed with an overdoses of MS 222 (Sandoz, Basel) followed by trans-section of the spinal cord at 0.3 *FL*, after which the positions were once more checked by dissecting the muscle tissue. These investigations confirmed that the electrodes were positioned properly into the selected muscle tissues without interfering with other muscles. None of the electrodes changed position during the experiments (Fig. 1B). The bundle of electrode wires was pulled through a flexible silicone tube (1.5 mm inner diameter) that was closed at both ends with silicon glue. The tube protected the leads, prevented contact with water, prevented the fish from being entangled in the wires (air-filled tube floats), and transmitted the movements of the fish better to the collector. Particular care was taken in attaching the electrode wires to the skin of the fish with suture thread and in fixing the tube to the first spine of the dorsal fin such that the fish was not allowed to bump the electrode wires into the tank walls.

Synchronisation of on- and offset of fast-starts between EMG and film was established using a random pulse generator. Pulses were visualised via a LED on the edge of the water tank and simultaneously stored with the EMGs on magnetic tape. The instruments for amplification and registration, including an ink-jet recorder (Siemens, type S), were similar to those used by Osse (1969), who described details of the measuring procedures. Amplification was set at 10^3 ; filters of low and high cut-off were set at 0.12 kHz (second order) and 2.5 kHz (fourth order), respectively, appropriate for dealing with motion artefacts that especially could become troublesome during fast motions. An instrumentation tape FM mode recorder (Bell and Howell; type CPR 4010) was used to store the signals. The connection between fish and apparatus was modified by applying a 14-pole collector, positioned just above the surface of the water. The analogue EMG signals of every muscle type were digitised using an AD-conversion system for a Macintosh computer with a time interval of 0.05 ms between samples (GWI-625 Macadios II 12-bit Data Acquisition Board, Keithley Instruments B.V.). We used very expanded time scales for EMG-analyses and in the illustrations to be able to resolve individual spikes within bursts, as described by Jayne and Lauder (1994), as well as lag times among bursts. The times of on- and offset of EMGs during the starts were quantified to the nearest millisecond using custom software. Values will be presented as means \pm S.D.

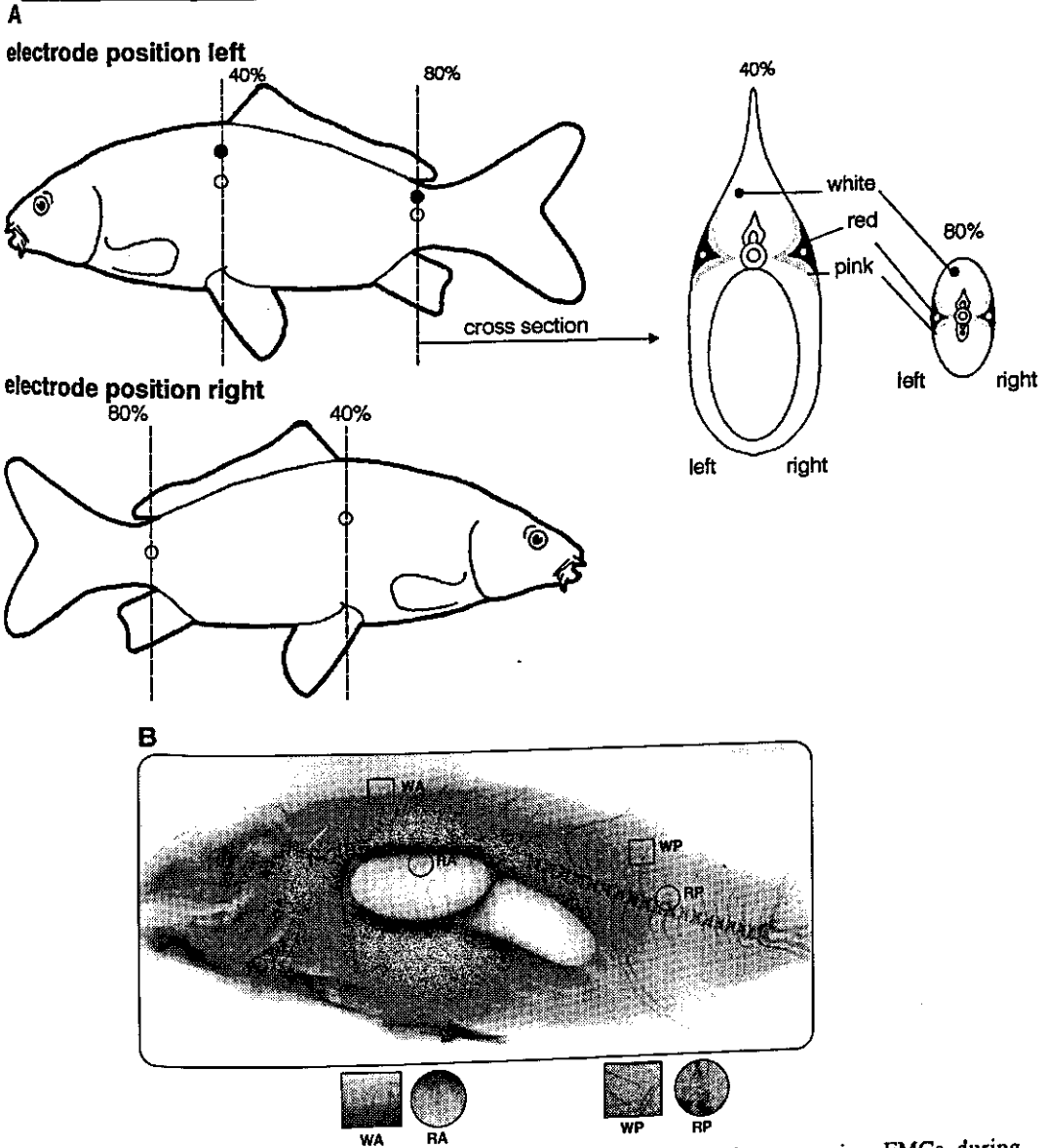


Fig. 1. (A) Schematic drawing showing the electrode positions used for measuring EMGs during different fast-starts. The positions for white and red muscle tissue are indicated by black and white dots, respectively. On the right side only red muscle tissue was used for EMG recordings. For strain calculations (based on the outlines of the fish during the swimming movement) both red and white muscle tissue (left and right side) were used at 40 % and 80 % of the fork length (as indicated); (B) X-ray picture of a carp showing the implanted electrodes. The positions are indicated by rectangles (white muscle tissue) and by circles (red muscle tissue) and are magnified below the X-ray picture. The distance between the two bared electrode tips was approximately 2-3 mm at each muscle site. W, white muscle; R, red muscle; A, anterior; P, posterior.

RESULTS

EMGs and muscle strain variations during C- and S-starts

C-start

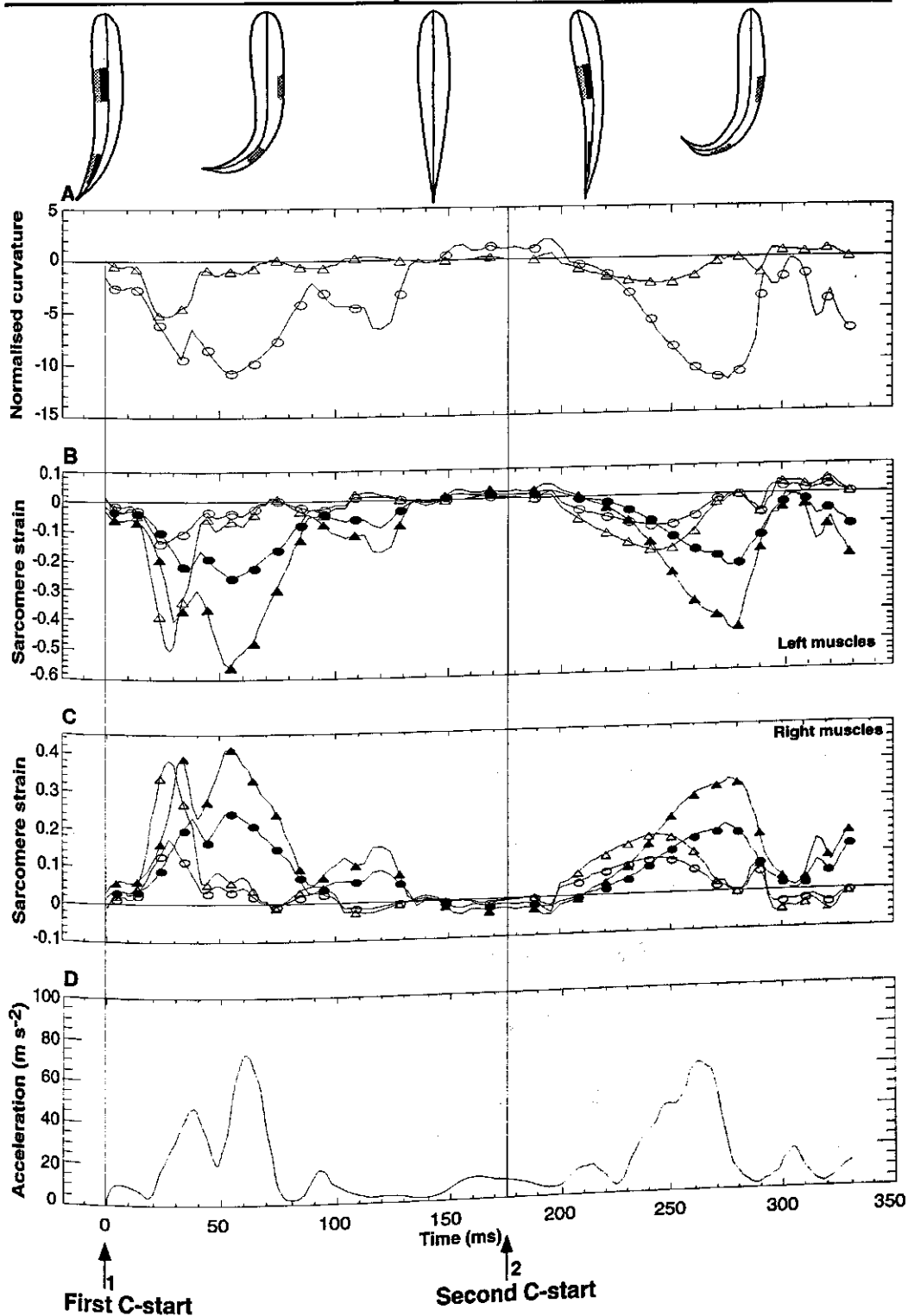
C-starts of carp occurred very suddenly and fast with high accelerations and large angles of turn. Table 1 shows the average maximum sarcomere strains and the EMG durations during the different stages of the fast-starts investigated. In Figs 2 and 3 (with a parallel time scale on the X-axis) sarcomere strains and EMGs are shown during a typical C-start of a carp (films and EMGs were recorded simultaneously). The fish shapes with the various muscle activities (red muscle EMG: shaded bars; white muscle EMG: black bars) are shown above the figures. The shaded and black bars under each EMG in Fig. 3 represent the periods of muscle fibre lengthening and shortening, respectively. We distinguished two C-starts: a type 1 C-start (at $t=0$ ms, arrow 1) where the fish was initially at a standstill, and a type 2 C-start (at $t=176$ ms, arrow 2) where the fish already had an initial speed. The type 2 C-start followed very quickly after the first start (typically within 500 ms). The beginning of a C-start (stage 1) was characterised by the onset of large ipsilateral muscle activity; stage 2 set in at the onset of contralateral muscle activity.

Type 1 C-start: starting from a standstill

Fig. 2B (strain of left fibres) shows that in the type 1 C-start the carp started from a resting position and subsequently bent to the left. After the fish was 'disturbed' not only left white axial muscle fibres (both anterior, 0.4 *FL*, and posterior, 0.8 *FL*) were synchronously active ($t=0$ ms, see

Fig. 2. Normalised curvature of the fish body and sarcomere strain of red and white axial muscle fibres at 0.4 *FL* (anterior) and at 0.8 *FL* (posterior) during a typical C-start of a carp (only 20 % of the measured and calculated data are shown). Simultaneously the EMGs of the different muscle fibres were recorded (as shown in Fig. 3). The fish shapes with these various muscle activities (red muscle activity, shaded bars; white muscle activity, black bars) are shown above the figure. Two types of C-starts are shown: starting from a standstill at $t=0$ ms (arrow 1 at bottom, curvatures are approximately zero) and starting with an initial speed at $t=176$ ms (arrow 2). The beginning of a C-start was defined as the starting moment of a large ipsilateral muscle activity (see Fig. 3); (A) Normalised curvature FL/R (where *FL* is fork length and *R* is local radius of curvature) of the fish body during the C-start. Anterior, triangles; posterior, circles. Curvature was positive for bending to the right and negative for bending to the left. When both anterior and posterior curvatures are zero, the fish is lying in a straight position; (B-C) Sarcomere strains of red (triangles) and white (circles) muscle fibres on the left and right side of the fish body during the C-start. Anterior, open symbols; posterior, filled symbols. Positive strains indicate muscle fibre lengthening; negative strains indicate muscle fibre shortening; (D) Acceleration (derived from velocity data) of the fish at 0.3 *FL* (where *FL* is fork length) during the C-start.⇒

How carp activate trunk muscles during C- and S-starts



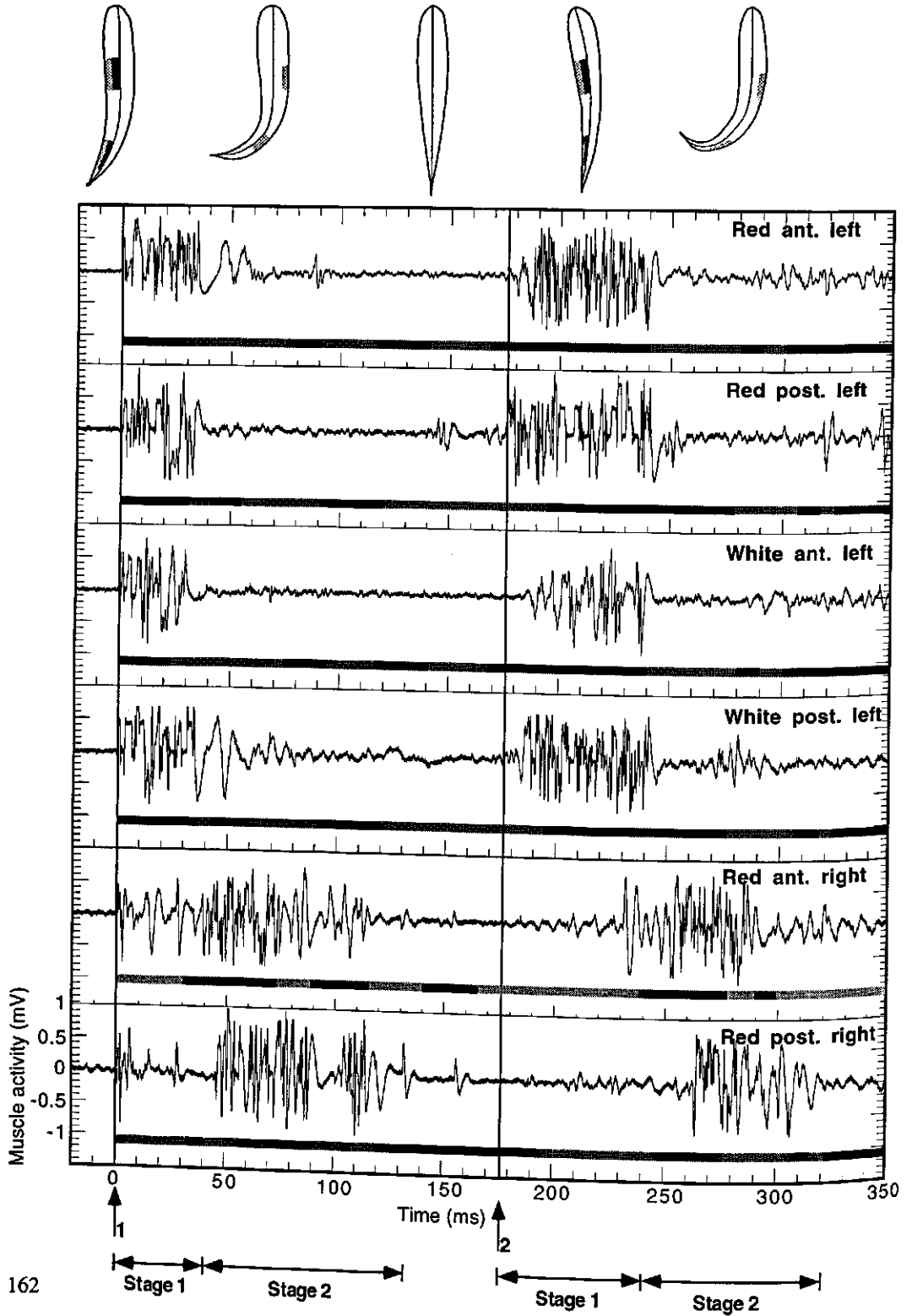


Fig. 3) but interestingly also left red anterior and posterior fibres. The antero-posterior or red-white delay in onset times of ipsilateral muscle activity was less than 1 ms during this stage 1. Red anterior and posterior and white anterior fibres showed EMG activity for approximately 35 ms (see Table 1) and white posterior fibres slightly longer (43.8 ± 4.6 ms, $N=9$). Maximum sarcomere strains for right fibres were anteriorly reached at $t=28$ ms (red: 0.40; white: 0.25) and posteriorly 6 ms later, at $t=34$ ms (red: 0.44; white: 0.31, see Fig. 2C). See also the second dominant peak (posteriorly) at $t=55$ ms.

Stage 2 set in when the activity of left fibres decreased to practically 0 and red anterior (at $t=42$ ms, contralateral EMGs, Fig. 3) and posterior fibres (at $t=46$ ms) at the right side of the body became active and the fish bent back to the resting position. Contralateral EMG durations, approximately 75 ms, were more than twice as long as ipsilateral EMG durations (see Table 1), which resulted in very extreme and rapid changing bending patterns (Fig. 2). Between the end of the type 1 start, at $t=135$ ms, and the beginning of the type 2 start, at $t=176$ ms, the maximum sarcomere strain was approximately 0.04 (red posterior fibres).

Type 2 C-start: starting with an initial speed

The type 2 C-start typically followed shortly after the type 1 start. In stage 1 red fibres were active prior to white fibres, but the antero-posterior delay in EMG onset (which is very common for cyclic swimming) was less than approximately 10 ms (Fig. 3). Anteriorly, the EMG onset of left muscle at approximately $t=176$ ms (type 2 C-start) resulted 68 ms later in a maximum strain for right fibres, at $t=244$ ms (red: 0.16; white: 0.094, see Fig. 2C). Posteriorly, the maximum strain for right fibres was reached at $t=274$ ms, which was 98 ms after the EMG onset of left muscle (red: 0.31; white: 0.18). In general right fibres reached their maximum strain 28-98 ms after the EMG onset of left fibres.

In stage 2, starting at approximately $t=240$ ms, anterior fibres started their activity approximately 35 ms prior to posterior fibres (Fig. 3). Practically no delay was present between the offset of ipsilateral EMGs and the onset of contralateral EMGs.

Comparing EMGs of different C-starts

In type 2 C-starts, ipsilateral EMG durations were almost twice as long as in type 1 C-starts (see Fig. 3 and Table 1). The total EMG durations from begin to end were longer in the type 2 start, approximately 144 ms (stage 1: 64 ms; stage 2: 80 ms) than in the type 1 start, approximately 119 ms.

Fig. 3. EMG signals (mV) of red and white anterior (ant.) and posterior (post.) muscle fibres at the left side and red anterior and posterior muscle fibres at the right side of the body during the C-start (as shown in Fig. 2). The shaded and black bars under each EMG represent the periods of muscle fibre lengthening and shortening, respectively, as presented in Fig. 2. The fish shapes with the various muscle activities (red muscle activity, shaded bars; white muscle activity, black bars) are shown above the figure. The time scale on the X-axis runs parallel with the time scale in Fig. 2. The kinematic stages during the type 1 (arrow 1) and type 2 (arrow 2) C-start are indicated. ←

Sarcomere strains and accelerations

The average maximum sarcomere strains during all C-starts was higher in red, approximately 0.28, than in white fibres, approximately 0.17 ($N=18$, see Table 1). No antero-posterior differences in strain were found. During a short period of time both red anterior (between $t=72-90$ ms) and red posterior fibres (between $t=90-120$ ms) at the right side of the body were stretched during activity after which the initial very fast bending to the left slowly decreased (compare Figs 2C and 3). This eccentric activity also occurred in the type 2 C-start in red anterior (between $t=231-240$ ms) and red posterior (between $t=261-280$ ms) fibres at the right side of the body.

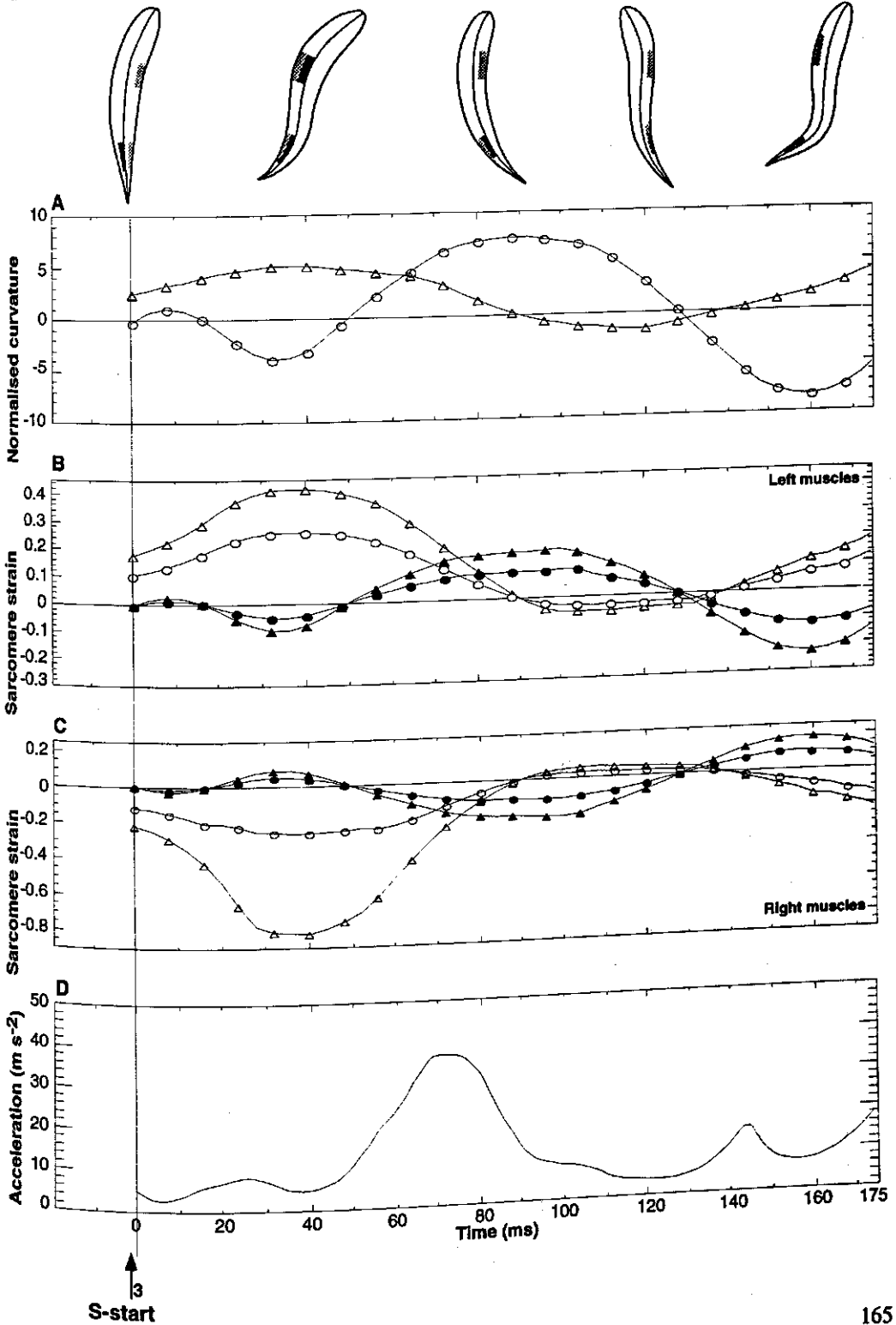
Fig. 2D shows the acceleration of the carp at 0.3 FL during the two C-starts. In the initial 20 ms of the type 1 start large accelerations of up to 50 m s^{-2} were already achieved. The acceleration during this start showed approximately four peaks. The main peak, approximately 72 m s^{-2} , occurred approximately 62 ms after the beginning of the start. The type 2 C-start showed three (smaller) peaks, with the largest acceleration (approximately 62 m s^{-2}) occurring approximately 90 ms after the beginning of the start.

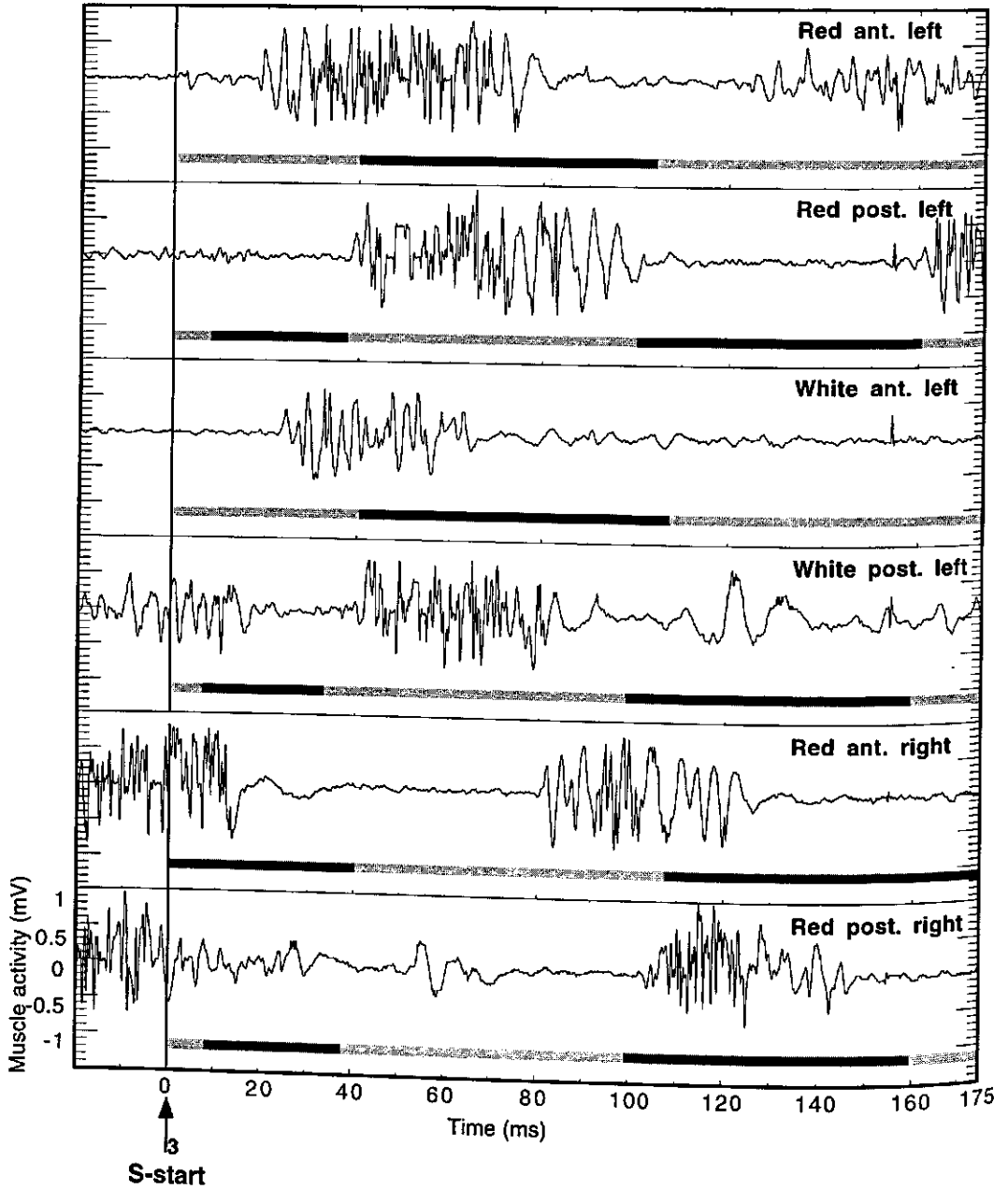
S-start

Carp performed S-starts with lower accelerations and smaller angles of turn compared to C-starts. Figs 4 and 5 (with a parallel time scale on the X-axis) show sarcomere strains and muscle activities during a typical escape S-start of a carp (films and EMGs were recorded simultaneously). The fish shapes with the various muscle activities (red muscle EMG: shaded bars; white muscle EMG: black bars) are shown above the figures. The shaded and black bars under each EMG in Fig. 5 represent the periods of muscle fibre lengthening and shortening, respectively. During S-starts the anterior and posterior part of the body were curved opposite making a subdivision into two stages based on ipsi- and contralateral EMGs very difficult to apply. The S-start here is therefore described in terms of an

Fig. 4. Normalised curvature of the fish body and sarcomere strain of red and white axial muscle fibres at 0.4 FL (anterior) and at 0.8 FL (posterior) during a typical S-start of a carp (only 50 % of the measured and calculated data are shown). Simultaneously the EMGs of different muscle fibres were recorded (as shown in Fig. 5). The fish shapes with these various muscle activities (red muscle activity, shaded bars; white muscle activity, black bars) are shown above the figure. The S-starts began at $t=0$ ms when the carp started to bend after being triggered (initially in a straight position); (A) Normalised curvature FL/R (where FL is fork length and R is local radius of curvature) of the fish body during the S-start. Anterior, triangles; posterior, circles. Curvature was positive for bending to the right and negative for bending to the left. When both anterior and posterior curvatures are zero, the fish is lying in a straight position; (B-C) Sarcomere strains of red (triangles) and white (circles) muscle fibres on the left and right side of the fish body during the S-start. Anterior, open symbols; posterior, filled symbols. Positive strains: muscle fibre lengthening; negative strains: muscle fibre shortening; (D) Acceleration (derived from velocity data) of the fish at 0.3 FL (where FL is fork length) during the S-start. \Rightarrow

How carp activate trunk muscles during C- and S-starts





initial (stage 1) and an opposite (stage 2) S-shape (with initial and opposite EMGs leading to these S-shapes), based on the curvature of the anterior body midline (see Fig. 4A). Stage 1 began when the carp started to bend after being 'disturbed' (initially in straight position) and ended when the initial S-shape was reached and stage 2 set in. Stage 2 ended when the opposite S-shape was reached after which a variable behaviour followed.

An initial low swimming speed led to an anterior bending to the right through contractions of red, and very likely also white, right anterior fibres prior to $t=0$ ms (see Figs 4 and 5). Simultaneously, red posterior fibre contractions (right side) resulted in a small right posterior curvature between $t=0$ and 18 ms, immediately followed by a bending to the left through contracting left white posterior fibres (this activity is not completely shown in Fig. 5 as it partly occurred before $t=-20$ ms). These contractions were not part of the S-start.

In Fig. 4 the carp began the actual S-start at $t=0$ ms (stage 1, arrow 3) while swimming very slowly with minor curvatures. At approximately $t=20$ ms the first actual left EMGs (both red and white, see Fig. 5) resulted in an initial S-shape at $t=118$ ms when a maximum left anterior curvature was reached (see Fig. 4A). At that moment the tail was already curved to the right and stage 2 set in. The opposite S-shape of the carp at $t=160$ ms was a result of red (and possibly also white) anterior EMGs at the right side at $t=80$ ms (right anterior bending) and of both red and white left posterior EMGs at approximately $t=40$ ms (left posterior bending, see Fig. 5).

Onsets and durations of EMGs

During all S-starts investigated ($N=9$) a very specific sequence of EMGs occurred at one side of the body (the left in this case, see Fig. 5): red anterior ($t=18$ ms), white anterior (at $t=22$ ms), red posterior (at $t=38$ ms) and white posterior (at $t=42$ ms). The delay in onset of EMGs was approximately 4 ms between red and white fibres (at the same longitudinal location) and approximately 20 ms between anterior and posterior fibres (at the same side of the fish body).

Initial EMG durations in S-starts were longer than ipsilateral EMG durations in the type 1 C-start: white anterior 43.1 ± 2.3 ms, red anterior 56.3 ± 2.5 ms and red posterior 68.1 ± 2.4 ms ($N=9$, see Table 1).

Fig. 5. EMG signals (mV) of red and white anterior (ant.) and posterior (post.) muscle fibres at the left side and red anterior and posterior muscle fibres at the right side of the body during the S-start (as shown in Fig. 4). The shaded and black bars under each EMG represent the periods of muscle fibre lengthening and shortening, respectively, as presented in Fig. 4. The fish shapes with the various muscle activities (red muscle activity, shaded bars, white muscle activity: black bars) are shown above the figure. The time scale on the X-axis runs parallel with the time scale in Fig. 4. ←

Sarcomere strains and accelerations

The maximum sarcomere strain for right anterior fibres (red: 0.06; white: 0.031, see Fig. 4B,C) was reached at $t=104$ ms, approximately 85 ms after the onset of left muscle EMGs. The maximum sarcomere strain for right posterior fibres was reached at $t=160$ ms (red: 0.185; white: 0.105), approximately 120 ms after the onset of left posterior muscle EMGs. The time between the onset of initial EMGs and the opposite maximum sarcomere strains was much longer in S-starts than in C-starts. The average maximum sarcomere strains during S-starts was higher in anterior fibres (red: 0.39 ± 0.02 ; white: 0.25 ± 0.03 , $N=9$) than in posterior fibres (red: 0.18 ± 0.01 ; white: 0.11 ± 0.006 , $N=9$). Also in S-starts muscle lengthening occurred in both anterior and posterior fibres, at both sides of the fish body, while they were active (eccentric activity).

S-starts of carp occurred at much lower accelerations than C-starts with displacements more in line with the body axis (see Fig. 4D). After a slow start, a peak acceleration close to 40 m s^{-2} occurred at approximately $t=73$ ms.

Table 1. Maximum sarcomere strain and durations of muscle activities during fast-starts. The sequence of muscle activity within each fast-start is indicated by the letters in subscript. From the muscle fibre types indicated with '--' no data were recorded. Strain data are expressed as relative values, only positive strains were used. See Results for further explanation. $N=9$ (total number of recordings per type of fast-start) for all values except for strain data during the C-starts, where $N=18$ (data from both C-start types combined). Values are presented as means \pm S.D.

Muscle fibre type	Mean maximum strain	Average duration of EMGs (in ms)			
		Type 1 C-start (no initial speed)		Type 2 C-start (initial speed)	
		<i>Ipsilateral</i>	<i>Contralateral</i>	<i>Ipsilateral</i>	<i>Contralateral</i>
C, red anterior	0.28 ± 0.18	$35.2\pm 1.9_1$	$77.4\pm 4.8_2$	$60.0\pm 3.8_1$	$60.0\pm 2.7_3$
C, red posterior	0.28 ± 0.14	$34.0\pm 2.1_1$	$74.1\pm 3.8_3$	$64.6\pm 4.0_1$	$55.8\pm 2.6_4$
C, white anterior	0.17 ± 0.15	$33.4\pm 1.9_1$	--	$53.2\pm 2.3_2$	--
C, white posterior	0.18 ± 0.09	$43.8\pm 4.6_1$	--	$58.7\pm 1.9_2$	--
		Escape S-start			
		<i>Initial S</i>	<i>Opposite S</i>		
S, red anterior	0.37 ± 0.02	$56.3\pm 2.5_2$	$47.2\pm 2.6_6$		
S, red posterior	0.18 ± 0.01	$68.1\pm 2.4_1$	$60.3\pm 3.0_4$		
S, white anterior	0.25 ± 0.03	$43.1\pm 2.3_3$	--		
S, white posterior	0.11 ± 0.006	--	$45.9\pm 3.2_5$		

DISCUSSION

Stages during fast-starts were difficult to define because muscle fibres at the left and right side of the body axis were sometimes active simultaneously. We therefore defined stages of S-starts based on the curvature of the anterior body midline (which only gave an indication of the actual stages): an initial and an opposite S-shape (see also Results), and stages of C-starts based on EMGs. As different solutions might appear when describing these stages differently we compared fast-start types based on features like curvature, sarcomere strain and duration and moment of EMGs.

The following major conclusions can be drawn from our analysis of the escape behaviour of carp. (1) Carp were able to uncouple red and white muscle activity during escape S-starts whereas this uncoupling was not (or less) present during the Mauthner initiated C-starts. (2) Red muscle were active during all fast-starts investigated which led us to believe that these muscle do contribute to force enhancement. (3) Our findings corresponded with the additive model of muscle fibre function (see Jayne and Lauder, 1994). (4) The antero-posterior delay in EMG onset was virtually absent during stage 1 of C-starts, making a very fast escape possible. (5) The delay between ipsilateral EMG onset and the following contralateral maximum bending was not constant for the various starts. (6) Escape S-starts and C-starts of carp can at any phase override continuous swimming motor patterns (see also Jayne and Lauder, 1993). (7) C-starts of carp are controlled differently on a neuronal level than escape S-starts.

Simultaneous EMGs of red and white muscle

A recurrent finding for vertebrate locomotion is that as power output and speed of movement increase, faster fibres are sequentially recruited in addition to (but not at the exclusion of) slower fibre types (Grillner, 1981; Armstrong, 1981). Jayne and Lauder (1993, 1994) found in bluegill sunfish (*Lepomis macrochirus*) that both red and white fibres were utilised at high speeds, although low. They suggested that during rapid unsteady swimming the intensity of red muscle activity decreased (although present) while the intensity of white muscle activity increased. In this view slower fibres are mainly used to power slow- and medium-speed movements, whereas both slow and fast fibres are used during fast movements (Jayne and Lauder, 1994). This 'additive' model of muscle fibre function could also be applied to all fast-starts we investigated, as we found only red muscle activity during continuous swimming whereas red and white muscle activity occurred simultaneously during fast-starts. Our results also showed that red and white muscle activity periods at a given longitudinal location needed not to be necessarily synchronous and could be uncoupled (more or less), depending on the type of escape response. In our study this uncoupling took place during escape S-starts of carp (Fig. 5) and we suggest that in this way mechanically sub-optimal patterns of force generation can be avoided. During C-starts, on the contrary, the uncoupling between red and white muscle activity periods seemed hardly present, possibly because it just cannot occur during these Mauthner-initiated starts.

Corresponding with the 'additive' model of muscle fibre function is the size principle of recruiting motoneurons (Henneman *et al.*, 1965): red fibres are innervated by the smallest motoneurons and

white fibres by both small and large motoneurons (Fetcho, 1986; Westerfield *et al.*, 1986). The same neuro-anatomy of these smallest motoneurons innervating red muscle has however also been used to support the prediction of no red muscle activity during escape responses (Fetcho, 1991). Red fibres only reach a maximum shortening velocity of approximately 5.5 L s^{-1} and are consequently quickly 'overruled' by the much faster white fibres (approximately 15 L s^{-1} , see Materials and methods). Van Leeuwen (1992) reported that, in the light of the above mentioned facts, the activity of red fibres seems a hindrance to locomotion in vigorous intermittent swimming of carp, as their work output is negative. Earlier studies suggested that carp red muscle operated at 50 % of their maximum force generating capacity (Rome and Sosnicki, 1991; Spierts and van Leeuwen, 1999) and therefore their use was considered to be unlikely during escape responses. Our findings of red muscle activity (anteriorly and posteriorly) during both stages of C- and S-starts however contradict these plausible predictions.

To investigate whether red fibres were able to contribute to force generation at all during fast-starts, we compared EMGs and muscle fibre lengthening and shortening of red fibres in Figs 3 and 5 (shaded and black bars, respectively). We considered delay times between initial electrical activity and the full mechanical response of approximately 60 ms and 105 ms for red anterior and posterior fibres, respectively (e.g. Altringham *et al.*, 1993; Rome *et al.*, 1993; van Leeuwen, 1995). Our findings suggest that during fast-starts red fibres could contribute to muscle fibre shortening at the beginning of their mechanical response for a very short period of time (before the full response is reached) and hence could contribute to force generation, although little. After red fibres started to buckle (due to the much faster contracting white fibres) the fish skin actually showed small foldings and no contribution to forward thrust was made anymore. Most of the force generation and the subsequent bending of the carp during fast-starts however is produced by white fibres, fibres that have a much shorter delay time between initial electrical activity and the full mechanical response (see later).

The differences in muscle activities in fast-starts between our study and other studies could very well be species- and water temperature related. Also the varying innervation of axial muscle among different fish taxa might partially account for observed variation in fibre recruitment (Bone, 1978). Future research will be needed to clarify these issues.

The antero-posterior delay in onset of EMGs

In the type 1 C-start the antero-posterior delay in the onset of EMGs was virtually absent in stage 1. This was also found by Kashin *et al.* (1979) during bursts of rapid movement of carp (*Cyprinus carpio*) and by Jayne and Lauder (1993) during escape responses of the bluegill sunfish (*Lepomis macrochirus*). In stage 2 of this start (red fibres) the delay was higher (approximately 4 ms) and in the type 2 C-start the antero-posterior delay increased to approximately 10 ms in stage 1 and to approximately 35 ms for red fibres in stage 2. In S-starts this delay was 20-25 ms for red and white fibres. Van Leeuwen (1995) hypothesised that the antero-posterior delay would be virtually absent during intermittent swimming and fast-starts (first tail beat), because positive work is likely to be done over the whole trunk by intermediate and fast muscle fibres (intermittent swimming in carp, van Leeuwen *et al.*, 1990; van Leeuwen, 1992; fast-start of sculpin, Johnston *et al.*, 1993; Johnston *et*

al., 1995). The pattern of co-ordination between muscle segments during the first tail beat of a C-start and the absence of this synchronous muscle activity in S-starts might also be connected to the different neural patterns controlling these starts. The smallest antero-posterior delay, occurring during the first tail beat of type 1 C-starts, was less than 1 ms. When assuming a distance of approximately 9 cm between the anterior and posterior electrodes in our carp, it is clear that very high conduction velocities of the Mauthner system were achieved (which also applies to stage 1 of the type 2 C-start). We therefore suggest that during the Mauthner neurones (and associated networks) initiated C-starts a synchronous muscle activity at different body segments during the first tail beat prevents a slow escaping reaction. This very fast conduction velocity was obviously not achieved in the second tail beat of C-starts and in S-starts. These latter larger antero-posterior delays were very similar to the ones found during cyclic swimming which were detected for several species and were approximately 30 ms (van Leeuwen, 1995). The underlying causes for differences between various fast-starts in antero-posterior delays in onsets of EMGs however are still unknown and should be investigated in more detail.

Durations of EMGs

An interesting and puzzling finding in our study was that the delay between ipsilateral EMG onset and the following contralateral (maximum) bending was small in the type 1 C-start, higher in the type 2 C-start and highest during the S-start. This might be connected to the (earlier mentioned) different neural patterns controlling these starts, but a more detailed study is needed to clarify these findings. In C-starts the time between the offset of stage 1 and the onset of stage 2 was less than 8 ms which agrees with findings of Jayne and Lauder (1993). In S-starts and in stage 1 of C-starts (except for red fibres in stage 1 of the type 1 C-start) the EMGs showed posterior propagation, resulting in longer durations of posterior EMGs. This longitudinal variation in stage 1 EMG durations confirms earlier findings by van Leeuwen *et al.* (1990) during intermittent swimming of carp and by Jayne and Lauder (1993) during the escape response of the bluegill sunfish (*Lepomis macrochirus*.) but is opposite to the results of studies on cyclic swimming (Williams *et al.*, 1989; van Leeuwen *et al.* 1990; Jayne and Lauder, 1993; Wardle and Videler, 1993). The similar durations of anterior and posterior EMGs in stage 2 of C-starts in our study (but with an earlier on- and offset anteriorly) were also found by Jayne and Lauder (1993). Stage 2 EMGs in C-starts were longer than contralateral EMGs in S-starts. This might be explained by the fact that after ipsilateral contractions in C-starts the fish 'slows down' its strong ipsilateral curving of the body by an early and long activation of contralateral muscles (even before the maximum ipsilateral curvature is reached) after which the bending process is reversed.

Accelerations of the fish at 0.3 FL

The main acceleration peak during C-starts, approximately 72 m s^{-2} , occurred when the carp was bending from its C-shape to the resting position. Between two main acceleration peaks during C-starts (Fig. 2D) a minimum value occurred which was probably caused by an approximate rotation around the fish centre of mass at 0.3 FL, while ongoing bending caused head and tail to move with large

accelerations. The lower maximum accelerations in S-starts, approximately 40 m s^{-2} , occurred between two opposite S-shapes which coincided with a tail fin movement of high lateral velocity and considerable angle with the anterior body axis (Fig. 4D). At that moment the thrust produced by the fish is indeed expected to be large. In a study of Spierts and van Leeuwen (1999) maximum accelerations were found of approximately 54 m s^{-2} and 40 m s^{-2} for C-starts and S-starts of carp, respectively. Reported maximum accelerations during fast-starts vary greatly between different studies (see review Domenici and Blake, 1997). When comparing accelerations during fast-starts from different studies, factors such as fish species, fish size, water temperature and filming must be considered.

Eccentric activity

Based on experimental data on fish muscle (e.g. Altringham *et al.*, 1993; Rome *et al.*, 1993) we assumed delay times between initial electrical activity and the full mechanical response of approximately 25 and 45 ms for white anterior and posterior fibres, respectively (see also van Leeuwen, 1995, the delay times for red fibres are mentioned before). When considering these delay times our data show that both anterior and posterior muscle fibres were active whilst lengthening at certain moments during both C- and S-starts. This eccentric activity confirms earlier studies of e.g. van Leeuwen (1990, carp, *Cyprinus carpio*), Johnston *et al.* (1995, fast-starts of short-horned sculpin, *Myoxocephalus scorpius*) and Franklin and Johnston (1997, escape responses of the Antarctic rock cod, *Notothenia coriiceps*) in which anterior, middle and posterior fibres were activated while being stretched. Muscle fibres that are active whilst lengthening in an escape response (as found in our study) initially absorb power. This might work advantageous for the transmission of force from the fish to the water, because (1) the muscle fibres are already activated before the actual bending of the fish body sets in (an advantage in time) and (2) the actin-myosin bindings occur in a more optimal (concerning force production) part of the force-velocity curve (see also Franklin and Johnston, 1997, and Curtin and Woledge, 1996).

ACKNOWLEDGEMENTS

We thank Dr M. Muller for his advises on data acquisition and Mr W.A. Valen for help in preparing the illustrations. This research were supported by Earth and Life Sciences (ALW), which is subsidised by the Netherlands Organisation for Scientific Research (NWO).

REFERENCES

- ALTRINGHAM, J.D., WARDLE, C.S. AND SMITH, C.I. (1993). Myotomal muscle function at different locations in the body of a swimming fish. *J. Exp. Biol.* **182**, 191-206.
- ARMSTRONG, R.B. (1981). Recruitment of muscles and fibres within muscles in running animals. *Symp. Zool. Soc. Lond.* **48**, 289-304.
- BONE, Q. (1978). Locomotor muscle. In *Fish physiology*, vol. 7, *Locomotion* (ed. W.S. Hoar and D.J. Randall), pp 361-424. New York: Academic Press.
- CURTIN, N.A. AND WOLEDGE, R.C. (1996). Power at the expense of efficiency in contraction of white muscle fibres from dogfish *Scyliorhinus canicula*. *J. Exp. Biol.* **199**, 593-601.
- DOMENICI, P. AND BLAKE, R.W. (1991). The kinematics and performance of the escape response in the angelfish (*Pterophyllum eimekei*). *J. Exp. Biol.* **156**, 187-205.
- DOMENICI, P. AND BLAKE, R.W. (1997). Review: The kinematics and performance of fish fast-start swimming. *J. Exp. Biol.* **200**, 1165-1178.
- EATON, R.C., BOMBARDIERE, R.A. AND MEYER, D.L. (1977). The Mauthner-initiated startle response in teleost fish. *J. Exp. Biol.* **66**, 65-85.
- FETCHO, J.R. (1986). The organisation of the motoneurons innervating the axial musculature of vertebrates. I. Goldfish (*Carrasius auratus*) and mudpuppies (*Necturus maculosus*). *J. Comp. Neurol.* **249**, 521-550.
- FETCHO, J.R. (1991). Spinal network of the Mauthner cell. *Brain Behav. Evol.* **37**, 298-316.
- FRANKLIN, C.E. AND JOHNSTON, I.A. (1997). Muscle power output during escape responses in an Antarctic fish. *J. Exp. Biol.* **200**, 703-712.
- GRILLNER, S. (1981). Control of locomotion in bipeds, tetrapods, and fish. In *Handbook of Physiology*, section 1, vol. II, *Motor Control*, part 2 (ed. V.B. Brooks), pp 1179-1236. Bethesda, MD: American Physiological Society.
- HENNEMAN, E., SOMJEN, G. AND CARPENTER, D.O. (1965). Functional significance of cell size in spinal motoneurons. *J. Neurophysiol.* **28**, 560-580.
- HOOGLAND, R. MORRIS, D. AND TINBERGEN, N. (1956). The spines of sticklebacks (*Gasterosteus* and *Pygosteus*) as a means of defence against predators (*Perca* and *Esox*). *Behaviour* **10**, 205-236.
- JAYNE, B.C. AND LAUDER, G.V. (1993). Red and white muscle activity and kinematics of the escape response of the bluegill sunfish during swimming. *J. Comp. Physiol. A.* **173**, 495-508.
- JAYNE, B.C. AND LAUDER, G.V. (1994). How swimming fish use slow and fast muscle fibers: implications for models of vertebrate muscle recruitment. *J. Comp. Physiol. A.* **175**, 123-131.
- JOHNSTON, I.A., FRANKLIN, C.E. AND JOHNSON, T.P. (1993). Recruitment patterns and contractile properties of fast muscle fibres isolated from rostral and caudal myotomes of the short-horned sculpin. *J. Exp. Biol.* **185**, 251-265.
- JOHNSTON, I.A., LEEUWEN, J.L. VAN, DAVIES, M.L.F. AND BEDDOW, T. (1995). How fish power predation fast-starts. *J. Exp. Biol.* **198**, 1851-1861.
- KASAPI, M.A., DOMENICI P., BLAKE, R.W. AND HARPER, D. (1993). The kinematics and performance of escape responses of the knifefish *Xenomystus nigri*. *Can. J. Zool.* **71**, 189-195.
- KASHIN, S.M., FELDMAN, A.G. AND ORLOVSKY, G.N. (1979). Different modes of swimming in the

- carp, *Cyprinus carpio* L. *J. Fish Biol.* **14**, 403-405.
- KIMMEL, C.B., EATON, R.C. AND POWELL, S.L. (1980). Decreased fast-start performance of zebrafish larvae lacking Mauthner neurons. *J. Comp. Physiol.* **140**, 343-351.
- OSSE, J.W.M. (1969). Functional morphology of the head of the perch (*Perca fluviatilis* L.): an electromyographic study. *Neth. J. Zool.* **19**, 289-392.
- OSSE, J.W.M., OLDENHAVE, M. AND SCHIE, B. VAN (1972). A new method for insertion of wire electrodes in electromyography. *Electromyography* **12**, 59-62.
- ROME, L.C. AND SOSNICKI, A.A. (1991). Myofilament overlap in swimming carp. II. Sarcomere length changes during swimming. *Am. Physiol. Soc.* **260**, 289-296.
- ROME, L.C., SWANK, D. AND CORDA, D. (1993). How fish power swimming. *Science.* **261**, 340-343.
- SPIERTS, I.L.Y. AND LEEUWEN, J.L. VAN (1999). Kinematics and muscle dynamics of C- and S-starts of carp (*Cyprinus carpio* L.). *J. Exp. Biol.* **202** (4), 393-406.
- VAN LEEUWEN, J.L. (1992). Muscle function in locomotion. In *Mechanics of animal locomotion, Advances in Comparative and Environmental Physiology*, vol. 11 (ed. R. MCN. ALEXANDER), pp 191-250. Heidelberg: Springer-Verlag.
- VAN LEEUWEN, J.L. (1995). The action of muscles in swimming fish. *Exp. Physiol.* **80**, 177-191.
- VAN LEEUWEN, J.L., LANKHEET, M.J.M., AKSTER, H.A. AND OSSE, J.W.M. (1990). Function of red axial muscles of carp (*Cyprinus carpio*): recruitment and normalised power output during swimming in different modes. *J. Zool.* **220**, 123-145.
- WARDLE, C.S. AND VIDELER, J.J. (1993). The timing of the EMG in the lateral myotomes of mackerel and saithe at different swimming speeds. *J. Fish Biol.* **42**, 347-359.
- WEBB, P.W. (1976). The effect of size on the fast-start performance of rainbow trout *Salmo gairdneri*, and a consideration of piscivorous predator-prey interactions. *J. Exp. Biol.* **65**, 157-177.
- WEBB, P.W. AND BLAKE, R.W. (1985). Swimming. In *Functional vertebrate morphology* (ed. M. Hildebrand, D.M. Bramble, K. Liem and D.B. Wake), pp 110-128. Cambridge: Harvard University Press.
- WEIHS, D. (1973). The mechanism of rapid starting of slender fish. *Biorheology* **10**, 343-350.
- WESTERFIELD, M., McMURRAY, J.V. AND EISEN, J.S. (1986). Identified motoneurons and their innervation of axial muscles in the zebrafish. *J. Neurosc.* **10**, 259-298.
- WILLIAMS T.L., GRILLNER, S., SMOLJANINOV, V.V., WALLÉN, P., KASHIN, S. AND ROSSIGNOL, S. (1989). Locomotion in lamprey and trout: the relative timing of activation and movement. *J. Exp. Biol.* **143**, 559-566.

8

Expression of titin isoforms during the ontogeny of carp (*Cyprinus carpio* L.) in relation to fast-swimming

Igor L.Y. Spierts

Experimental Zoology Group, Wageningen Institute of Animal Sciences (WIAS), Wageningen
Agricultural University, Marijkeweg 40, 6709 PG Wageningen;
The Netherlands

SUMMARY

Titin is a striated-muscle specific protein that spans the distance between the Z- and M-line of the sarcomere. The elastic I-band segment of the titin molecule is held responsible for developing passive tension and for maintaining the central position of thick filaments in contracting sarcomeres. Different muscle types express isoforms of titin differing in molecular mass. To elucidate the relation between the occurrence of titin isoforms and the functional properties of fibre types during fast swimming at different ages of fish, I investigated the presence of titin in carp larval muscle fibres (*Cyprinus carpio* L.) and compared our findings with data of adult carp muscle titins. Gel-electrophoresis revealed that the titin isoform was larger in adult than in larval muscle. Apparently the molecular structure of titin changed during ontogeny. A previous study showed that the size of titin was correlated to the functioning of different muscles during swimming. Fish larvae (6.5-8 mm total length) are subjected to low Reynolds-number regimes ($Re < 500$) during swimming and therefore require special features to overcome effects of friction. How do these larvae generate the power to swim in their environment? The smaller titin isoforms of carp larvae, compared to adults, may contribute to regaining some power needed for swimming as an elastic deformation. The smaller a titin isoform, the more passive tension is required for stretching the muscle fibre to a certain extend. During fast swimming of larvae negative power is accumulated in the passively stretching fibres at the convex side of the body axis, generated by the activity of fibres at the concave side, and is only released in the opposite bending. Fish larvae may increase the elastic contribution to the tail beat by absorbing power as elastic energy in their titin isoforms during the initial bending that is subsequently released in the following bending.

INTRODUCTION

Teleost larvae often hatch at quite small lengths (Moser, 1996). In most cases the larval body form differs substantially from the juvenile form, and a metamorphosis is, therefore, seen during the larval development. Numerous functional systems are adjusted for larval needs shortly after hatching, but still incomplete for adult functioning (Osse and van den Boogaart, 1997). Generally pectoral fins are present yet lacking finrays and sometimes even these are absent (Bruton, 1979). The median fins have the form of a continuous finfold without bony or cartilaginous support, but having collagenous rods, actinotrichia (Géraudie, 1977, 1984; Géraudie and Landis, 1982). The larvae start feeding on external energy sources soon after hatching because eggs are mostly small, especially in pelagic fish. Rapid growth of organs and systems is observed during the early larval period.

Coinciding with the development of lepidotrichia as fin rays, the swimming behaviour of fish larvae changes remarkably. Osse (1990) described the ontogeny of swimming behaviour in carp. He found a change from anguilliform towards carangiform swimming in growing carp larvae. Young carp larvae initially swam with a large amplitude over their entire body in a low Reynolds-regime where friction is still important. Possibly, the viscous environment favours an anguilliform type of swimming of the larvae because the animal does not gain much thrust from inertial forces. Axial muscle of fish larvae differ from that of adult fish. Adult fish mostly have a triangular red zone at the

level of the horizontal septum separated by a pink or intermediate zone from the white bulk of the muscle mass (Johnston *et al.*, 1977). Yolk-sac larvae have an inner 'larval white' muscle mass surrounded by a superficial monolayer of red muscle fibres, larval red muscle. During the free-swimming larval stage the adult patterns of muscle fibre type distribution and the differences in metabolism between the red aerobic fibres and the white anaerobic fibres develop (Hinterleitner *et al.*, 1987). It is suggested that red muscle fibres in larvae are mainly involved in the uptake and transfer of oxygen until the gills are fully developed (El-Fiky *et al.*, 1987; Hinterleitner *et al.*, 1987). So regarding the early differentiation of muscle the question rises: Which muscles do fish larvae use for swimming?

Carp larvae (at approximately 22 °C) generally start swimming and feeding 2-3 days after hatching (before that time they attach to a substratum). Part of this swimming behaviour are attempts to hold their position in the water by undulatory movements of the body and the finfolds. The burst-like mode of swimming which is typical for older fish also occurs. El-Fiky *et al.* (1987) suggested that superficial red fibres of Cyprinid larvae actually are mainly used for respiratory functions and that all larval swimming behaviour is powered by the deeper mass of, still oxidative, 'larval white' fibres. But how do these inner 'larval white' muscles generate enough power to overcome the effects of friction so that velocities over 20 bodylengths s⁻¹ can be realised?

In an earlier study Spierts *et al.* (1997) suggested a correlation between the function of different muscle fibres of carp and the size (and other properties) of the giant elastic muscle protein titin. The understanding of the molecular basis of muscle elasticity has improved greatly from increased knowledge of this particular molecule. Titin is a giant protein that spans from the Z-line to the M-line of the sarcomere (Wang, 1985; Maruyama, 1986, 1994; Trinick, 1991). The I-band segment of titin consists of series-coupled immunoglobulin (Ig)-like domains, each containing approximately 100 residues, and an unique domain rich in proline (P), glutamate (E), lysine (K) and valine (V), referred to as the PEVK domain (Labeit and Kolmerer, 1995). This region is thought to function as a molecular spring that maintains the central position of the thick filaments in the sarcomere and that develops passive tension upon sarcomere stretch (Horowitz *et al.*, 1986; Fürst *et al.*, 1988; Wang *et al.*, 1991, 1993; Granzier *et al.*, 1996). Different muscles express size variants of titin (isoforms) that result from differential splicing in the elastic region of titin (Labeit and Kolmerer, 1995). The smaller a titin isoform, the more passive tension is required to obtain a similar strain. Gel-electrophoresis of single fibres under strictly defined conditions revealed that the molecular mass of titin was larger in red than in white fibres of adult carp (Spierts *et al.*, 1997). For both white and red fibres the molecular mass of titin in posterior muscle fibres was larger than in anterior muscle fibres. During continuous swimming, red fibres are exposed to larger changes in sarcomere strain than white fibres, due to their more lateral position and close to longitudinal fibre orientation. Posterior fibres also undergo larger changes in strain than anterior fibres. Spierts *et al.* (1997) proposed that sarcomere strain is one of the functional parameters that modulates the expression of different titin isoforms in axial muscle fibres of carp.

The differences in swimming behaviour between carp larvae and adults led me to investigate whether these differences are accompanied by differences in titin isoforms. My hypothesis is that in larvae shorter titin isoforms (requiring larger stress for the same strain) will be found to restrict the

form changes of the swimming larvae and to increase the elastic contribution to the tail beat. This is possibly required also because the ratio between muscle mass and beating surface is still very small in fish larvae. Short molecules might also help to increase the resonant frequency of the beating tail and thereby provide the required high frequency for swimming in a low Reynolds-regime. To tackle these questions I measured and calculated lateral body curvature as a function of position and time in carp larvae. Second, I used the curvature data and measured muscle fibre orientations to calculate strain variations of larval anterior and posterior red and early white muscle fibres. Finally, gel-electrophoresis was used to investigate the presence of titin isoforms in carp larvae and a comparison with titin isoforms of adult carp was made, to be related to the differences in sarcomere strain and fast swimming behaviour between larval and adult carp.

MATERIALS AND METHODS

Preparations

Carp eggs were artificially fertilised and kept in well aerated tanks (24.5 °C). The larvae were fed using *Artemia nauplii ad lib.* Approximately 105 larvae of common carp (*Cyprinus carpio* L.); 6.5-8 mm total length, *TL*, were used: 100 for gel electrophoresis and 5 for the swimming experiments. Three adult common carp (*Cyprinus carpio* L., 22-24 cm fork length, *FL*), bred in the laboratory at 23 °C and fed on commercial fish food (Trouvit pellets; Trouw and Co. Putten) were used for gel electrophoresis.

Swimming recordings

High-speed motion films were made to derive sarcomere length changes (muscle strain) during fast swimming at two positions along the body, 0.4 and 0.8 *TL* (measured from the tip of the snout), in red and white axial muscle fibres of five carp larvae (Fig. 1). Fast swimming of the larvae was elicited by touching their tails with a small diameter (approximately 0.2 mm) steel wire. Swimming events were filmed using a high speed video camera at 500 frames s⁻¹ (NAC colour High Speed Video system HSV 1000 FRS with a Super-VHS video tape recorder type V-306; Reinka B.V., Breda). The films were shadow-images (Arnold and Nuttall-Smith, 1974) of larvae put in a small (25 x 35 mm) glass aquarium lit dorsally. Water temperature was approximately 21-22 °C. Video scenes were selected on basis of the following criteria: (1) the fish should swim in a straight line for more than one complete swimming cycle, (2) the fish should not swim near the aquarium edge nor near the bottom, and (3) the fish should swim in a horizontal plane. The selected video scenes were digitised using the media 100 QX video capturing package (Transtec B.V.) running on a power Macintosh 8600 computer.

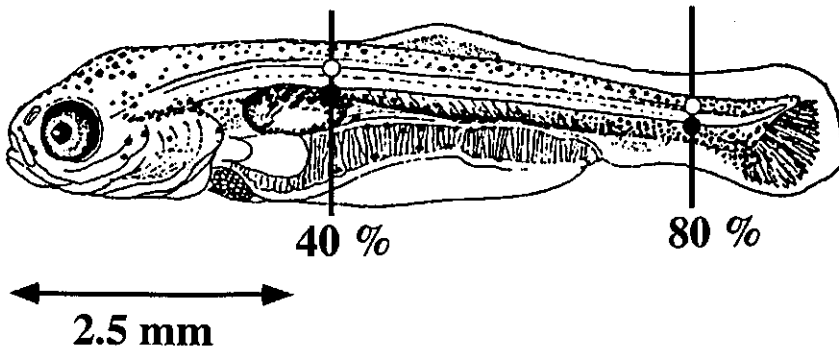


Fig. 1. Schematic drawing of a 7.5 mm (*TL*) carp larva showing the positions used for calculating the muscle fibre strain in red and white muscle tissue at the left and right side of the fish body at 0.4 and 0.8 *TL*. The positions for red and white muscle tissue are indicated by respectively black and white dots.

Calculation of muscle fibre strain

The outlines of the larvae during fast swimming were printed onto A4-paper sheets at 2 ms intervals and were digitised relative to fixed reference points, using an *x,y*-data-tablet (Calcomp 9100). For each side of the body, approximately 100 points were used. The points were distributed non-equidistantly. The shortest distances were used for the strongest curvatures of the outline. The estimated maximum error of the digitising process was 0.5 mm, which is approximately 0.03 % of the total length of the larvae at the used enlargement. For successive frames, a longitudinal axis of the fish during the swimming event was calculated from its digitised outlines and the absolute curvature was determined, using equations 1-3 from Spierts and van Leeuwen (1999). Axis data were smoothed as a function of position down the trunk and curvature data were smoothed as a function of time, following van Leeuwen *et al.* (1990). The total length (*TL*) divided by the local radius of the curvature (*R*) gave the normalised curvature (*TL/R*) and was defined as positive for curvature to the right and as negative for curvature to the left.

Sarcomere strains of red and white muscle fibres at 0.4 and 0.8 *TL* (Fig. 1) during fast swimming were calculated using equations 4-7 from van Leeuwen *et al.* (1990), which describe the observed thickening at the concave side of the body and the thinning at the convex side. In the calculation, it was assumed that when the trunk was straight the fibres were at their resting length. Five larvae were used for the strain calculations, and of every larva a fast swimming scene was filmed and digitised. For fast swimming carp larvae a mean sarcomere strain and a mean maximum sarcomere strain (i.e. the average of 5 maximum values, 1 per filmed scene) was calculated for each muscle type and location. Due to possible buckling effects occurring in red fibres at the concave side during fast swimming, for which the calculations did not compensate, I only included

positive strains of the sarcomere (of both the left and right side of the body during a filmed scene) in the results.

Muscle fibre orientations of carp larvae

To correct strain calculations for the orientation of the different muscle fibres the angles with respect to the median and frontal plane of the fish were used. As in carp larvae of approximately 6.5-8 mm *TL* both red and white muscle fibres run almost parallel to the body axis at 0.4 and 0.8 *TL*, I assumed angles of 0-3° with respect to both the median and the frontal plane of the fish.

Gel electrophoresis

Approximately 100 complete carp larvae were anaesthetised with MS 222 (Sandoz, Basel) and decapitated. After killing three adult carp with an overdoses of MS 222, followed by trans-section of the spinal cord at 0.3 *FL*, I quickly dissected white anterior (at 0.4 *FL*) and red posterior (at 0.8 *FL*) axial muscles.

The decapitated carp larvae, fibre bundles of adult carp, and fibre bundles of rabbit semitendinosus muscle (adult New Zealand, 2.6 kg) were quickly frozen in liquid N₂ and pulverised to a fine powder using a mortar and pestle bathed in liquid N₂. I rapidly added the powder to a tenfold excess of 1.1X solubilisation buffer (50 mmol l⁻¹ TRIS-Cl, 2 % SDS, 10 % glycerol, 80 mmol l⁻¹ DTT, 30 µl/ml Pyronin Y, pH 6.8 at 25 °C) in a homogeniser that was present in a water bath of 80 °C (see also Granzier and Irving, 1995). After solubilising the sample for 90 sec it was cooled down and analysed with SDS-PAGE using 2.7-12 % polyacrylamide gradient gels with a Fairbanks buffer (Fairbanks *et al.*, 1971) for quantifying titin at room temperature.

To obtain a high-molecular-mass standard for comparison, I co-electrophoresed samples from semitendinosus muscle of rabbit. The muscle samples of adult carp were co-electrophoresed for further comparison with the larval samples.

Gel staining

For Coomassie Blue staining, gels were soaked in 150 ml of 25 % v/v isopropanol, 10 % v/v acetic acid for 15 min before switching to 0.1 % w/v Coomassie-Brilliant Blue R-250 in 25 % isopropanol, 10 % acetic acid for 15h. Gels were destained in 5 % isopropanol, 10 % acetic acid for 3 hours (see also Granzier and Wang, 1993). Gels were overrun 2-3 hours to increase resolution. The migration distances of carp and rabbit skeletal muscle proteins were determined using video densitometry and normalised to nebulin of rabbit semitendinosus muscle.

Statistics

All data calculated in this study appeared to be normally distributed (Shapiro and Wilk, 1965). Statistical analysis of the sarcomere strains of red and white anterior and posterior muscle fibres and

of the anterior and posterior curvatures during fast swimming of carp larvae was performed using a univariate analysis of variance procedure (ANOVA; SAS 6.11, SAS Institute Inc., Cary, USA); *t*-test and least significant difference (LSD) of means (Sokal and Rohlf, 1981). Statements of statistical significance are based on $P \leq 0.05$ unless specified otherwise (Sokal and Rohlf, 1981; Rohlf and Sokal, 1981). Values are presented as means \pm S.D.

RESULTS

Fast swimming responses of carp larvae

Fast swimming of carp larvae occurred very sudden (within approximately 30 ms) and involved high frequency tail beats (up to approximately 33 Hz). The larvae rapidly overcame viscous friction caused by the Reynolds-regime these larvae were subjected to ($200 \leq Re \leq 500$) and quickly gained speed. Fig. 2 is a typical example of a fast swimming response of a 7.5 mm TL carp larva showing the calculated central axes. The turning rate and total turning angle during this swimming sequence were low and therefore this movement was not an escape response but a straight forward fast swimming mode characterised by high frequency alternating S-shapes. The displacements of the fish larvae were approximately in line with the body axis.

At $t=0$ ms the larva was not in a (straight) resting position, but had an initial S-shape (Figs 2 and 3A) due to the preceding swimming motion in a clear direction (arrow). At approximately $t=16$ ms the larva already had an opposite S-shape. The bending of the flexible body axis of the fish larva during this swimming event (Fig. 2) can also be seen in Fig. 3A, showing the anterior and posterior normalised body curvature TL/R (TL , total length; R , local radius of curvature, Fig. 3 represents the same fast swimming response as shown in Fig. 2). Although the largest mean normalised body curvature during these fast swimming modes occurred posteriorly ($0.8 TL$), 2.61 ± 1.58 ($N=5$), there was no significant difference with the mean normalised curvature anteriorly ($0.4 TL$), 1.57 ± 0.81 ($N=5$). During these fast swimming modes the maximum curvature at one side of the body (anterior or posterior) was always reached within approximately 7-10 ms (e.g. Fig. 3A, anteriorly at $t=16$ ms) after lying in an, almost, straight body position (e.g. Fig. 3A, $t=11$ ms). During this maximum curvature, maximum sarcomere strains were reached at the convex side of the fish body (see Fig. 3B,C).

Strain variations in muscle fibres

The sarcomere strains at the left and right side of the body axis are shown in Fig. 3B,C, respectively (see also Table 1). From the figure it is clear that red and white anterior fibres had similar

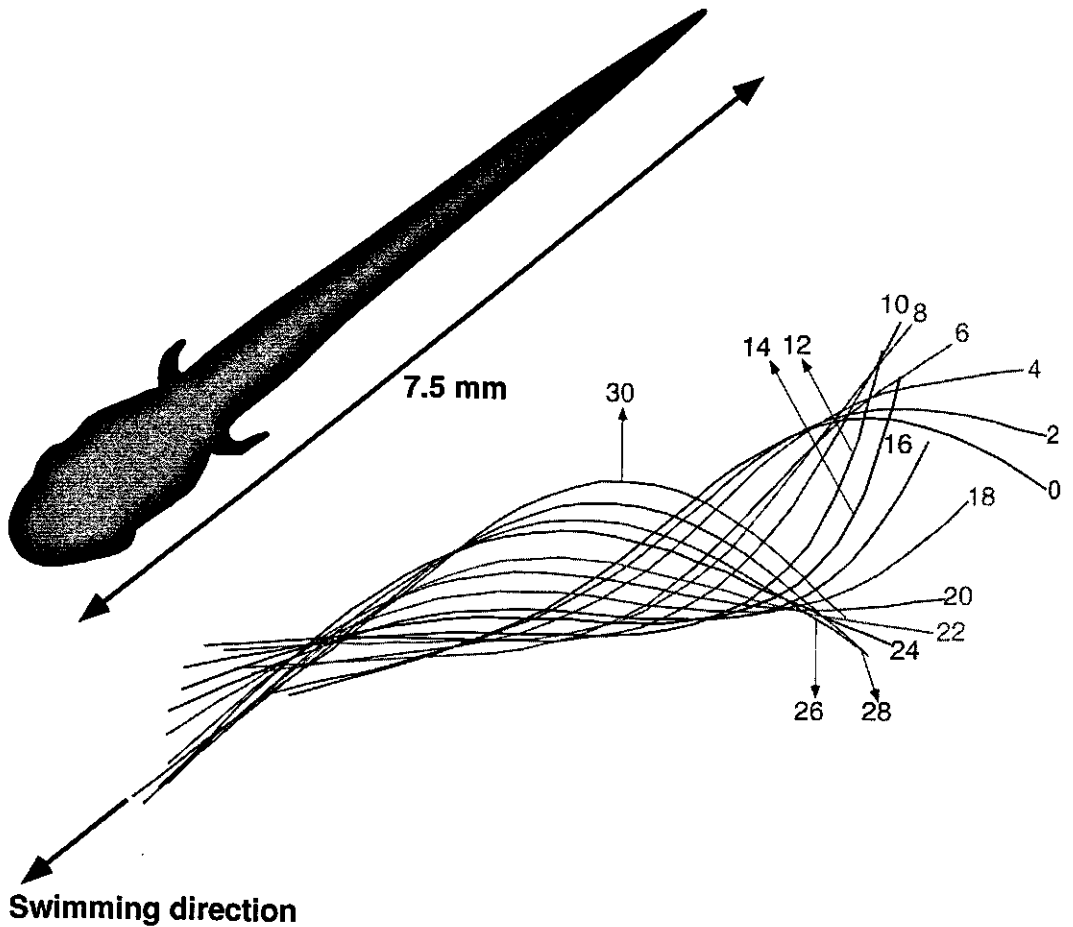


Fig. 2. A typical example of a fast swimming response of a 7.5 mm (TL) carp larva (the outline shows the larvae in a resting position from a dorsal point of view). The larva is already swimming with an initial speed at $t=0$ ms. The central axes of the larvae during fast swimming are shown every 2 ms. For every calculated axis 31 points were used. Times between tracings are in ms from $t=0$ ms. The tail beat frequency here is approximately 33 Hz.

sarcomere strains during the response. At the posterior side red and white fibres also showed similar strains. Table 1 presents the results from a statistical comparison of the mean sarcomere strains and the mean maximum sarcomere strains ($N=10$ is the total number of muscle tissue sections used; 5 carp larvae). Mean sarcomere strains during fast swimming of carp larvae did not significantly differ between anterior (0.107 ± 0.055 , $N=10$) and posterior fibres (0.115 ± 0.068 , $N=10$) or between red

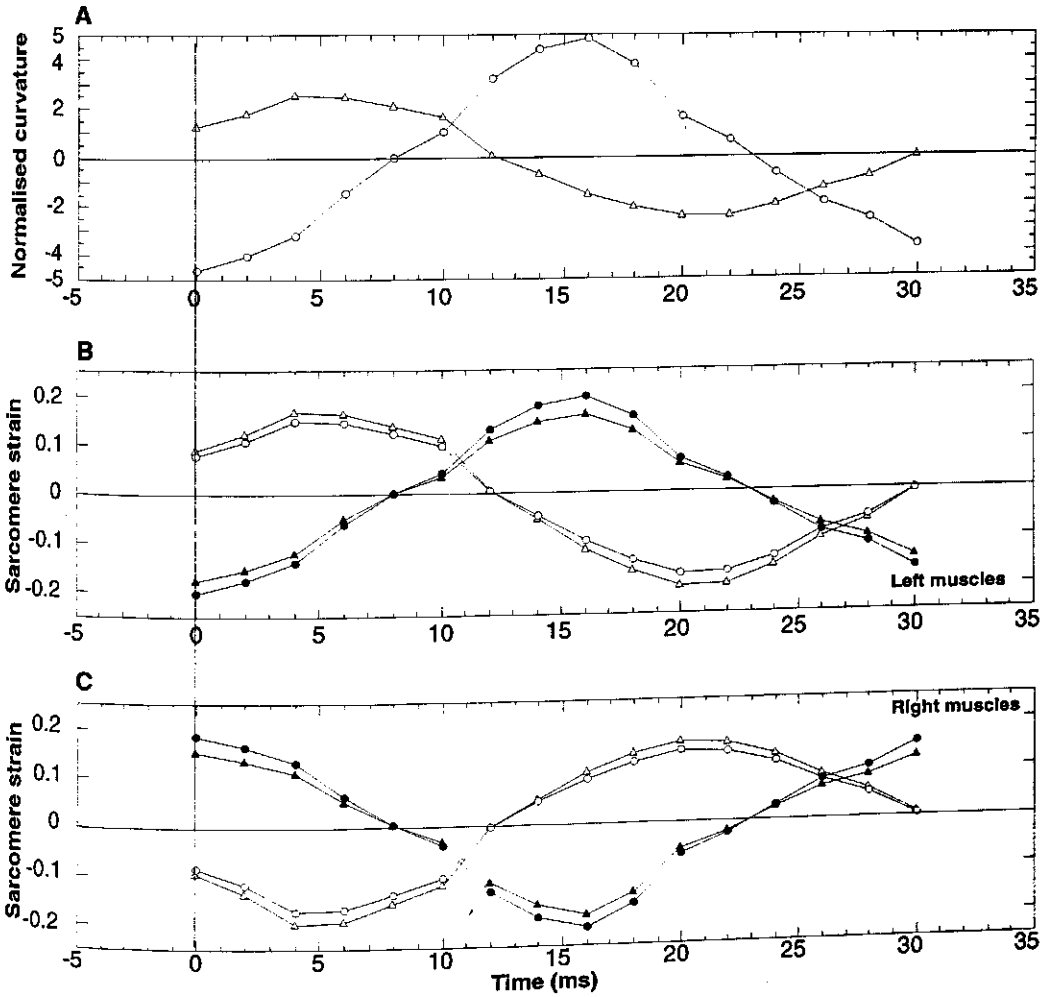


Fig. 3. Normalised curvature of the fish body and sarcomere strain of red and white axial muscle fibres at 0.4 TL (anterior) and at 0.8 TL (posterior) during a typical fast swimming response of a 7.5 mm (TL) carp larva. This response represents the same fast swimming response as shown in Fig. 2. The larva is already swimming with an initial speed at $t=0$ ms; (A) Normalised curvature TL/R (where TL is the total length and R is local radius of curvature) of the anterior (0.4 TL, triangles) and posterior (0.8 TL, circles) length and R is local radius of curvature) of the anterior (0.4 TL, triangles) and posterior (0.8 TL, circles) part of the fish body during the fast swimming. When both anterior and posterior curvatures are zero the fish is lying in a straight position; (B-C) Sarcomere strain of red (triangles) and white (circles) anterior muscle fibres at the left and right side of the fish body, (open symbols) and posterior (filled symbols) muscle fibres at the left and right side of the fish body, respectively, during fast swimming. Positive strains, muscle fibre lengthening; negative strains, muscle fibre shortening.

(0.117 ± 0.066 , $N=10$) and white fibres (0.105 ± 0.059 , $N=10$). Mean maximum sarcomere strains neither differed significantly between anterior (0.194 ± 0.016 , $N=10$) and posterior fibres (0.211 ± 0.018 , $N=10$). Red muscle fibres however had significantly larger mean maximum sarcomere strains (0.213 ± 0.014 , $N=10$) than white fibres (0.182 ± 0.011 , $N=10$).

Table 1. Mean sarcomere strains during fast swimming of carp larvae. Within each section of a column (mutually distinguished by blank lines) different letters (a,b) indicate a significant difference ($P \leq 0.05$). N , total number of muscle tissue sections used for determining the mean strain and the mean maximum strain (five carp larvae, 6.5-8 mm *TL*). Values are means \pm S.D.

Sarcomere strain → Muscle fibre type ↓	N	Mean strain	Mean maximum strain
Anterior, total	10	0.107 ± 0.055^a	0.194 ± 0.016^a
Posterior, total	10	0.115 ± 0.068^a	0.211 ± 0.018^a
Red, total	10	0.117 ± 0.066^a	0.213 ± 0.014^a
White, total	10	0.105 ± 0.059^a	0.182 ± 0.011^b

Gel-electrophoresis

Rabbit semitendinosus muscle samples (adult New Zealand) were used as high-molecular-mass standards and were either electrophoresed side by side with carp samples or mixed with carp samples. Fig. 4 shows a low porosity-gel of complete carp larvae samples and of adult carp fibre bundles (white anterior and red posterior muscles). Carp titin consisted of a doublet, T1 and T2 (Fig. 4, e.g. lane 3 and 8 for larval muscle and lane 7 and 9 for adult muscle). T2 is considered a degradation product of the parent molecule, T1, a process that may occur during sample preparation (Wang, 1985). In most skeletal muscles considerable degradation was found, with the exception of rabbit semitendinosus muscle which is known to be relatively insensitive to degradation (Wang *et al.*, 1991).

Spierts *et al.* (1997) found that white anterior and red posterior muscle of adult carp possessed the smallest and largest titin isoforms, respectively. The present study confirmed that adult white anterior muscle T1 (Fig. 4, lane 9) indeed migrated further into the gel than adult red posterior muscle T1 (Fig. 4, lane 7, see also Table 2), which can also be observed in lane 1 of Fig. 4, where these two muscle samples were mixed in one lane.

T1 of carp axial muscle (larval as well as adult samples) had a higher mobility than T1 of rabbit semitendinosus muscle (Fig. 4, adult red posterior and white anterior muscle T1: compare lane 7 and 9 with lane 10; larval muscle T1: compare lane 2 with lane 3 and see lane 6 and Table 2). This can also be observed in Fig. 5A, which is an amplification of an SDS-PAGE (adult white anterior muscle T1: compare lane 1 with lane 2; larval muscle T1: compare lane 1 with lane 3).

The difference in mobility between larval carp muscle T1 and adult carp muscle T1 is clearly visible: larval muscle T1 (Fig. 4, lane 3 and 8) migrated further than both white anterior (Fig. 4, lane

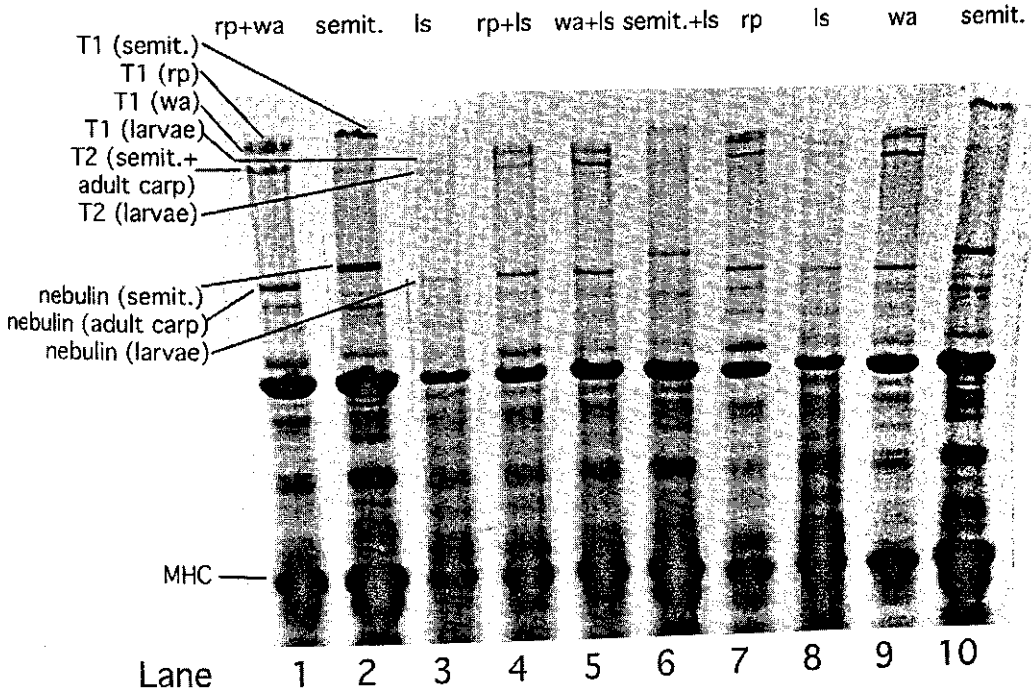


Fig. 4. SDS-PAGE of complete carp larvae and of adult carp fibre bundles. Carp axial muscles titin consists of a doublet, T1 and T2. Semitendinosus muscle from rabbit (adult New Zealand) was used as a high-molecular-mass standard, and titin of this muscle had a lower mobility than all carp muscle T1 (larval as well as adult, compare *lane 2 and 10 with lanes 1, 3 and 6-8*). semit., rabbit semitendinosus muscle; MHC, myosin heavy chain; Adult carp axial muscle: r, red; w, white; a, anterior; p, posterior; ls, complete carp larvae samples. See text for further details.

1 and 9) and red posterior muscle T1 of adult carp (Fig. 4, lane 1 and 7, see also Table 2). This is also shown in Fig. 5A, where adult white anterior and larval muscle samples were electrophoresed side by side (lane 2 and 3, respectively), and in Fig. 5B, where larval and adult red posterior muscle samples were electrophoresed side by side (lane 2 and 3, respectively).

When adult and larval muscle samples were mixed in one lane (in a low, C1, and a high, C2, concentration of the sample loaded in the lane: Fig. 5A,B, lane 4 and 5, respectively) this difference was more difficult to see as the larval 'T1 band' was 'thinner' and less visible in all the gels (less

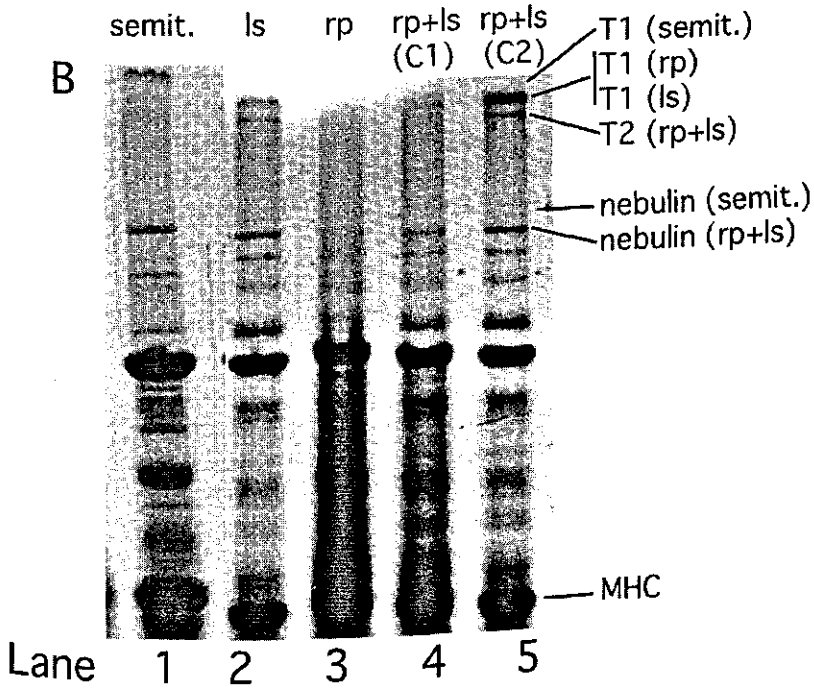
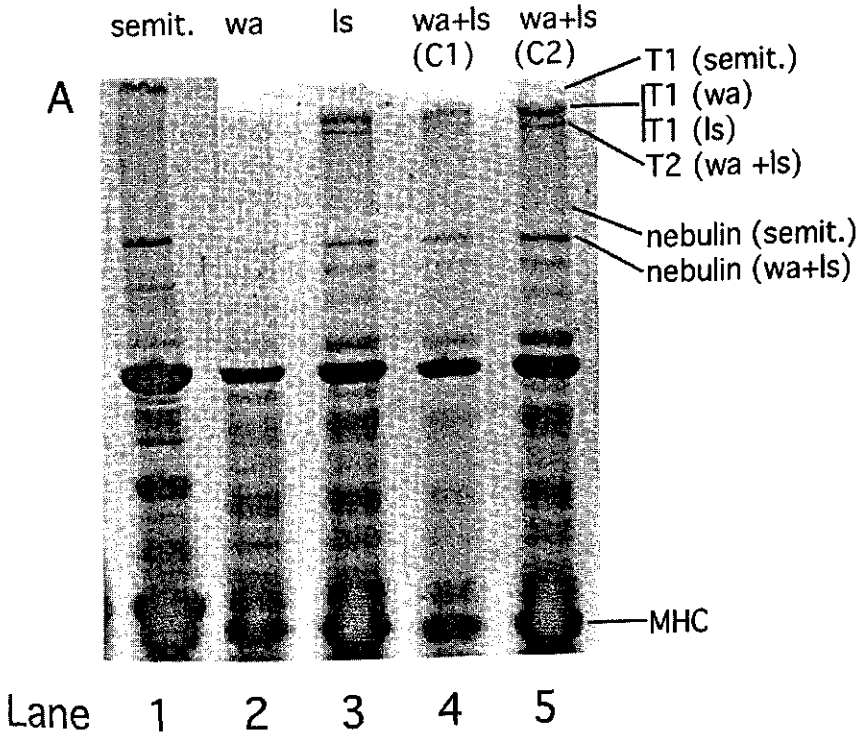
concentrated sample) than adult muscle T1. However, when higher concentrated mixed samples (C2) were loaded in a lane the difference between larval and adult muscle T1 seemed to be somewhat clearer in comparison to the lower concentrated mixed samples (C1). The distance from rabbit semitendinosus muscle T1 to carp adult muscle T1 was clearly smaller than its distance to larval muscle T1 (Fig. 4, compare lane 6 and 7).

Nebulin, which is thought to regulate thin filament length (Kruger *et al.*, 1991), of different adult carp muscle did not vary in mobility (Spierts *et al.*, 1997) but migrated further into the gel than that of rabbit semitendinosus muscle (Fig. 4, compare lane 1 and 2 and lane 9 and 10, and see Table 2). Nebulin of carp larvae muscle migrated slightly further into the gel than nebulin of adult carp muscle (Fig. 4, lane 3 and 4 and lane 7 and 8, and see Table 2), suggesting that carp larval thin filament length is slightly shorter than carp adult thin filament length (which is reported to be approximately 0.95 μm ; van Leeuwen *et al.*, 1990).

Table 2. Relative mobility of adult and larval carp skeletal muscle proteins and of rabbit semitendinosus muscle proteins. The migration distances were determined using video densitometry and normalised to nebulin of rabbit semitendinosus muscle, which was loaded in all lanes of the gels used to determine these migration distances. Adult carp muscle data are derived from Spierts *et al.* (1997).

Protein→ Muscle ↓	Titin T1	Titin T2	Nebulin
Adult carp red posterior	0.40		
red anterior	0.41	0.49	1.15
white posterior	0.42		
white anterior	0.43		
Larval carp	0.45	0.50	1.16
Rabbit semitendinosus	0.36		1.0

Fig. 5. Amplification of SDS-PAGE of fibre bundles. (A) Complete larval samples and adult white anterior muscle samples (smallest adult carp muscle T1 found) electrophoresed side by side (lane 2 and 3) or mixed in one lane at different concentrations (lane 4 and 5). Larval muscle T1 migrated a little further into the gel than adult white anterior muscle T1. (B) Complete larval samples and adult red posterior muscle samples (largest adult carp muscle T1 found) electrophoresed side by side (lane 2 and 3) or mixed in one lane at different concentrations (lane 4 and 5). Larval muscle T1 migrated further into the gel than adult red posterior muscle T1. semit., rabbit semitendinosus muscle; MHC, myosin heavy chain; Adult carp axial muscle: r, red; w, white; a, anterior; p, posterior. ls, complete carp larvae samples. Concentration (in μl) of the sample loaded in the lane: C1, low; C2, high. See text for further details.⇒



DISCUSSION

Although titin is an important constituent of muscle (approximately ten percent of the protein present in a muscle fibre) relatively little is known of the occurrence of different isoforms of titin. Its late discovery as an important constituent of muscle is caused by its extreme susceptibility to rapid post-mortem degradation. Throughout the ontogeny of species different isoforms are expected which may be highly relevant for a better understanding of muscle structure and function. During growth of fish from larva to adult large changes occur in swimming and the influence of friction on it, feeding and respiration, probably leading to a variety of spatially separated muscle zones with their own functions. Fish muscle therefore seems to be a promising model for such studies.

I studied presumed differences in titin isoforms of larval and adult carp muscle, in fibres that differ greatly in location (distance to and angle with respect to the body axis) and function. The relationship of these different titin isoforms with fast swimming and the subsequent maximum sarcomere strains will also be discussed.

Fish larvae muscle

Small fish (6.5-8 mm *TL*) are subject to a Reynolds-regime in the range of approximately 250-500 during fast swimming (approximately 5-8 bodylengths s^{-1}). In this Reynolds-range the influence of friction on swimming can not be neglected and the fish larvae are actually dragging water while swimming in it. These larvae therefore need to have special features to overcome friction during swimming. But what is the special equipment?

Fast swimming of small fish larvae is characterised by high frequency body curvatures and tail beats, which is explained as an adaptation to overcome the effects of friction. What are their tools to accomplish that? Red muscle fibres are thought to be mainly involved in the uptake and transfer of oxygen until the gills are fully developed (El-Fiky *et al.*, 1987; Hinterleitner *et al.*, 1987). In an experiment of El-Fiky *et al.* (1987) cytochrome oxidase (COX) was used as a semi-quantitative indicator of changes in the aerobic capacity of different muscle portions in Cyprinid larvae. A few days after hatching distinct COX activity was observed. It was not until 2 weeks after hatching before the anaerobic iso-enzyme of LDH (M4) was the strongest fraction in the electropherograms of total body homogenates. These findings led El-Fiky *et al.* (1987) to suggest that in the early stages of fish larvae swimming was almost entirely aerobic, being powered by the deeper mass of 'white' fibres. Small Cyprinid larvae at this stage do not show the sustained straightforward, burst-like, mode of swimming typical for older fish. The swimming behaviour of small Cyprinid larvae is at this stage however dominated by attempts to hold their position in the water and characterised by jerky and erratic fast movements which are always very brief and powered by the deep (aerobic) muscle mass. But even this swimming behaviour takes large amounts of power per unit mass. How do the inner muscles generate enough power to swim so fast?

Sarcomere strain

As initially the inner muscle fibres run almost parallel to the body axis without the complex three-dimensional folding pattern, as seen in adult fish, the strains these fibres are exposed to during fast swimming must be considerable. One limiting factor for very high strains is that these inner muscle fibres are situated very close to the body axis. This fact also accounts for the small differences in the mean sarcomere strain and the mean maximum sarcomere strain I found between red and white and between anterior and posterior fibres of carp larvae, a difference that becomes however larger in older fish. Although the mean maximum sarcomere strains I found for fast swimming carp larvae (approximately 20 %) was indeed considerable, it was not extremely high compared to the mean maximum strains of adult muscle fibres during fast-starts. In older fish the orientation of the fibres with respect to the body axis and the distance to the axis do become important for the maximum strain that occurs and for possible differences in maximum strain between various fibres. During fast-starts of adult carp indeed larger differences occurred in mean maximum sarcomere strains (compared to the maximum strains of carp larvae, as reported here), approximately 20 % anteriorly and posteriorly, 25 % for red fibres and 15 % for white fibres (see Spierts and van Leeuwen, 1999). But how exactly are these inner 'larval white' fibres, that mainly power larval swimming, able to generate enough power to overcome the friction effects and reach maximum sarcomere strains of approximately 20 % during fast swimming and velocities of over 20 bodylengths s⁻¹?

Titin in relation to larval swimming

Following an earlier suggestion by Spierts *et al.* (1997) that a close relation may exist between functional differences (in power generation for specific swimming movements) and sarcomere structure, I investigated the titin molecule in muscles of carp larvae and looked for a possible correlation with the strain findings. Wang *et al.* (1991) suggested that skeletal muscle cells may control and modulate elasticity and compliance and the elastic and stiffness limit of the sarcomere by selective expression of specific titin size isoforms. For larval and adult carp muscle this also seems to be the case in such a way that the titins of sarcomeres are adapted to the swimming behaviour the fish uses most. The titin isoforms of carp larvae appeared to be smaller than any titin isoform reported by Spierts *et al.* (1997) for adult carp muscle. They found different titin isoforms for different muscle types and within one muscle type of carp at different positions along the body axis. As continuous swimming is the most used swimming mode in time in adult carp, sarcomere strain during this cyclic swimming, and consequently the required stress for the production of a certain elastic strain, was hypothesised to be one of the functional variables modulating the expression of different titin isoforms in axial muscle fibres, thus reducing energy loss during the cyclic loading of muscle fibres. During fast-starts (a very inefficient mode of swimming) however Spierts and van Leeuwen (1999) calculated that adult carp anterior red muscle fibres reached a mean maximum sarcomere strain of 39 %. The passive tension required for such large strains was 20 kPa, of which 14 kPa was titin-based and 6 kPa was intermediate filament-based (Spierts *et al.*, 1997). So stretching red fibres in adult carp during fast-starts required a fair amount of tension compared to the maximum active tension that can

be generated by these muscle fibres when assuming they actively participate in power generation (approximately 150 kPa, Spierts and van Leeuwen, 1999). Fish larvae on the contrary swim most of their time very fast implying that an adapted titin molecule for reducing energy loss during slow continuous swimming is not very logical. As carp larvae muscle fibres possess smaller titin isoforms than adult muscle fibres the passive tension required for stretching their titin during fast swimming (for which they do not yet seem to have specialised muscles) is likely to be considerable compared to the maximum active tension that can be generated by larval muscles.

A smaller titin isoform has a shorter elastic segment in the I-band than a larger titin isoform (Horowitz, 1992; Granzier and Irving, 1995; Granzier *et al.*, 1996). As the strain of the elastic segment is the fundamental determinant of the amount of passive tension that will be developed (Fürst *et al.*, 1988; Wang *et al.*, 1991, 1993; Labeit and Kolmerer, 1995; Granzier *et al.*, 1996), it can be predicted that in larval carp muscle fibres the elastic titin segment should increase passive tension more steeply with increasing sarcomere length than is the case for adult carp muscle fibres (see Figs 2 and 3 in Spierts *et al.*, 1997). For the, mostly, fast swimming carp larvae this might work advantageous as the fibres at the convex side of the body axis are passively pre-stretched considerably by the activity of the fibres at the concave side of the body axis and consequently store elastic energy in their titin. The 'almost' parallel orientation of larval muscle fibres with respect to the body axis increases this effect. The elastic energy that is stored in titin during this pre-stretch is probably released in great extent in the shortening period of these fibres, as titin-based sarcomere length-passive tension curves show little hysteresis in this particular range of sarcomere lengthening (see e.g. Wang *et al.*, 1991). In this view contracting fibres at the concave side of the body axis generate positive power by their own contraction and simultaneously store elastic energy in the titins of the passively stretching fibres at the convex side. This energy however is only released in the opposite bending of the body. In this view the larvae fully use the stretching of titin during sarcomere lengthening of fibres at the convex side. Observation of carp larval swimming behaviour by analysing many films revealed that during fast swimming the initial frequency of a curvature wave along the body was much lower (1.5-2 times lower) than the second and following frequencies of curvatures. This finding supports the hypothesis that during fast swimming stretching titin in the initial bending also provides (stored) energy for the following bending, possibly resulting in a stronger frequency of body curvatures.

I hypothesise that there is a relation between the swimming mode mostly used by carp larvae, fast swimming, and the size of their titin isoforms. During fast swimming the small titin isoforms in carp larval muscle fibres store elastic energy in the initial bending of the body which is released in the following bending and hence may increase the elastic contribution to the tail beat. Further research however is required to quantify the energetic consequences of these features of muscle for swimming of small fish larvae.

ACKNOWLEDGEMENTS

I gratefully acknowledge Prof. Dr. J.W.M. Osse for valuable discussions, Dr. J.L. van Leeuwen for usage of the curvature and strain programmes and Mr. J. Samallo and Mr. H. Schipper for superb technical assistance. This work was made possible by the Netherlands Organisation for Scientific Research, Institution of Life Sciences.

REFERENCES

- ARNOLD, G.P. AND NUTTALL-SMITH, P.B.N. (1974). Shadow cinematography of fish larvae. *Mar. Biol.* **28**, 51-53.
- BRUTON, M.N. (1979). Breeding of *Clarias gariepinus*. *Trans. Zool. Soc. London* **35**, 7-45.
- EL-FIKY, N., HINTERLEITNER, S. AND WIESER, W. (1987). Differentiation of swimming muscles and gills, and development of anaerobic power in the larvae of Cyprinid fish (Pisces, Teleostei). *Zoomorph.* **107**, 126-132.
- FAIRBANKS, G., STECK, T.L. AND WALLACH, D.F.H. (1971). Electrophoretic analysis of the major polypeptides of the human erythrocyte membrane. *Electrophoresis* **10**, 2606-2617.
- FÜRST, D.O., OSBORNE, M., NAVE, R. AND WEBER, K. (1988). The organisation of titin filaments in the half-sarcomere revealed by monoclonal antibodies in immunoelectron microscopy: a map of ten nonrepetitive epitopes starting at the Z-line extends close to the M-line. *J. Cell. Biol.* **106**, 1563-1572.
- GERAUDIE, J. (1977). Initiation of the actinotrichial development in early fin bud of the fish, *Salmo*. *J. Morph.* **151**, 353-362.
- GERAUDIE, J. (1984). Fine structural comparative peculiarities of the developing dipnoan dermal skeleton in the fins of *Neoceratodus* larvae. *Anat. Rec.* **209**, 115-123.
- GERAUDIE, J. AND LANDIS, W.J. (1982). The fine structure of the developing pelvic fin dermal skeleton in trout, *Salmo gairdneri*. *Am. J. Anat.* **163**, 141-156.
- GRANZIER, H.L.M. AND WANG, K. (1993). Gel electrophoresis of giant proteins: Solubilization and silver-staining of titin and nebulin from single muscle fibre segments. *Electrophoresis* **14**, 56-64.
- GRANZIER, H.L.M., IRVING, T. (1995). Passive tension in cardiac muscle: the contribution of collagen, titin, microtubules and intermediate filaments. *Bioph. J.* **68**, 1027-1044.
- GRANZIER H.L.M., HELMES, M. AND TROMBITÁS, K. (1996). Nonuniform elasticity of titin in cardiac myocytes: a study using immunoelectron microscopy and cellular mechanics. *Bioph. J.* **70**, 430-442.
- HINTERLEITNER, S., PLATZER, U. AND WIESER, W. (1987). Development of the activities of oxidative, glycolytic and muscle enzyme during early larval life in three families of freshwater fish. *J. Fish Biol.* **30**, 315-326.
- HOROWITS, R. (1992). Passive force generation and titin isoforms in mammalian skeletal muscle. *Bioph. J.* **61**, 392-398.
- HOROWITS, R., KEMPNER, E.S., BISHOP, M. AND PODOLSKY, R.J. (1986). A physiological role for titin and nebulin in skeletal muscle. *Nature* **323**, 160-163.

- JOHNSTON, I.A., DAVISON, W. AND GOLDSPIK, G. (1977). Energy metabolism of carp swimming muscles. *J. Comp. Physiol.* **114**, 203-216.
- KRUGER, M., WRIGHT, J. AND WANG, K. (1991). Nebulin as a length regulator of thin filaments of vertebrate skeletal muscles: correlation of thin filament length, nebulin size, and epitope profile. *J. Cell Biol.* **115**, 97-107.
- LABBET, S. AND KOLMERER, B. (1995). Titins: giant proteins in charge of muscle ultrastructure and elasticity. *Science* **270**, 293-296.
- MARUYAMA, K. (1986). Connectin an elastic filamentous protein of striated muscle. *Int. Rev. Cytol.* **104**, 81-114.
- MARUYAMA, K. (1994). Connectin, an elastic protein of striated muscle. *Biophys. Chem.* **50**, 73-85.
- MOSER, H.G. (1996). *The early stages of fishes in the california current region*. California Cooperative Oceanic Fisheries Investigations, Atlas no. 33. Kansas: Allen Press, Inc. 1505 pp.
- OSSE, J.W.M. (1990). Form changes in fish larvae in relation to changing demands of function. *Neth. J. Zool.* **40**, 362-385.
- OSSE, J.W.M. AND BOOGAART, J.G.M. VAN DEN (1997). Size of flatfish larvae at transformation, functional demands and historical constraints. *J. Sea Res.* **37**, 229-239.
- ROHLF, F.J. AND SOKAL, R.R. (1981). *Statistical Tables*, second edition. New York: W.H. Freeman and Company. 219 pp.
- SHAPIRO S.S. AND WILK, M.B. (1965). An analysis of variance test for normality (complete samples). *Biometrika* **52**, 591-611.
- SOKAL, R.R. AND ROHLF, F.J. (1981). *Biometry*, second edition. New York: W.H. Freeman and Company. 859 pp.
- SPIERTS, I.L.Y., AKSTER H.A. AND GRANZIER, H.L. (1997). Expression of titin isoforms in red and white muscle fibres of carp (*Cyprinus carpio* L.) exposed to different sarcomere strains during swimming. *J. Comp. Physiol. B.* **167**, 229-239.
- SPIERTS, I.L.Y. AND VAN LEEUWEN, J.L. (1999). Kinematics and muscle dynamics of C- and S-starts of carp (*Cyprinus carpio* L.). *J. Exp. Biol.* **202** (4), 393-406.
- TRINICK, J. (1991). Elastic filaments and giant proteins in muscle. *Curr. Opin. Cell. Biol.* **3**, 112-118.
- VAN LEEUWEN, J.L., LANKHEET, M.J.M., AKSTER, H.A. AND OSSE, J.W.M. (1990). Function of red axial muscles of carp (*Cyprinus carpio*): recruitment and normalised power output during swimming in different modes. *J. Zool.* **220**, 123-145.
- WANG, K. (1985). Sarcomere associated cytoskeletal lattices in striated muscle. Review and hypothesis. In *Cell and Muscle Motility 6* (ed. J.W. Shay), pp 315-369. New York: Plenum Publ. Comp.
- WANG K., McCARTER R., WRIGHT J., BEVERLY J. AND RAMÍREZ-MITCHELL R. (1991). Regulation of skeletal muscle stiffness and elasticity by titin isoforms: a test of the segmental extension model of resting tension. *Proc. Natl. Acad. Sci. USA* **88**, 7101-7105.
- WANG K., McCARTER R., WRIGHT J., BEVERLY J. AND RAMÍREZ-MITCHELL R. (1993). Viscoelasticity of the sarcomere matrix of skeletal muscles. The titin-myosin composite is a dual-stage molecular spring. *Bioph. J.* **64**, 1161-1177.

Summary/Samenvatting

Igor L. Y. Spierts

Experimental Zoology Group, Wageningen Institute of Animal Sciences (WIAS), Wageningen
Agricultural University, Marijkeweg 40, 6709 PG Wageningen;
The Netherlands

Submitted to: The Netherlands Journal of Zoology.

SWIMMING AND MUSCLE STRUCTURE IN FISH

In this series of studies the relations between swimming behaviour of fish in general and extreme swimming responses in particular (called fast starts or escape responses) and the structure and ontogeny of the muscle system was investigated. Special attention was paid to relate functional differences between anterior and posterior parts of the axial myotomal muscles of fish to differences in their structural design. In the past considerable knowledge has been accumulated concerning the muscular system. There are however still many unsolved questions. What for example is the influence of swimming in different fish species on the ontogeny of their muscles. How is the development of the muscle system reflecting functional demands (e.g. strength of fibre, elastic properties etc.) and what is the relationship between muscle development on a molecular scale and a macro scale? These and other questions will partly be addressed in this study.

Initially the larval muscle system and its function was investigated in general as fish larvae swim in a different hydrodynamic environment, compared to adult fish, characterised by the importance of viscous forces which can not be neglected (Osse, 1990). In contrast to adults, the different muscles during the early stages of life of many fish species (e.g. *Rutilus rutilus*, *Alburnus alburnus*, *Leuciscus cephalus*, *Clupea harengus*, *Clarias gariepinus*) have an aerobic metabolism (El-Fiky *et al.*, 1987). In yolk-sac larvae of *Clarias gariepinus* for example, at a time when gill development is still insufficient and muscle rely for oxygen supply on diffusion through the body surface, both the superficial red muscle layer as well as the inner 'larval white' muscle mass are aerobic. The superficial red layer initially only consisted of a monolayer. At the moment the gills started to develop the superficial red layer acquired additional fibres along the horizontal septum, resulting in a double layer of red fibres at this location. The differences in metabolism between the red aerobic fibres and the white anaerobic fibres develop during the free-swimming larval stage of e.g. roach (*Rutilus rutilus*) and rainbow trout (*Salmo gairdneri*) and the adult pattern of muscle fibre type distribution emerges (Hinterleitner *et al.*, 1987). As this development probably occurs in relation to gill development, it is thought that the red layer of yolk-sac larvae has a negligible role in swimming but an important role in respiratory (El-Fiky *et al.*, 1987). Once the adult pattern of muscle fibre type distribution has developed the actual differences between the various muscles can be studied in great detail.

The effects of transmission of forces on the structure and function of different muscle fibre types and at different locations along the body axis were studied during swimming of adult carp (*Cyprinus carpio* L.). The connection between muscle fibres and collagen fibres, myotendinous junctions (MTJs), was investigated electron-microscopically. Especially during extreme swimming movements such as escape fast-starts large forces are imposed on the muscular system and mainly on the MTJs. During these life-saving swimming movements large sarcomere strains (relative to sarcomere slack length) occurred. Muscle fibres in the tail region (together with the connective tissue) play an important role in the transmission of force produced by more anterior fibres. Posterior fibres have a longer phase of eccentric activity (active while being stretched) than the anterior fibres and will therefore develop greater forces (van Leeuwen *et al.*, 1990; van Leeuwen, 1995). It was therefore expected that greater forces in these posterior fibres would be accompanied by stronger MTJs (a greater membrane amplification). Posterior (80 % of the fork length, *FL*) muscle fibres of carp indeed

had much larger myotendinous surface areas than anterior fibres (40 % FL) and consequently can transmit larger forces and 'bear' larger loads during swimming. Red muscle fibres of carp had a larger membrane amplification at the MTJs than white fibres. Red fibres are active at lower tail beat frequencies (longer cycle times) than white fibres and for longer periods of time, resulting in a longer duration of the load on the junction of red fibres. Tidball and Daniel (1986) proposed that the degree of membrane amplification at MTJs not only depends on the magnitude but also on the duration of load on the junction. Curtis (1961) and Rand (1964) showed that the mechanical behaviour of cell membranes is dependent on loading time. Cells can survive a certain shear load (caused by applying either a large load for a short time or a small load for a longer time) by reducing the stress on the membrane through an amplification of the membrane area. It was therefore suggested that the larger membrane amplification at the MTJs of carp red muscle fibres may be related to the longer duration of the load on the junction in this fibre type.

Not only the MTJs were subjected to large forces during fast-starts (accompanied by large strain fluctuations). High demands will also be imposed on the muscle system itself and the series elastic elements within the sarcomere unit, such as the titin filaments (Wang *et al.*, 1991). This may be reflected in the type and structure of the elastic elements as different isoforms of titin seem to exist (Wang *et al.*, 1991; Granzier and Wang, 1993a,b). To help elucidate the relation between the possible occurrence of different titin isoforms and the functional properties of different fibre types, the presence of different titin isoforms in red and white anterior and posterior fibres of the axial muscles of adult carp was investigated. Titin is a striated-muscle-specific giant muscle protein that spans the distance from the Z- and M-lines of the sarcomere (Wang, 1985; Maruyama, 1986, 1994; Trinick, 1991). The elastic segment of titin in the I-band is thought to function as a molecular spring that is responsible for maintaining the central positions of the thick filaments in contracting sarcomeres and develops passive tension upon sarcomere stretch (Horowitz *et al.*, 1986; Fürst *et al.* 1988; Wang *et al.*, 1991, 1993; Granzier *et al.*, 1996). Gel-electrophoresis of single fibres of carp revealed that the molecular mass of titin was larger in red than in white fibres. For both red and white fibres the molecular mass of titin was larger in posterior than in anterior muscle fibres. Thus depending on the fibre type and its location along the body axis different titin isoforms were expressed. Furthermore the contribution of titin to passive tension and stiffness of red anterior and red posterior fibres was determined in micro-mechanical experiments. It appeared that more passive tension and stiffness was needed to stretch fibres with smaller titin isoforms (red anterior fibres) to a certain sarcomere length than in fibres with larger titin isoforms (red posterior fibres). Continuous swimming is the most frequently used swimming mode in adult carp and is driven by the activity of red muscle. During this type of swimming sarcomere strain is larger in red muscle fibres, which have larger titin isoforms, than in the three-dimensionally folded white muscle tissue, due to differences in distance between the sarcomere and the body axis and differences in fibre arrangement between both types. As during cyclic swimming local curvature increases from anterior to posterior the sarcomere strain is consequently larger in posterior fibres, which have larger titin isoforms. The finding that exactly those fibres that are exposed to the largest sarcomere strains during continuous swimming also possessed the largest titin isoforms led to the suggestion that titin isoform and sarcomere strain are correlated in order to minimise energy loss during cyclic loading of muscle fibres.

Summary/Samenvatting

However, it was still unknown how large the maximum sarcomere strains actually were during the most extreme swimming responses of adult carp. Therefore a study on the kinematics and muscle dynamics of escape fast-starts of carp was conducted. Adult carp perform escape C- or S-starts, based on the typical body curvature of the fish during these movements. During the Mauthner initiated C-starts (Eaton *et al.*, 1977; Kimmel *et al.*, 1980) adult carp made a large angle of turn directed away from the stimulus (approximately 150°) with a high acceleration at 0.3 FL of up to 72 m s^{-2} . The maximum sarcomere strains (both anteriorly and posterior) were approximately 27 % for red fibres and approximately 16.5 % for white fibres. During escape S-starts however maximum strain in anterior fibres was more than twice that of posterior fibres with an angle of turn of approximately 70° . This large anterior peak curvature enabled the fish to control the direction of escape better but with lower accelerations at 0.3 FL (approximately 40 m s^{-2}). Little is known about the neuronal mechanisms controlling S-starts. The largest strains occurred in red anterior fibres during S-starts (39 %). It was found that during continuous and intermittent swimming the largest strains (red posterior fibres, approximately 5 %) occurred in fibres with the largest titin isoforms. This enabled these fibres to attain large strain amplitudes with relatively low passive tensions.

It was surprising to find that in all fast-starts both red and white muscle were simultaneously active at a given longitudinal location, whereas only red muscle were active during continuous swimming. Red fibres could contribute to muscle fibre shortening at the beginning of their mechanical response for a very short period of time (before the full response was reached). This implies that red fibres hence could contribute to force generation during these extremely fast swimming modes, although little. Red and white muscle at a given longitudinal location were not necessarily active synchronously and could be uncoupled during escape S-starts. In this way mechanically sub-optimal patterns of force generation can be avoided. Both anterior and posterior muscle were active whilst lengthening at certain moments during C- and S-starts. Muscle fibres that are active whilst lengthening in an escape response initially absorb power. This might work advantageous for the transmission of force from the fish to the water, because (1) the muscle fibres are already activated before the actual bending of the fish body sets in (an advantage in time) and (2) the actin-myosin bindings occur in a more optimal (concerning force production) part of the force-velocity curve (see also Franklin and Johnston, 1997, and Curtin and Woledge, 1996).

Fish larval swimming on the other hand is very different from adult swimming. Small carp larvae of approximately 6.5-8 mm total length are subjected to relatively low Reynolds-number regimes of approximately $200 \leq Re \leq 500$ and therefore require special features to overcome effects of friction. As superficial red fibres of Cyprinid larvae are mainly used as a respiratory organ (see earlier), larval swimming behaviour is mainly powered by the inner 'larval white' fibres (El-Fiky *et al.*, 1987). But how exactly are these inner 'larval white' fibres able to generate enough power to overcome these friction effects and reach velocities of over 20 bodylength s^{-1} ? As small carp larvae and adults show large differences in their swimming behaviour the sarcomere strain ranges during fast swimming of larvae were investigated, together with their size of titin. During fast swimming of carp larvae all muscle fibres showed maximum sarcomere strains of approximately 20 %, whereas their titin appeared to be shorter than any titin isoform found in adult muscle. Apparently the molecular structure of titin changed in the course of ontogeny. This shorter titin isoform (requiring larger stress for the

same strain, compared to a larger titin isoform) is thought (1) to help restricting form changes of the swimming larvae and (2) to increase the elastic contribution to the tail beat by elastic energy storage in this titin isoform during the initial bending that is subsequently released in the following bending. Such molecules possibly also increase the resonant frequency of the beating tail and thereby provide the required high frequency for swimming in a relatively low Reynolds-regime.

The present study corroborates the idea that strong relations exist between the structural design of the muscular system, from micro- to macro-level, and its functions, also in diverse levels, in a fish's specific habitat. Starting at a structural level, differences in muscle function during swimming of fish can be used in an effort to explain and possibly predict morphological differences between the various muscle types and even within the same muscle type.

ZWEMMEN EN SPIERSTRUCTUUR IN VISSSEN

In deze serie van studies zijn de relaties tussen het zwemgedrag van vissen in het algemeen en extreme zwemreacties in het bijzonder (de zogenaamde snelle starten) en de structuur en ontogenie van het spiersysteem onderzocht. Speciale aandacht werd besteed aan het relateren van functionele verschillen tussen anterior en posterior gelegen delen van de axiale myotomale spieren van vissen aan verschillen in hun structurele ontwerp. In het verleden is een aanzienlijke hoeveelheid kennis verzameld van het spiersysteem. Er blijven echter nog steeds vele onbeantwoorde vragen. Wat is bijvoorbeeld de invloed van het zwemmen van verschillende soorten vissen op de ontogenie van hun spieren? Hoe reflecteert de ontwikkeling van het spiersysteem functionele eisen (bijvoorbeeld de sterkte van een spiervezel en diens elastische eigenschappen, etc.) en wat is de relatie tussen spierontwikkeling op een microscopische dan wel macroscopische schaal? Deze en andere vragen zullen gedeeltelijk aan de orde komen in deze studie.

In eerste instantie werd het larvale spiersysteem en zijn functie in het algemeen onderzocht. Vislarven zwemmen in een andere hydrodynamische omgeving, vergeleken met adulte vissen, die gekarakteriseerd wordt door visceuse krachten die niet verwaarloosd kunnen worden (Osse, 1990). Spieren hebben tijdens de vroege levensstadia van vele vissoorten (bijvoorbeeld *Rutilus rutilus*, *Alburnus alburnus*, *Leuciscus cephalus*, *Clupea harengus*, *Clarias gariepinus*) een aërobe metabolisme, in tegenstelling tot adulte vissen (El-Fiky *et al.*, 1987). In bijvoorbeeld larven van *Clarias gariepinus* die nog een dooierzak bezitten zijn, op een moment dat de ontwikkeling van de kieuwen nog steeds onvoldoende is en spieren voor hun zuurstof behoefte voornamelijk afhankelijk zijn van diffusie door het lichaamsoppervlak, zowel de oppervlakkig gelegen rode spierlaag als de dieper gelegen 'larvale witte' spieren aërobe. De oppervlakkige gelegen rode spieren bestaat in eerste instantie uit een enkele laag cellen. Op het moment dat de kieuwen zich beginnen te ontwikkelen ontstaan nieuwe oppervlakkig gelegen rode spiervezels langs het horizontale septum, wat resulteert in een dubbele laag rode vezels op deze plek. De verschillen in metabolisme tussen de aërobe rode spieren en de anaërobe witte spieren ontstaan gedurende het stadium waarin vislarven vrij beginnen te zwemmen, zoals bijvoorbeeld bij de blankvoorn (*Rutilus rutilus*) en de regenboog forel (*Salmo gairdneri*), waarna het adulte patroon van de distributie van spiervezeltypen komt te voorschijn

(Hinterleitner *et al.*, 1987). Aangezien deze ontwikkeling waarschijnlijk optreedt in relatie tot de ontwikkeling van de kieuwen wordt verondersteld dat de rode spierlaag van vislarven die nog een dooierzak bezitten een verwaarloosbare rol heeft bij het zwemmen maar een belangrijke rol bij het ademen (El-Fiky *et al.*, 1987). Wanneer het adulte patroon van spiervezel distributie zich eenmaal ontwikkeld heeft kunnen de verschillen tussen de diverse spieren in detail bestudeerd worden.

De effecten van krachtoverdrachten op de structuur en functie van verschillende spiervezeltypen op verschillende plekken langs de lichaamsas werden bestudeerd in relatie tot het zwemmen van adulte karpers (*Cyprinus carpio* L.). De verbinding tussen spiervezels en collageenvezels, de zogenaamde spierpees-overgangen (SPO), werd electronen-microscopisch bestudeerd. Vooral tijdens zeer snelle zwembewegingen zoals ontsnapingsreacties worden grote krachten uitgeoefend op het spiersysteem en met name op de SPO. Gedurende deze levensreddende zwembewegingen worden de sarcomeren in grote mate gerekt (relatief ten opzichte van hun rustlengte). Spiervezels in de staartregio spelen (tezamen met het bindweefsel) een belangrijke rol in de transmissie van krachten die door de meer anterior gelegen spiervezels geproduceerd zijn. Posterior gelegen spiervezels hebben een langere fase van excentrische activiteit (activiteit terwijl ze rekken) dan de anterior gelegen spiervezels en zullen daarom grotere krachten ontwikkelen (van Leeuwen *et al.*, 1990; van Leeuwen, 1995). Er werd daarom verwacht dat deze grotere krachten in de posterior gelegen vezels gepaard zouden gaan met sterkere SPO (groter membraanoppervlak). Posterior gelegen spiervezels (op 80% van de vorklengte, *FL*) van karpers hadden inderdaad een groter membraanoppervlak op de SPO dan anterior gelegen spiervezels (40% *FL*) en kunnen daardoor grotere krachten overbrengen en ondergaan tijdens het zwemmen. Rode spiervezels van karpers hadden een groter membraanoppervlak op de SPO dan witte vezels. Rode vezels zijn actief tijdens lagere frequenties van de staartslag (langere duur van de cyclus) dan witte vezels en gedurende een langere periode. Dit resulteert in het feit dat de krachten die werken op de SPO van rode vezels langere aanhouden. Tidball en Daniel (1986) suggereerden dat de mate van oppervlaktevergroting van het membraan in SPO niet alleen afhankelijk is van de grootte maar ook van de duur van de krachten die werken op de verbinding. Curtis (1961) en Rand (1964) lieten zien dat het mechanisch gedrag van celmembranen afhankelijk is van de duur van de last. Cellen kunnen een bepaalde hoeveelheid afschuifkrachten overleven (veroorzaakt door een grote last gedurende een korte periode of een kleine last gedurende een langere periode aan te brengen) door de spanning op het membraan te reduceren via vergroting van het membraan oppervlak. Er werd daarom gesuggereerd dat het grotere membraanoppervlak in SPO van rode spiervezels van karpers gerelateerd zou kunnen zijn aan de langere duur van de last op de spier-pees verbinding in dit type spiervezel.

Niet alleen de SPO zijn onderhevig aan grote krachten tijdens de snelle starten van vissen (die gepaard gaan met grote fluctuaties in de rek van spiervezels). Er worden ook grote eisen gesteld aan het spiersysteem zelf en aan de serie elastische elementen binnen de sarcomeer eenheid, zoals de titine filamenten (Wang *et al.*, 1991). Aangezien er verschillende titine isoformen bestaan kunnen deze eisen ook gereflecteerd zijn in het type elastische elementen en in de structuur ervan (Wang *et al.*, 1991; Granzier en Wang, 1993a,b). Om de relatie tussen de mogelijke aanwezigheid van verschillende titine isoformen en de functionele eigenschappen van de diverse vezeltypen op te helderen werd de aanwezigheid van verschillende titine isoformen in rode en witte anterior en posterior gelegen vezels van de axiale spieren van karpers onderzocht. Titine is een zeer groot eiwit dat voorkomt in

dwarsgestreepte spieren en de afstand overbrugt tussen de Z- en de M-lijnen in een sarcomeer (Wang, 1985; Maruyama, 1986, 1994; Trinick, 1991). Er wordt verondersteld dat het elastische segment van titine in de I-band functioneert als een moleculaire veer die verantwoordelijk is voor het handhaven van de centrale positie van dikke filamenten in contraherende sarcomeren en die passieve spanning ontwikkelt tijdens sarcomeerrek (Horowitz *et al.*, 1986; Fürst *et al.* 1988; Wang *et al.*, 1991, 1993; Granzier *et al.*, 1996). Gel-electrophorese van individuele spiervezels van de karper bracht liet zien dat de moleculaire massa van titine groter was in rode dan in witte vezels. Voor zowel rode als witte vezels was de moleculaire massa van titine groter in posterior gelegen vezels dan in anterior gelegen spiervezels. Dus, afhankelijk van het type spiervezel en diens locatie langs de lichaamsas van de vis werden verschillende titine isoformen tot expressie gebracht. De bijdrage van titine aan de passieve spanning en stijfheid van rode anterior en posterior gelegen vezels werd ook bepaald door middel van micro-mechanische experimenten. Er bleek meer passieve spanning en stijfheid nodig te zijn om spiervezels met een klein titine isoform (rode anteriore vezels) tot een bepaalde sarcomeerlengte op te rekken dan spiervezels met een groter titine isoform (rode posterioere vezels). Continu zwemmen is de meest (in tijd) gebruikte zwemwijze van adulte karpers en wordt uitgevoerd door de activiteit van rode spieren. Tijdens dit continu zwemmen is de rek van de sarcomeren groter in rode spiervezels (die een groter titine isoform bezitten) dan in de drie-dimensionaal gevouwen witte spieren ten gevolge van verschillen tussen de beide spiervezeltypen in de afstand tussen het sarcomeer en de lichaamsas en in de wijze waarop de vezels gearrangeerd zijn. Omdat tijdens cyclisch zwemmen de lokale lichaamscurvatuur toeneemt van anterior naar posterior is de rek van posterior gelegen vezels groter, vezels die een groter titine isoform bezitten. Het feit dat precies die vezels die onderhevig zijn aan de grootste sarcomeerrekken tijdens continu zwemmen ook de grootste titine isoformen bezaten leidde tot de suggestie dat titine isoformen en sarcomeerrek zodanig gecorreleerd zijn dat de energieverliezen gedurende het cyclische belasten van spiervezels minimaal zullen zijn.

Het was echter nog steeds onbekend hoe groot de maximale sarcomeerrekken daadwerkelijk waren gedurende de meest extreme zwemwijzen van adulte karpers. Om deze vraag te beantwoorden werd daarom een studie naar de kinematica en spierdynamica van snel ontsnappende karpers uitgevoerd. Adulte karpers vertonen ofwel een C-start ofwel een S-start (gebaseerd op de typische lichaamskromming van de vis tijdens deze bewegingen) wanneer ze ontsnappen. Tijdens de Mauthner geïnitieerde C-starten (Eaton *et al.*, 1977; Kimmel *et al.*, 1980) draaien adulte karpers met een grote hoek (ongeveer 150°) weg van de stimulus met hoge versnellingen op $0.3 FL$ die kunnen oplopen tot 72 m s^{-2} . De maximale sarcomeerrek (zowel anterior als posterior) bedroeg ongeveer 27 % voor rode vezels en ongeveer 16.5 % voor witte vezels. Tijdens S-starten was de maximale sarcomeerrek echter meer dan twee keer zo groot in anteriore vezels dan in posterioere vezels en draaiden de karpers met een hoek van ongeveer 70° weg van de stimulus. Deze grotere anteriore curvatuur stelde de vis in staat om de richting waarin hij wegzwemt beter te kunnen controleren, echter met lagere versnellingen op $0.3 FL$ (ongeveer 40 m s^{-2}). Er is nog weinig bekend over het neurale mechanisme dat ten grondslag ligt aan deze S-starten. De grootste rekken traden op in rode anterior gelegen vezels tijdens S-starten (39 %). Tijdens continu en intermitterend zwemmen traden de grootste rekken (rode posterior gelegen vezels, ongeveer 5 %) op in vezels met de grootste titine isoformen. Deze vezels waren daardoor in staat om grote rekken te bereiken met relatief lage passieve spanningen.

Summary/Samenvatting

Het was opmerkelijk dat tijdens alle snelle starten zowel rode als witte spieren gelijktijdig actief waren op een bepaalde positie langs de lichaamsas van de vis, terwijl tijdens continu zwemmen enkel de rode spieren actief waren. Rode spieren konden aan het begin van hun mechanische reactie gedurende een erg korte periode een bijdrage leveren aan spierverkorting (voordat de volledige reactie bereikt was). Dit impliceert dat rode vezels daarom konden bijdragen aan krachtsproductie tijdens deze extreem snelle zwemwijzen, alhoewel gering. Rode en witte spieren op een bepaalde positie langs de lichaamsas van de vis waren niet noodzakelijkerwijs synchroon actief. Hun activiteiten konden losgekoppeld worden tijdens S-starten, waardoor mechanisch sub-optimale patronen van krachtsproductie vermeden kunnen worden. Op bepaalde momenten tijdens C- en S-starten waren zowel anterior als posterior gelegen spieren actief terwijl ze uitrekten. Spiervezels die tijdens een ontsnappingsreactie van een vis actief zijn terwijl ze uitrekken absorberen in eerste instantie vermogen. Dit kan gunstig zijn voor de transmissie van krachten van de vis op het water, omdat (1) de betreffende spiervezels al geactiveerd zijn voordat de eigenlijke buiging van het visselichaam inzet (een tijdsvoordeel dus) en (2) de actine-myosine bindingen plaatsvinden in een optimaler deel (voor wat betreft krachtsproductie) van de kracht-snelheids curve (zie ook Franklin en Johnston, 1997, en Curtin en Woledge, 1996).

Het zwemmen van vislarven echter is zeer verschillend van het zwemmen van adulte vissen. Kleine karperlarven van ongeveer 6.5-8 mm totale lengte zijn onderhevig aan relatief lage Reynolds-getal gebieden van ongeveer $200 \leq Re \leq 500$ en hebben daarom speciale kenmerken nodig om de effecten van wrijving te overwinnen. Het zwemmen van Cyprinid larven wordt voornamelijk uitgevoerd door de dieper gelegen 'larvale witte' spiervezels (El-Fiky *et al.*, 1987), aangezien de oppervlakkig gelegen rode spiervezels voornamelijk gebruikt worden als een ademhalingsorgaan (zie eerder). Maar hoe zijn deze dieper gelegen 'larvale witte' spiervezels precies in staat om genoeg vermogen te genereren om de effecten van wrijving te overwinnen en snelheden te bereiken van meer dan 20 lichaamslengten s^{-1} ? Aangezien larvale en adulte karpers grote verschillen vertonen in hun zwemgedrag werden de rekken van de sarcomeren tijdens snel zwemmen van deze larven onderzocht, tezamen met de grootte van hun titine. Tijdens het snel zwemmen van karperlarven vertoonden alle spiervezels maximale rekken van ongeveer 20 %, terwijl hun titine korten bleek te zijn dan welk titine isoform dan ook dat gevonden was in spieren van adulte karpers. Kennelijk veranderde de moleculaire structuur van titine gedurende de ontogenie. Verondersteld wordt dat dit kortere titine isoform (dat dus meer spanning vereist voor de zelfde hoeveelheid rek in vergelijking met een groter titine isoform) (1) de vormveranderingen van de zwemmende larve helpt te beperken en (2) de elastische bijdrage aan de staartslag vergroot door middel van opslag van elastische energie in dit titine isoform gedurende de initiële buiging welke vervolgens vrijkomt in de daaropvolgende buiging. Zo'n moleculen verhogen mogelijk ook de resonerende frequentie van de staartslag en dragen zo bij aan de vereiste hoge frequentie die nodig is voor het zwemmen in een relatief laag Reynolds-getal gebied.

de huidige studie bevestigt het idee dat er sterke relaties bestaan tussen het structurele ontwerp van het spiersysteem, van micro- tot macro-niveau, en diens functies, ook op diverse niveaus, in de specifieke omgeving van een vis. Startend op het structurele niveau kunnen verschillen in spierfunctie tijdens het zwemmen van vissen gebruikt worden in een poging om morfologische verschillen tussen diverse spiertypen en zelfs binnen hetzelfde spiertype te verklaren en mogelijk zelfs te voorspellen.

REFERENCES

- CURTIS, A.S.G. (1961). Timing mechanics in the specific adhesion of cells. *Exp. Cell Res.* **8**, S107-S122.
- CURTIN, N.A. AND WOLEDGE, R.C. (1996). Power at the expense of efficiency in contraction of white muscle fibres from dogfish *Scyliorhinus canicula*. *J. Exp. Biol.* **199**, 593-601.
- EATON, R.C., BOMBARDIERE, R.A. AND MEYER, D.L. (1977). The Mauthner-initiated startle response in teleost fish. *J. Exp. Biol.* **66**, 65-85.
- EL-FIKY, N., HINTERLEITNER, S. AND WIESER, W. (1987). Differentiation of swimming muscles and gills, and development of anaerobic power in the larvae of Cyprinid fish (Pisces, Teleostei). *Zoomorph.* **107**, 126-132.
- FRANKLIN, C.E. AND JOHNSTON, I.A. (1997). Muscle power output during escape responses in an antarctic fish. *J. Exp. Biol.* **200**, 703-712.
- FÜRST, D.O., OSBORNE, M., NAVE, R. AND WEBER, K. (1988). The organisation of titin filaments in the half-sarcomere revealed by monoclonal antibodies in immunoelectron microscopy: a map of ten nonrepetitive epitopes starting at the Z-line extends close to the M-line. *J. Cell. Biol.* **106**, 1563-1572.
- GRANZIER, H.L.M. AND WANG, K. (1993a). Gel electrophoresis of giant proteins: Solubilization and silver-staining of titin and nebulin from single muscle fibre segments. *Electrophoresis* **14**, 56-64.
- GRANZIER, H.L.M. AND WANG, K. (1993b). Passive tension and stiffness of vertebrate skeletal muscle and insect flight muscle: the contribution of weak crossbridges and elastic filaments. *Biophys. J.* **65**, 2141-2159.
- GRANZIER H.L.M., HELMES, M. AND TROMBITÁS, K. (1996). Nonuniform elasticity of titin in cardiac myocytes: a study using immunoelectron microscopy and cellular mechanics. *Bioph. J.* **70**, 430-442.
- HINTERLEITNER, S., PLATZER, U. AND WIESER, W. (1987). Development of the activities of oxidative, glycolytic and muscle enzyme during early larval life in three families of freshwater fish. *J. Fish Biol.* **30**, 315-326.
- HOROWITS, R., KEMPNER, E.S., BISHOP, M. AND PODOLSKY, R.J. (1986). A physiological role for titin and nebulin in skeletal muscle. *Nature* **323**, 160-163.
- KIMMEL, C.B., EATON, R.C. AND POWELL, S.L. (1980). Decreased fast-start performance of zebrafish larvae lacking Mauthner neurons. *J. Comp. Physiol.* **140**, 343-351.
- MARUYAMA, K. (1986). Connectin an elastic filamentous protein of striated muscle. *Int. Rev. Cytol.* **104**, 81-114.
- MARUYAMA, K. (1994). Connectin, an elastic protein of striated muscle. *Biophys. Chem.* **50**, 73-85.
- OSSE, J.W.M. (1990). Form changes in fish larvae in relation to changing demands of function. *Neth. J. Zool.* **40**, 362-385.
- RAND, R.P. (1964). Mechanical properties of the red cell membrane. II. Viscoelastic breakdown of the membrane. *Biophys. J.* **4**, 303.
- TIDBALL, J.G. AND DANIEL, T.L. (1986). Myotendinous junctions of tonic muscle cells: structure and loading. *Cell tissue Res.* **245**, 315-322.
- TRINICK, J. (1991). Elastic filaments and giant proteins in muscle. *Curr. Opin. Cell. Biol.* **3**, 112-118.
- VAN LEEUWEN, J.L. (1995). The action of muscles in swimming fish. *Exp. Physiol.* **80**, 177-191.

Summary/Samenvatting

- VAN LEEUWEN, J.L., LANKHEET, M.J.M., AKSTER, H.A. AND OSSE, J.W.M. (1990). Function of red axial muscles of carp (*Cyprinus carpio*): recruitment and normalised power output during swimming in different modes. *J. Zool.* **220**, 123-145.
- WANG, K. (1985). Sarcomere associated cytoskeletal lattices in striated muscle. Review and hypothesis. In *Cell and Muscle Motility 6* (ed. J.W. Shay), pp 315-369. New York: Plenum Publ. Comp.
- WANG, K., McCARTER, R., WRIGHT, J., BEVERLY, J. AND RAMÍREZ-MITCHELL, R. (1991). Regulation of skeletal muscle stiffness and elasticity by titin isoforms: a test of the segmental extension model of resting tension. *Proc. Natl. Acad. Sci. USA* **88**, 7101-7105.
- WANG, K., McCARTER, R., WRIGHT, J., BEVERLY, J. AND RAMÍREZ-MITCHELL, R. (1993). Viscoelasticity of the sarcomere matrix of skeletal muscles. The titin-myosin composite is a dual-stage molecular spring. *Bioph. J.* **64**, 1161-1177.

References

References

- A**HERNE, W.A. AND DUNNILL, M.S. (1982). *Morphometry*, 205 pp. London: E. Arnold Ltd.
- AKSTER, H.A. (1983). A comparative study of fibre type characteristics and terminal innervation in head and axial muscle of the carp (*Cyprinus carpio* L.): a histochemical and electron-microscopical study. *Neth. J. Zool.* **33**, 164-188.
- AKSTER, H.A. (1985). Morphometry of muscle fibre types in the carp (*Cyprinus carpio* L.): relationships between structural and contractile characteristics. *Cell Tissue Res.* **241**, 193-201.
- AKSTER, H.A. AND OSSE, J.W.M. (1978). Muscle fibres in head muscles of the perch *Perca fluviatilis* (L), Teleostei. A histochemical and electromyographical study. *Neth. J. Zool.* **28**, 94-110.
- AKSTER, H.A., GRANZIER, H.L.M. AND FOCANT, B. (1989). Differences in I-band structure, sarcomere extensibility and electrophoresis of titin between two muscle fibre types of the perch (*Perca fluviatilis* L.). *J. Ultrastruct. Res. Mol. Struct. Res.* **102**, 109-121.
- AKSTER, H.A., GRANZIER, H.L.M. AND KEURS, H.E.D.J. TER (1985). A comparison of quantitative ultrastructural and contractile characteristics of muscle fibre types of the perch, *Perca fluviatilis* L. *J. Comp. Physiol. B* **155**, 685-691.
- AKSTER, H.A., WAL, J.W. VAN DE AND VEENENDAAL, T. (1995). Interaction of force transmission and sarcomere assembly at the muscle-tendon junctions of carp (*Cyprinus carpio*): ultrastructure and distribution of titin (connectin) and α actinin. *Cell. Tissue Res.* **281**, 517-524.
- ALEXANDER, R. MCN. (1969). Orientation of muscle fibres in the myomeres of fish. *J. Mar. Biol. Assoc. UK* **49**: 263-290.
- ALEXANDER, R. MCN. (1975). *The chordates*, pp. 142-154. London: Cambridge University Press.
- ALEXANDER, R. MCN. (1978). *Fish swimming: size and shape related to energy consumption*. Proc. of the Zodiac Symposium on Adaptation, pp. 44-47. Wageningen: Pudoc Wageningen.
- ALEXANDER, R. MCN. AND GOLDSPIK G. (1977). *Mechanics and energetics of animal locomotion*, pp. 18-22. London: Chapman and Hall.
- ALTRINGHAM, J.D. AND JOHNSTON, I.A. (1990a). Modelling muscle power output in a swimming fish. *J. Exp. Biol.* **148**, 395-402.
- ALTRINGHAM, J.D. AND JOHNSTON, I.A. (1990b). Scaling effects in muscle function: power output of isolated fish muscle fibres performing oscillatory work. *J. Exp. Biol.* **151**, 453-467.
- ALTRINGHAM, J.D., WARDLE, C.S. AND SMITH, C.I. (1993). Myotomal muscle function at different locations in the body of a swimming fish. *J. Exp. Biol.* **182**, 191-206.
- ARMSTRONG, R.B. (1981). Recruitment of muscles and fibres within muscles in running animals. *Symp. Zool. Soc. Lond.* **48**, 289-304.
- ARNOLD, G.P. AND NUTTALL-SMITH., P.B.N. (1974). Shadow cinematography of fish larvae. *Mar. Biol.* **28**, 51-53.
- B**AINBRIDGE, R. (1958). The speed of swimming as related to size and to the frequency and amplitude of tail beat. *J. Exp. Biol.* **40**, 23-56.
- BATTY, R.S. (1984). Development of swimming movements and musculature of larval herring (*Clupea harengus*). *J. Exp. Biol.* **110**, 217-229.

- BERTIN, L. (1958). Modifications des nageoires. In *Traité de Zoologie*, tome XIII (ed. P.P. Grassé), pp. 710-747. Paris: Masson et Cie.
- BIKERMAN, J.J. (1968). Stresses in proper adhins. In *The science of adhesive joints*, second edition, pp. 192-263. New York, London: Academic Press.
- BLIGHT, A.R. (1977). The muscular control of vertebrate swimming movements. *Biol. Rev.* **52**, 181-218.
- BODDEKE, R., SLIJPER, E.J. AND STELT, A. VAN DER (1959). *Histological characteristics of the body musculature of fish in connection with their mode of life*, Proceedings, Series C, Vol. LXII, pp. 576-588. Koninklijke Nederlandse Akademie van Wetenschappen.
- BONE, Q. (1978). Locomotor muscle. In *Fish Physiology*, vol. VII. (ed. W.S. Hoar and D.J. Randall), pp. 361-424. New York: Academic Press.
- BONE, Q., MARSHALL, N.B. AND BLAXTER, J.H.S. (1995). *Biology of fish*, second edition. London: Chapman and Hall, 332 pp.
- BREDER, C.M. (1926). The locomotion of fish. *Zoologica* (NY) **4**, 159-297.
- BREMNER, H.A. AND HALLETT, I.C. (1985). Muscle fiber-connective tissue junctions in the fish blue grenadier (*Macruronus novaezelandiae*). A scanning electron microscopy study. *J. Food Sc.* **50**, 975-980.
- BRETT, J.R. (1964). The respiratory metabolism and swimming performance of young sockeye salmon. *J. Fish. Res. Bd. Can.* **21**, 1183.
- BRUTON, M.N. (1979). Breeding of *Clarias gariepinus*. *Trans. Zool Soc. London* **35**, 7-45.
- C**AMPBELL, N.A. (1996). *Biology*, fourth edition. New York: The Benjamin/Cummings Publishing Company, Inc. 1206 pp.
- CANFIELD, J.G. AND ROSE, G.J. (1993). Activation of Mauthner neurons during prey capture. *J. Comp. Physiol. A* **172**, 611-618.
- CAREY, F.G. AND TEAL, J.M. (1966). Heat conservation in tuna fish muscle. *Proc. Nat. Acad. Sci. U.S.A.* **56**, 1464-1469.
- CAREY, F.G. AND TEAL, J.M. (1969). Regulation of body temperature by the bluefin tuna. *Comp. Biochem. Physiol.* **28**, 205-213.
- CHILDRESS, S. (1981). *Mechanics of swimming and flying*. Cambridge: Cambridge University Press. 155 pp.
- COUGHLIN, D.J., VALDES L. AND ROME L.C. (1996). Muscle length changes during swimming in scup: sonomicrometry verifies the anatomical high-speed cine technique. *J. Exp. Biol.* **199**, 459-463.
- CURTIN, N.A. AND WOLEDGE, R.C. (1996). Power at the expense of efficiency in contraction of white muscle fibres from dogfish *Scyliorhinus canicula*. *J. Exp. Biol.* **199**, 593-601.
- CURTIS, A.S.G. (1961). Timing mechanics in the specific adhesion of cells. *Exp. Cell Res.* **8**, S107-S122.

DANIEL, T.L. (1984). Unsteady aspects of aquatic locomotion. *Amer. Zool.* **24**, 121-134.

References

- DAVIES, L.F., JOHNSTON, I.A. AND WAL, J.W. VAN DE (1995). Muscle fibres in rostral and caudal myotomes of the Atlantic cod (*Gadus morhua* L.) have different mechanical properties. *Physiol. Zool.* **68**, 673-697.
- DE BOOR, C. (1978). *A Practical Guide to Splines*. Berlin: Springer.
- DEHOFF, R.T. AND RHINES, F.N. (1968). *Quantitative microscopy*. New York: McGraw-Hill. 422 pp.
- DICKINSON, M.H. (1996). Unsteady mechanisms of force generation in aquatic and aerial locomotion. *Amer. Zool.* **36**, 537-554.
- DOMENICI, P. AND BATTY, R.S. (1994). Escape manoeuvres of schooling *Clupea harengus*. *J. Fish Biol.* **45**, (Suppl. A): 97-110.
- DOMENICI, P. AND BLAKE, R.W. (1991). The kinematics and performance of the escape response in the angelfish (*Pterophyllum eimekei*). *J. Exp. Biol.* **156**, 187-205.
- DOMENICI, P. AND BLAKE, R.W. (1993a). Escape trajectories in angelfish (*Pterophyllum eimekei*). *J. Exp. Biol.* **177**, 253-272.
- DOMENICI, P. AND BLAKE, R.W. (1993b). The effect of size on the kinematics and performance of angelfish (*Pterophyllum eimekei*) escape responses. *Can. J. Zool.* **71**, 2319-2326.
- DOMENICI, P. AND BLAKE, R.W. (1997). Review. The kinematics and performance of fish fast-start swimming. *J. Exp. Biol.* **200**, 1165-1178.
- DOS REMEDIOS, C.G. AND GILMOUR, D. (1978). Is there a third type of filament in striated muscles? *J. Biochem. (Tokyo)* **84**, 235-238.
- DROST, M.R. AND BOOGAART, J.G.M. VAN DEN (1986). The energetics of feeding strikes in larval carp, *Cyprinus carpio* L. *J. Fish Biol.* **29**, 371-379.

- E**ATON, R.C., BOMBARDIERE, R.A. AND MEYER, D.L. (1977). The Mauthner-initiated startle response in teleost fish. *J. Exp. Biol.* **66**, 65-85.
- EATON, R.C., NISSANOV, J. AND DIDOMENICO, R. (1991). The role of the Mauthner cell in sensimotor integration by the brainstem escape network. *Brain Behav. Evol.* **37**, 272-285.
- EISENBERG, B.R. (1983). Quantitative ultrastructure of mammalian skeletal muscle. In *Handbook of Physiology*, section 10 (ed. L.D. Peachey and R.H. Adrian), pp. 73-112. Bethesda, MD: American Physiological Society.
- EISENBERG, B.R. AND MILTON, R.L. (1984). Muscle fibre termination at the tendon in the frog's sartorius: A stereological study. *Am. J. Anat.* **171**, 273-284.
- EL-FIKY, N., HINTERLEITNER, S. AND WIESER, W. (1987). Differentiation of swimming muscles and gills, and development of anaerobic power in the larvae of Cyprinid fish (Pisces, Teleostei). *Zoomorph.* **107**, 126-132.

- F**AIRBANKS, G., STECK, T.L. AND WALLACH, D.F.H. (1971). Electrophoretic analysis of the major polypeptides of the human erythrocyte membrane. *Electrophoresis* **10**, 2606-2617.
- FETCHO, J.R. (1986). The organisation of the motoneurons innervating the axial musculature of vertebrates. I. Goldfish (*Carassius auratus*) and mudpuppies (*Necturus maculosus*). *J. Comp. Neurol.* **249**, 521-550.

- FETCHO, J.R. (1991). Spinal network of the Mauthner cell. *Brain Behav. Evol.* **37**, 298-316.
- FRANKLIN, C.E. AND JOHNSTON, I.A. (1997). Muscle power output during escape responses in an antarctic fish. *J. Exp. Biol.* **200**, 703-712.
- FRITH, H.R. AND BLAKE, R.W. (1991). Mechanisms in the startle response in the northern pike, *Esox lucius*. *Can. J. Zool.* **69**, 2831-2839.
- FÜRST, D.O., OSBORNE M., NAVE R. AND WEBER K. (1988). The organisation of titin filaments in the half-sarcomere revealed by monoclonal antibodies in immunoelectron microscopy: a map of ten nonrepetitive epitopes starting at the Z-line extends close to the M-line. *J. Cell. Biol.* **106**, 1563-1572.
- G**EEERLINK, P.J. (1983). Pectoral fin kinematics of *Coris formosa* (Teleostei, Labridae). *Neth. J. Zool.* **33**, 515-531.
- GEERLINK, P.J. (1986). *Pectoral fins, aspects of propulsion and breaking in Teleost fish*, Thesis. Groningen: University of Groningen. 154 pp.
- GERAUDIE, J. (1977). Initiation of the actinotrichial development in early fin bud of the fish, *Salmo*. *J. Morph.* **151**, 353-362.
- GERAUDIE, J. (1984). Fine structural comparative peculiarities of the developing dipnoan dermal skeleton in the fins of *Neoceratodus* larvae. *Anat. Rec.* **209**, 115-123.
- GERAUDIE, J. AND LANDIS, W.J. (1982). The fine structure of the developing pelvic fin dermal skeleton in trout, *Salmo gairdneri*. *Am. J. Anat.* **163**, 141-156.
- GRANZIER, H.L.M. AND IRVING, T. (1995). Passive tension in cardiac muscle: the contribution of collagen, titin, microtubules and intermediate filaments. *Biophys. J.* **68**, 1027-1044.
- GRANZIER, H.L.M. AND WANG, K. (1993a). Gel electrophoresis of giant proteins: Solubilization and silver-staining of titin and nebulin from single muscle fibre segments. *Electrophoresis* **14**, 56-64.
- GRANZIER, H.L.M. AND WANG, K. (1993b). Passive tension and stiffness of vertebrate skeletal muscle and insect flight muscle: the contribution of weak crossbridges and elastic filaments. *Biophys. J.* **65**, 2141-2159.
- GRANZIER, H.L.M., AKSTER, H.A. AND KEURS, H.E.D.J. TER (1991). Effect of filament length on the force-sarcomere length relation of skeletal muscle. *Am. J. Physiol.* **260**, C1060-C1070.
- GRANZIER, H.L.M., HELMES, M. AND TROMBITÁS, K. (1996). Nonuniform elasticity of titin in cardiac myocytes: a study using immunoelectron microscopy and cellular mechanics. *Biophys. J.* **70**, 430-442.
- GRANZIER, H.L.M., WIERSMA, J., AKSTER, H.A. AND OSSE, J.W.M. (1983). Contractile properties of a white- and a red-fibre type of the m. hyohyoideus of the carp (*Cyprinus carpio* L.). *J. Comp. Physiol.* **149**, 441-449.
- GRAY, J. (1933). Studies in animal locomotion I. The movement of fish with special reference to the eel. *J. Exp. Biol.* **10**, 88-104.
- GRILLNER, S. (1981). Control of locomotion in bipeds, tetrapods, and fish. In *Handbook of Physiology*, section 1, vol. II, Motor Control, part 2 (ed. V.B. Brooks), pp 1179-1236. Bethesda, MD, USA: American Physiological Society.

References

- H**ALLETT, I.C. AND BREMNER, H.A. (1988). Fine structure of the myocommata-muscle fibre junction in hoki (*Macruronus novaezelandiae*). *J. Sc. Food Agric.* **44**, 245-261.
- HANAK, H. AND BÖCK, P. (1971). Die Feinstruktur de Muskel-Sehnverbindung von Skelett- und Herzmuskel. *J. Ultrastruct. Res.* **36**, 68-85.
- HARPER, D.G. AND BLAKE, R.W. (1990). Fast-start performance of rainbow trout *Salmo gairdneri* and northern pike *Esox lucius*. *J. Exp. Biol.* **150**, 321-342.
- HENNEMAN, E., SOMJEN, G. AND CARPENTER, D.O. (1965). Functional significance of cell size in spinal motoneurons. *J. Neurophysiol.* **28**, 560-580.
- HERTEL, H. (1966). *Structure, form and movement*. New York: Reinhold Publishing Corp. 251 pp.
- HESS, F. AND VIDELER, J.J. (1984). Fast continuous swimming of saithe (*Pollachius virens*): A dynamic analysis of bending movements and muscle power. *J. Exp. Biol.* **109**, 229-251.
- HIGGINS, P.J. AND THORPE, J.E. (1990). Hyperplasia and hypertrophy in the growth of skeletal muscle in juvenile Atlantic salmon *Salmo salar* L. *J. Fish Biol.* **37**, 505-519.
- HILL, A.V. (1938). The heat of shortening and the dynamic constants of muscle. *Proc. R. Soc. Lond. B* **126**, 136-195.
- HINTERLEITNER, S., PLATZER, U. AND WIESER, W. (1987). Development of the activities of oxidative, glycolytic and muscle enzyme during early larval life in three families of freshwater fish. *J. Fish Biol.* **30**, 315-326.
- HOOGLAND, R. MORRIS, D. AND TINBERGEN, N. (1956). The spines of sticklebacks (*Gasterosteus* and *Pygosteus*) as a means of defence against predators (*Perca* and *Esox*). *Behaviour* **10**, 205-236.
- HOROWITS, R. (1992). Passive force generation and titin isoforms in mammalian skeletal muscle. *Bioph. J.* **61**, 392-398.
- HOROWITS, R., KEMPNER, E.S., BISHOP, M. AND PODOLSKY, R.J. (1986). A physiological role for titin and nebulin in skeletal muscle. *Nature* **323**, 160-163.
- HUDSON, R.C.L. (1973). On the function of white muscles in teleosts at intermediate swimming speeds. *J. Exp. Biol.* **58**, 509-522.
- I**SHIKAWA, H., SAWADA, H. AND YAMADA, E. (1983). Surface and internal morphology of skeletal muscle. In *Handbook of Physiology* (ed. L.D. Peachey and R.H. Adrian), pp. 1-21. Bethesda, MD: American Physiological Society.
- J**AYNE, B.C. AND LAUDER, G.V. (1993). Red and white muscle activity and kinematics of the escape response of the bluegill sunfish during swimming. *J. Comp. Physiol. A* **173**, 495-508.
- JAYNE, B.C. AND LAUDER, G.V. (1994). How swimming fish use slow and fast muscle fibers: implications for models of vertebrate muscle recruitment. *J. Comp. Physiol. A* **175**, 123-131.
- JAYNE, B.C. AND LAUDER, G.V. (1995). Red muscle motor patterns during steady swimming in largemouth bass: effects of speed and correlation's with axial kinematics. *J. Exp. Biol.* **198**, 1575-1587.

- JOHNSTON, I.A., DAVISON, W. AND GOLDSPINK, G. (1977). Energy metabolism of carp swimming muscles. *J. Comp. Physiol.* **114**, 203-216.
- JOHNSTON, I.A., FRANKLIN, C.E. AND JOHNSON, T.P. (1993). Recruitment patterns and contractile properties of fast muscle fibres isolated from rostral and caudal myotomes of the short-horned sculpin. *J. Exp. Biol.* **185**, 251-265.
- JOHNSTON, I.A., SIDELL, B.D. AND DRIEDZIC, W.R. (1985). Force-velocity characteristics and metabolism of carp muscle fibres following temperature acclimation. *J. Exp. Biol.* **119**, 239-249.
- JOHNSTON, I.A., WARD, P. AND GOLDSPINK, G. (1975). Studies on the swimming musculature on the rainbow trout. I. Fibre types. *J. Fish. Biol.* **7**, 451-458.
- JOHNSTON, I.A., LEEUWEN, J.L. VAN, DAVIES, M.L.F. AND BEDDOW, T. (1995). How fish power predation fast-starts. *J. Exp. Biol.* **198**, 1851-1861.
- JOHNSTON, I.A., PATTERSON, S., WARD, P. AND GOLDSPINK, G. (1974). The histochemical demonstration of microfibrillar adenosine triphosphatase activity in fish muscle. *Can. J. Zool.* **52**, 871-877.
- K**ANNUS, P., JOZSA, L., KVIST, M., LEHTO, M. AND JÄRVINEN, M. (1992). The effect of immobilisation on myotendinous junction: an ultrastructural, histochemical and immunohistochemical study. *Acta Physiol. Scand.* **144**, 387-394.
- KARNOVSKY, M.J. (1965). A formaldehyde glutaraldehyde fixative of high osmolality for use in electronmicroscopy. *J. Cell Biol.* **27**, 137A-138A.
- KASAPI, M.A., DOMENICI, P., BLAKE, R.W. AND HARPER, D. (1993). The kinematics and performance of escape responses of the knifefish *Xenomystus nigri*. *Can. J. Zool.* **71**, 189-195.
- KASHIN, S.M. AND SMOLYANINOV, V.V. (1969a). Concerning the geometry of fish trunk muscles. *J. Ichthyol.* (Engl. Transl. Vopr. Ikhti.) **9**, 923-925.
- KASHIN, S.M. AND SMOLYANINOV, V.V. (1969b). On the question of the geometrical arrangement of body muscles in fish. *J. Ichthyol.* (Engl. Transl. Vopr. Ikhti.) **9**, 1139-1142.
- KASHIN, S.M., FELDMAN, A.G. AND ORLOVSKY, G.N. (1979). Different modes of swimming in the carp, *Cyprinus carpio* L. *J. Fish Biol.* **14**, 403-405.
- KELLERMAYER, M.S.Z., SMITH, S.B., GRANZIER, H.L. AND BUSTAMANTA, C. (1997). Folding-unfolding transitions in single titin molecules characterised with laser tweezers. *Science* **276**, 112-116.
- KIMMEL, C.B., EATON, R.C. AND POWELL, S.L. (1980). Decreased fast-start performance of zebrafish larvae lacking Mauthner neurons. *J. Comp. Physiol.* **140**, 343-351.
- KORNELIUSSEN, H. (1973). Ultrastructure of myotendinous junctions in myxine and rat. Specializations between the plasma membrane and the lamina densa. *J. Anat. Entwickl. Gesch.* **142**, 91-101.
- KRUGER, M., WRIGHT, J. AND WANG, K. (1991). Nebulin as a length regulator of thin filaments of vertebrate skeletal muscles: correlation of thin filament length, nebulin size, and epitope profile. *J. Cell Biol.* **115**, 97-107.

LABEIT, S. AND KOLMERER, B. (1995). Titins: giant proteins in charge of muscle ultrastructure and elasticity. *Science* **270**, 293-296.

References

- LAZARIDES, E. (1982). Intermediate filaments: a chemically heterogeneous, developmentally regulated class of proteins. *Annu. Rev. Biochem.* **51**, 219-250.
- LIGHTHILL, M.J. (1971). Large-amplitude elongated-body theory of fish locomotion. *Proc. R. Soc. Lond.* **179B**, 125-138.
- LINDSEY, C.C. (1978). Form, function and locomotory habitats in fish. In *Fish Physiology*, vol. VII (ed. W.S. Hoar and D.J. Randall), pp. 1-100. London: Academic Press.
- LINKE, W.A., IVEMEYER, M., OLIVIERI, N., KOLMERER, B., RUEGG, J.C. AND LABETT, S. (1996). Towards a molecular understanding of the elasticity of titin. *J. Mol. Biol.* **261**, 62-71.
- LIPSCHUTZ, M.M. (1969). *Theory and Problems of Differential Geometry. Schaum's Outline Series.* New York: McGraw-Hill. 269 pp.
- LUBKIN, J.L. (1957). A theory of adhesive scarf joints. *J. Appl. Mech.* **24**, 255-260.

- M**ARUYAMA, K. (1986). Connectin an elastic filamentous protein of striated muscle. *Int. Rev. Cytol.* **104**, 81-114.
- MARUYAMA, K. (1994). Connectin, an elastic protein of striated muscle. *Biophys. Chem.* **50**, 73-85.
- MERZ, W.A. (1967). Die Streckenmessung an gerichteten Strukturen im Mikroskop und ihre Anwendung zur Bestimmung von Oberflächen-Volumen-Relationen im Knochengewebe. *Mikroskope.* **22**, 132.
- MOSER, H.G. (1996). *The early stages of fishes in the california current region.* California Cooperative Oceanic Fisheries Investigations, Atlas no. 33. Kansas: Allen Press, Inc. 1505 pp.

- N**ACHLAS, M.M., TSOU, K.-C., SOUZA, E. DE, CHENG, C.-S. AND SELIGMAN, A.M. (1957). Cytochemical demonstration of succinic dehydrogenase by the use of a new p-nitrophenyl substituted ditetrazole. *J. Histochem. Cytochem.* **5**, 420-436.
- NAG, A.C. AND NURSALL, J.R. (1972). Histogenesis of white and red muscle fibres of trunk muscles of a fish *Salmo gairdneri*. *Cytobios.* **6**, 227-246.
- NELSON, J.S. (1994). *Fish of the world*, third edition. New York: John Wiley and Sons. 600 pp.
- NIJSSSEN, H. AND GROOT, S.J. DE (1987). *De vissen van Nederland.* Utrecht: Stichting Uitgeverij van de Koninklijke Nederlandse Natuurhistorische Vereniging. 224 pp.

- O**SSE, J.W.M. (1969). Functional morphology of the head of the perch (*Perca fluviatilis* L.): an electromyographic study. *Neth. J. Zool.* **19**, 289-392.
- OSSE, J.W.M. (1990). Form changes in fish larvae in relation to changing demands of function. *Neth. J. Zool.* **40**, 362-385.
- OSSE, J.W.M. AND BOOGAART, J.G.M. VAN DEN (1997). Size of flatfish larvae at transformation, functional demands and historical constraints. *J. Sea Res.* **37**, 229-239.
- OSSE, J.W.M. AND DROST, M.R. (1989). Hydrodynamics and mechanics of fish larvae. *Pol. Arch. Hydrobiol.* **36**, 455-465.
- OSSE, J.W.M., OLDENHAVE, M. AND SCHIE, B. VAN (1972). A new method for insertion of wire

- electrodes in electromyography. *Electromyography* **12**, 59-62.
- P**AGE, S.G. AND HUXLEY, H.E. (1963). Filament lengths in striated muscle. *J. Cell Biol.* **19**, 369-390.
- PRICE, M. (1984). Molecular analysis of intermediate filament cytoskeleton--a putative load bearing structure. *Am. J. Physiol.* **246**, H566-H572.
- PRICE, M.G. AND SANGER, J.W. (1983). Intermediate filaments in striated muscle. A review of structural studies in embryonic and adult skeletal and cardiac muscle. In *Cell and muscle motility*, vol. 3. (ed. R.M. Dowben and J.W. Shay), pp. 1-40. New York: Plenum Press.
- PROCTOR, C., MOSSE, P.R.L. AND HUDSON, R.C.L. (1980). A histochemical and ultrastructural study of the development of the propulsive musculature of the brown trout, *Salmo trutta* L., in relation to its swimming behaviour. *J. Fish Biol.* **16**, 309-329.
- R**AND, R.P. (1964). Mechanical properties of the red cell membrane. II. Viscoelastic breakdown of the membrane. *Biophys. J.* **4**, 303.
- RAYNER, J.M.V. (1985). Vorticity and propulsion mechanics in swimming and flying vertebrates. In *Principles of construction in fossil and recent reptiles*, Konzepte SFB 230 Heft 4, pp. 89-118.
- RICHTER, C.J.J., EDING, E.J., VERRETH, J.A.J. AND FLEUREN, W.L.G. (1995). African catfish *Clarias gariepinus*. In *Broodstock Management and Egg and Larval Quality* (ed. N.R. Bromage and R.J. Roberts), pp. 242-276. Oxford, London: Blackwell Science.
- ROHLF, F.J. AND SOKAL, R.R. (1981). *Statistical tables*, second edition. New York: W.H. Freeman and Company. 219 pp.
- ROME, L.C. AND SOSNICKI, A.A. (1991). Myofilament overlap in swimming carp. II. Sarcomere length changes during swimming. *Am. Physiol. Soc.* **260**, 289-296.
- ROME, L.C., SWANK, D. AND CORDA, D. (1993). How fish power swimming. *Science*. **261**, 340-343.
- ROME, L.C., FUNKE, R.P., ALEXANDER, R. MCN., LUTZ, G., ALDRIDGE, H., SCOTT, F. AND FREADMAN, M. (1988). Why animals have different muscle fibre types. *Nature* **335**: 824-827.
- ROMEIS, B. (1968). *Mikroskopische Technik*, 16e edition. München: Oldenbourg Verlag. 757 pp.
- ROYET, J.P. (1991). Stereology: A method for analysing images. *Prog. Neurobiol.* **37**, 433-474.
- S**CAPOLO, P.A., VEGETTI, A., MASCARELLO, F. AND ROMANELLO, M.G. (1988). Developmental transitions of myosin isoforms and organisation of the lateral muscle in the teleost *Dicentrarchus labrax* (L.). *Anat. Embryol.* **178**, 287-295.
- SCHATTENBERG, P.J. (1973). Licht- und elektronenmikroskopische Untersuchungen über die Entstehung der Skelettmuskulatur von Fischen. *Z. Zellforsch. Mikrosk. Anat.* **143**, 569-586.
- SCHIAFFINO, S. AND REGGIANI, C. (1996). Molecular diversity of myofibrillar proteins: gene regulation and functional significance. *Physiol. Rev.* **76**, 371-409.
- SHAPIRO S.S. AND WILK, M.B. (1965). An analysis of variance test for normality (complete samples). *Biometrika* **52**, 591-611.
- SOKAL, R.R. AND ROHLF, F.J. (1981). *Biometry*, second edition. New York: W.H. Freeman and Company. 859 pp.

References

- SOSNICKI, A.A., LOESSER, K.E. AND ROME, L.C. (1991). Myofilament overlap in swimming carp I. Myofilament lengths of red and white muscles. *Am. J. Physiol.* **260** (Cell Physiol 29), C283-C288.
- SPIERTS, I.L.Y. AND LEEUWEN, J.L. VAN (1999). Kinematics and muscle dynamics of C- and S-starts of carp (*Cyprinus carpio* L.). *J. Exp. Biol.* **202** (4), 393-406.
- SPIERTS, I.L.Y., AKSTER H.A. AND GRANZIER, H.L. (1997). Expression of titin isoforms in red and white muscle fibres of carp (*Cyprinus carpio* L.) exposed to different sarcomere strains during swimming. *J. Comp. Physiol. B.*, **167** 543-551.
- SPIERTS, I.L.Y., AKSTER, H.A., VOS, I.H.C. AND OSSE, J.W.M. (1996). Local differences in myotendinous junctions in axial muscle fibres of carp (*Cyprinus carpio* L.). *J. Exp. Biol.* **199**, 825-833.
- STICKLAND, N.C., WHITE, R.N., MESCALL, P.E., CROOK, A.R. AND THORPE, J.E. (1988). The effect of temperature on myogenesis in embryonic development of the Atlantic salmon (*Salmo salar* L.). *Anat. Embryol.* **178**, 253-257.
- STREET, S.F. (1983). Lateral transmission of tension in frog myofibres: a myofibrillar network and transverse cytoskeletal connections are possible transmitters. *J. Cell. Physiol.* **114**, 346-364.
- SYMMONS, S. (1979). Notochordal and elastic components of the axial skeleton of fish and their function in locomotion. *J. Zool. Lond.* **189**, 157-206.
- T**IDBALL, J.G. (1983). The geometry of actin filament-membrane associations can modify adhesive strength of the myotendinous junction. *Cell Motil.* **3**, 439-447.
- TIDBALL, J.G. (1984). Myotendinous junctions: morphological changes and mechanical failure associated with muscle cell atrophy. *Exp. Mol. Path.* **40**, 1-12.
- TIDBALL, J.G. AND CHAN, M. (1989). Adhesive strength of single muscle cells to basement membrane at myotendinous junctions. *J. Appl. Physiol.* **67**, 1063-1069.
- TIDBALL, J.G. AND DANIEL, T.L. (1986). Myotendinous junctions of tonic muscle cells: structure and loading. *Cell tissue Res.* **245**, 315-322.
- TIDBALL, J.G. AND QUAN, D.M. (1992). Reduction in myotendinous junction surface area of rats subjected to 4-day spaceflight. *J. Appl. Physiol.* **73**, 59-64.
- TRINICK, J. (1991). Elastic filaments and giant proteins in muscle. *Curr. Opin. Cell. Biol.* **3**, 112-118.
- TROMBITÁS, K., JIN, J.P. AND GRANZIER, H. (1995). The mechanically active domain of titin in cardiac muscle. *Circ. Research* **77**(4), 856-861.
- TROTTER, J.A. (1990). Interfiber tension transmission in series-fibered muscles of the cat hindlimb. *J. Morph.* **206**, 351-361.
- TROTTER, J.A. (1993). Functional morphology of force transmission in skeletal muscle: A brief review. *Acta Anat.* **146**, 205-222.
- TROTTER, J.A. AND BACA, J.M. (1987). The muscle-tendon junctions of fast and slow fibres in the garter snake: Ultrastructural and stereological analysis and comparison with other species. *J. Muscle Res. Cell Motil.* **8**, 517-526.
- TROTTER, J.A., CORBETT, K. AND AVNER, B.P. (1981). Structure and function of the murine muscle-tendon junction. *Anat. Rec.* **201**, 293-302.

- TROTTER, J.A., EBERHARD, S. AND SAMORA, A. (1983a). Structural domains of the muscle-tendon junction. 1. The internal lamina and the connecting domain. *Anat. Rec.* **207**, 573-591.
- TROTTER, J.A., EBERHARD, S. AND SAMORA, A. (1983b). Structural connections of the muscle-tendon junction. *Cell Motil.* **3**, 431-438.
- TROTTER, J.A., HSI, K., SAMORA, A. AND WOFYSY, C. (1985a). A morphometric analysis of the muscle-tendon junction. *Anat. Rec.* **213**, 213-226.
- TROTTER, J.A., SAMORA, A. AND BACA, J.M. (1985b). Three-dimensional structure of the murine muscle-tendon junction. *Anat. Rec.* **213**, 16-25.
- VAN DER STELT, A. (1968). *Spiemechanica en myotoombouw bij vissen*, Thesis. Amsterdam: University of Amsterdam. 94 pp.
- VAN LEEUWEN, J.L. (1992). Muscle function in locomotion. In *Mechanics of animal locomotion* (ed. R. MCN. ALEXANDER), *Advances in Comparative and Environmental Physiology*, vol. 11. pp. 191-250. Heidelberg: Springer-Verlag.
- VAN LEEUWEN, J.L. (1995). Review article: The action of muscles in swimming fish. *Exp. Physiol.* **80**, 177-191.
- VAN LEEUWEN, J.L., LANKHEET, M.J.M., AKSTER, H.A. AND OSSE, J.W.M. (1990). Function of red axial muscles of carp (*Cyprinus carpio* L.) recruitment and normalised power output during swimming in different modes. *J. Zool. Lond.* **220**, 123-145.
- VAN RAAMSDONK, W. (1978). *De ontwikkeling van de rompmusculatuur van Brachydanio rerio (de zebravis)*, Thesis. Amsterdam: University of Amsterdam. 125 pp.
- VAN RAAMSDONK, W., POOL, C.W. AND KRONNIE, G. TE (1987). Differentiation of muscle fibre types in the teleost *Brachydanio rerio*. *Anat. Embryol.* **153**, 137-155.
- VAN RAAMSDONK, W., KRONNIE, G. TE, POOL, C.W. AND LAARSE, W. VAN DE (1980). An immune histochemical and enzymic characterisation of the muscle fibres in myotomal muscle of the teleost *Brachydanio rerio*, Hamilton-Buchanan. *Acta Histochem.* **67**, 200-216.
- VERRETH, J.A.J. AND BIEMAN, J. DEN (1987). Quantitative feed requirements of African catfish (*Clarias gariepinus* Burchell) larvae fed with decapsulated cysts of *Artemia*. I. The effect of temperature and feeding level. *Aquaculture* **63**, 251-267.
- VERRETH, J.A.J., TORREELE, E., SPAZIER, E., SLUISZEN, A. VAN DER, ROMBOUT, J.H.W.M., BOOMS, R. AND SEGNER, H. (1992). The development of a functional digestive system in the African catfish *Clarias gariepinus* (Burchell). *J. World Aquacult. Soc.* **23**, 286-298.
- VIDELER, J.J. (1975). On the interrelationships between morphology and movement in the tail of the Cichlid fish *Tilapia nilotica* (L.). *Neth. J. Zool.* **25**, 143-154.
- VIDELER, J.J. (1985). Fish swimming movements: a study of one element of behaviour. *Neth. J. Zool.* **35**, 170-185.
- VIDELER, J.J. (1992). Wateraap of geboren verdrinker? Vergelijking van zwemprestaties van mens en dier. In *Biologie, Mechanica en Sport*, Biologische Raad Reeks, KNAW (ed. J.W.M. Osse, G.J. van Ingen Schenau, P. Voogt and C.M. van den Heuvel), pp. 107-130. Amsterdam.
- VIDELER, J.J. (1993). *Fish swimming*. London: Chapman and Hall. 260 pp.

References

- VIDELER, J.J. AND HESS, F. (1984) Fast continuous swimming of two pelagic predators, saithe (*Pollachius virens*) and mackerel (*Scomber scombrus*): a kinematic analysis. *J. Exp. Biol.* **109**, 209–228.
- VIERA, V.L.A. AND JOHNSTON, I.A. (1992). Influence of temperature on muscle-fibre development in larvae of the herring *Clupea harengus*. *Mar. Biol.* **112**, 333–341.
- WAINWRIGHT, S.A., BIGGS, W.D., CURRY, J.D. AND GOSLINE, J.M. (1976). *Mechanical design in organisms*. London: Edward Arnold. 423 pp.
- WANG K. (1985). Sarcomere associated cytoskeletal lattices in striated muscle. Review and hypothesis. In *Cell and Muscle Motility 6* (ed. J.W. Shay), pp 315–369. New York: Plenum Publ. Company.
- WANG, K. AND RAMÍREZ-MITCHELL, R. (1983). A network of transverse and longitudinal intermediate filaments is associated with sarcomeres of adult vertebrate skeletal muscle. *J. Cell. Biol.* **96**, 562–570.
- WANG K., McCARTER R., WRIGHT J., BEVERLY J. AND RAMÍREZ-MITCHELL R. (1991). Regulation of skeletal muscle stiffness and elasticity by titin isoforms: a test of the segmental extension model of resting tension. *Proc. Natl. Acad. Sci. USA* **88**, 7101–7105.
- WANG K., McCARTER R., WRIGHT J., BEVERLY J. AND RAMÍREZ-MITCHELL R. (1993). Viscoelasticity of the sarcomere matrix of skeletal muscles. The titin-myosin composite is a dual-stage molecular spring. *Bioph. J.* **64**, 1161–1177.
- WARDLE, C.S. AND VIDELER, J.J. (1980). Fish swimming. In *Aspects of Animal Movement* (ed. H.Y. Elder and E.R. Trueman), pp. 125–150. Cambridge: Cambridge University Press.
- WARDLE, C.S. AND VIDELER, J.J. (1993). The timing of the EMG in the lateral myotomes of mackerel and saithe at different swimming speeds. *J. Fish Biol.* **42**, 347–359.
- WARDLE, C.S., VIDELER, J.J. AND ALTRINGHAM J.D. (1995). Review. Tuning in to fish swimming waves: body form, swimming mode and muscle function. *J. Exp. Biol.* **198**, 1629–1636.
- WEATHERLEY, A.H. (1990). Approaches to understanding fish growth. *Trans. Am. Fish. Soc.* **119**, 662–672.
- WEBB, P.B. (1975). Hydrodynamics and energetics of fish propulsion. *Bull. Fish. Bd. Can.* **190**, 1–158.
- WEBB, P.W. (1975). Acceleration performance of rainbow trout *Salmo gairdneri* and green sunfish *Lepomis cyanellus*. *J. Exp. Biol.* **63**, 451–465.
- WEBB, P.W. (1976). The effect of size on the fast-start performance of rainbow trout *Salmo gairdneri*, and a consideration of piscivorous predator-prey interactions. *J. Exp. Biol.* **65**, 157–177.
- WEBB, P.W. (1978a). Effects of temperature on fast-start performance of rainbow trout, *Salmo gairdneri*. *J. Fish. Res. Board Can.* **35**, 1417–1422.
- WEBB, P.W. (1978b). Fast-start performance and body form in seven species of teleost fish. *J. Exp. Biol.* **74**, 211–226.
- WEBB, P.W. (1984a). Bodyform, locomotion and foraging in aquatic vertebrates. *Am. Zool.* **24**, 107–120.
- WEBB, P.W. (1984b). Form and function in fish swimming. *Sc. American* **251**, 58–68.
- WEBB, P.W. (1993). Swimming. In *The Physiology of Fishes*. Marine Science Series (ed. D.H. Evans), pp. 47–73. London: CRC Press.

- WEBB, P.W. AND BLAKE, R.W. (1985). Swimming. In *Functional Vertebrate Morphology* (ed. M. Hildebrand, D.M. Bramble, K. Liem and D.B. Wake), pp 110-128. Cambridge: Harvard University Press.
- WEBB, P.W. AND SKADSEN J.M. (1980). Strike tactics of *Esox*. *Can. J. Zool.* **58**, 1462-1469.
- WEBB, P.W. AND WEIHS, D. (1983). *Fish biomechanics*. New York: Preager. 398 pp.
- WEIBEL, E.R. (1979). *Stereological methods. Practical Methods for Biological Morphometry*, vol. 1, pp. 1-415. New York: Academic Press.
- WEIBEL, E.R. AND BOLENDER, R.P. (1973). Stereological techniques for electron microscopic morphometry. In *Principles and Techniques of Electron Microscopy. Biological Applications*, vol. 3 (ed. M.A. Hayat), pp. 237-297. New York: Van Nostrand Reinhold Company.
- WEIHS, D. (1972). A hydrodynamical analysis of fish turning manoeuvres. *Proc. R. Soc. Lond. B* **182**, 59-72.
- WEIHS, D. (1973). The mechanism of rapid starting of slender fish. *Biorheology* **10**, 343-350.
- WESTERFIELD, M., McMURRAY, J.V. AND EISEN, J.S. (1986). Identified motoneurons and their innervation of axial muscles in the zebrafish. *J. Neurosc.* **10**, 259-298.
- WILLIAMS T.L., GRILLNER, S., SMOLJANINOV, V.V., WALLÉN, P., KASHIN, S. AND ROSSIGNOL, S. (1989). Locomotion in lamprey and trout: the relative timing of activation and movement. *J. Exp. Biol.* **143**, 559-566.
- WOLTRING, H. (1986). A Fortran package for generalised, cross-validatory spline smoothing and differentiation. *Adv. Engng Software* **8**, 104-113.

DANKWOORD

Tja, eenmaal op deze plek in het proefschrift beland mag ik wel zeggen dat ik blij ben het einde in zicht te hebben. Natuurlijk was de hele periode op EDC voor mij een geweldige ervaring die ik nooit had willen missen. Als ik toen wist wat ik nu weet, na vier en een half jaar, zou ik me met nog meer enthousiasme op dit promotieonderzoek geworpen hebben. Vele mensen hebben mij in raad en daad bijgestaan en dat was lang niet altijd in wetenschappelijk opzicht. Aangezien het niet ondenkbaar is dat ik hier iemand vergeet te vermelden, zal ik mezelf maar alvast deels gaan indekken door alle collegas' en iedereen die ook maar enigszins bijgedragen heeft aan de leuke tijd die ik op EDC had van harte te bedanken voor de interesse, gezelligheid en hulp. Aangezien er te veel mensen zijn die een rol gespeeld hebben tijdens mijn promotie-periode zal ik me hier beperken tot het noemen van degenen die direct betrokken zijn geweest bij het onderzoek en bij het leven buiten het onderzoek.

Allereerst Jan Osse en Rie Akster, die het project opgestart hebben en mij uitstekend begeleidden. Vele (al dan niet) verhitte discussies, openhartige gesprekken en aandacht hebben geresulteerd in het werk dat hier gepresenteerd is. Vooral Rie Akster was in de beginperiode van mijn promotie erg belangrijk omdat zij door haar zeer vakkundige kijk op spieronderzoek de rode draad in mijn project mede vorm en inhoud wist te geven. Rie, je bent er nu niet meer om dit te lezen of het van mij persoonlijk te horen, maar ik ben er van overtuigd dat jij op welke wijze dan ook beseft hoe belangrijk je voor mij bent geweest. Bedankt voor alle steun, aandacht en gedeelde vreugde en verdriet. Toen ik vier en een half jaar geleden begon aan dit onderzoek kon ik nooit vermoeden dat jij twee en een half jaar later zo ernstig ziek zou worden. Je ziekteperiode was voor iedereen die er nauw bij betrokken was erg zwaar, en voor mij dus ook. Niet alleen het feit dat je iemand waarmee je zo'n tijd een kamer deelde ziet lijden, maar ook nog eens het feit dat ik een geweldige begeleidster van mijn onderzoek kwijtraakte maakte de laatste twee jaar van mijn promotie behoorlijk zwaar. Je staat in elk geval in mijn geheugen gegrift als een erg lieve, zorgzame en sympathieke vrouw. Ik denk dat het gedicht vooraan in dit proefschrift, ongeveer een week voordat je stierf geschreven, verder voldoende zegt. Zonder jou Rie was dit proefschrift er zeer zeker niet geweest.

Jan Osse heeft mij vanaf de eerste minuut dat ik hem ken letterlijk en figuurlijk gebiologeerd. Zijn onvermoeibare enthousiasme voor biologie en wetenschap werken zeer aanstekelijk en stimulerend op mij. De steun die ik van hem kreeg na de dood van Rie was bijzonder welkom, dank daarvoor. Ook de sociale bijeenkomsten (bijvoorbeeld Schotse kroegen) waren altijd erg gezellig. Het samen 'in elkaar draaien' van het zwemhoofdstuk was een hele 'bevalling', maar wél een geweldige ervaring. Na alle 'Osse-travel' verhalen heb ik er spijt van dat ik dát nooit echt zelf meegemaakt heb, maar wel genoeg van gehoord heb via verhalen van anderen. Of het een gemis is weet ik zo net nog niet, maar waarschijnlijk wel een onvergetelijke ervaring.

Jos van den Boogaart (paranimf 1) is op vele verschillende wijzen een soort van rots in de branding geweest. Vele uurtjes hebben wij kletsend doorgebracht over zowat alles wat een mens ook maar enigszins kan dwarszitten of bezighouden. Bedankt hiervoor. Zijn ongekende handigheid en inventiviteit kwamen eigenlijk nog het meest sprekend naar voren tijdens het 'gebroken-sleutel-in-slot-incident', waarbij Jos op uiterst 'subtiele' en creatieve manier een functionele oplossing vond. Dat niet iedereen dit waardeerde begrijp ik nog steeds niet.

Natuurlijk is ook Johan van Leeuwen, de secondant en 'adviseur' (zoals het in de oorspronkelijke project-aanvraag beschreven staat), binnen mijn promotie-onderzoek van onschatbare waarde geweest, vooral bij het volbrengen van dit werk. Hij wist, ondanks een drukke baan in Leiden, toch altijd weer tijd voor me te vinden. Na Rie's overlijden nam hij zonder enige aarzeling de begeleiding van haar over en heeft dit met veel vakkundigheid volbracht. Het feit dat wij beiden 'zwart-wit denkers' zijn leidde tot discussies en telefoontjes die niet altijd even rustig verliepen als misschien wel gewenst was, maar het heeft wel resultaat gehad. Jouw directheid spreekt mij erg aan en maakte de samenwerking voor mij erg plezierig.

Henk Granzier heeft mij in 1996 met open armen ontvangen in zijn laboratorium in Pullman, waar ik gedurende ruim vier maanden werkte aan het tot stand komen van het titine artikel. Bij hem heb ik erg veel geleerd en veel leuke mensen ontmoet. Bedankt hiervoor Henk! Alle overige mensen op het laboratorium van Henk die bijgedragen hebben aan de goede tijd die ik er heb gehad wil ik ook bedanken. Speciaal Michiel Helmes die mij in het begin wegwijs maakte in Pullman en onderdak bood. De 'coffeebreaks' waren een welkome afwisseling van de dagelijkse beslommeringen. Vooral de ritjes in je oude auto vergeet ik niet snel. In de vroege ochtend naar de 'fish-trap' bij de stuwdam om 'Golden Salmon' op de meest creatieve manieren te vangen waren onvergetelijk. Vele van deze ritjes eindigden uiteindelijk in het gezamenlijk staren naar de karpers die vrolijk uit het water sprongen in het midden van het meer en ons schenen uit te lachen.

Veel dank ben ik ook verschuldigd aan Henk 'histochemie' Schipper, John 'gel' Samallo, Arie 'EMG' Terlouw, Ingrid 'kletsen' Vos, Anke en Hilda 'zou je het secretariaat een middagje willen overnemen?' Hana en Valk (respectievelijk), Wim 'foto's' Valen, Mees 'data verwerking' Muller en natuurlijk niet te vergeten Sander 'maatje' Kranenbarg (paranimf 2).

Alle vrienden buiten het werk bedank ik ook voor de interesse en vriendschap. Pa, ma, Indra en Mirjam: bedankt dat jullie altijd voor mij klaarstaan.

De laatsten zullen de eersten zijn, oftewel niemand minder dan mijn kersverse vrouw. Jij kwam precies op het juiste moment in mijn leven en hebt mij door dik en dun volledig gesteund. Ook voor jou was het niet altijd even gemakkelijk, zeker niet toen ik in de VS zat. Partner zijn van een wetenschapper is soms erg vermoeiend, maar dáár heb jij nooit blijk van gegeven. Zonder jou was dit zeker niet tot stand gebracht. Heel, héél veel dank lieve Bianca!

CURRICULUM VITAE

Igor Leo Yvonne Spierts werd op 9 december 1969 in Stein geboren. Vanaf zijn tweede jaar woonde hij in Landgraaf waar hij zijn schooltijd begon. In 1988 behaalde hij zijn VWO diploma aan het Eijkhagen-college in Landgraaf, waarna hij begon met de studie Biologie aan de Landbouwniversiteit te Wageningen. Tijdens zijn studie heeft hij diverse practica begeleid voor studenten van de studierichtingen Biologie, Zoötechniek en Humane Voeding. Zijn eerste afstudeervak was een onderzoek betreffende het hypothalamus-hypofyse-bijnier systeem in relatie tot stress bij varkens, uitgevoerd aan de vakgroep Fysiologie van Mens en Dier. Aansluitend hierop werd voor dezelfde vakgroep een stage en een tweede afstudeervak verricht waarbij de invloed van beperkt voedingsniveau op de fysiologie en het gedrag van mannelijke kalveren gedurende een maaltijd en in een 'novel environment test' werd onderzocht. Dit werk werd uitgevoerd op het Agricultural Research Station in Lennoxville, Québec, Canada. Na een rondreis van enige maanden door Canada werd de studie voortgezet met een laatste afstudeervak Functionele Diermorfologie aan de vakgroep Experimentele Diermorfologie en Celbiologie (EDC). Hij werkte daar onder leiding van Rie Akster aan de groei en ontwikkeling van spieren bij larven van de Afrikaanse meerval in relatie tot verschillende zwembewegingen. Na een rondreis van vier maanden door Australië studeerde hij in 1994 *cum laude* af en begon aansluitend als onderzoeker-in-opleiding (OIO) aan een promotieonderzoek bij de vakgroep EDC. In 1996 bracht hij vier maanden door op de Washington State University in Pullman, Washington (VS) waar hij onder leiding van Henk Granzier onderzoek verrichtte naar het spiereiwit titine. Dit werkbezoek werd gefinancierd met behulp van een Fulbright AIO/OIO grant, verstrekt door 'the Netherlands America Commission for Educational Exchange' (NACEE) en resulteerde in een wetenschappelijke publicatie. Het in dit proefschrift beschreven onderzoek werd gefinancierd door de Nederlandse Organisatie voor Wetenschappelijk Onderzoek (NWO), Stichting Levenswetenschappen (SLW), projectnummer 805-28.266, en resulteerde tot nu toe in vier verschenen publicaties en een opgestuurde publicatie (elk in internationale vakbladen). Drie andere publicaties worden nog bewerkt.

LIST OF PUBLICATIONS

Research articles (refereed)

- Akster, H.A., J.A.J. Verreth, I.L.Y. Spierts, T. Berbner, M. Schmidbauer and J.W.M. Osse (1995). Muscle growth and swimming in larvae of *Clarias gariepinus* (Burchell). *ICES Marine Science Symposia* **201**, 45-50.
- Spierts, I.L.Y., H.A. Akster, I.H.C. Vos and J.W.M. Osse (1996). Local differences in myotendinous junctions in axial muscle fibres of carp (*Cyprinus carpio* L.). *Journal of Experimental Biology* **199**, 825-833.
- Spierts, I.L.Y., H.A. Akster and H.L. Granzier (1997). Expression of titin isoforms in red and white muscle fibres of carp (*Cyprinus carpio* L.) exposed to different sarcomere strains during swimming. *Journal of Comparative Physiology B* **167**, 543-551.
- Spierts, I.L.Y. and J.L. van Leeuwen (1999). Kinematics and muscle dynamics of C- and S-starts of carp (*Cyprinus carpio* L.). *Journal of Experimental Biology*: **202** (4), 393-406.

Abstracts and other small publications

- Akster, H.A, J.A.J. Verreth, I.L.Y. Spierts, T. Berbner, M. Schmidbauer and J.W.M. Osse (1993). Muscle growth and swimming in larvae of *Clarias gariepinus* (Burchell). *ICES Marine Symposia, Actes du Symposium, Mass rearing of juvenile Fish, 21-23 june 1996*.
- Spierts, I.L.Y., H.A. Akster, I.H.C. Vos and J.W.M. Osse (1995). Differences in membrane area between myotendinous junctions of red and white and of anterior and posterior muscle fibres of carp (*Cyprinus carpio* L.). *European Journal of Morphology* **33**, 326.
- Spierts, I.L.Y., H.A. Akster, I.H.C. Vos and J.W.M. Osse (1995). Differences in membrane area between myotendinous junctions of red and white and of anterior and posterior muscle fibres of carp (*Cyprinus carpio* L.). *Nederlandse Anatomen Vereniging, 157e wetenschappelijke vergadering, 6 en 7 januari 1995, Lunteren*, 11.
- Spierts, I.L.Y. , H.A. Akster, I.H.C. Vos and J.W.M. Osse (1995). Differences in membrane area between myotendinous junctions of red and white and anterior and posterior axial muscle fibres of carp (*Cyprinus carpio* L.). *The Society for Experimental Biology, St. Andrews Meeting 3-7 april 1995, Animal and Cell Abstracts*, A12.30, 37.
- Spierts, I.L.Y. and H.A. Akster (1996). Local differences in myotendinous in axial muscle fibres of carp (*Cyprinus carpio* L.). *Biophysical Journal* **70** (part 2 of 2), Tu-Pos173, A293.

Spierts, I.L.Y. H.A. Akster and H.L. Granzier (1998). Expression of titin isoforms in red and white muscle fibres of carp (*Cyprinus carpio* L.) exposed to different sarcomere strains during swimming. *The Society for Experimental Biology, Annual Meeting, University of York, 23-27 March 1998, Abstracts Animal and Cell Biology*, A8.1, 29.